

Identification of polymer types, additives and simultaneous quantification of trace organic chemical sorption behavior on sub μ -particles in environmental samples

Julia Reichel

Vollständiger Abdruck der von der TUM School of Engineering and Design der Technischen Universität München zur Erlangung einer

Doktorin der Naturwissenschaften (Dr. rer. Nat.)

genehmigten Dissertation.

Vorsitz: Prof. Dr. Martin Elsner

Prüfer*innen der Dissertation:

1. Prof. Dr.-Ing. Jörg E. Drewes
2. Priv-Doz. Dr. rer. nat. Thomas Letzel
3. Prof. Dr.-Ing. Martin Jekel

Die Dissertation wurde am 12.10.2023 bei der Technischen Universität München eingereicht und durch die TUM School of Engineering and Design am 23.11.2023 angenommen.

Acknowledgement

I am grateful to all those who have contributed to the realization of my dissertation at the Chair of Urban Water Systems Engineering. First and foremost, I extend my deepest gratitude to PD Dr. Johanna Grassmann for her remarkable dedication and intensive guidance throughout the entirety of my doctoral work. Her insightful mentorship and encouragement have been instrumental in shaping both the trajectory and quality of my research. I am honored to acknowledge Prof. Dr.-Ing. Jörg Drewes for graciously providing me with the opportunity to conduct my research within his institute. His expertise and willingness to share his insights have been invaluable assets in the development of my work. A special note of appreciation goes to PD Dr. Thomas Letzel for his exceptional contributions and guidance, which have enriched the depth and scope of my dissertation. I am indebted to Dr. Oliver Knoop for his technical expertise, which has enriched the scientific rigor of my work.

Special thanks to Prof. Dr.-Ing. Martin Jekel for his participation as examiner.

I would like to extend thanks to my colleagues, including Andrea Vogel, Dr. Lara Stadlmaier, Dr. Mohammed Al-Azzawi, Dr. Christoph Schwaller, Franziska Bedacht, Astrid Götz, Dr. Matin Funck, Dr. Elisabeth von der Esch and all the other colleagues of the institute and the project team SubjTrack.

I am also grateful to my students, namely Katrina Templeton, Tom Hackbarth, Carolin Feierabend, Lea-Marie Kiesecker, Patrick Rieder, and Barbara Rösch, for their enthusiastic engagement and contributions.

A sincere thank you to the company Gerstel for providing the necessary technical equipment and the active support by Thomas Wagner.

Lastly, I extend my heartfelt thanks to my family and friends for their unending support, understanding and patience.

To everyone mentioned here and those whose names might not appear, your collective support, expertise, and encouragement have been invaluable in making this dissertation a reality. I am profoundly grateful for each individual's contribution and look forward to carrying forward the knowledge and experiences gained during this enriching journey.

Abstract

The proliferation of micro- and nanoplastic particles in the environment is a global problem. However, not only the particles alone can cause problems, but also contaminants present in the environment that sorb onto the particles, such as pesticides, insecticides or pharmaceuticals. Until now, the investigation of micro- and nanoplastic particles with sorbed TOrCs has only been possible with complex extraction procedures. In this work, a novel analytical technique named TD-Pyr-GC/MS was established and validated for the identification and quantification of sorbed TOrCs and the polymer type.

This dissertation initially addresses method development and validation of TD-Pyr-GC/MS. Using selected reference substances (phenanthrene, triclosan and α -cypermethrin) and defined reference particles of polystyrene (PS), polyethylene (PE), and polymethyl methacrylate (PMMA), controlled sorption experiments were performed. The method development was comprised of not only specifying the appropriate choice of sample preparation but also the identification of the optimal thermodesorption (TD) conditions. Thereby the temperature has to be chosen in such a way that the selected TOrCs desorb in the first step. During the TD step, almost no decomposition of the polymers occurred. The subsequent pyrolysis step is used for polymer identification. For optimal conditions, the TD temperature was set at 200 °C and the pyrolysis temperature at 800 °C. In conclusion, a method was developed to identify TOrCs on particles, regardless of particle size (both micro- and nanoparticles).

In the second part of this dissertation, the focus was on sorption as a function of particle size, polymer type, mixture of TOrCs used, and aging of the particles. Based on the previously developed TD-Pyr-GC/MS method, sorption experiments were conducted with the selected TOrCs and reference particles. For a comprehensive analysis, these studies were the first to examine TOrC concentrations in both phases, aqueous and particulate. Findings suggest that sorption is polymer- and size-dependent. PE particles exhibited the highest sorption rate compared to PS and PMMA particles, with approximately the same particle size. The high sorption on PS nanoparticles is mainly due to the high number of particles and the higher specific surface area. At the same time, it was demonstrated that quantification of TOrCs directly from nanoparticles by TD-Pyr-GC/MS is possible. Simultaneous sorption of the TOrCs phenanthrene, triclosan and α -cypermethrin onto PS nanoparticles and PE microparticles, showed no competing effects for PS nanoparticles. Thus, phenanthrene sorbed more strongly to PE microparticles in the presence of triclosan and α -cypermethrin.

In the third part, the application of TD-GC/MS was used to determine the concentration of phenanthrene in the aqueous phase of an ecotoxicological experiment. This study was conducted in collaboration with the Chair of Aquatic Systems Biology. Using the freshwater organism *G. roeseli*, it has been shown that the presence of microplastic particles (polyamides) as well as sediment particles did not negatively affect the organism considering sublethal and lethal effects. Thus, microplastics and sediment particles significantly reduced phenanthrene levels by their presence, so that the lethal effect for *G. roeseli* was solely caused by higher phenanthrene concentrations.

The application of TD-Pyr-GC/MS in the field of micro- and nanoplastic analysis showed that identification and quantification of TOxCs directly from the particle is possible after validation of the appropriate method. No complex extraction steps are necessary in advance, so that an analysis can be performed in less than two hours. Combining a new analytical technique for micro- and nanoplastic particles and analytical sorption research, this work offers new and fast analytical methods, which could be effectively employed for instance in fate studies using laboratory-scale wastewater treatment plants or in ecotoxicological experiments.

Zusammenfassung

Die Verbreitung von Mikro- und Nanopartikeln aus Kunststoff in der Umwelt ist ein globales Problem. Nicht nur die Partikel selbst können Probleme verursachen, sondern auch in der Umwelt vorhandene Schadstoffe, die an die Partikel sorbiert werden, wie z.B. Pestizide, Insektizide oder Pharmazeutika. Die Untersuchung von Mikro- und Nanoplastikpartikeln mit sorbierten TOrcs war bisher nur mit aufwendigen Extraktionsverfahren möglich. In dieser Arbeit wurde eine neue Analysetechnik (TD-Pyr-GC/MS) zur Identifizierung und ggf. Quantifizierung der sorbierten TOrcs und des Polymertyps etabliert und validiert.

Diese Dissertation befasst sich zunächst mit der Methodenentwicklung und Validierung der TD-Pyr-GC/MS. Unter Verwendung ausgewählter Referenzsubstanzen (Phenanthren, Triclosan und α -Cypermethrin) und definierter Referenzpartikel aus Polystyrol (PS), Polyethylen (PE) und Polymethylmethacrylat (PMMA) wurden kontrollierte Sorptionsversuche durchgeführt. Die Methodenentwicklung umfasst neben der Auswahl einer geeigneten Probenvorbereitung auch die Bestimmung der optimalen Thermodesorptionstemperatur (TD). Die Temperatur muss so gewählt werden, dass die ausgewählten TOrcs im ersten TD-Schritt desorbiert werden. Während der Thermodesorption findet noch keine vollständige Fragmentierung der Polymere statt. Der anschließende Pyrolyseschritt dient der Polymeridentifizierung. Für optimale Bedingungen wurde die TD-Temperatur auf 200 °C und die Pyrolysetemperatur auf 800 °C eingestellt. Zusammenfassend lässt sich sagen, dass eine Methode zur Identifizierung von TOrcs auf Partikeln entwickelt wurde, unabhängig von der Partikelgröße (sowohl Mikro- als auch Nanopartikel).

Im zweiten Teil dieser Dissertation lag der Schwerpunkt auf der Sorption in Abhängigkeit von der Partikelgröße, dem Polymertyp, der Mischung der verwendeten TOrcs und der Alterung der Partikel. Basierend auf der zuvor entwickelten TD-Pyr-GC/MS Methode wurden Sorptionsexperimente mit den ausgewählten TOrcs und Referenzpartikeln durchgeführt. Diese Studien waren die ersten, die TOrc-Konzentrationen in beiden Phasen, wässrig und auf Partikeln, untersuchten. Es konnte gezeigt werden, dass die Sorption polymer- und größenabhängig ist. PE-Partikel zeigten die höchste Sorptionsrate im Vergleich zu PS- und PMMA-Partikeln, die in etwa die gleiche Partikelgröße aufwiesen. Eine hohe Sorption auf die PS-Nanopartikel ist hauptsächlich auf die hohe Partikelanzahl und die höhere spezifische Oberfläche zurückzuführen. Gleichzeitig konnte jedoch gezeigt werden, dass die Quantifizierung von TOrcs direkt aus Nanopartikeln mittels TD-Pyr-GC/MS möglich ist. Die gleichzeitige Sorption der TOrcs Phenanthren, Triclosan und α -Cypermethrin an PS-Nanopartikeln und PE-Mikropartikeln zeigte

keine konkurrierenden Effekte für die PS-Nanopartikel. Phenanthren wurde in Gegenwart von Triclosan und α -Cypermethrin stärker an PE-Mikropartikel adsorbiert.

Im dritten Teil wurde die TD-GC/MS zur Bestimmung der Konzentration von Phenanthren in der wässrigen Phase eines ökotoxikologischen Experiments eingesetzt. Diese Studie wurde in Zusammenarbeit mit dem Lehrstuhl für Aquatische Systembiologie durchgeführt. Anhand des Süßwasserorganismus *G. roeseli* konnte durch subletale, letale und analytische Untersuchungen gezeigt werden, dass die Anwesenheit von Mikroplastikpartikeln (Polyamid) und Sedimentpartikeln keine negativen Auswirkungen auf den Organismus hat. Mikroplastik- und Sedimentpartikel reduzierten die Phenanthrenkonzentration sogar signifikant, so dass *G. roeseli* erst bei höheren Phenanthrenkonzentrationen starb.

Die Anwendung der TD-Pyr-GC/MS auf dem Gebiet der Mikro- und Nanokunststoffanalytik hat gezeigt, dass die Identifizierung und Quantifizierung von TOCs direkt aus dem Partikel nach Validierung der entsprechenden Methode möglich ist. Es sind keine aufwendigen Extraktionsschritte notwendig, so dass eine Analyse in weniger als 2 h durchgeführt werden kann. Durch die Kombination einer neuartigen Analysetechnik für Mikro- und Nanopartikel und der analytischen Sorptionsforschung stellt diese Arbeit eine neue und schnelle Analyseverfahren zur Verfügung, die für Laborkläranlagen oder für ökotoxikologische Experimente geeignet ist.

Content

List of Abbreviations.....	xii
List of Figures	xiv
List of Tables	xvi
1 Introduction	1
1.1 Analytical methods for micro- and nanoplastic particles	1
1.2 Current analytical strategies to detect sorbed TOrCs on micro- and nanoplastic particles in aqueous environment.....	3
1.2.1 Polymer properties that influence the sorption process	4
1.2.2 General strategies to identify sorbed TOrCs.....	5
2 Research significance, goals and hypotheses.....	10
3 State-of-the-art of analytical methods.....	14
3 Material and Methods.....	14
3.1 Instrumental Systems	14
3.1.1 TD-GC/MS	15
3.1.2 TD-Pyr-GC/MS.....	15
3.2 Chemicals.....	16
3.2.1 Selection of particles	16
3.2.2 Selection of TOrCs.....	18
3.2.3 Sample preparation of suspended micro- and nanoparticles.....	20
3.2.4 Verification of TOrCs via the Alkanes Calibration Standard.....	22
3.2.5 Data evaluation of the TD-Pyr-GC/MS	23
4 Analysis – Coupling of thermodesorption- and pyrolysis-GC/MS in one analytical setup.....	27
4.1 Sample preparation, method development and validation for a TD-Pyr-GC/MS method..	28
4.1.1 Rationale.....	28
4.1.2 Experimental Section	33
4.2 Results and Discussion	36

4.2.1 Preliminary results – analysis of the aqueous phase	36
4.2.2 Sources of contaminations and sample preparation	37
4.2.3 Choice of the final thermal desorption temperature	38
4.2.4 Desorption behavior of the TOrCs phenanthrenes, α -cypermethrin and triclosan.....	38
4.2.5 Sorption of TOrCs on reference particles	39
4.2.6 Quantification of micro- and nanoplastic particles by TD-Pyr-GC/MS	39
4.2.7 Quantification of TOrCs (preliminary experiments)	41
4.3 Conclusion.....	42
5 Ad- and Absorption behavior on reference particles depends on particle size and shape / particle type / mixture of TOrCs / aging of particles	43
5.1 Rationale	44
5.2 Experimental section	49
5.3 Results and Discussion	54
5.3.1 Sorption onto PS micro- and nanoplastic particles	54
5.3.2 Quantification – Sorption of different TOrCs concentrations onto PS nanoparticles...54	
5.3.3 Ad- and Absorption behavior on reference particles depends on particle type.....55	
5.3.4 Ad- and absorption behavior on reference particles depends on mixture of TOrCs ...56	
5.3.5 Ad- and absorption behavior on reference particles depends on aging of particles ...57	
5.4 Conclusion.....	58
6 Sublethal and lethal effects of particles in <i>in vitro</i> and <i>in vivo</i> assays depend on particle type and size	60
6.1 Rationale	60
6.1.1 Experimental Section	62
6.2 Results and Discussion	64
6.3 Conclusion.....	64
7 Overall conclusions, prospects and future research challenges	65
7.1 Impacts and Conclusions of the Research Results	65

7.2 Remaining Challenges and Suggestions for Future Research	66
7.2.1 Screening of different micro- and nanoplastic polymers and TOrCs	66
7.2.2 Application in screening procedures for ecotoxicological and laboratory tests	67
7.2.3 Quantification of sorbed TOrCs by TD-Pyr-GC/MS compared with modeling	67
References	68
Appendix I	77
Appendix II	96
Appendix III	113
Appendix IV	130
Appendix V	156

List of Abbreviations

CBs	Chlorinated benzenes
CIS	Cooled injection system
DAD	Diode array detector
ECD	Electron Capture Detection
EtOH	Ethanol
FD	Fluorescence detector
FFF	Field flow fractionation
FLD	fluorescence detector
FTIR	Fourier transform infrared spectroscopy
GC/MS	Gas chromatography / mass spectrometry
HCHs	Hexachlorocyclohexanes
HDPE	High-density polyethylene
HOCs	Hydrophobic organic chemicals
HPLC	High performance liquid chromatography
HR/MS	High resolution / mass spectrometric
LDPE	Low-density polyethylene
MS	mass spectrometry
PA	Polyamide
PAHs	Polycyclic aromatic hydrocarbons
PCBs	Polychlorinated biphenyls
PDMS	polydimethylsiloxane
PE	Polyethylene
PET	Polyethylene terephthalate
PHCs	Polyhalogenated carbazoles
PLA	Poly lactide
PMMA	Polymethylmethacrylate
PP	Polypropylene
PS	Polystyrene
Pyr-GC/MS	Pyrolysis gas chromatography mass spectrometry
RI	Retention index
RT	Retention time
SBSE	Stir bar sorptive extraction

TD-Pyr- GC/MS	Thermal extraction/desorption-pyrolysis-gas chromatography/mass spectrometry
TDU	Thermal desorption unit
TED-GC/MS	Thermal extraction desorption gas chromatography mass spectrometry
T _g	Glass transition temperature
TGA	Thermogravimetric analysis
TIC	Total ion chromatogram
TOrCs	Trace organic compounds
UV	Ultraviolet

List of Figures

FIGURE 1: WORKFLOW OF SAMPLE PREPARATION OF SORPTION EXPERIMENTS ON MICRO- AND NANOPLASTICS FOR ANALYTICAL DETECTION METHODS. (1) MIXING AND (2) INCUBATION OF THE PARTICLES AND TORCs FOR A SPECIFIED TIME IN AQUEOUS SOLUTION. (3) SEPARATION OF THE PARTICLES AND THE AQUEOUS PHASE. PREPARATION OF EITHER THE AQUEOUS PHASE OR THE PARTICLES, DEPENDING ON THE ANALYTICAL TECHNIQUE. (4) ANALYSIS IS BASED ON EITHER A GAS CHROMATOGRAPHIC METHOD FOLLOWED BY HIGH RESOLUTION/MASS SPECTROMETRIC (HR/MS), MASS SPECTROMETRIC (MS) OR ELECTRON CAPTURE DETECTION (ECD) ANALYSIS, OR HIGH PERFORMANCE LIQUID CHROMATOGRAPHY (HPLC) FOLLOWED BY MS/MS, MS, ULTRAVIOLET (UV), DIODE ARRAY DETECTOR (DAD) OR FLUORESCENCE DETECTOR (FLD). OTHER ANALYTICAL METHODS INCLUDE LIQUID SCINTILLATION COUNTER AND SPECTROPHOTOMETER. (ADAPTED FROM REICHEL ET AL., 2021 (APPENDIX I)).....	5
FIGURE 2: COMPREHENSIVE OVERVIEW OF RESEARCH HYPOTHESES, RESEARCH TASKS, AND PUBLICATIONS OF THIS DISSERTATION.....	11
FIGURE 3: FLOWCHART OF THE TD-PYR-GC/MS ANALYSIS. FIRST, (A) THE SAMPLE IS THERMODESORBED (120 – 280 °C), THEREBY DESORBING THE VOLATILE SUBSTANCES AND CRYOFOCUSING THEM IN THE COOLED INJECTIONS SYSTEM (CIS) AT –50 °C. THIS IS FOLLOWED BY A TRANSFER TO THE GC COLUMN WITH AN MS ANALYSIS (TD-GC/MS). THE SAME SAMPLE (B) IS SUBSEQUENTLY PYROLYZED AT 800 °C, FOLLOWED BY A GC/MS ANALYSIS (PYR-GC/MS). THE EVALUATIONS ARE CARRIED OUT USING THE TD-CHROMATOGRAM AND THE PYROGRAM. ADOPTED FROM REICHEL ET AL., 2020 [65].	15
FIGURE 4: LEFT: STRUCTURE OF THE TD-GC/MS (ANALYSIS VIA GERSTEL TWISTER®), RIGHT: STRUCTURE OF THE COUPLED TD-GC/MS + PYR-GC/MS, ADAPTED FROM REICHEL ET AL., 2020 (APPENDIX II)	16
FIGURE 5: INCUBATION OF THE TORCs AND THE POLYMERS OVER A PERIOD OF TIME. THE PARTICLES (1) ARE SCRAPED FROM THE PARTICLE AFTER FILTRATION AND FREEZE-DRIED. THEN A MAXIMUM AMOUNT OF 80 µg IS WEIGHED INTO A PYROLYSIS TUBE AND ANALYZED VIA TD-PYR-GC/MS. THIS IS FOLLOWED BY AN EVALUATION OF THE TORCs VIA THE TD CHROMATOGRAM AND THE POLYMERS VIA THE PYROGRAM. THE FILTRATE (2) IS EITHER DISCARDED (A) OR A DEUTERATED STANDARD IS ADDED FOR FURTHER ANALYSIS (B). THE FILTRATE IS THEN MIXED WITH A GERSTEL TWISTER® AND STIRRED FOR 1 H AND THEN PLACED IN A THERMODESORPTION (TD) TUBE. THE ANALYSIS IS PERFORMED VIA TD-GC/MS. THE TORC IS EVALUATED VIA THE TD CHROMATOGRAM, ADAPTED FROM REICHEL ET AL., 2022 (APPENDIX III)	22
FIGURE 6: SAMPLE ANALYSIS PROCEDURE: FILTRATION OF THE SAMPLE TO SEPARATE PARTICLES AND AQUEOUS PHASE. SUBSEQUENT APPLICATION OF THE PARTICLES INTO THE PYROLYSIS TUBES. DEPENDING ON THE TEST SETUP, A NON-TARGET ANALYSIS (SCAN MODE) OR A TARGET ANALYSIS (SIM MODE) CAN BE PERFORMED. FINALLY, A TD-PYR-GC/MS ANALYSIS IS PERFORMED. ADAPTED FROM REICHEL ET AL., 2020 (APPENDIX II)	28
FIGURE 7: STEPS TO DEVELOP AN OPTIMIZED METHOD: A) PYROLYSIS TUBES, B) APPLICATION OF PARTICLES INTO PYROLYSIS TUBES AND WEIGHING, C) PYROLYSIS ADAPTER D) DURING ANALYSIS IN TD-PYR-GC/MS.....	33

FIGURE 8: FLOWCHART OF A TD-PYR-GC/MS ANALYSIS. THE SAMPLE (A) IS THERMODESORBED (120 / 200 280°C) TO DESORB THE VOLATILE TORCS. THE SUBSTANCES ARE CRYOFOCUSED IN THE COOLED INJECTION SYSTEM (CIS) AT -50°C. THE ANALYSIS IS PERFORMED BY GC/MS (TD-GC/MS). THE SAME SAMPLE (B) IS PYROLYZED AT 800°C AND ANALYZED BY GC/MS (PYR-GC/MS). THE EVALUATIONS ARE PERFORMED WITH THE TD CHROMATOGRAM AND THE PYROGRAM. ADAPTED FROM REICHEL ET AL., 2020 (APPENDIX II)	35
FIGURE 9: INCREASE OF STYRENE DIMER DURING BLANK MEASUREMENTS WITH FILAMENT 1 AND DECREASE AFTER CHANGING THE FILAMENT	38
FIGURE 10: BOXPLOTS OF PEAK AREAS NORMALIZED TO POLYMER MASS VERSUS WEIGHED-IN MASS FOR ALL POLYMERS. THE PEAK AREA VALUES INCLUDE THE SIGNALS OF ALL SELECTED CHARACTERISTIC POLYMER FRAGMENTS IN BOTH TD AND PYR.	40
FIGURE 11: POLLUTANTS WHICH INTERACT VIA DE- AND ADSORPTION WITH MICRO- AND NANOPLASTIC PARTICLES	44
FIGURE 12: SORPTION OF TORCS IS INFLUENCED BY POLYMER AND PARTICLE TYPE (1), SIZE (2), SHAPE (3) AND MIXTURE OF TORCS (4)	45
FIGURE 13: INTERACTIONS OF MICRO- AND NANOPLASTIC PARTICLES AND TORCS DEPENDING ON THEIR SPECIFIC PROPERTIES.	47
FIGURE 14: SAMPLE PREPARATION WORKFLOW: FIRST, THE TORCS AND MICROPLASTIC PARTICLES ARE INCUBATED IN AQUEOUS SOLUTION. SUBSEQUENTLY, THE SAMPLE IS FILTERED. THE FILTRATE (1) IS MIXED WITH THE DEUTERATED STANDARD AND STIRRED FOR 1 H WITH THE TWISTER. THE TWISTER IS ADDED TO THE TD TUBE AND ANALYZED VIA TD-GC/MS. THE TORC IS ANALYZED VIA THE TD CHROMATOGRAM (A). THE PARTICLES (2) ARE SCRAPED OFF THE FILTER WITH A SPATULA, PLACED IN A VIAL AND FREEZE DRIED. THE DRIED PARTICLES ARE WEIGHED DIRECTLY INTO THE PYROLYSIS TUBE AND ANALYZED BY TD-PYR-GC/MS. THE TD CHROMATOGRAM IS USED TO EVALUATE THE VOLATILES (A), AND THE PYROGRAM IS USED FOR THE POLYMERS (B). ADAPTED FROM REICHEL ET AL., 2022 (APPENDIX III)	49

List of Tables

TABLE 1: OVERVIEW OF POTENTIAL AND LIMITATIONS OF OPTICAL [6, 7, 26, 27, 29-31, 43] AND THERMAL [16, 20, 21, 24, 26, 27, 29, 40, 41] ANALYTICAL METHODS FOR THE DETECTION OF MICRO- AND NANOPLASTICS.....	3
TABLE 2: POLYMER PROPERTIES AND THEIR INFLUENCE ON SORPTION PROCESSES	4
TABLE 3: SUMMARY OF GC/MS AND HPLC METHODS FOR THE ANALYSIS OF SORBED TORCs ON PLASTIC PARTICLES ADAPTED FROM REICHEL ET AL., 2021 [80] (APPENDIX I).....	7
TABLE 4: INVESTIGATED POLYMER TYPES, STRUCTURAL FORMULA, LOG D AND SIZES.....	17
TABLE 5: SELECTED REFERENCE TORCs	19
TABLE 6: RI FOR PHENANTHRENE, A-CYPERMETHRIN AND TRICLOSAN CALCULATED FROM THE RT. RI FROM NIST DATABASE ARE SHOWN AS COMPARISON	23
TABLE 7: CHARACTERISTIC PYROLYSIS FRAGMENTS OF SELECTED POLYMERS FOR IDENTIFICATION	24
TABLE 8: CHARACTERISTIC SIGNALS OF SELECTED TORCs FOR IDENTIFICATION	25
TABLE 9: SUMMARY OF GC/MS-METHODS TO ANALYZE SORBED SUBSTANCES ON VARIOUS MICROPLASTIC PARTICLES LIKE POLYETHYLENE (PE), POLYSTYRENE (PS), POLYAMIDE (PA), POLYVINYL CHLORIDE (PVC), POLYPROPYLENE (PP), POLYETHYLENE TEREPHTHALATE (PET) AND POLYMETHYL METHACRYLATE (PMMA), ADOPTED FROM REICHEL ET AL., 2021.....	30
TABLE 10: CHARACTERISTIC SIGNALS FOR MS ANALYSIS AND PROPERTIES OF SELECTED TORCs.....	51
TABLE 11: PROTOCOLS APPLIED TO THE AGING OF MICRO- AND NANOPLASTIC PARTICLES	52
TABLE 12: CHARACTERISTIC PYROLYSIS PRODUCTS OF THE SELECTED POLYMERS FOR IDENTIFICATION.....	52
TABLE 13: INFLUENCE ON THE PARTIAL PYROLYSIS (TD) PRODUCTS AT 200°C FOR PA AND PS PARTICLES DURING THERMAL DESORPTION, ADAPTED BY AL-AZZAWI ET AL., 2020 (APPENDIX IV)	58
TABLE 14: MASS AND NUMBER OF POLYSTYRENE PARTICLES, ADAPTED FROM REICHEL ET AL., 2020 (APPENDIX 1)	59
TABLE 15: OVERVIEW: CURRENT LITERATURE REGARDING AQUATIC ORGANISMS AND MICROPLASTICS (MP) AND TORCs.....	61
TABLE 16: COMPOSITION OF THE ISO MEDIUM FOR A 20 L APPROACH; SUBSTANCES DISSOLVED IN WATER.....	62
TABLE 17: PHENANTHRENE CONCENTRATION RANGE IN THE GAMMARIDS EXPERIMENT WITH THE ENVIRONMENTAL SAMPLE WITHOUT ADDITIVES (CONTROL), PMMA MICROPLASTIC PARTICLES (MP) AND SEDIMENT	63

1 Introduction

The spread of micro- and nanoplastics is considered a global challenge and a recognized risk to the aquatic and terrestrial environment [1-3]. Commonly, plastic particles in the environment are considered to be either primary or secondary. Primary plastic particles are produced intentionally and refer to particles produced in their specific size range. Once synthetic polymers are exposed to natural processes in the aquatic environment, weathering and mechanical stress lead to fragmentation of larger plastic parts into more and smaller particles of different shapes and sizes [4-6]. Thus, large macroplastics are turning into micro- and nanoplastics. The term "microplastics" was first proposed by Thompson et al. in 2004 [7]. No standard definition of the term "microplastic" has been defined for a long time [1, 4, 8-11]. In a recently published ISO standard, an attempt was made to standardize the terms (DIN CEN ISO/TR 21960). Macroplastics are defined as all plastic parts larger than 5 mm, microplastics are particles between 1 μm and 1,000 μm in size, and nanoplastics are smaller than 1 μm . Plastic particles above 1 mm and smaller than 5 mm are defined as "large microplastic".

Micro- and nanoplastic particles could pose a risk to human health [12]. Nanoparticles could penetrate cells potentially causing adverse effects [13-15]. In addition to the risk of the pure polymers, their properties determine their bioavailability and potential to sorb toxic pollutants, especially in aquatic environments [9]. This influences the transport and diffusion of pollutants which may lead to a transfer of pollutants to biota [1, 16-18]. Relevant pollutants can be divided into two groups: (i) hydrophobic chemicals adsorbing from the environment due to their affinity for the hydrophobic surface of plastics and (ii) additives, monomers and oligomers present as constituents of polymers [19]. The sorption processes depend mainly on the composition of the polymer and can be categorized into adsorption on the surface or absorption into the polymer structure [20-22]. Another aspect of particular importance is the size of the plastic particles [16, 23]. Smaller plastic particles show enhanced physicochemical interactions due to an increased surface area and moreover have a greater potential to be ingested by organisms, bioaccumulate, and enter the human food chain [1, 9]. Due to the described problems with micro- and nanoplastic particles, a reliable and reproducible analysis of these is essential.

1.1 Analytical methods for micro- and nanoplastic particles

For the analysis of micro- and nanoplastic particles, there is no specific analytical method that can determine all relevant parameters such as particle size, composition, mass, sorbed trace organic compounds (TOCs), surface area, porosity, or aging effects. Considering the analysis of

micro- and nanoplastic particles, many challenges arise: the sample should be homogeneous, microplastic should be free of organic substances (e.g. biofilms) and inorganics (e.g. sand). Therefore, a costly and time-consuming sample preparation is necessary [24-26]. An initial standardization was carried out by DIN CEN ISO/TR 21960 (Plastics – Environmental aspects – State of knowledge and methodologies). A multitude of different techniques is used. However, the application of several different methods can lead to a lack of comparability of the data [3, 24, 27]. A general method for the analysis of microplastics is the physical examination of the particles (microscopy), prior to chemical characterization (spectroscopy or thermal analysis) [27].

Visual analysis offers the simplest and cheapest way to identify microplastic particles. However, the biggest limitation here is the particle size which must be larger than 500 μm [6, 24, 27, 28]. Since plastic particles in the environment are often not identifiable as such, it can easily lead to false positive or false negative results. To enable identification of smaller synthetic polymers, the current state-of-the-art is the use of Fourier transform infrared spectroscopy (FTIR) and Raman spectroscopy [4, 7, 24, 29]. Using FTIR, it is possible to distinguish synthetic polymers from other organic and inorganic particles. In the case of microplastics, micro-FTIR can be used [6, 26, 27, 30, 31].

Another suitable analytical method is Raman spectroscopy for the identification of microplastics [32, 33]. Polymer particles are identified based on their specific frequencies of backscattered light after irradiation with a laser beam [24]. Again, the evaluation is performed with the assignment of spectra to reference databases [34-36]. FTIR and Raman spectroscopy are both non-contact analytical techniques. However, interference can occur due to the presence of pigments. FTIR and Raman spectroscopy analyses are very time consuming and costly, however, automated mapping can reduce the time required for both FTIR and Raman analyses [33, 37]. A newly developed online coupling of Raman microscopy and Field Flow Fractionation (FFF) analysis with the aid of optical tweezers also enables nanoplastics analysis (5 μm - 200 nm) [38].

Other analytical methods for polymer identification are based on thermal methods [24, 39]. An established thermal analysis method is thermal extraction-desorption gas chromatography-mass spectrometry (TED-GC/MS) coupled with thermogravimetric analysis (TGA) [26, 40]. A defined amount of polymer is heated over a temperature gradient. The volatile substances are collected with an adsorber material and subsequently analyzed by GC/MS. Another method is pyrolysis GC/MS (Pyr-GC/MS) [29, 41, 42]. In all pyrolysis methods, the polymers are fragmented using high temperatures. The resulting characteristic degradation products can then be analyzed by GC/MS and cross-checked against databases (e.g., NIST) in order to allow polymer identification

[26, 27, 40, 41]. A new method that allows uncomplicated measurement of sorbed trace substances and polymers is thermodesorption-pyrolysis gas chromatography mass spectrometry (TD-Pyr-GC/MS), an application that has been developed as part of this work.

Table 1 summarizes the current analytical techniques (optical and thermal) for micro- and nanoplastic particles and their limitations regarding particle size, polymer identification and quantification, and their potential to analyze sorbed TOrCs. Often, multiple methods, e.g., microscopic and spectroscopic techniques, are used in parallel to identify plastics in an environmental sample [27].

Table 1: Overview of potential and limitations of optical [6, 7, 26, 27, 29-31, 43] and thermal [16, 20, 21, 24, 26, 27, 29, 40, 41] analytical methods for the detection of micro- and nanoplastics

Method Parameter	Optical Analysis		Thermal Analysis		
	FTIR	Raman	TED-GC/MS	Pyr-GC/MS	TD-Pyr-GC/MS
Particle Size	✓	✓	-	-	-
Size Restriction	≥ 10 µm	≥ 1 µm	-	-	-
Polymer Identification	✓	✓	✓	✓	✓
Polymer Quantification	✓	✓	✓	✓	- (so far)
Destructive	-	-	✓	✓	✓
TOrC analysis	-	-	- (so far)	- (so far)	✓

1.2 Current analytical strategies to detect sorbed TOrCs on micro- and nanoplastic particles in aqueous environment

Recently published reviews have summarized the sorption of TOrCs on micro- and nanoplastics with a focus on the influence of physical properties (size, surface area, crystallinity) [17, 44-46]. In addition, the interactions between TOrCs and polymers, sorption mechanisms, and ecotoxicological factors are considered.

The sorption processes depend especially on the nature of the polymer and can be categorized into adsorption on the surface or absorption into the polymer matrix [20-22]. [47]. In the case of interaction between polymers and TOrCs, the term sorption is used. This is due to the fact that the dominant process cannot clearly be identified and both processes can occur simultaneously [48, 49]. A further classification is made by the type of sorption process. Chemical sorption is the formation of covalent bonds, which is often irreversible and depends on the ability of the compounds to interact with each other. Physical sorption processes, on the other hand, are mostly

non-covalent intermolecular interactions such as van der Waals bonds [48, 50]. Sorption of persistent TOrCs to plastic debris in aquatic systems is most commonly classified as physical processes. Nevertheless, more specific compound-dependent binding such as hydrogen bonding and π - π -surface interactions or cavity formation can occur within the polymeric material [48, 51]. Various parameters such as particle size and surface area, polymer type or hydrophobicity influence the sorption of TOrCs onto micro- and nanoplastic particles.

1.2.1 Polymer properties that influence the sorption process

Different polymer properties significantly influence the sorption process. In addition to the polymer type, particle size and particle shape, it is mainly the hydrophobicity of the polymer that influences the sorption capacity of a hydrophobic TOrC. Hydrophobicity is considered one of the most important driving mechanisms of organic compounds from water onto solid particles [48, 52]. Decisive for this is the Log D value as a measure of the hydrophobicity of a molecule, for the distribution of a sorbate in solution for sorbing to a given solid, taking into account the pH influence of functional groups [53]. In addition, the density of the polymer, its crystallinity and the glass transition temperature also influence sorption. Table 2 describes the polymer properties and their influence on the sorption process.

Table 2: Polymer properties and their influence on sorption processes

Polymer property	Effect on sorption process
Crystallinity	Higher absorption rates in amorphous regions or amorphous polymers, lower for crystalline fractions [5, 54, 55]
Density	Influences the speed of the sorption process [56]
Glass transition temperature (T_G)	Classification of amorphous regions into rubbery or glassy. Conditioned by this the function of the mobility of the polymer chains [23, 48, 57-59].
Hydrophobicity	Affinity of the chemical to sorb onto the particle and affinity of the polymer to TOrC [48, 52, 53].
Size	Influences volume-to-surface ratio, capacity and velocity of sorption [60-62]
Surface	Number of adsorption sites, capacity and speed of sorption [16, 18, 49, 63]
Structure	Distance between the individual polymer chains [59, 64]

1.2.2 General strategies to identify sorbed TOrcs

The analysis of sorbed TOrcs on polymers in a liquid phase can be performed either via the aqueous phase, the gas phase, or directly via particle analysis [20, 21, 65, 66]. Established analytical methods include GC/MS, HPLC-DAD, (U)HPLC-MS/MS, UV spectrometer, or liquid scintillation counting [66-69].

Figure 1 shows the schematic progress of a laboratory test setup for the determination of sorbed substances. The reference particles are incubated in an aqueous phase with selected TOrcs for a defined period of time. The aqueous phase can be varied with respect to pH, humic acid content or salt content in order to simulate specific environmental conditions [70-72].

After incubation, separation of the aqueous and particle phases must take place by centrifugation or filtration [23, 65, 73]. This is followed by analysis of the sorbed substance by direct particle analysis or by solvent extraction of the TOrcs from the particle (e.g., n-hexane, dichloromethane) [74, 75]. Another possibility for the determination of TOrcs is the analysis of the aqueous phase via liquid/liquid extraction or by a passive sampler [52, 66, 76, 77]. Based on the residual concentration in the aqueous phase, an indirect statement can be made about the amount of sorbed substances on the particles [78].

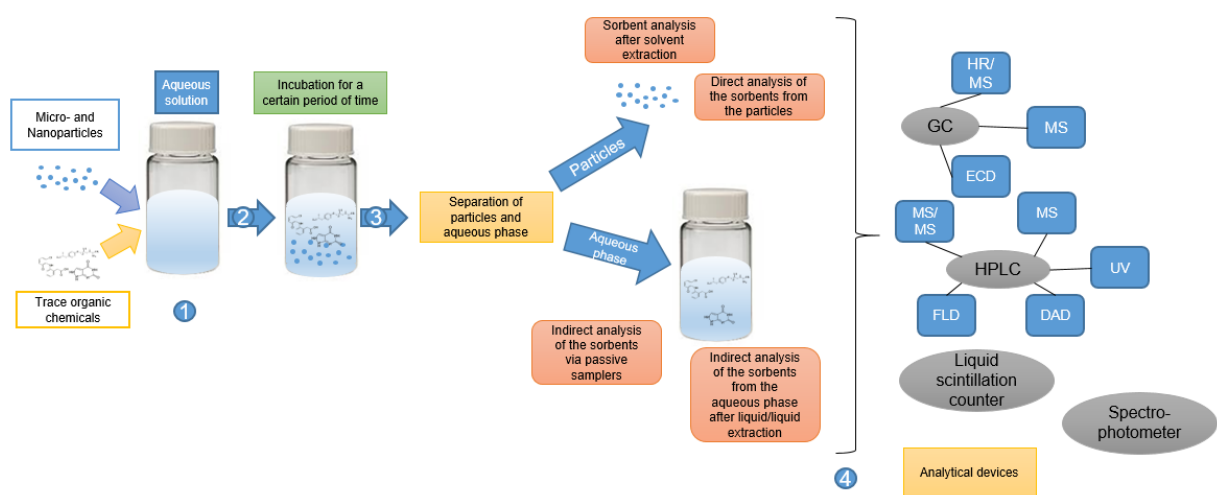


Figure 1: Workflow of sample preparation of sorption experiments on micro- and nanoplastics for analytical detection methods. (1) Mixing and (2) incubation of the particles and TOrcs for a specified time in aqueous solution. (3) Separation of the particles and the aqueous phase. Preparation of either the aqueous phase or the particles, depending on the analytical technique. (4) Analysis is based on either a gas chromatographic method followed by high resolution/mass spectrometric (HR/MS), mass spectrometric (MS) or electron capture detection (ECD) analysis, or high performance liquid chromatography (HPLC) followed by MS/MS, MS, ultraviolet (UV), diode array detector (DAD) or fluorescence detector (FLD). Other analytical methods include liquid scintillation counter and spectrophotometer. (Adapted from Reichel et al., 2021 (Appendix I))

1.2.2.1 GC/MS analysis

The most established method for the analysis of volatile substances sorbed onto plastic particles is GC/MS analysis [16, 21, 70, 79]. By means of GC/MS analysis the aqueous, particulate, and gas phases can be examined regarding sorbed TOrCs [21, 52, 74]. GC/MS analysis of sorbed substances can usually be performed in a time-saving and automated manner after sample preparation (2-3 h / sample). Coupling to an MS allows target and non-target analyses of the sorbed substances [21, 80].

Further developments of the pyrolysis process allow not only an analysis of the polymer, but also an identification of possible additives or sorbed substances. Processes for this purpose include sequential pyrolysis, double-shot pyrolysis, thermogravimetric analysis (TGA), solvent extraction, or a thermodesorption (TD) unit coupled with pyrolysis [41, 42, 65, 81]. A detailed description of the methods is discussed in the review by Reichel et al. (2021) [80].

1.2.2.2 HPLC analysis

In contrast to GC/MS, high performance liquid chromatography (HPLC) analysis cannot be used to analyze sorbed TOrCs directly from the particle [82-84]. After separation of the particles by for instance filtration, the supernatant can be analyzed. Other methods include solvent extractions of the sorbed TOrCs from the particles or solid phase extraction. HPLC is coupled with an ultraviolet (UV) detector, a diode array detector (DAD), a fluorescence detector (FD), or a mass spectrometer [73, 82, 85, 86]. An overview of studies performed with HPLC is provided in Table 3.

Table 3: Summary of GC/MS and HPLC methods for the analysis of sorbed TORCs on plastic particles adapted from Reichel et al., 2021 [80] (Appendix I)

Particle Type	Particle Size (μm)	Sorbate	Analytical Method	Analyzed Phase	Reference
PE	260	Phenanthrene, Tonalide, Benzophenone	GC/MS after extraction with cyclohexane	Particle (Extraction)	[21]
PE, PS	PE: 260, PS: 250	Atrazine, Benzotriazole, Caffeine, Carbamazepine, Carbendazim, DEET, Diazinon, Diclofenac, Ibuprofen, MCPA, Mecoprop, 4-Nonylphenol, Phenanthrene, Propiconazole, Tris(2-chloroisopropyl)-phosphate (TCPP), Tebuconazole, Terbutryn, Torasemide, Triclosan	GC/MS, LC-MS/MS after extraction with cyclohexane	Particle (Extraction)	[70]
PA, PE, PVC, PS	<250	n-Hexane, Cyclohexane, Benzene, Toluene, Chlorobenzene, Ethylbenzoate, Naphtalene	Headspace GC/MS or in-tube-microextraction	Gaseous phase	[20]
PS (aged)	125 – 250	Various aliphatics and aromatics	GC/MS headspace from three-phase system	Gaseous phase	[87]
PE, PS, Fullerene, Sediment	PE: 10-180 PS: 0.07	17 Polychlorinated biphenyls (PCBs)	GC/MS after extraction with pentane-dichloromethane	Aqueous phase via passive sampler	[16]
PE, PP, PS	320 – 440	8 Polycyclic aromatic hydrocarbons (PAHs), 4 Hexachlorocyclohexanes (HCHs), 2 Chlorinated benzenes (CBs)	GC-ECD after extraction with n-hexane	Aqueous phase and PDMS phase	[52]
PP	450 – 850	Tonalide, Musk xylene, Musk ketone	GC/MS after extraction with n-hexane and dichloromethane	Particle (extraction)	[79]
PS, PE, PET	PE: 3-16 PS: 10 PET: < 300	38 PCB congeners	GC-HRMS after soxhlet extraction with dichloromethane	Particle (extraction)	[88]

PE, PP (environmental samples)	< 500	PCBs (IUPAC nos. 28, 52, 101, 118, 138, 153, 180)	GC-ECD after soxhlet extraction with dichloromethane	Particle (extraction)	[89]
PS	2; 1; 0.1	Eighteen unsubstituted hydrophobic organic chemicals (HOCs)	GC/MS after liquid / liquid extraction	Aqueous phase via passive sampler	[76]
PE, PS, PVC	< 150	Five polyhalogenated carbazoles (PHCs)	GC/MS after washing with n- hexane and dichloromethane	Particle (extraction)	[74]
PE, PP, PS	100 – 150	9-Nitroanthracene	GC/MS after liquid/liquid extraction	Aqueous phase	[66]
PP	450-850	3,6-Dibromocarbazole and 1,3,6,8- Tetrabromocarbazole	GC/MS after extraction with n- hexane and dichloromethane	Particle (extraction)	[75]
PS, PE, PMMA	PS: 40, 41, 0.078 PMMA: 48 PE: 48	Phenanthrene, Triclosan, α -Cypermethrin	TD-Pyr-GC/MS	Particle (directly)	[65]
PS	0.5, 0.235, 0.80, 30, 50, 102, 170	Phenanthrene, Nitrobenzene	HPLC	Supernatant	[23]
PE, PP, PS, PVC	< 200	Tylosin	HPLC+DAD	Supernatant	[82]
PA, PE, PET, PS, PVC, PP	100, 150	Sulfamethoxazole	HPLC	Supernatant	[90]
PBAT, PE, PS	PBAT: 2338 \pm 486, PE: 2628 \pm 623 / Reference Particles: PE: 400 PS: 250	Phenanthrene	HPLC-UV	Supernatant	[73]

PE, PS, soil	PE: 225 ± 41 PS: 313 ± 48	Triclosan	HPLC+UV	Methanol extraction of the particles	[91]
PE, PS, PP, PA, PVC	75 – 180	Sulfadiazine, Amoxicillin, Tetracycline, Ciprofloxacin, Trimethoprim	HPLC+UV	Supernatant	[92]
PS	75.4, 106.9, 150.5, 214.6	Triclosan	HPLC+UV	Supernatant	[60]
PS	0.07	Phenanthrene, Anthracene, Fluoranthene, Pyrene, Benzo[a]anthracene, Chrysene, Benzo[b]fluoranthene, Benzo[k]fluoranthene, Benzo[a]pyrene, Benzo[g,h,i] perylene	HPLC+FD	Extraction via Polyoxymethylene sheets	[86]
PS (aged)	50.4 ± 11.9	Atorvastatin, Amlodipine	HPLC+UV	Supernatant	[93]
PET	< 150	4-Chlorophenol, 2,4,6-Trichlorophenol, Fulvic acid	HPLC+UV	Supernatant	[94]
PP (aged)	< 180	Triclosan	HPLC+UV	Supernatant	[95]
PP, LD-PE, HD- PE, PVC	63 – 125	Enrofloxacin, Ciprofloxacin, Norfloxacin, 5- Fluorouracil, Methotrexate, Flubendazole, Fenbendazole, Propranolol, Nadolol	HPLC+DAD	Supernatant	[96]
PS (weathered)	139 – 207	4-Hydroxybenzophenone, Benzophenone-1, ethylhexyl methoxycinnamate, Octocrylene	UHPLC-MS/MS	Supernatant	[97]
PVC, PLA	PLA: 250 - 550 PVC: 75-150	Tetracycline, Ciprofloxacin	HPLC	Supernatant	[98]
nano-PS, carboxyl- functionalized polystyrene nano-PS-COOH	Nano-PS: 0.05 Nano-PS- COOH: 0.055	Norfloxacin, Levofloxacin	HPLC+FD	Supernatant	[99]
PE, PS, PP	< 280	Tetracycline	HPLC-FD	Supernatant	[67]
PE	250 – 280	Carbamazepine, 4- methylbenzylidene camphor, Triclosan, 17α- ethinyl estradiol	HPLC-PAD (Solid phase extraction)	Supernatant	[100]
PE	150	Sulfamethoxazole	HPLC+UV	Supernatant	[101]

2 Research significance, goals and hypotheses

Micro- and nanoplastics are considered wide spread contaminants in the environment. However, current analytical methods are mainly designed for a size range from 1 μm to 5 mm. Analytical methods are still lacking, especially in the sub- μ particle range (50 nm - 100 μm), to identify sorbed substances and polymer types. The aim of this dissertation within the BMBF funded project 'Subtrack' was to develop a suitable method for the thermal extraction/desorption pyrolysis-GC/MS (TD-Pyr-GC/MS) in order to allow the identification of sorbed substances and the identification of polymer types in one analytical step. In addition, sorption processes of selected trace substances, e.g. pesticides, were investigated on different reference (sub)-microparticles as well as on real polymer samples. So far, either the sorbed TOrcs on the particles or the concentration of TOrcs in the aqueous phase have been studied. A mass balance of both phases was missing so far and is presented in this work. The aim is to investigate the sorption processes of sorbed TOrc in both phases. In collaboration with project partners, it was also possible to apply the developed TD-Pyr-GC/MS method for real ecotoxicological samples. To achieve these goals, three main topics were set for the thesis:

1. The development of a reproducible method for sorbed trace compounds on micro- and nanoplastic particles using TD-Pyr-GC/MS. The author hypothesized that *by coupling thermodesorption and pyrolysis GC/MS (TD-Pyr-GC/MS) trace substances on reference micro- and nanoplastic particles can be quantified and polymer types can be identified in one single analytical step.*
2. The application of the developed method to analyze sorption processes and different trace substance concentration on micro- and nanoplastic particles. In addition, the influence of various types of polymers on sorption is considered. The author hypothesized that *the ad- and absorption behavior depends on the particle size, particle type, mixture of trace substances and organic matter and pH of the aqueous phase.*
3. Application of the developed TD-Pyr-GC/MS method for ecotoxicological samples. The author hypothesized that *sublethal and lethal effects of particles in in vitro and in vivo assays depends on particle type and size.*

Figure 2 summarize the research hypotheses and research tasks for analysis, applications and publications.

Chapter	Objective	Research Task	Hypothesis	Publication
4	Development of a method for the analysis of trace organic substances and polymers in one analytical set-up (TD-Pyr-GC/MS).	System optimizations	#1: By coupling thermodesorption and pyrolysis-GC/MS (TD-Pyr-GC/MS) trace substances on reference micro- and nanoplastic particles can be quantified and polymer types can be identified in one single analytical step.	Reichel et al., 2020: Systematic development of a Simultaneous Determination of Plastic Particle Identity and Adsorbed Organic Compounds by TD-Pyr-GC/MS. <i>Molecules</i> 2020, 25, 4985
		Temperature optimization (GC/MS)		
5	Investigation of sorption processes as a function of time, trace organic substance concentrations and mixtures of trace substances via TD-Pyr-GC/MS.	Comprehensive analysis of the aqueous (TD-GC/MS) and the particulate phase (TD-Pyr-GC/MS)	#2: Ad- and Absorption behavior on reference particles depends on a) Particle size and shape → the smaller the particle, the larger the relative surface, the higher the adsorption rate b) Particle type c) Mixture of trace substances → competition between substances depending on their structure (e.g. p-systems) and hydrophobicity d) Aging of particles	Reichel et al., 2022: A Novel Analytical Approach to Assessing Sorption of Trace Organic Compounds into Micro- and Nanoplastic Particles. <i>Biomolecules</i> 2022, 12, 953
		Preliminary tests for quantitative analysis of sorbed trace substances		
	Influence of various sample preparation methods on different polymers (TD-Pyr-GC/MS)	Characterization of the polymers before and after the sample preparation methods		Co-Author: Al-Azzawi et al., 2020: Validation of Sample Preparation Methods for Microplastic Analysis in Wastewater Matrices – Reproducibility and Standardization. <i>Water</i> 2020, 12, 2445
6	Influence of the trace substance phenanthrene on gammarids (<i>G. roeselii</i>) in the presence of microplastics and natural sediments.	Quantitative analysis of the aqueous phase via TD-GC/MS	#3: Sublethal (e.g., behavior of aquatic organism, changes in biomarkers) and lethal effects of particles in <i>in vitro</i> and <i>in vivo</i> assays depend on particle type (plastic or silica) and size → Ad-, Ab- and Desorption behavior of trace substances determine effects by influencing e.g. bioavailability of trace substances	Co-Author: Bartonitz et al., 2020: Modulation of PAH toxicity on the freshwater organism <i>G. roeselii</i> by microplastic. <i>Environmental Pollution</i> 2020, 260, 113999

Reichel et al., 2021: Organic Contaminants and Interactions with Micro- and Nano-Plastics in the Aqueous Environment: Review of Analytical Methods. *Molecules* 2021, 26, 1164

Figure 2: Comprehensive overview of research hypotheses, research tasks, and publications of this dissertation

Paper I: “Organic Contaminants and Interactions with Micro- and Nano-Plastics in the Aqueous Environment: Review of Analytical Methods” (Reichel et al., 2021, *Molecules*, 26, 1164)

This article provides an overview of current analytical methods (gas chromatography, liquid chromatography and ultraviolet-visible spectroscopy) for identifying sorbed TOrcs on micro- and nanoplastic particles, which are addressed in chapters 4 and 5. It also discusses the influences on sorption, such as polymer properties, particle sizes, and age of the polymers. The paper is presented in APPENDIX I.

Paper II: “Systematic development of a Simultaneous Determination of Plastic Particle Identity and Adsorbed Organic Compounds by Thermodesorption-Pyrolysis GC/MS (TD-Pyr-GC/MS)” (Reichel et al., 2020, *Molecules*, 25, 4985)

This research paper is presented as chapter 4, which addresses the development of a new method for the analysis of sorbed TOrcs on plastic particles in one analytical setup. In this context, identification of both TOrcs and polymers is possible with TD-Pyr-GC/MS. The focus of this study is on the development and validation of the method. For this purpose, defined micro- and nanoplastic particles and selected TOrcs are used. The paper is presented in APPENDIX II.

Paper III: “A Novel Analytical Approach Assessing Sorption of Trace Organic Compounds into Micro- and Nanoplastic Particles” (Reichel et al., 2022, *Biomolecules*, 12, 953)

In this study, the sorption processes of selected TOrcs and micro- or nanoplastic particles in aqueous solution were investigated. The TOrcs content in the aqueous phase (TD-GC/MS) as well as of the particles were determined. It was shown that quantification of the TOrcs content of nanoplastic particles by TD-Pyr-GC/MS is possible. The topic is presented as chapter 5 of this dissertation thesis. The paper is presented in APPENDIX III.

Paper IV (Co-author): “Validation of Sample Preparation Methods for Microplastic Analysis in Wastewater Matrices – Reproducibility and Standardization” (Al-Azzawi et al., 2020, *Water*, 12, 2445)

During experiments, TD-Pyr-GC/MS was employed to investigate the influence of treatment of various micoplastic polymers of Fenton reagent and H₂O₂ based on the resulting chromatograms and pyrograms. These were compared with those of untreated microplastics. The treatment served an age simulation experiment and is presented in chapter 5. The paper is attached as APPENDIX IV.

Paper V (Co-author): “Modulation of PAH toxicity on the freshwater organism *G. roeseli* by microplastic” (Bartonitz et al., 2020, *Environmental Pollution*, 360, 113999)

In this study, quantitative determination of TOC phenanthrene was performed by TD-GC/MS in the aqueous phase. In combination with ecotoxicological experiments using the organism *G. roeseli*, conclusions could be drawn on the toxicity of microplastics in the presence of phenanthrene. This topic is presented as chapter 6 and the paper is attached as APPENDIX V.

3 State-of-the-art of analytical methods

Depending on the particle size and type, different analytical methods are available to analyse the particles themselves and the TOrcs sorbed onto the particles. [80]. Optical analysis methods such as Raman spectroscopy or FTIR can be used to analyse the particles quantitatively and to analyse the particle size and shape [102, 103]. However, both methods are limited in size [24, 29, 104, 105]. Thermal analysis methods such as pyrolysis gas chromatography-mass spectrometry (Pyr-GC/MS) can be used to analyse TOrcs or additives in polymers [106, 107]. The analysis of TOrcs sorbed to particles in a liquid phase can be performed either via the aqueous phase, the gas phase or on the particles [20, 21, 66]. Various techniques such as GC/MS, HPLC-DAD, UHPLC-MS/MS or UV spectrometer are commonly used for this purpose [67, 68, 108]. The sample preparation for the investigation of sorption kinetics, properties or processes is the same in most cases [80]: Selected micro- or nanoplastic particles are incubated with defined TOrcs for a certain period of time. Subsequently, the aqueous phase is separated from the particle phase. The final analysis of the sorbed TOrcs can be performed either on the filtrate or on the particles.

3 Material and Methods

3.1 Instrumental Systems

Within the scope of this work, the combined TD-Pyr-GC/MS or the TD-GC/MS has been used for analyses. This is an instrument that can be modified to analyze either trace substances in the aqueous phase using a Gerstel Twister (TD-GC/MS) or trace substances and polymers (TD-Pyr-GC/MS). The process of a TD-Pyr-GC/MS measurement is shown in Figure 3.

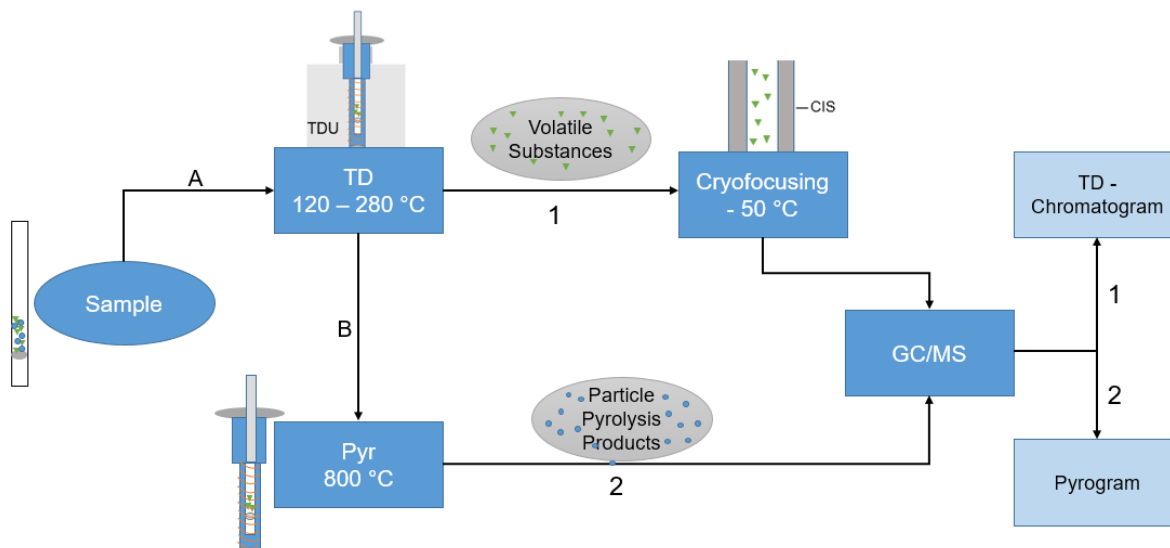


Figure 3: Flowchart of the TD-Pyr-GC/MS analysis. First, (A) the sample is thermodesorbed (120 – 280 °C), thereby desorbing the volatile substances and cryofocusing them in the Cooled Injections System (CIS) at -50 °C. This is followed by a transfer to the GC column with an MS analysis (TD-GC/MS). The same sample (B) is subsequently pyrolyzed at 800 °C, followed by a GC/MS analysis (Pyr-GC/MS). The evaluations are carried out using the TD-Chromatogram and the Pyrogram. Adopted from Reichel et al., 2020 [65].

3.1.1 TD-GC/MS

The TD-GC/MS consists of a Gerstel Thermal Desorption Unit (TDU) 2, a Cooled Injections System (CIS) 4 with Controller C506, and an Agilent 7890B gas chromatograph equipped with a DB-5MS Ultra Inert column coupled with an electron ion source to an Agilent 5977B MSD mass spectrometer. TD-GC/MS is used in combination with the stir bar sorptive extraction (SBSE) method to determine TORCs concentrations in aqueous matrices. The SBSE materials used are Gerstel Twister® (Gerstel GmbH & Co. KG, Mühlheim an der Ruhr, Germany) and SorbStars (Mercury Instruments GmbH, Vohenstrauß, Germany).

3.1.2 TD-Pyr-GC/MS

The setup of the combined TD-Pyr-GC/MS is basically the same as the TD-GC/MS. A pyrolysis module was integrated into the Gerstel TDU 2 (Figure 4). With the Gerstel MPS robotic^{pro} the particle samples are directly transferred into the pyrolysis unit. The setup of the further steps of analysis is the same as for TD-GC/MS. A pre-programmed temperature protocol (see chapter 4) is executed to evaporate the volatile substances during an initial step. The volatile substances are trapped in the CIS and then applied to the GC column while increasing the temperature. The sample is now subjected to pyrolysis and the pyrolysis products are analyzed. The detailed method parameters and the MS parameters are described in Appendix II.

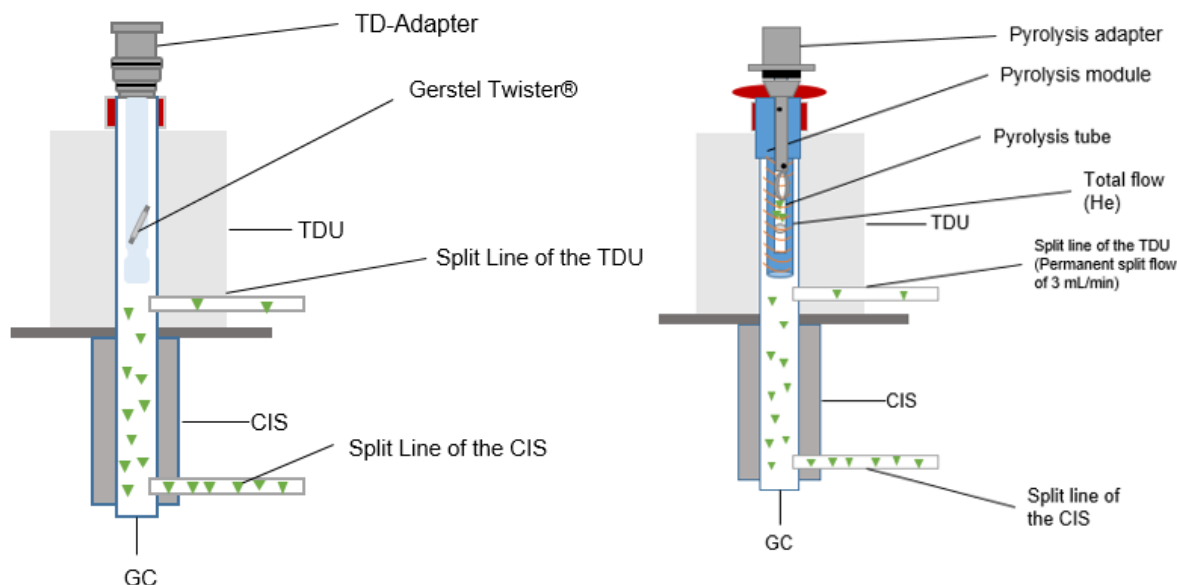


Figure 4: Left: structure of the TD-GC/MS (analysis via Gerstel Twister®), right: structure of the coupled TD-GC/MS + Pyr-GC/MS, adapted from Reichel et al., 2020 (Appendix II)

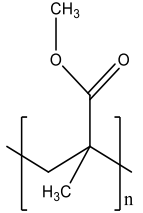
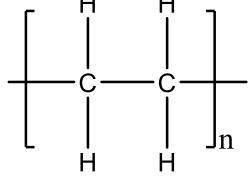
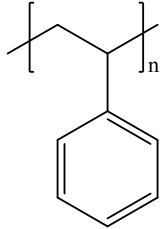
3.2 Chemicals

3.2.1 Selection of particles

All reference particles employed were additive-free. The polystyrene (PS), polymethyl methacrylate (PMMA) and polyethylene (PE) particles were provided by BS Partikel GmbH (Mainz, Germany). An overview of the polymers and sizes used is shown below in Table 4.

According to the manufacturer BS-Partikel GmbH one drop of particle-ethanol suspension has a volume of 20 μL . In preliminary tests, the dry mass of one drop was determined for PS 41 μm and PS 78 nm for further adsorption experiments (Table 5).

Table 4: Investigated polymer types, structural formula, log D and sizes

Polymer	Mean Particle size [μm]	Structural formula	Log D (pH 7)	Storage	Number of particles per drop	Dry mass per drop [mg]	Number of drops for 10 mg
PMMA	48		1.62	Dry, technical grade powder			
PE	48		-0.30	Dry, technical grade powder			
PS	40		-0.2	Dry, technical grade powder			
	41		Suspended in EtOH	$1.3 \cdot 10^6$	1.15 ± 0.08	9	
	0.078		Suspended in EtOH	$1.9 \cdot 10^{14}$	1.37 ± 0.03	7	

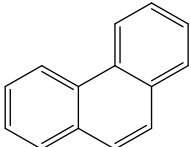
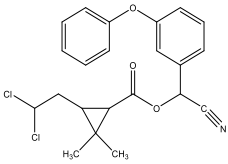
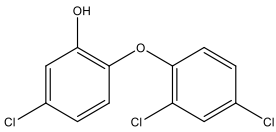
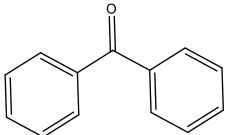
For the experiment in the Al-Azzawi et al (2020) paper, the following additional polymers were analyzed [109]: polyamide (PA), polyethylene terephthalate (PET), polylactide (PLA), and polypropylene (PP).

3.2.2 Selection of TOrCs

Six trace organic substances were selected considering their different structural formula, log D values, and environmental relevance (Table 5). They were chosen to represent a variety of sources and degrees of hydrophobicity.

For all TOrCs, standard solutions were prepared by dissolving the solid in methanol (MeOH), because they are poorly soluble in water [20]. The standard solutions and diluted standards were stored in the dark at 8 °C as suggested by Wang et al. (2019) [23]. The final MeOH content in the samples ranged from 0.1 to 3 % (v/v).

Table 5: Selected reference TOxCs

Substance class	Substance	Monoisotopic mass [g/mol]	Environmental relevance	Structural formula	Log D (pH 7)*	Van der Waals surface Area [\AA^2]*
Polycyclic aromatic hydrocarbons	Phenanthrene	178.08	High toxicity, mutagenic [110], typical waste water pollutant [21]		3.95	261
Pyrethroide	Cypermethrin	415.07	Used against pests [111], adverse effects in rats regarding fertility [112]		5.44	571
Polychlorinated phenoxyphenols	Triclosan	289.54	Added to personal care products due to its antiseptic property [113]		5.80	340
Others	Benzophenone	182.07	Component of sunscreens [114], typical wastewater pollutant [21]		3.43	270

3.2.3 Sample preparation of suspended micro- and nanoparticles

The sample preparation in this work can be divided into two main areas: particle analysis (TD-Pyr-GC/MS) and the analysis of an aqueous phase (TD-GC/MS).

Basically, sample preparation of the particulate samples always proceeds in the same way, regardless of whether trace substances are sorbed or not. Dry particles that were not previously in suspension were weighed and applied directly to the pyrolysis tubes. If the particles are in a suspension, they must be separated from the aqueous phase. For the separation of the particles, centrifugation as well as filtration were tested to identify the most suitable method.

Filtration

Filtration was performed using a vacuum filtration unit (Sartorius, Göttingen, Germany) and Nucleopore hydrophilic membrane filters with a pore size of 0.03 μm (Whatman / GE Healthcare, Marlborough, USA). This setup was used for filtration of all particle types and sizes. After separation of the particles and the aqueous phase, the particles were scraped off the filter using a spatula and placed in a vial and frozen at -8 °C in the refrigerator for a maximum of 4 h. The particles were then dried for 20 min in the freeze-dryer Alpha 1-2 LDplus (Christ, Osterode am Hartz, Germany).

Centrifugation

As part of the method optimization, the separation of the aqueous and particle phases by centrifugation was investigated as an alternative to filtration. Centrifugation was performed with a multi-application centrifuge (NuAir, Plymouth, USA). Centrifugation was tested with PE 48 μm , PS 40 μm and PMMA 48 μm microplastic particles in an aqueous suspension at 1 g/L. The samples were centrifuged between 0.5 and 12 h at 3,000 – 5,000 RCF.

Filtrate analysis – TD-GC/MS

There are two options for the filtrate (see Figure 5). Either the filtrate is discarded (2A) or the filtrate is analyzed for TOrcs concentrations (2B). The adsorption behavior of selected trace organic substances in aqueous media has been tested with Gerstel Twister® and SorbStars and analyzed via TD-GC/MS. Both methods are developed for extraction of non-polar compounds, i.e., the higher the log D value of the trace organic substance, the better it adsorbs and the higher the recovery rate will be. Since the Gerstel Twisters® are magnetic, it is possible to use the Gerstel Twister® as a magnetic stirrer. By stirring TOrcs are extracted by means of adsorption of the trace substances onto the polydimethylsiloxane (PDMS) coating [115, 116]. A Cimarec i Poly

15 stirrer 100 -240 V (Thermo Scientific, Waltham, USA) is used. By reconditioning the Gerstel Twister®, it is possible to use the Gerstel Twister® up to 50 times [114, 117]. The reconditioning is carried out in the Tube Conditioner TC2 (Gerstel GmbH, Mühlheim an der Ruhr, Germany). The procedure is independent of the GC/MS measurement, which excludes contaminations of the GC/MS system. SorbStars are disposable products that – in contrast to Gerstel Twisters® – are to be shaken for the adsorption of trace substances [26]. The SorbStars are intended as a replacement for the Gerstel Twister®, as these are disposable products that do not require reconditioning.

For the quantification of TOrCs, calibration curves were created for analysis with Gerstel Twister® and TD-GC/MS. For GC/MS an isotopically labeled reference was added as an internal mass spectrometric standard. Stock solutions of standards were produced in methanol. The final analysis volume for Gerstel Twister® analyses was always 10 mL. Gerstel Twisters® were added and stirred for 60 min at 1,000 rpm at room temperature. The Gerstel Twisters® were removed, washed with ultra-pure water (Arium® pro Ultrapure Water System, Sartorius, Göttingen, Germany) and dried with a lint-free tissue. Subsequently the stir bar was transferred into the thermodesorption tube for subsequent TD-GC/MS analysis.

Chemical analysis – TD-GC/MS

The Gerstel Twister® and TD-GC/MS analysis were adopted from Ochiai et al. (2005) [118]. However, the temperature for cryofocussing was set to -50 °C instead of -150 °C. Helium was used as carrier gas.

Particle analysis – TD-Pyr-GC/MS

The weight of 30 - 80 µg was checked with the Cubis® Ultramicro Balance (Sartorius, Göttingen, Germany) in triplicate determination. Thermodesorption and pyrolysis of polymers was prone to contamination. Therefore, sources of contamination such as the choice of pyrolysis tubes, the correct weighing, the pyrolysis adapters and the TD-Pyr-GC/MS itself were optimized in preliminary tests. A detailed description can be found in chapter 4.1.2. Also experiments to identify the appropriate thermodesorption temperature were carried out and are described in chapter 4.2.

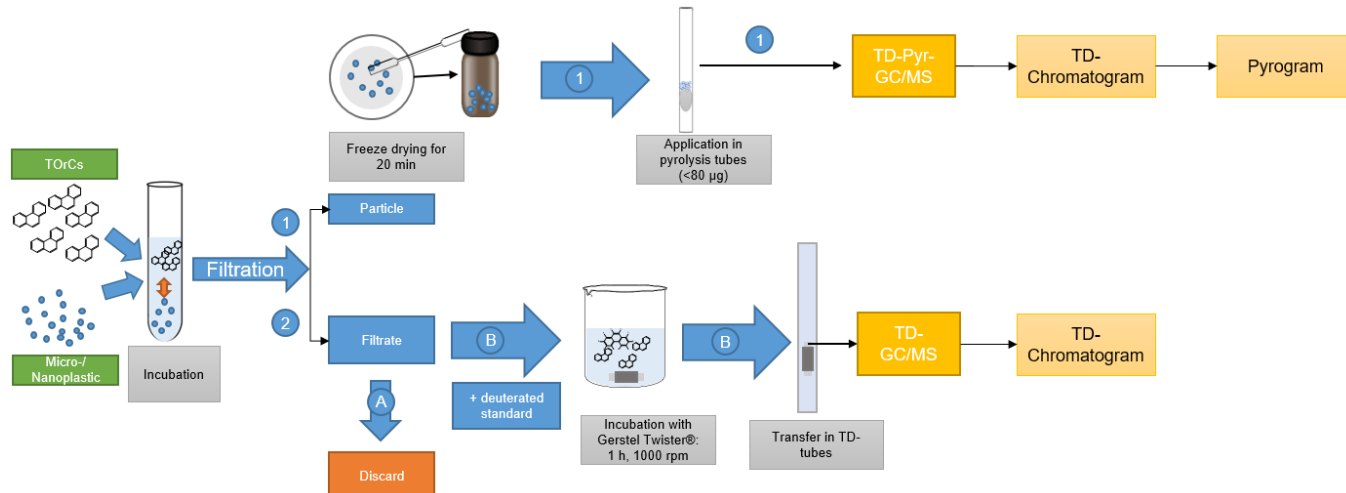


Figure 5: Incubation of the TOxCs and the polymers over a period of time. The particles (1) are scraped from the particle after filtration and freeze-dried. Then a maximum amount of $80 \mu\text{g}$ is weighed into a pyrolysis tube and analyzed via TD-Pyr-GC/MS. This is followed by an evaluation of the TOxCs via the TD chromatogram and the polymers via the pyrogram. The filtrate (2) is either discarded (A) or a deuterated standard is added for further analysis (B). The filtrate is then mixed with a Gerstel Twister® and stirred for 1 h and then placed in a thermodesorption (TD) tube. The analysis is performed via TD-GC/MS. The TOxC is evaluated via the TD chromatogram, adapted from Reichel et al, 2022 (Appendix III)

3.2.4 Verification of TOxCs via the Alkanes Calibration Standard

By using an alkane calibration standard, retention times (RT) can be normalized to obtain Kováts retention indices (RI). These are independent of the chromatographic method and can be used to identify a substance. The RI is calculated by interpolation between two adjacent alkanes eluting before and after the substance of interest. For temperature-programmed GC, the Kováts retention index was calculated as follows [119]:

$$I^T = 100 \left[\frac{t_{Ri}^T - t_{Rz}^T}{t_{R(z+1)}^T - t_{Rz}^T} + z \right]$$

- I^T : Kováts index
- t_R^T : retention time
- z : number of carbon atoms that elutes before the compound of interest
- i : compound itself

Rearranging the equation allowed calculation of the predicted retention time for a compound with a known RI. A calibration standard for C8 to C40 alkanes (Supelco / Merck, Darmstadt, Germany) was used to calculate the RI for phenanthrene, α -cypermethrin, and triclosan for TD-GC/MS

analysis. In addition, the RI for phenanthrene in Pyr-GC/MS analysis was calculated. The RI values obtained were then compared with the NIST database (Table 6).

Table 6: RI for phenanthrene, α -cypermethrin and triclosan calculated from the RT. RI from NIST database are shown as comparison

	TOrC	RI (calculated)	RI (NIST)
TD-GC/MS	phenanthrene	1,791	1,775±14
	α -cypermethrin 1	2,824	2,780±24
	α -cypermethrin 2	2,846	2,780±24
	Triclosan	2,104	2,214±N/A
Pyr-GC/MS	phenanthrene	1,810	1,775±14

Based on these data, the selected TOrCs could be identified using the alkane standard in combination with MS spectra and NIST data base.

3.2.5 Data evaluation of the TD-Pyr-GC/MS

Polymers

In the conducted experiments, the polymer types PS, PE and PMMA were mainly used for method development and sorption tests. Based on their respective characteristic substances, the polymers can be identified:

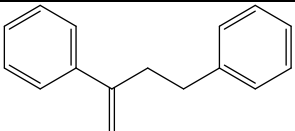
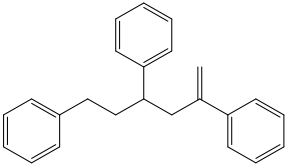

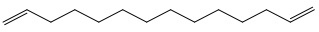
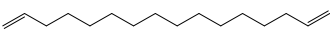
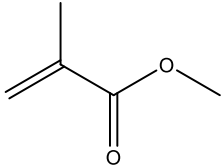
PS: Characteristic substances that can be used to identify PS are the styrene mono-, di- and trimer. However, the monomer is also found in environmental samples as it is also present in biogenic polymers such as chitin or wool fibers [29]. It is also found as a pyrolysis product in other polymers such as PVC and in the quartz wool used [120]. Depending on the radical initiator used in the production of PMMA, the pyrolysis of PMMA may also release the styrene monomer. Therefore, only the dimer and trimer serve as final indicator substances for PS samples (Table 7).

PE: Decomposition into small aliphatic chains (saturated, monounsaturated and diunsaturated hydrocarbons) is typical for PE [40, 121, 122]. Monounsaturated and saturated hydrocarbons also occur naturally in environmental matrices, as they result, for example, from the degradation of fatty acids and lipids [123]. Therefore, only the diunsaturated hydrocarbons are used for the identification of PE [26] (Table 7).

PMMA: The only pyrolysis product that could be reproducibly detected for PMMA was methyl methacrylate (Table 7). While a clearly defined peak is seen in the pyrogram of methyl

methacrylate, the peak in the thermodesorption is broad and elongated with several local maxima. This could indicate overloading of the GC column. Therefore, for the evaluation of PMMA over methyl methacrylate, only the peak in the pyrogram is considered.

Table 7: Characteristic pyrolysis fragments of selected polymers for identification

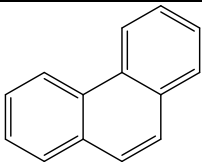
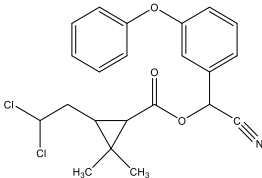
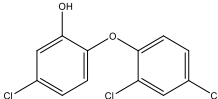
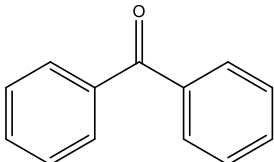
Polymer type	Characteristic pyrolysis fragments	Formula	Molecular weight [g/mol]	m/z (intensity ratio [%])*	Structure
PS	3-butene-1,3-diyldibenzene (styrene dimer)	C ₁₆ H ₁₆	208	91 (100), 104 (27), 130 (23), 208 (30)	
	5-hexene-1,3,5-triyltribenzene (styrene trimer)	C ₂₄ H ₂₄	312	91 (100), 117 (32), 194 (19), 207 (25)	
PE	1,12-tridecadiene	C ₁₃ H ₂₄	180	55 (52), 81 (44), 67 (38), 95 (26)	
	1,13-tetradecadiene	C ₁₄ H ₂₆	194	81 (42), 95 (27), 109 (13)	
	1,15-hexadecadiene	C ₁₆ H ₃₀	222	55 (63), 81 (50), 96 (45), 69 (37)	
PMMA	Methyl methacrylate	C ₅ H ₈ O ₂	100	41(77), 69 (100), 100 (57)	

* intensity ratio to largest peak in spectra

TOrCs

In the same way as the polymers, the TOrCs were determined on the basis of characteristic signals in the chromatograms (Table 8).

Table 8: Characteristic signals of selected TOrCs for identification

Substance	Characteristic signals [m/z]	Boiling point [°C] at 760 mmHg	Structure
Phenanthrene	178	337.4±9.0	
α-Cypermethrin	163, 184, 209	511.3 ±50	
Triclosan	290, 288, 218, 63	344.6±42.0	
Benzophenone	182		

The mass spectrometer was operated in full-scan mode (m/z range 40 to 550) with electron impact ionization (70V) for non-target analysis. For target analysis the TOrCs were measured with characteristic signals in SIM Mode. For phenanthrene, e.g., the m/z value was set to 178. Data analysis of the TD-Chromatogram was conducted with Mass Hunter Workstation Software (Ver.B.08.000, Agilent). The identification of the substances was ensured via the MS spectra and comparison with the NIST database, the RI and comparison with external standards.

Calibration curves were constructed using the respective TOrCs for quantification of TOrCs concentrations in the aqueous phase. In each case, a fixed internal deuterated standard was added as a control. The samples were also spiked with the internal standards in each case to avoid measurement fluctuations. For the evaluation, the peak area of the trace substance was divided by the peak area of the internal standard. All aqueous analyses via Gerstel Twister and TD-GC/MS were performed at least in duplicate.

For normalization of the data obtained by TD-Pyr-GC/MS analysis, the peak areas obtained after specific extraction were divided by the weighed weight of the sample.

4 Analysis – Coupling of thermodesorption- and pyrolysis-GC/MS in one analytical setup

Hypothesis #1: By coupling thermodesorption and pyrolysis-GC/MS trace substances on reference micro- and nanoplastic particles can be quantified and polymer types can be identified in one analytical setup

Established methods to analyze TOrCs on micro- and nanoplastic particles were based on extracting the TOrCs from the particles [21] with subsequent headspace analysis [20, 87] or using radioisotopic marked TOrCs [80, 108, 124]. The goal of this work was to develop an innovative application of thermodesorption-pyrolysis-gas chromatography/mass spectrometry (TD-Pyr-GC/MS) in order to enable identification of potentially sorbed pollutants, the type of polymer, and even additives in one analytical setup. For doing so, initially the trace substances were desorbed from the particles by thermodesorption and analyzed using GC/MS. Subsequently the polymers were decomposed by pyrolysis and the decomposition products and by this the type of polymer and contained additives were identified via GC/MS analysis. Thus, it was hypothesized that *by coupling thermodesorption and pyrolysis-GC/MS trace substances on reference micro- and nanoplastic particles can be quantified and polymer types can be identified in one analytical setup*. To test this hypothesis, three different polymer types (PE, PS and PMMA) and three TOrCs (phenanthrene, α -cypermethrin and triclosan) were selected. After detailed sample preparation development (e.g., filtration, freeze – drying and application into the pyrolysis tubes) of the micro- and nanoplastic particles, method development was performed for TD-Pyr-GC/MS. For this purpose, pure reference particles were measured to find an optimal thermal desorption method and to ensure reliable identification of the polymers. In the TD step, complete disintegration of the polymers does not yet take place. In the second step, the individual TOrCs were sorbed onto the particles and then analyzed by TD-Pyr-GC/MS. The process steps of a sample preparation including measurement are illustrated in Figure 6.

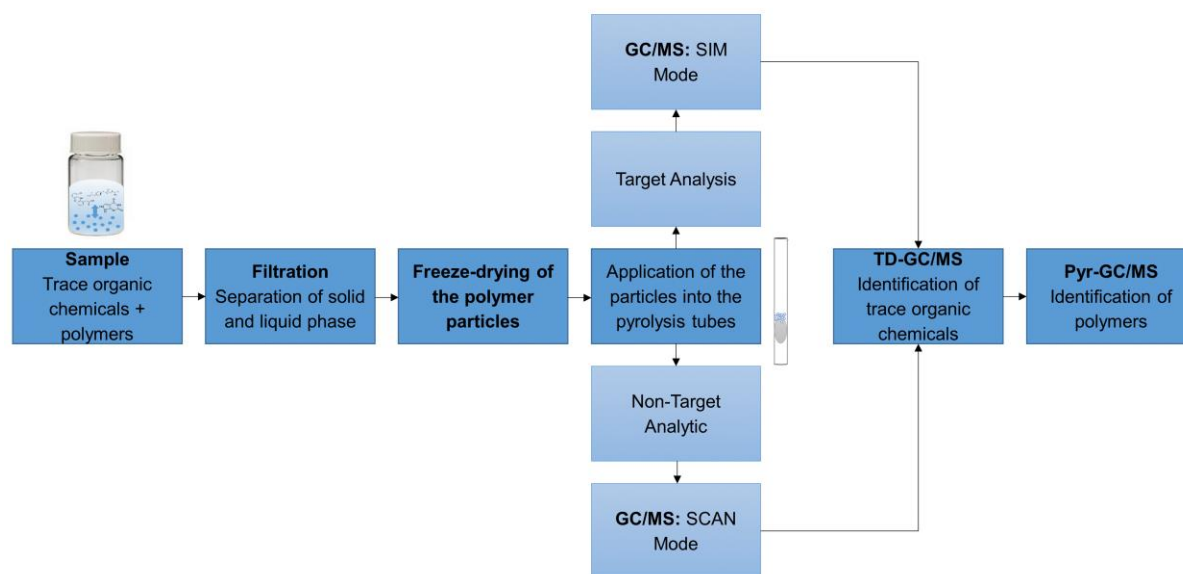


Figure 6: Sample analysis procedure: Filtration of the sample to separate particles and aqueous phase. Subsequent application of the particles into the pyrolysis tubes. Depending on the test setup, a non-target analysis (SCAN mode) or a target analysis (SIM mode) can be performed. Finally, a TD-Pyr-GC/MS analysis is performed. Adapted from Reichel et al., 2020 (Appendix II)

4.1 Sample preparation, method development and validation for a TD-Pyr-GC/MS method

4.1.1 Rationale

Micro- and submicro- and nanoplastics may potentially not only be harmful by themselves but also serve as vectors due to ad- or absorbed contaminants. Analysis of these sorbed contaminants is challenging and requires several analytical steps [4, 20, 21, 70]. Particles in an aqueous solution must be separated from the liquid phase by e.g., centrifugation or filtration [23, 65]. After separation of the two phases, the TOrcs can now be determined indirectly via the aqueous phase using liquid/liquid extraction or a passive sampler [52, 76, 77]. An analysis of the gas phase can also be performed [52, 87]. An analysis of the sorbed TOrcs from the particles can be achieved via solvent extraction (e.g., n-hexane, dichloromethane) [21, 74, 75]. Another method is the direct analysis of TOrcs from the particle without further preparation or extraction steps using TD-Pyr-GC/MS. This allows identification or quantification of the TOrcs and determination of the polymer type in one analytical setup. The final analysis is performed by GC/MS or GC/ECD [4, 65].

Table 9 summarizes various studies and their analytical methods that have investigated the sorption of TOrCs onto micro- and nanoplastics. An overview of further analytical methods is given in the review article by Reichel et al. (2021).

There are methods that have been developed specifically for polymer analysis, such as thermal extraction-desorption gas chromatography-mass spectrometry (TED-GC/MS), analytical double-shot pyrolysis and sequential pyrolysis. These methods have also shown that the detection of additives and the identification of polymers is possible with one analytical setup [41, 42, 81, 125].

Analysis – Coupling of thermodesorption- and pyrolysis-GC/MS in one analytical setup

Table 9: Summary of GC/MS-methods to analyze sorbed substances on various microplastic particles like polyethylene (PE), polystyrene (PS), polyamide (PA), polyvinyl chloride (PVC), polypropylene (PP), polyethylene terephthalate (PET) and polymethyl methacrylate (PMMA), adopted from Reichel et al., 2021

Particle Type	Particle Size (µm)	Sorbate	Analytical Method	Analyzed Phase	Reference
PE	260	Phenanthrene, Tonalide, Benzophenone	GC/MS after extraction with cyclohexane	Particle (Extraction)	[13]
PE, PS	PE: 260, PS: 250	Atrazine, Benzotriazole, Caffeine, Carbamazepine, Carbendazim, DEET, Diazinon, Diclofenac, Ibuprofen, MCPA, Mecoprop, 4-Nonylphenol, Phenanthrene, Propiconazole, Tris(2-chloroisopropyl)-phosphate (TCPP), Tebuconazole, Terbutryn, Torasemide, Triclosan	GC/MS, LC-MS/MS after extraction with cyclohexane	Particle (Extraction)	[26]
PA, PE, PVC, PS	<250	n-Hexane, Cyclohexane, Benzene, Toluene, Chlorobenzene, Ethylbenzoate, Naphtalene	Headspace GC/MS or in-tube-microextraction	Gaseous phase	[5]
PS (aged)	125–250	Various aliphatics and aromatics	GC/MS headspace from three-phase system	Gaseous phase	[44]
PE, PS, Fullerene, Sediment	PE: 10–180 PS: 0.07	17 Polychlorinated biphenyls (PCBs)	GC/MS after extraction with pentane-dichloromethane	Aqueous phase via passive sampler	[45]
PE, PP, PS	320–440	8 Polycyclic aromatic hydrocarbons (PAHs), 4 Hexachlorocyclohexanes (HCHs), 2 Chlorinated benzenes (CBs)	GC-ECD after extraction with n-hexane	Aqueous phase and PDMS phase	[4]

Analysis – Coupling of thermodesorption- and pyrolysis-GC/MS in one analytical setup

PP	450–850	Tonalide, Musk xylene, Musk ketone	GC/MS after extraction with n-hexane and dichloromethane	Particle (extraction)	[46]
	PE: 3–16				
PS, PE, PET	PS:10 PET: <300	38 PCB congeners	GC-HRMS after soxhlet extraction with dichloromethane	Particle (extraction)	[65]
PE, PP (environmental samples)	<500	PCBs (IUPAC nos. 28, 52, 101, 118, 138, 153, 180)	GC-ECD after soxhlet extraction with dichloromethane	Particle (extraction)	[66]
PS	2; 1; 0.1	Eighteen unsubstituted hydrophobic organic chemicals (HOCs)	GC/MS after liquid / liquid extraction	Aqueous phase via passive sampler	[41]
PE, PS, PVC	<150	Five polyhalogenated carbazoles (PHCs)	GC/MS after washing with n-hexane and dichloromethane	Particle (extraction)	[39]
PE, PP, PS	100–150	9-Nitroanthracene	GC/MS after liquid/liquid extraction	Aqueous phase	[21]
PP	450–850	3,6-Dibromocarbazole and 1,3,6,8- Tetrabromocarbazole	GC/MS after extraction with n-hexane and dichloromethane	Particle (extraction)	[40]

PS, PE, PMMA	PS: 40, 41, 0.078 PMMA: 48 PE: 48	Phenanthrene, Triclosan, α -Cypermethrin	TD-Pyr-GC/MS	Particle (directly)	[20]
--------------	--	---	--------------	------------------------	------

4.1.2 Experimental Section

Prior to actual method development on the TD-Pyr GC/MS instrument (Figure 7d), optimizations had to be made on the choice of pyrolysis tubes (Figure 7a), particle application and weighing (Figure 7b), and cleaning of the transport adapters (Figure 7d), to minimize contamination and carryover. The detailed steps of those optimizations are described in chapter 4.2. In the following the final method parameters are presented.

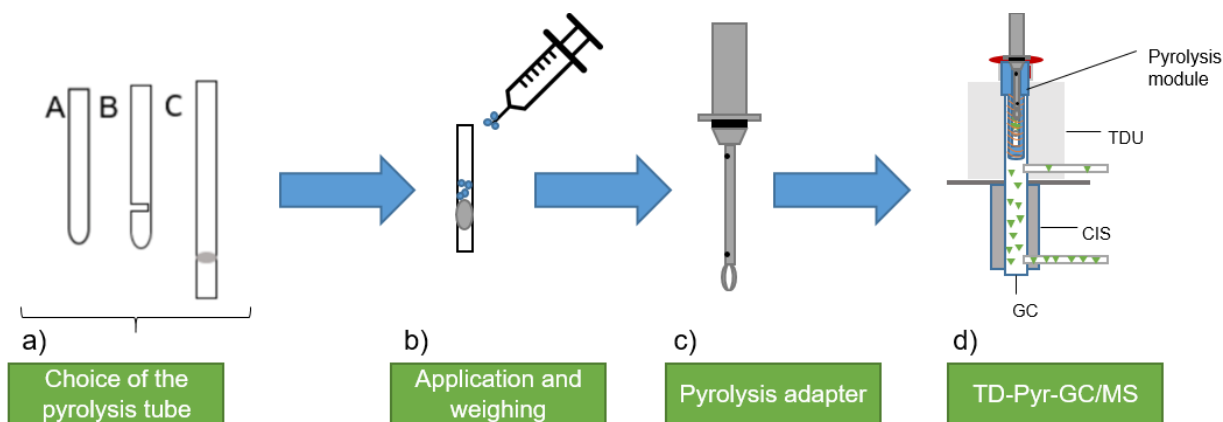


Figure 7: Steps to develop an optimized method: a) pyrolysis tubes, b) application of particles into pyrolysis tubes and weighing, c) pyrolysis adapter d) during analysis in TD-Pyr-GC/MS.

a) Choice of the pyrolysis tube

One of the first tasks was to determine the most suitable type of pyrolysis tube for application and analysis of polymer particles, Figure 1. Three different pyrolysis tubes were tested. The weight of the pyrolysis tubes ranged from 90 to 110 mg. All were made of quartz glass and were purchased from Gerstel GmbH (Mühlheim an der Ruhr, Germany). The design of the pyrolysis tube is an essential aspect regarding possible carryover [126] as well as accurate analysis. Therefore, the following tube types were tested (Figure 7a): pyrolysis tubes (A) with one open and one closed end with a length of 17 mm, (B) with one open and one closed end with an additional slot of 17 mm length and (C) with two open ends and a length of 25 mm sealed with quartz wool. Quartz wool is thus used only in type (C) and is in contact with the sample. After application of the quartz wool into the pyrolysis tubes, it was heated at 100 °C for 30 min to remove possible contamination.

b) Application and weighing of micro- sub μ - and nanoparticles

In order to measure the particles with TD-Pyr-GC/MS, they have to be applied into pyrolysis tubes. For the development of the appropriate TD method, the dry particles were applied without filtration; for all sorption experiments in aqueous suspension, the particles were filtered out. For this purpose, the particles are scraped off the filters after filtration and applied to a glass vial.

Since moist particles are easier to handle than dry ones, in the first preliminary tests the particles were weighed directly into the prepared pyrolysis tubes (type C) after filtration and freeze-dried. For the final method, the particles were first freeze-dried for 15 min and either applied directly into the pyrolysis tubes or stored for a maximum of 24 h in the refrigerator at 4 °C. Subsequently, the particles are weighed into the baked pyrolysis tubes. Flattened cannula tips are used for transfer into the pyrolysis tubes (Figure 7b). By using an ultra-fine balance, it is ensured that between 20 and 80 µg of particles are weighed to avoid overloading of the GC/MS system. Each sample is weighed three times and the mean value is then taken. Each sample is also run at least in duplicate.

c) Pyrolysis adapters

During preliminary tests, the pyrolysis adapters turn out to be a source of polymer contamination. Therefore, a cleaning protocol was established, which was carried out with the adapters after each measurement. For this, the lower part of each adapter was submerged in 0.5 mL dichloromethane in a glass vial and placed in an ultrasonic bath for 15 min. The adapters were then rinsed with ultra-pure water and dried at 100 °C for 15 min.

d) TD-Pyr-GC/MS – Temperature optimization

The aim of this study is to develop an innovative analytical method of combined thermodesorption and pyrolysis gas chromatography/mass spectrometry (TD-GC/MS + Pyr-GC/MS) to enable the identification of sorbed TOrCs and polymer type in a single analytical setup. In the first step, the TOrCs are desorbed from the particles by thermodesorption and analyzed by GC/MS. In the second step, the polymers are decomposed by pyrolysis and the characteristic decomposition products and thus the type of polymer and additives contained are identified by GC/MS analysis. The analytical procedure is visualized in Figure 8. In order to find a suitable thermodesorption temperature, three different temperatures were selected: 120 / 200 / 280°C. For the temperature optimization, preliminary tests were first performed without sorbed TOrCs. The aim is that the thermodesorption temperature is high enough to desorb the volatile substances. At the same time, however, the temperature must be low enough to prevent degradation of the polymers. These are analyzed in the second pyrolysis step. The detailed method development is described in the article Reichel et al. (2020) (Appendix II).

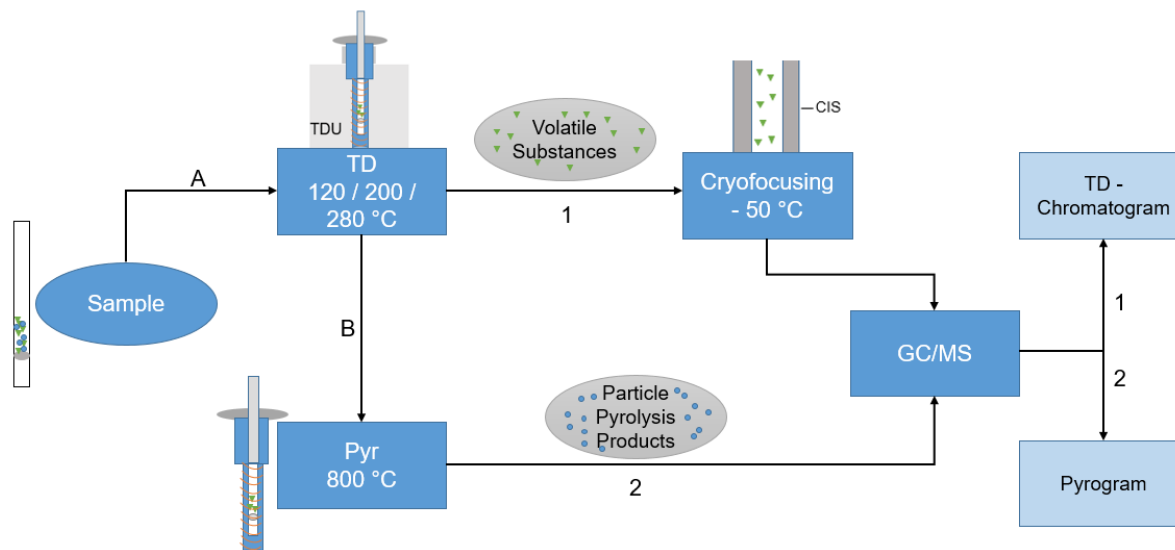


Figure 8: Flowchart of a TD-Pyr-GC/MS analysis. The sample (A) is thermodesorbed (120 / 200 / 280 °C) to desorb the volatile TOrcs. The substances are cryofocused in the Cooled Injection System (CIS) at -50 °C. The analysis is performed by GC/MS (TD-GC/MS). The same sample (B) is pyrolyzed at 800 °C and analyzed by GC/MS (Pyr-GC/MS). The evaluations are performed with the TD chromatogram and the pyrogram. Adapted from Reichel et al., 2020 (Appendix II)

TD-GC/MS: In the first step of thermal desorption (TD-GC/MS), samples are heated to a pre-programmed temperature to desorb the volatile substances. The optimal TD temperature was determined during method development and set at 200 °C [65].

Pyr-GC/MS: In the second step, pyrolysis (Pyr-GC/MS) is performed to pyrolyze all substances. Sufficient depolymerization of all tested micro- and nanoplastic particles was achieved with a temperature of 320 °C. Contamination can be avoided with this temperature selection.

Preliminary sorption experiments

Sample preparation of Micro- and Nanoparticles

The samples were analyzed by TD-Pyr-GC/MS (Figure 8). The subsequent sorption experiments with the TOrcs phenanthrene, α -cypermethrin and triclosan were performed analogously. The particle concentration was kept constant at 1 g/L, and the trace substance concentration was varied between 100 μ g/L and 1,000 μ g/L. The stock solution of all trace compounds was prepared at a concentration of 1,000 mg/L in methanol (MeOH) and diluted in MeOH in further dilution steps. The experiments for the SCAN and SIM mode measurements were performed on PS 78 nm particles. All experiments were performed in triplicate on two different days, i.e., a total of six replicates.

In another preliminary test for sorption analysis, two TOrCs (benzophenone and phenanthrene) were used without particles. Therefore, calibration solutions with different concentrations of benzophenone and phenanthrene, respectively, were prepared and analyzed by TD-Pyr-GC/MS using the pyrolysis quartz tubes. 10 mL of the respective TOrC solution was added to a closed glass test tube. The solution was shaken for 1 h at room temperature (Vortex-Mixer Genie 2, Scientific Industries, New York, USA). From this solution, 10 μ L was pipetted into a pyrolysis tube. All assays were performed in duplicate. In order to avoid contamination, the pyrolysis tubes were stored in individual glass vials for each concentration. The vials containing the tubes were then placed in a freeze dryer where the sample was frozen at -60 °C for 15 min and then dried at -60 °C and 0.3 mbar for 30 min. In a second step, the samples were analyzed by TD-GC/MS only. Samples were placed directly into a TDU glass tube.

4.2 Results and Discussion

The application of TD-Pyr-GC/MS is of advantage in the rapid analysis of samples, since no extraction steps are necessary and a direct particle analysis can be performed. Sorbed TOrCs and the polymer type can be identified in one analytical set-up. This is mainly useful for e.g., ecotoxicological investigations or spiked samples of wastewater treatment processes at laboratory or pilot scale.

4.2.1 Preliminary results – analysis of the aqueous phase

Centrifugation and filtration methods were tested to separate the particulate from the aqueous phase. Centrifugation was performed with a multi-application centrifuge (NuAir, Plymouth, USA). Centrifugation was tested with PE 48 μ m, PS 40 μ m and PMMA 48 μ m microplastic particles in an aqueous suspension at 1 g/L. The samples were centrifuged between 0.5 and 12 h at 3,000 – 5,000 RCF. However, no permanent separation of the aqueous phase and the particles was observed even when applying longer centrifugations. For this reason, filtration was used for all further experiments.

Analysis of the filtrate was performed using passive samplers. The Gerstel Twister® and the SorbStars were tested. In preliminary tests the extraction capacity of SorbStar in ultra-pure water was tested with phenanthrene. However, no reproducible measurements could be carried out with the SorbStar. If the SorbStar is used in large sample vessels, it floats on the surface. The consecutive measurements show results that are tenfold lower than those of the Gerstel Twister®. If the SorbStar is shaken in test tubes so that it is completely immersed in solution, the subsequent measurement is aborted by the device. Most likely, a too high water content penetrated into the

SorbStar leading to this aborting due to freezing of the tubings. Therefore, the SorbStars were discarded subsequently as an alternative to the Gerstel Twisters®.

4.2.2 Sources of contaminations and sample preparation

Summary of the study published in Reichel et al., 2020

Sample carryover is a well-known problem in Pyr-GC/MS of synthetic polymers [39]. To avoid those contamination, the choice of the pyrolysis tube is crucial (see Figure 7a, type C). In the closed tube of type (A), the carrier gas flow is non-uniform, while in the slotted tube of type (B), a more uniform carrier gas flow is ensured [126]. (C) is open at both ends, which should improve the carrier gas flow. Since carryover was observed with type A and B pyrolysis tubes, but measurements with tube type C showed good results and significantly reduced the problem of contamination. Type C tubes were used for all further temperature optimization experiments and sorption experiments. After each measurement, the pyrolysis adapters (Figure 7c) should be cleaned with dichloromethane for 15 min in an ultrasonic bath. In addition, in order to identify possible contamination at an early stage, an empty pyrolysis tube was measured as a blank after each sample measurement. In this way, carryovers can be detected and eliminated at an early stage. Overloading of the GC column must be avoided to produce reproducible and evaluable peaks. This was achieved by accurately weighing and discarding samples with weights of above 80 µg.

After each TD-Pyr-GC/MS analysis run, an empty pyrolysis tube was measured to check the system for contamination. Especially during polystyrene measurements, carryover of the styrene trimer occurred, which could also be detected in the following measurements. Since the sequence of sample analysis consisted not only of PS samples but also of other polymer types (PE, PMMA), it could be established that the styrene trimer peaks were not induced by the actual samples. Rather, they can be characterized as impurities in the system. These results indicate occasional detachment or formation of the trimer due to accumulation of analytes in the system. Upon closer inspection of the pyrolysis module, black dots and soot discoloration were visible on the filament. Figure 9 shows the peak size identified as styrene trimer desorbed in blank tube measurements at 280 °C. The measurements with the contaminated filament 1 exhibited a clear increase in the peak area of the styrene trimer. Therefore, the filament was replaced by a new one (filament 2). Subsequent sample analysis improved substantially in terms of the detection of styrene trimers in the blank tubes. According to the experience gained from these measurements, the filament life can be estimated to about 300 - 350 runs for the pyrolysis of polymer particles.

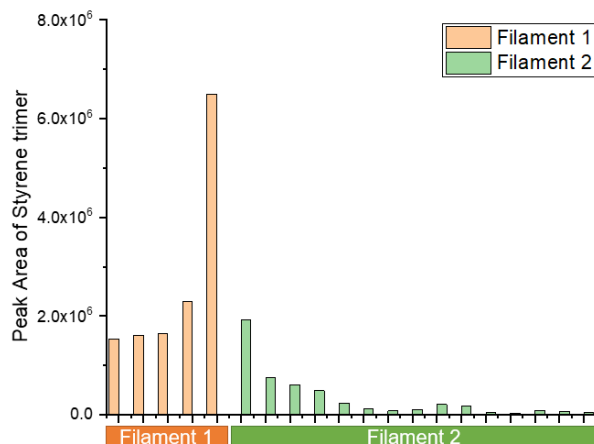


Figure 9: Increase of styrene dimer during blank measurements with filament 1 and decrease after changing the filament

4.2.3 Choice of the final thermal desorption temperature

Summary of the study published in Reichel et al., 2020

The final thermal desorption (TD) temperature was set at 200 °C. 120 °C is too low to achieve quantitative desorption of most TOCs. However, a TD temperature of 280 °C is too high for the analysis of thermolabile substances. For the reference PMMA particles, a noticeable increase in the characteristic substances already occurred in the thermodesorption with the increase of TD temperature. The results of the PS microplastic particles indicate that the storage of the particles also plays a role. Compared to the PS41 µm particles suspended in ethanol, the dry stored PS40 µm particles show a larger amount of characteristic substances already in the thermal desorption. The characteristic substances for the PE particles are independent of the choice of TD temperature. They are only visible in the pyrogram.

4.2.4 Desorption behavior of the TOCs phenanthrenes, α-cypermethrin and triclosan.

Summary of the study published in Reichel et al., 2020

In the current study, the trace compounds phenanthrene, α-cypermethrin, and triclosan were sorbed onto the reference particles PMMA 48 µm, PE 48 µm, PS 78 nm, PS 41 µm, and PS 40 µm (1 g/L each) for 1 h at the two final concentrations of 1,000 µg/L and 100 µg/L, respectively.

The highest sorption for the selected TOCs occurred onto the PS 78 nm nanoparticles. Phenanthrene (1000 µg/L) sorbed onto the particles as follows: PMMA << PS 40 µm < PS 41 µm < PE 48 µm < PS 78 nm. For phenanthrene at a concentration of 100 µg/L, sorption was observed only on PS (78 nm) and PE particles. Sorption of α-cypermethrin on particles was generally lower compared to phenanthrene and followed order: PS 41 µm < PS 40 µm < PE 48 µm < PMMA

48 μm < PS78 nm. When α -cypermethrin was applied at a concentration of 100 $\mu\text{g/L}$, sorption was observed only on PS 78 nm and PE particles. Triclosan at the concentration of 1,000 $\mu\text{g/L}$ sorbed only on PS 78 nm and PE 48 μm particles. When triclosan was applied at a concentration of 100 $\mu\text{g/L}$, sorption was not observed on any particle type. However, identifying sorption kinetics and individual detection limits of the selected TOrCs are beyond the scope of this study.

4.2.5 Sorption of TOrCs on reference particles

Summary of the study published in Reichel et al., 2020

In order to assess the tendency of TOrCs to desorb from particles, the percentage of phenanthrene desorption during TD was considered. On the PE particles nearly 100% of the phenanthrene desorbed during thermodesorption. The PS 78 nm particles also showed a desorption of 90%. The PS particles (41 and 40 μm) present a desorption between 25 and 60%. These clear differences may be due to the different storage of the particles. The PS 41 μm particles were suspended in ethanol, while the PS 40 μm particles were stored dry. Comparing the different concentrations (1,000 $\mu\text{g/L}$ and 100 $\mu\text{g/L}$) of phenanthrene applied, the concentration does not seem to significantly affect desorption for PE, PS 40 μm , and PS 78 nm particles. These results suggest that desorption behavior depends on both particle size and particle type. The TOrCs α -cypermethrin and triclosan were both completely desorbed within TD.

It is recommended to measure the substances in SIM mode for target analysis. The peak areas and thus the sensitivity increased in the SIM mode for all trace substances: phenanthrene (+33% \pm 2%), α -cypermethrin (+54% \pm 12%), and triclosan (+58% \pm 12%).

4.2.6 Quantification of micro- and nanoplastic particles by TD-Pyr-GC/MS

In order to find out whether a quantification of the polymers by TD-Pyr-GC/MS is possible, to normalize the data, the peak areas of the characteristic substance fragments (Table 8) of the respective polymer were added and divided by the mass weighed-in. For example, for PS, the peak areas of the dimer and trimer in the TD and Pyr were added and divided by the weighed particle mass. Figure 10 shows boxplots for all polymer particles analyzed. Outliers were eliminated by applying Grubbs test. For PMMA 48 μm there was the highest signal of peak area / mass, while for PE 48 μm it was the lowest. This could be due in part to the peaks obtained for methyl methacrylate. The peaks are very large and wide, which is unfavorable for the automatic integration of the Masshunter evaluation program. On the other hand, it could be due to the different patterns of thermal desorption for the polymers. While PMMA exclusively forms methyl methacrylate as a characteristic substance, both PE and PS form a range of pyrolysis products

[120]. In addition to the selected characteristic PS fragments, a large amount of styrene (monomer) is obtained during thermal decomposition. The PS monomer was not included in the characteristic PS fragments because it can also be formed in natural matrices, e.g., by decomposition of chitin [29]. While PS forms only three significant decomposition products, PE exhibits a variety of alkanes, alkenes, and dienes [120]. This could be a reason for the comparatively low signal when only three characteristic polymer fragments are considered. If only the three PS particles (40 μm , 41 μm , 78 nm) are considered, an approximate estimate of the amount of polymer contained is possible. In summary, the results indicate that this type of evaluation is only useful when the same polymer type is to be compared. However, this would still have to be verified in mixed samples with other polymers.

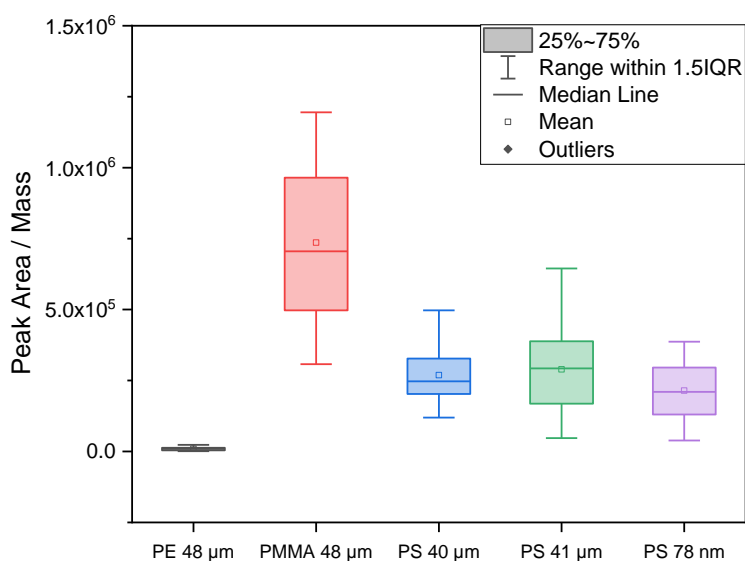


Figure 10: Boxplots of peak areas normalized to polymer mass versus weighed-in mass for all polymers. The peak area values include the signals of all selected characteristic polymer fragments in both TD and Pyr.

One reason for the high deviations may be the weighing-in process: On the one hand, there may be invisible particles on the upper and outer rim of the pyrolysis tube, which are weighed in but not pyrolyzed. Second, after weighing, the pyrolysis transport adapters are placed on the pyrolysis tubes. This process may result in additional loss of particles, especially if the particles were placed close to the edge of the capillary tube. Since only a small amount of <80 μg is weighed in, any smallest particle loss can result in large outliers.

At the current state, quantification of the amount of polymer by TD-Pyr-GC/MS is not feasible. However, a reliable identification of the polymer is possible.

4.2.7 Quantification of TOrCs (preliminary experiments)

In the initial quantification experiments, an attempt was made to reproduce a calibration curve of benzophenone without particles using the established parameters of TD-Pyr-GC/MS. For this purpose, the TOrCs solution was filled directly to the pyrolysis tubes.

However, it was concluded that no reproducible data could be measured. Furthermore, impurities were also found in the blank samples without benzophenone. In addition, the peak areas obtained were much lower than for TOrCs sorbed to polymer particles.

In order to overcome these inaccuracies, several strategies were used:

- The pyrolysis tubes were placed in individual glass vials for freeze-drying according to the concentration they contained to avoid cross-contamination during drying.
- The transport adapters were cleaned with dichloromethane before use, although they were not exposed to polymer particles.
- Additional pyrolysis steps after TD, as well as steps to measure empty pyrolysis tubes, were introduced to exclude signal accumulation.
- The GC instrument was baked out at 320 °C prior to measurements to exclude accumulation of TOrCs in the instrument.
- Thus, to achieve higher reproducibility, the pyrolysis module was disassembled for some measurements. For these, the samples were placed directly into the TDU glass tubes connected to the TDU adapters. The glass tubes were cleaned with acetonitrile and ultrapure water and dried at 100 °C. However, this resulted in signal accumulation.
- A higher TD temperature (280 °C instead of 200 °C) was used to increase the vapor pressure of the TOrCs. This change resulted in lower signals with high blank values and low reproducibility.
- In the pyrolysis tubes, the TOrC sorb directly onto the smooth glass surface. To obtain a more comparable surface to the polymer particles, the samples were pipetted onto the quartz wool. However, it was not possible to always reproducibly apply the solution droplets only to the quartz wool or only to the glass tube wall. For future experiments, inertized (e.g., with hydrofluoric acid) pyrolysis tubes should be tested.

However, even considering this strategy, reproducible data could not be generated. This method of quantification was therefore discarded.

4.3 Conclusion

Until now, double-shot pyrolysis or sequential pyrolysis GC/MS could detect additives in polymers, but not organic trace compounds [41, 42]. The results of this study confirm that TD-Pyr-GC/MS can identify both TOrCs and polymers in one analytical setup. Within a very short experimental time (<2 h), individual samples can be analyzed without the need for complex and contaminating steps of TOrCs extraction. The micro- or nanoplastic particles are separated by filtration from the liquid phase and then freeze-dried. For analysis, the samples are placed in pyrolysis tubes. Depending on the assay, a target analysis (SIM mode) or a non-target analysis (SCAN mode) can be performed.

The following goals were achieved by the TD-Pyr-GC/MS method development and validation:

- Identification of sorbed TOrCs on micro- and nanoparticles is possible, regardless of polymer type and size. Therefore, TD-Pyr-GC/MS is one of the few analytical methods that is also practical for nanoparticles.
- The optimum TD temperature was identified at 200 °C. This temperature ensures that the volatiles elute in the TD step while generating few pyrolysis products.
- The optimum pyrolysis temperature is 800 °C. All reference polymers (PS, PE, PMMA) were able to fragmentate completely at this temperature without leaving residues in the system.
- Possible applications of the TD-Pyr-GC/MS are for rapid qualitative analysis of e.g., ecotoxicological studies or fate studies of evaluating wastewater treatment processes at laboratory or pilot scale.

Thus, the hypothesis that by ‘coupling thermodesorption and pyrolysis-GC/MS trace substances on reference micro- and nanoplastic particles can be quantified and polymer types can be identified in one analytical setup’ can partially be accepted. In further experiments (see chapter 5) also quantification was successfully established.

5 Ad- and Absorption behavior on reference particles depends on particle size and shape / particle type / mixture of TOrCs / aging of particles

Hypothesis #2: Ad- and Absorption behavior on reference particles depends on

- a) Particle size and shape → the smaller the particle, the larger the relative surface, the higher the adsorption rate
- b) Particle type
- c) Mixture of trace substances → competition between substances depending on their structure (e.g. p-systems) and hydrophobicity
- d) Aging of particles

In general, sorption of TOrCs on particles can be distinguished into chemical and physical sorption. Chemical sorption is the name given to the formation of covalent bonds, which is often irreversible and depends on the ability of the components to interact with each other. Physical sorption processes, on the other hand, are usually non-covalent intermolecular interactions such as van der Waals bonds with hydrophobic surfaces on particles [48, 50]. Due to a porous polymer structure and the resulting large surface area of micro- and nanoplastic particles, both adsorption to the particle surface and absorption of TOrCs into the particle are relevant [20]. In most cases, the dominant process (adsorption or absorption) cannot be clearly identified, since both processes can occur simultaneously [48, 49]. Due to the hydrophobicity of plastics and their high surface-to-volume ratio, hydrophobic organic compounds readily sorb to micro- and nanoplastics. Persistent organic trace substances can thereby be transported into the environment and accumulate there [9, 11, 127, 128]. To enable evaluation of those accumulation detailed knowledge about sorption processes on particles and how are they influenced is crucial. Thus, it was hypothesized that *ad- and absorption behavior depend on particle size and shape, particle type, the mixture of trace substances, and organic matter and pH of the aqueous phase*. To test this hypothesis, three different polymer types (PS, PE, PMMA) and different polymer sizes at the micro- and nanoscale were selected. In addition, three TOrCs (phenanthrene, triclosan, α -cypermethrin) were chosen for the sorption studies. TD-Pyr-GC/MS and TD-GC/MS methods developed in Chapter 4 were used to determine the TOrCs concentrations as well on the particles and in the aqueous phase.

Ad- and Absorption behavior on reference particles depends on particle size and shape / particle type / mixture of TOrCs / aging of particles

5.1 Rationale

Micro- and nanoplastic particles can serve as both a source and a sink for TOrCs in the environment (Figure 11). Microplastic particle itself must be considered a pollutant, since monomers, additives, plasticizers and others can be desorbed. On the other hand, the sorption of TOrCs on the particles may pose a risk to the environment, due to sorbed antibiotics, heavy metals und polycyclic aromatic hydrocarbons and other TOrCs [4, 54, 63, 64, 87, 129, 130].

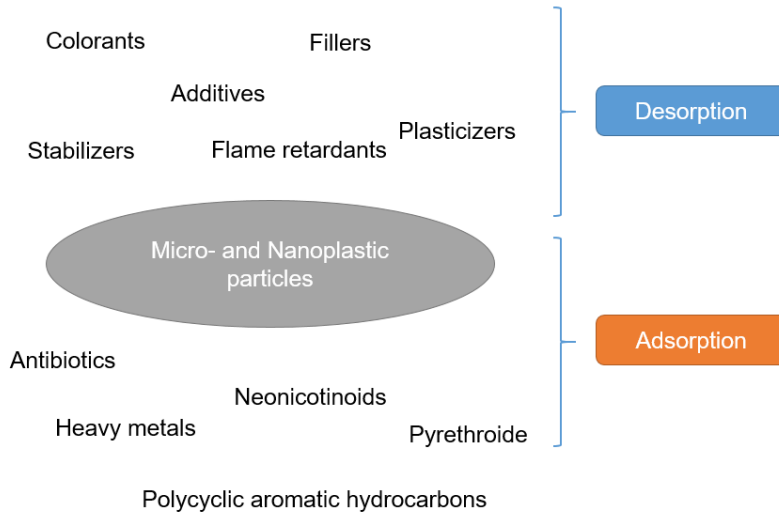


Figure 11: Pollutants which interact via de- and adsorption with micro- and nanoplastic particles

Sorption analysis is a challenge because sorption is influenced by many different parameters such as pH, temperature, and salinity of the liquid phase or the polymer type or age of the polymers [16, 131].

Therefore, in the following section sorption behavior of selected reference particles are analyzed and discussed as a function of their size and shape, particle type, and TOrCs mixture (Figure 12).

Ad- and Absorption behavior on reference particles depends on particle size and shape / particle type / mixture of TOrcs / aging of particles

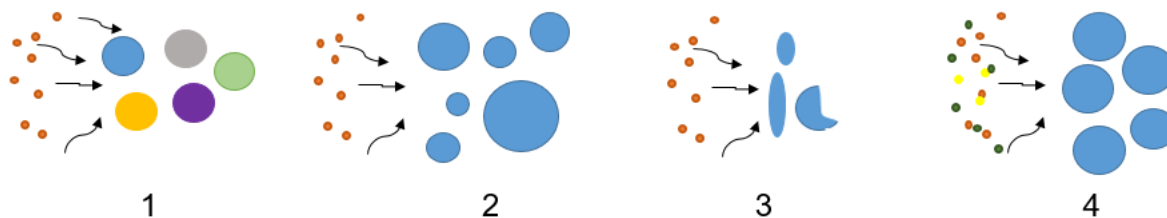


Figure 12: Sorption of TOrcs is influenced by polymer and particle type (1), size (2), shape (3) and mixture of TOrcs (4)

Ad- and Absorption behavior on reference particles depends on particle size and shape

Micro- and nanoplastic particles can result from the fragmentation of larger plastic pieces through photolytic, mechanical, and biological degradation without significant chemical degradation [8, 132, 133]. The smaller the particles, the greater the surface area, thus, smaller particles are expected to be of greater ecotoxicological relevance and cell wall mobility increases as the capacity to adsorb TOrcs increases [18, 49, 63]. However, the effective surface area of nano-sized particles can be limited by aggregation by increasing the hydrodynamic diameter [9, 49, 134]. Aggregation can occur between two similar (homoaggregation) or two different (heteroaggregation) particles [4]. Aggregation is usually controlled by the ionic strength and valence of the electrolytes in the surrounding medium, but the polymer coating of the particles can also play a role [4, 135].

By means of nanofragmentation, microplastic particles can further disintegrate into nanoplastic [9, 49, 134]. Already with other particle types (e.g., titanium particles or magnesium oxide particles) it could be shown that the relative sorption increases, the smaller the particle becomes [136, 137]. These statements could be supported by research with micro- and nanoplastics: the sorption of polychlorinated biphenyls on nano-PS is 1-2 orders of magnitude higher than on micro-PE. However, it is questionable to what extent those data can be transferred to nanoplastics [138]. To enable comparison of data, the methods for detection, analysis and toxicological assessment of nanoplastics, which are currently still in their initial stages, must first be improved [139].

Ad- and Absorption behavior on reference particles depends on particle type

Various previous studies showed that the sorption is polymer dependent. Plastic polymers can be categorized as either crystalline, semi-crystalline or amorphous, which describes their structure. Amorphous polymers consist of randomly arranged polymer chains. In contrast, semi-crystalline describes portions of rigidly arranged crystalline moieties that are located in looser amorphous regions [5, 51]. Compared to amorphous polymers or regions of polymers, the crystalline fractions

Ad- and Absorption behavior on reference particles depends on particle size and shape /
particle type / mixture of TOrCs / aging of particles

have a lower affinity and rate for incorporation into a polymer matrix [5, 54]. The hydrophobic bonds are less stable in amorphous materials than in crystalline materials [140]. TOrCs require a high amount of energy to break and absorb the lattice structure of polymer chains associated with crystalline domains [48]. The amorphous region within polymers can be classified as either glassy or rubbery, which is also an indication of sorption capacity [19].

Hydrophobicity is considered one of the most important driving mechanisms of organic compounds from water into solid particles [48, 52]. Decisive for this is the Log D value as a measure of the hydrophobicity of a molecule, for the distribution of a sorbate in solution for sorbing to a given solid, taking into account the pH influence of functional groups [53].

Prior studies have noted that the density increase of the polymer decreases the velocity of diffusion into the polymer [22]. The study was set up to compare sorption of different molecular weight PAHs to Low-Density Polyethylene (LDPE) and High-Density Polyethylene (HDPE). It is possible that this characteristic is not limited to LDPE and HDPE, thus can be transferred to polymers of different types. However, the density of polymers with crystalline and amorphous components, such as HDPE, is determined by the ratio of crystallinity. As stated above, the amorphous region within polymers can be classified as either glassy or rubbery, which is also an indication of sorption capability [19]. The surface appearance is also important. Napper et al. (2015) showed that rough PE microplastic particles adsorbed more DDT and phenanthrene than smooth ones [141].

The glass transition temperature defines whether a polymeric rubber-like or glass-like material is present. Rubber-like polymers are normally above their glass transition temperature (T_g) values if they are not plasticized. At room temperature this results in greater flexibility, which facilitates sorption of impurities. Glassy polymers are usually below their T_g and are also referred to as condensed (glasslike) [64]. In general, rubbery polymers (such as HDPE, LDPE or PP) are expected to allow greater diffusion of impurities into the polymer than glassy polymers (such as PET or PVC) [53, 54]. Some polymer types, like PMMA and PS, are glassy at ambient temperature. Once they surpass the glass transition temperature, the amorphous fractions change into a rubbery state. In contrast, sorption to glassy polymers occurs through dissolution (absorption) and pore-filling mechanisms [58, 59]. However, there are exceptions such as polystyrene. The average sorption capacity is higher than the T_g predicts [4, 20, 52, 64]. A possible explanation for this is the presence of benzene. The benzene ring increases the distance between the polymer chains and can facilitate the adhesion and integration of impurities into the polymer [20, 64, 142]

Ad- and Absorption behavior on reference particles depends on particle size and shape / particle type / mixture of TOrcs / aging of particles

Ad- and Absorption behavior on reference particles depends on mixture of trace substances

During the sorption process, fluid chemicals are transferred to solids [143, 144]. In adsorption, chemical molecules are bound at the solid-liquid interface, while in absorption they penetrate the solid matrix of the particle [48, 144]. Adsorption to the particle surface includes ionic and van der Waals interactions, as well as covalent bonds. Absorption occurs due to the distribution of TOrcs within the polymer matrix, which is held by weak van-der-Waals forces. In this process, absorption is strongly dependent on various factors such as the hydrophobic properties of the TOrcs, the polymer type, and particle size. The interactions between the particles and the TOrcs depending on their specific properties are shown in Figure 13.

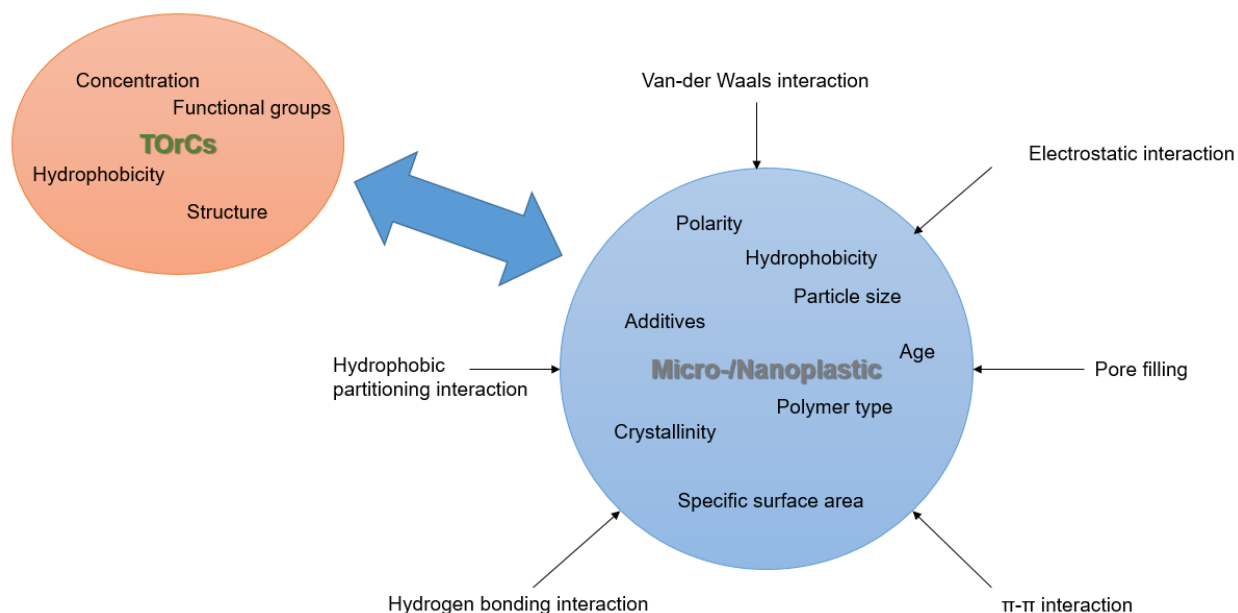


Figure 13: Interactions of micro- and nanoplastic particles and TOrcs depending on their specific properties.

Ad- and Absorption behavior on reference particles depends on aging of particles

One of the main challenge of microplastics in the environment is their low rate of degradation by means of natural processes [145]. Microplastics age due to UV irradiation, heat, chemical oxidation and physical abrasion, or biotic effects [11, 146]. In the aging process of microplastic, the physical integrity is lost and the polymer degrades at the weak points such as unsaturated double bonds, branched chains, carbonyl groups or hydroxyl groups at the ends [147]. As a result, the physicochemical properties of microplastics change: the average molecular weight and surface roughness increase, added additives are leached out, the particle size decreases, and

Ad- and Absorption behavior on reference particles depends on particle size and shape /
particle type / mixture of TOrCs / aging of particles

the specific surface area increases, which promotes the adsorption of TOrCs [148-154]. In the laboratory, the aging processes can be simulated, e.g., by heat treatment or chemical oxidations [148].

The aging of particles in this work was done with chemical treatment based on Fenton reaction, hydrogen peroxide (H_2O_2) and potassium hydroxide (KOH). The effects of the chemical treatment are studied by TD-Pyr-GC/MS. The chromatograms and pyrograms of selected untreated microplastic reference particles (PS, PE, polylactic acid (PLA), polyethylene terephthalate (PET), polyamide (PA) and polypropylene (PP)) are compared with those after simulated aging processes.

Ad- and Absorption behavior on reference particles depends on particle size and shape / particle type / mixture of TOrcs / aging of particles

5.2 Experimental section

The experiments to investigate the adsorption and absorption behavior of the selected TOrcs on the reference particle were performed based on the results obtained in Chapter 4.

In individual studies, after preliminary tests, the analyses were performed including the determination of TOrcs concentration in the aqueous phase and on the particles. PS (78 nm, 41 μ m), PMMA (48 μ m) and PE (48 μ m) were used as reference particles, and phenanthrene, triclosan and α -cypermethrin were chosen as environmentally relevant TOrcs. At a concentration of 1 mg/mL, the particles were shaken in ultrapure water for 1 h at room temperature. TOrcs were added at variable concentrations of 0.1 mg/L, 1 mg/L, 5 mg/L and 10 mg/L, respectively.

Nanoplastic particles (PS 78 nm) and microplastic particles (PE 48 μ m) at a concentration of 1 g/L were used to analyze the sorption of the mixture of TOrcs. The TOrcs concentration was 1 mg/L and 10 mg/L, respectively. These particles were selected because sorption equilibrium was quickly established after 1 hour in the sorption experiments. The general procedure and sample preparation workflow is shown in Figure 14.

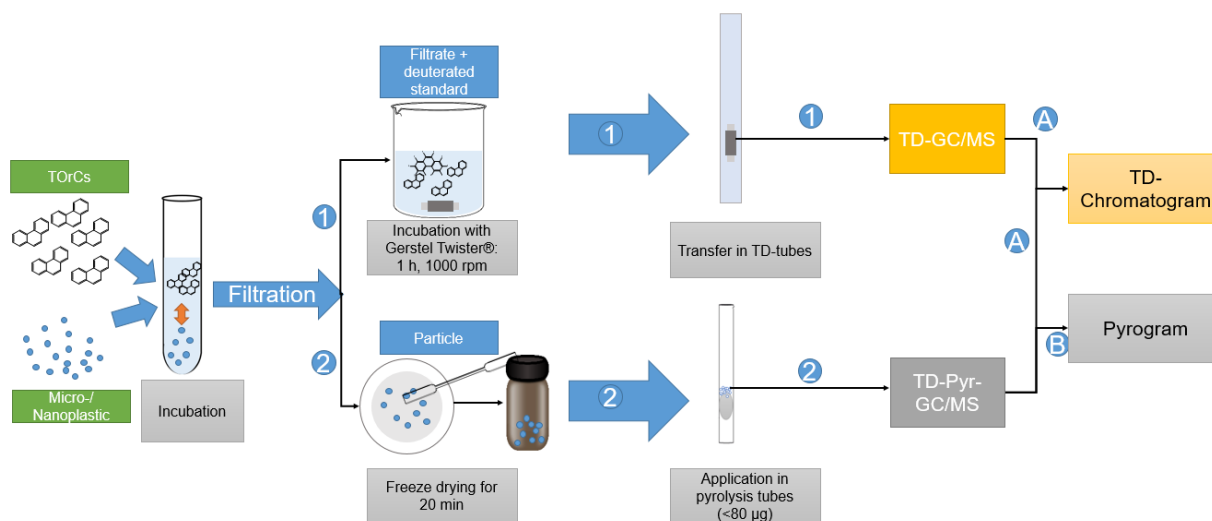


Figure 14: Sample preparation workflow: First, the TOrcs and microplastic particles are incubated in aqueous solution. Subsequently, the sample is filtered. The filtrate (1) is mixed with the deuterated standard and stirred for 1 h with the Twister. The Twister is added to the TD tube and analyzed via TD-GC/MS. The TOrc is analyzed via the TD chromatogram (A). The particles (2) are scraped off the filter with a spatula, placed in a vial and freeze dried. The dried particles are weighed directly into the pyrolysis tube and analyzed by TD-Pyr-GC/MS. The TD chromatogram is used to evaluate the volatiles (A), and the pyrogram is used for the polymers (B). Adapted from Reichel et al., 2022 (Appendix III)

Analysis of the aqueous phase via TD-GC/MS

For the quantification of TOrcs in the aqueous phase, calibration curves are created with Gerstel Twister® and TD-GC/MS. For GC/MS, an isotopically labeled reference is added as an internal

Ad- and Absorption behavior on reference particles depends on particle size and shape /
particle type / mixture of TOrcs / aging of particles

mass spectrometric standard for the specific TOrc (phenanthrene-d10 (50 ng/L), cypermethrin- (phenoxy-d5) (0.1 mg/L), and triclosan-d3 (0.01 mg/L)). Stock solutions of poorly water-soluble pollutants are produced in methanol. The dilution is carried out in tap water to a final volume of 10 mL. Gerstel Twisters® are added and stirred on a Thermo Fisher (USA) magnetic stirrer (15 positions) for 60 min at 1,000 rpm at room temperature. The Gerstel Twisters® are removed, washed with ultra-pure water and dried with a lint-free tissue. Subsequently, the stir bar is transferred into the thermodesorption tube for subsequent TD-GC/MS analysis.

The Gerstel Twister® and TD-GC/MS analysis are adopted from Ochiai et al. (2005) [118]. However, the temperature for cryofocussing is set to -50 °C instead of -150 °C. Helium is used as carrier gas. The mass spectrometer is operated in full-scan mode (m/z range 40 to 550) with electron impact ionization (70 V). Data analysis is conducted with Mass Hunter Workstation Software (Ver.B.08.000, Agilent). The identification of the substances is ensured via the MS spectra and comparison with the NIST database, the retention index (RI) and comparison with external standards.

Analysis of the particles via TD-Pyr-GC/MS

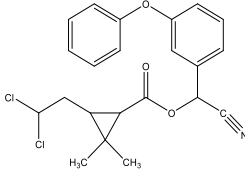
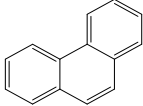
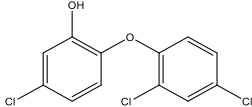
In order to analyze the sorbed TOrcs on the particles, particles were scraped off the filter after filtration using a spatula. After freeze-drying for 20 min, they were stored for a maximum of 24 h at 4 °C. Subsequently, they were weighed directly into the pyrolysis tubes with a maximum weight of 80 µg. Analysis was performed by TD-Pyr-GC/MS using the method finalized in Chapter 4.

Evaluation of TD-GC/MS and TD-Pyr-GC/MS data

The focus of the analysis via TD-GC/MS and TD-Pyr-GC/MS was on the identification of the selected TOrcs based on their characteristic signals (Table 10).

Ad- and Absorption behavior on reference particles depends on particle size and shape / particle type / mixture of TOrCs / aging of particles

Table 10: Characteristic signals for MS analysis and properties of selected TOrCs

Substance	Characteristic Signals (m/z)	Molecular weight (g/mol)	Van der Waals surface * (Å ²)	Structure
α-Cypermethrin	163, 184, 209	416	571	
Phenanthrene	178	178	261	
Triclosan	290, 288, 218, 63	290	319	

TD-GC/MS analysis: MS analysis of the selected TOrCs (Table 1) was performed in SIM mode. The TOrCs phenanthrene (m/z 178), triclosan (m/z 290), and α-cypermethrin (m/z 163) and their corresponding deuterated standards were determined based on their characteristic signals.

TD-Pyr-GC/MS: In the first step, i.e. thermal desorption, MS analysis was performed using a combined SIM/full scan mode. The SIM mode was used to analyze the characteristic signals of the selected TOrCs. With the full scan mode, it is additionally possible to identify the characteristic signals of the polymers. The MS analysis of the subsequent pyrolysis was performed in full scan mode to identify potential contaminations.

TD-GC/MS and TD-Pyr-GC/MS data were performed using Mass Hunter Workstation software (Ver.B.08.000, Agilent). Primary identification of individual compounds was performed using the MS spectrum and the NIST database. The data obtained were statistically analyzed for outliers using the Dixon' Q-test and Grubbs test (level 0.05). Significant outliers were not used for the final data evaluation.

Experimental setup for analysis of aging of particles

The experiments were performed with ultrapure water prepared on an arium® pro VF (Sartorius, Germany) with an ultrafilter. Hydrogen peroxide (H₂O₂ (30%)) was purchased from Merck, Germany, and Carl Roth, Germany. Potassium hydroxide (KOH, 10 wt%) was prepared from pure KOH (Merck, Germany) in Ultra-Pure Water. In order to minimize contamination by foreign particles, all reagents were filtered with 0.2 μm polycarbonate syringe filters prior to use. The following protocols (Table 11) were applied to the aging of the micro- and nanoplastic particles.

Ad- and Absorption behavior on reference particles depends on particle size and shape / particle type / mixture of TOrcs / aging of particles

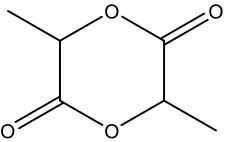
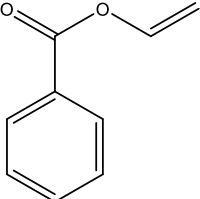
Table 11: Protocols applied to the aging of micro- and nanoplastic particles

Protocols	Temperature	Time
No treatment	None	None
Fenton (30 % H ₂ O ₂ + 20 g/L FeSO ₄)	Unregulated	10 min + 10 min cooling
H ₂ O ₂	60 °C	24 h
KOH (10 %)	60 °C	24 h

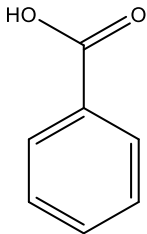
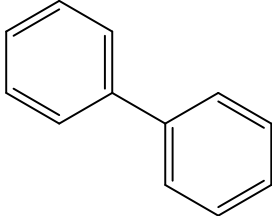
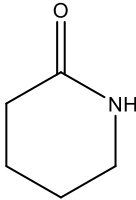
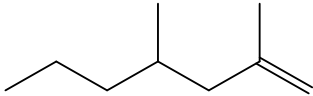
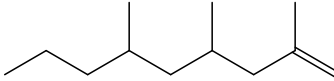
Analysis of aged microplastic particles via TD-Pyr-GC/MS

The reference particles of the polymers PS, PE (Ineos, London, UK), PLA (Nature Works, Minnetonka, MN, USA), PET (TPL, Zurich, Switzerland), PA (Lanxess, Cologne, Germany) and PP (Borealis, Vienna, Austria) were analyzed without treatment and each after treatment with Fenton reagent, KOH or H₂O₂ using TD-Pyr-GC/MS. TD-Pyr-GC/MS analyses were performed according to the method validated in Chapter 4. The particle sizes of the microplastic ranged from 80 – 330 µm. All experiments were performed in duplicate. The chromatograms or pyrograms were compared in order to detect possible changes in the untreated and treated polymers, regarding the characteristic pyrolysis products. The following characteristic pyrolysis products of the individual polymers were used for identification (Table 12).

Table 12: Characteristic pyrolysis products of the selected polymers for identification

Polymer type	Characteristic pyrolysis products	Formula	m/z (intensity ratio [%])*	Structure
PLA	Lactide	C ₆ H ₈ O ₄	28 (75), 45 (34), 56 (100), 144(1)	
PET	Vinyl benzoate	C ₉ H ₈ O ₂	51 (15), 77 (62), 105 (100)	

Ad- and Absorption behavior on reference particles depends on particle size and shape /
particle type / mixture of TOrcs / aging of particles

	Benzoic acid	$C_7H_6O_2$	51 (18), 122 (99), 77 (57)	
	1,1-Biphenyl	$C_{12}H_{10}$	28 (100), 76 (12), 154 (92)	
PA	Caprolactam	$C_6H_{11}NO$	55 (79), 67 (11), 85 (61), 113 (100)	
PP	2,4-Dimethylhept-1-ene	C_9H_{18}	43 (97), 70 (100), 83 (27), 126 (18)	
	2,4,6-trimethyl-1-nonene	$C_{12}H_{24}$	28 (100), 43 (59), 69 (88), 111 (33), 125 (13)	

* intensity ratio to largest peak in spectra

5.3 Results and Discussion

In the following section, the sorption of the selected TOrcs from micro- and nanoplastic particles is discussed, depending on the particle size, polymer type, and TOrcs mixture. Aged particles are also compared with unaged ones by TD-Pyr-GC/MS analysis.

5.3.1 Sorption onto PS micro- and nanoplastic particles

Summary of the study published in Reichel et al., 2020

In order to compare whether the sorption rate increases the smaller the particle and the larger the relative surface area are, spherical PS particles of different sizes (78 nm, 40 μm , 41 μm) were used. For the comparative study, the TOrcs phenanthrene, triclosan and α -cypermethrin were used at concentrations of 1 $\mu\text{g/mL}$ and 0.1 $\mu\text{g/mL}$. After a sorption time of 1 h, sorbed TOrcs were measured by TD-Pyr-GC/MS. Based on this data, the sorption efficiency of TOrcs as a function of peak area per particle surface was determined (Reichel et al., 2020/ Figure 8). Sorption onto nanoplastic particles (PS 78 nm) was highest in all sorption experiments (phenanthrene: PS 40 μm < PS 41 μm < PS 78 nm; α -cypermethrin (PS 41 μm < PS 40 μm < PS 78 nm). Sorption of triclosan on PS 41 μm and PS 40 μm could not be detected.

The results show that the higher sorption efficiency of nanoparticles is mainly due to the high particle number and higher specific surface area. In addition, it was shown that sorption performed better on 41 μm PS particles suspended in ethanol than on dry 40 μm particles.

5.3.2 Quantification – Sorption of different TOrcs concentrations onto PS nanoparticles

Summary of the study published in Reichel et al., 2022

Nanoplastics are shown to have strong hydrophobicity and increased sorption capacity for TOrcs due to their increasing surface ratio associated with fragmentation and other weathering processes [4, 113]. The aim of this experiment was to investigate whether a quantitative determination of sorbed TOrcs directly from the particle by TD-Pyr-GC/MS is possible. Already after 1 h the concentration of 1 mg/L phenanthrene is completely sorbed onto the particles, for the concentrations of 5 mg/L and 10 mg/L only concentrations less than 0.2 mg/L can be detected in the aqueous phase. For all initial concentrations of triclosan, the final concentration after 1 h incubation is below 1 mg/L in the aqueous phase. Observing the particle analysis (TD-Pyr-GC/MS), a clear increase of the triclosan concentration on the particles can also be seen. Compared to phenanthrene and triclosan, the remaining concentrations of α -cypermethrin and the deviations in the aqueous phase are significantly higher. However, a clear increase of the concentrations in the particulate phase can be demonstrated. For all three selected TOrcs a

Ad- and Absorption behavior on reference particles depends on particle size and shape /
particle type / mixture of TOrcs / aging of particles

possible quantification could be shown (Reichel et al., 2022/ Figure 5). A quantification of sorbed TOrcs could be shown here for the first time.

5.3.3 Ad- and Absorption behavior on reference particles depends on particle type

Summary of the study published in Reichel et al., 2020

Phenanthrene

Phenanthrene is a non-polar chemical and readily sorbs to non-polar polymers. The sorption results show that phenanthrene is no longer detectable in the aqueous filtrate of PE 48 μm and PS 78 nm particles after an exposure time of 1 h. The concentration of phenanthrene in the aqueous filtrate decreases with time (Reichel et al., 2022/Figure 2). The sorption results of the particle phase analysis (TD-Pyr-GC/MS) are confirmed by the aqueous phase results (TD-GC/MS). Deviations may occur due to the weight of the particles or incomplete pyrolysis of the particles. Substances with high hydrophobicity are generally readily adsorbed on PE [155]. PE is the least polar polymer of the studied polymers, thus the rapid sorption of the non-polar chemical is to be expected. The high sorption capacity of PE is also due to its increased diffusivity, which is based on its larger free volume, greater flexibility and mobility. This allows TOrcs to diffuse quickly into the material [64]. Prior studies have noted that next to hydrophobic interactions, for example PS can also engage in π - π -interactions [16, 20, 156]. These interactions are present in polymers, such as PS, which have benzene rings in their structure [131]. For example, a study by Hüffer and Hofmann (2016) reported that the enhanced adsorption of pharmaceuticals on PS microplastic particles is related to the strong interaction between the aromatic part of the polymer particles and the conjugated π -cloud of the aromatic structure of the adsorbed pharmaceuticals [20]. Nevertheless, sorption onto the PS 41 μm particles shows only a slight increase within 1 h to 48 h. The concentration in the aqueous phase decreases. PMMA is relatively polar. Even after 48 h, hardly any sorption was noticed both in the aqueous phase and in the particle analysis. The order of sorption after 48 h (sampling 1 h, 24 h, 48 h) is as follows: PMMA 48 μm < PS 41 μm < PE 48 μm < PS 78 nm.

Triclosan

Triclosan is symmetrical and therefore exhibits only low polarity. On the PS 78 nm particles, triclosan sorbed within 1 h, as evidenced by both the analysis of the particles and the aqueous phase (Reichel et al., 2022/Figure 3a). In contrast to the PS nanoparticles, sorption to the PS microparticles (PS 41 μm) and to the PMMA 48 μm particles is not complete even after 48 h (Reichel et al., 2022/Figure 3c, d). Due to the benzene rings in the structure of triclosan, it can

Ad- and Absorption behavior on reference particles depends on particle size and shape / particle type / mixture of TOrCs / aging of particles

form π - π interactions with those of PS [26]. This confirms the results of Li et al. (2019) and Ma et al. (2019) that increased sorption capacity is associated with decreasing particle size [60, 61]. The sorption of triclosan to the polymers is mainly due to hydrophobic, hydrogen-bonding and π - π -bonding interactions [157, 158]. Hydrophobicity is considered to be an important mechanism for sorption of organic compounds from water onto solid particles [48, 52]. Usually, to measure the hydrophobicity, the octanol-water partition coefficient (K_{ow} or $\log K_{ow}$) is used as a parameter [44]. Therefore, materials with high $\log K_{ow}$ values tend to be more readily absorbed by organic material due to their low affinity for water. The hydrophobic nature of microplastic particles contributes significantly to the sorption of TOrCs to microplastics [131]. The results of a study by Hüffer & Hoffmann, (2016) suggest that the molecular interactions between microplastics and organic compounds are mainly caused by hydrophobicity [20]. The sorption of triclosan to the PE particles is not completed within 48 h. However, the concentration in the aqueous phase decreases constantly (Reichel et al., 2022/Figure 3b). Analysis of the concentration of triclosan in the aqueous phase showed the following order: PMMA 48 μ m < PS 41 μ m < PE 48 μ m < PS78 nm. The particle phase gave the following results: PMMA 48 μ m = PS 41 μ m < PE 48 μ m < PS78 nm.

α -Cypermethrin

The concentration of α -cypermethrin in the aqueous phase is consistently very low for all polymers (Reichel et al., 2022/Figure 4a-d). The deuterated standard cypermethrin-(phenoxy-d5) was used as the reference substance for the aqueous phase. This may have influenced the measurements due to the presence of four isomers. Based on the particle data, the highest sorption to the PS 78 nm particles was found (Reichel et al., 2022/Figure 4a). α -Cypermethrin does not have a planar structure, which makes it difficult to bind to the benzene rings of the PS 41 μ m particles. A decrease in the measured concentration in the aqueous phase can nevertheless be seen (Reichel et al., 2022/Figure 4d). The benzene rings of α -cypermethrin cannot bind as effectively to the hydrogen groups of PE due to additional structural elements. Thus, the concentration on the particles remains relatively constant within the 48 h, while the concentration in the aqueous phase decreases slightly (Reichel et al., 2022/Figure 4b). PMMA has an amorphous structure into which the α -cypermethrin can absorb. The concentration in the aqueous phase decreases within the 48 h (Reichel et al., 2022/Figure 4c). Considering only the particulate phase, the sorption order is as follows: PE 48 μ m = PMMA 48 μ m < PS 41 μ m < PS 78 nm.

5.3.4 Ad- and absorption behavior on reference particles depends on mixture of TOrCs

Summary of the study published in Reichel et al., 2022

Ad- and Absorption behavior on reference particles depends on particle size and shape /
particle type / mixture of TOrCs / aging of particles

Considering the sorption of the selected TOrCs onto the PS 78 nm particles, only minor differences of the mixed TOrCs measurements compared to the single measurements can be seen. Thereby, the differences are still within the measurement deviations. One reason for this could be that after calculating the particle surface area of the total PS 78 nm particles used, there is still capacity. Thus, there is no competition for the occupancy of the particle surface (Reichel et al., 2022/Figure 6a).

In comparison, the single substances and the mixed TOrCs were sorbed on PE 48 μm . Phenanthrene sorbed more strongly onto the particles in the substance mixture than as a single substance (Reichel et al., 2022/Figure 6b). This could indicate an antagonistic effect, which was also found in the study by Bakir et al. (2012) with phenanthrene and DDT [58]. The sorption of triclosan and α -cypermethrin is not affected by the presence of the other TOrCs.

Comparing the sorption on PS 78 nm and PE 48 μm with an initial TOrCs concentration of 10 mg/L, the sorption on the nanoparticles is higher (Reichel et al., 2022/Figure 6c). This could be due to the higher particle surface to volume ratio.

5.3.5 Ad- and absorption behavior on reference particles depends on aging of particles

Summary of the study published in Al-Azzawi et al., 2020 (Co-Author)

Aging with KOH resulted in degradation of PLA and PET particles. Therefore, this method was excluded for subsequent analyses. Regarding the polymers PA and PS, the treatment with Fenton and H_2O_2 had an influence on their thermal stability. During the thermal desorption step at 200 °C, the ratio between the volatile pyrolysis products observed and the stable pyrolysis products at 800 °C was decreased after the treatment, especially for PA (Table 13). The amount of pyrolysis products that were volatile at 200 °C was reduced after applying the treatment and more pyrolysis products were stable until the second pyrolysis step at 800 °C. However, all polymers were still clearly identifiable in all cases.

Ad- and Absorption behavior on reference particles depends on particle size and shape / particle type / mixture of TOrCs / aging of particles

Table 13: Influence on the partial pyrolysis (TD) products at 200°C for PA and PS particles during thermal desorption, Adapted by Al-Azzawi et al., 2020 (Appendix IV)

Polymer type	Particle treatment	Pyrolysis products in TD (%) / Standard deviation (%)
PA	No treatment	74.5 / 19.0
	Fenton	17.1 / 12.7
	H ₂ O ₂	3.0 / 3.7
PS	No treatment	79.3 / 12.5
	Fenton	78.8 / 16.9
	H ₂ O ₂	71.9 / 10.9

The results indicate that a changes in particle surface area occur as a result of treatment with the selected reagents. Research indicates that the sorption capacity of trace substances increases on aged microplastics [150]. Experiments about sorption capacities with TOrCs analyzed via TD-Pyr-GC/MS should be considered in the future.

5.4 Conclusion

Based on the following results, it could be concluded that the sorption of the selected TOrCs onto micro- or nanoplastic particles is dependent on particle size, polymer type and mixture of TOrCs. In addition, TD-Pyr-GC/MS analysis showed differences in aged particles compared to unaged ones. It was demonstrated with the use of various polymers, PMMA (48 µm), PS (78 nm, 40 and 41 µm), PE (48 µm) and selected TOrCs (phenanthrene, triclosan, α-cypermethrin) that sorption is polymer dependent. Sorption measurements in a time period of 48 h (measuring points: 1 h, 24 h, 48 h) showed the generally highest sorption to PE particles. The sorption on PMMA and PS was significantly lower. Briefly, the sorption behaviors are as follows:

- Phenanthrene: PMMA 48 µm << PS 40 µm < PS 41 µm < PE 48 µm < PS 78 nm
- α-Cypermethrin: PS 41 µm < PS 40 µm < PE 48 µm < PMMA 48 µm < PS 78 nm
- Triclosan: PE 48 µm < PS 78 nm. No sorption on PS 41 µm, PS 40 µm and PMMA 48 µm was detected.

With the particle surface area calculations performed and the sorption experiments conducted on PS micro- and nanoplastic particles, it was shown that the higher sorption on the PS nanoparticles (78 nm) was mainly due to the higher number of particles and the higher specific surface area.

Ad- and Absorption behavior on reference particles depends on particle size and shape / particle type / mixture of TOrCs / aging of particles

An overview of the specific surface areas of the PS particles used as a function of particle size and number is shown in Table 14.

Table 14: Mass and number of polystyrene particles, adapted from Reichel et al., 2020 (Appendix 1)

Particle size [µm]	Particle type	Mass [µg]	Number of particles	Surface particles [m ²]
41	PS	22-63	586 – 1679	3.10*10 ⁻⁶ - 8.86*10 ⁻⁶
40	PS	23-64	660 – 1837	3.32*10 ⁻⁶ - 9.23*10 ⁻⁶
0.078	PS	29-69	1.12*10 ¹¹ – 2.67*10 ¹¹	2.14*10 ⁻³ - 5.10*10 ⁻³

At the same time, it was demonstrated for the first time that the newly developed technique of TD-Pyr-GC/MS is feasible to quantify sorbed TOrCs directly from nanoplastic particles. The quantification of TOrCs may be of particular interest for ecotoxicological and particle aging laboratory experiments.

Considering substance mixtures sorbed onto micro- and nanoplastic particles, agonistic and antagonistic effects are expected compared to single substances. In general, sorption in substance mixtures is dependent on particle size, polymer type, and surface-to-volume ratio. There were no competing effects within TOrCs for the PS 78 nm nanoparticles, while phenanthrene sorbed more strongly on PE 48 µm in the presence of triclosan and a-cypermethrin.

In laboratory experiments, pure microplastic particles were treated with H₂O₂ to simulate aging of the particles. The treated particles were subsequently analyzed by TD-Pyr-GC/MS. Based on the chromatograms and pyrograms, a change in PS and PA particles was observed. Since a previous study already indicated that the sorption capacity of aged microplastics is increased, this should be quantified during further experiments using TD-Pyr-GC/MS [150].

Thus, the hypothesis that **Ad- and Absorption behavior on reference particles depends on particle size and shape / particle type / mixture of TOrCs / aging of particles can be accepted.**

6 Sublethal and lethal effects of particles in *in vitro* and *in vivo* assays depend on particle type and size

Micro- and nanoplastic particles not only constitute environmental pollution, but can also have effects on aquatic organisms. Recent studies show negative effects on freshwater organisms [159-161]. For example, inhibition of reproduction or chronic toxicity and genotoxicity were found in the presence of PS particles (1 μm) in the organism *C. dubia* [161]. Due to the non-polar properties of microplastic particles, additional synergistic effects with TOxCs can occur. Thus, the presence alone of microplastics can significantly increase the presence of co-contaminants [159]. A study by Na et al. (2021) showed that the combination of microplastics and the TOxC benzophenone posed a synergistically amplified ecological risk to the organism *Daphnia magna* [162]. Thus, it was hypothesized that *sublethal* (e.g., behavior of aquatic organisms, changes in biomarkers) and lethal effects of particles in *in vitro* and *in vivo* assays depend on particle type (plastic or silica) and size (ad- ab- and desorption behavior of trace substances determine effects by influencing e.g., bioavailability of TOxCs). To test this hypothesis, ecotoxicological experiments with the freshwater organism *Gammarus roeselii* were conducted in collaboration with the Chair of Aquatic Systems Biology at TUM. Phenanthrene was used as a reference trace material, which was exposed to *G. roeselii* in combination with polyamide (PA) particles (40 – 63 μm) or sediment microparticles (45 – 53 μm). The remaining residual phenanthrene concentration in the aqueous phase was thereby analytically investigated by TD-GC/MS.

6.1 Rationale

Plastic particles smaller than 5 mm have reached a high occurrence (e.g., 100,000 articles per m^3) in waters and sediments and interact in many ways with organisms and the environment [163]. In about 50 % of all small aquatic freshwater organisms (macroinvertebrate samples) microplastic was found in concentrations up to 0.14 microplastic particles per mg tissue^{-1} [164]. Effects of microplastic accumulation may include toxic effects such as, disruption of the endocrine system, alterations in food intake and reproductive behavior, reduction in energy levels, and initiation of inflammatory responses [165-167]. As the size of the microplastic decreases, its availability and its potential to accumulate in the entire food network of freshwater invertebrates increases [168]. It is assumed that especially nanoparticles may penetrate into cells and by this provoke harmful effects [13-15]. For example, nanoplastic particles (100 nm) can be taken up by human gastric cells [14]. Scherer et al. (2017) proved that all freshwater invertebrates examined in the study have taken up microplastic. For *Daphnia magna*, for example, up to 6,180 particles

Sublethal and lethal effects of particles in *in vitro* and *in vivo* assays depend on particle type and size

h⁻¹ were recorded. The particle size that were offered had a size of 1 – 90 µm [168]. However, the particles are also excreted to a high degree [169]. Recent studies that deal with aquatic organisms and the effect of microplastics on these are summarized in Table 15.

It should be noted that microplastics can also serve as a vector for other substances [17]. TOrCs can be adsorbed on the plastic and ingested by organisms. Plastics may contain high levels of potentially bioavailable toxic substances such as TOrCs, which may pose a high ecotoxicological risk, especially in the early life stages of aquatic animals [170]. With regard to plastics and hydrophobic organic chemicals, it is argued that they can even form a complex cocktail that increases bioavailability for aquatic organisms and thus for humans [171]. A study by Horton et al., (2018) investigated the influence of microplastic particles in the presence of two pesticides [172].

Table 15: Overview: current literature regarding aquatic organisms and microplastics (MP) and TOrCs

Polymer Type	Particle size [µm]	Investigated organism	Main outcome	Reference
PS	0.07	<i>Daphnia magna</i>	<ul style="list-style-type: none"> Population growth was reduced reduced body size number and body size of neonated were lower 	[173]
	1	<i>Daphnia magna</i>	<ul style="list-style-type: none"> Exposed to two pesticides (dimethoate, deltamethrin) with or without PS particles PS particles alone: no effects Increasing pesticide concentrations: decreased mobility and increased mortality PS reduced the concentration of one pesticide (deltamethrin) 	[172]
	20-250 (powder), 0.02-200 µm (suspension)	<i>Daphnia magna</i> , <i>Artemia franciscana</i>	<ul style="list-style-type: none"> MP were found inside the guts Exponential correlation between MP uptake in the intestine and size of MP 	[174]
	1	<i>C. dubia</i>	<ul style="list-style-type: none"> Inhibition of reproduction and DNA damage Chronic toxicity and genotoxicity 	
PE	1 and 100	<i>Daphnia magna</i>	<ul style="list-style-type: none"> 1 µm particles are ingested and cause immobilization 100 µm particles had no visible effects 	[175]

Sublethal and lethal effects of particles in *in vitro* and *in vivo* assays depend on particle type and size

PE, PP	10 - 27	<i>Hyalella azteca</i>	<ul style="list-style-type: none"> • PP: were significantly more toxic than PE [160] • Chronic exposure to PE and PP: led to a significant decrease in growth and to a decrease in the reproduction
--------	---------	------------------------	---

6.1.1 Experimental Section

In collaboration with the Chair of Aquatic Systems Biology (TUM), microplastic experiments were carried out with the aquatic organisms *G. roeseli* and the TOxC phenanthrene. The aim of the experiment was to investigate the influence of microplastic particles or natural sediment particles on *G. roeseli* in the presence of phenanthrene. For this purpose, the aqueous phase of the preparation was analyzed with the Gerstel Twister® and TD-GC/MS. The procedure was analogous to the method described in Chapter 5.2. Instead of tap water, however, ISO medium was used (Table 16).

Table 16: Composition of the ISO medium for a 20 L approach; substances dissolved in water

	Amount (g)
CaCl ₂ *2H ₂ O	5.880
MgSO ₄ *7H ₂ O	2.460
NaHCO ₃	1.296
KCl	0.115

First, a calibration curve was generated for the measurements of phenanthrene in ISO-medium. Second, the measured and nominal concentrations of the exposure experiments were compared. A concentration of 0.5 ng/ml phenanthrene-d10 was added to each sample as an internal standard for correction. The concentrations for the calibration line started at 50 pg/mL and went up to 5 ng/mL. The sample solutions consisted of varying concentrations of phenanthrene, 0.5 ng/mL phenanthrene-d10 and ISO-medium. Measurements were performed in triplicates.

Animal experiments on *G. roeseli* were conducted at the Chair of Aquatic Systems Biology. The analytical concentration determination in the aqueous phase was carried out at the Chair of Urban Water Systems Engineering (TUM). For these measurements, solution mixtures of 50 µL of sample with 50 µL of phenanthrene-d10 (0.1 mg/L) and 9.9 mL ISO-Medium were prepared. Table 17 summarizes the phenanthrene concentration range to which the gammarids were exposed. Each concentration was applied to an environmental sample with microplastic particles,

Sublethal and lethal effects of particles in *in vitro* and *in vivo* assays depend on particle type and size

sediment, and a solvent control environment for comparison. The microplastic particles consisted of 40 – 63 µm sized PA particles with a particle concentration of 0.5 mg/L in each assay. The sediment was taken from the river Moosach.

Table 17: Phenanthrene concentration range in the gammarids experiment with the environmental sample without additives (Control), PMMA microplastic particles (MP) and sediment

Sample name	Time [h]	Concentration phenanthrene [mg/L]	Sample environment
Solvent control	0 + 48	0	0
Control	0 + 48	0	0
MP control	0 + 48	0	0
Sediment control	0 + 48 h	0	0
A	0 + 48	0.05	Control, MP & Sediment
B	0 + 48	0.075	Control, MP & Sediment
C	0 + 48	0.1	Control, MP & Sediment
D	0 + 48	0.25	Control, MP & Sediment
E	0 + 48	0.5	Control, MP & Sediment

Samples were taken at the beginning and after 48 hours of the experiment. 10 mL samples were transferred by pipette from each sample environment and frozen for storage. The frozen samples were thawed at 20 °C; 6 mL were taken. The samples were centrifuged with NuWind (NuAire, Plymouth, USA) at 1,000 rpm for 5 minutes. This was done to avoid a disturbance of the two-phase system (Gerstel Twister® and medium) by sediments or microplastics. From the centrifuged sample, 50 µL was transferred by pipette three times for a threefold concentration measurement with the Gerstel Twister®. This corresponded to a 200-fold dilution of the samples, which was necessary to avoid overloading the GC column. The samples were analyzed via TD-GC/MS.

6.2 Results and Discussion

Summary of the study published in Bartonitz et al., 2020 (Co-Author)

Particle exposure alone did not result in any effects in *G. roeseli*. The toxicity of phenanthrene regarding *G. roeseli* was reduced by the presence of sediment particles or PA particles after 24 h and 48 h. Also in the control samples, which contained neither sediment nor microplastic, a decrease in phenanthrene concentration after 48 h in aqueous medium was detected. Sorption to the glass surface of the containers cannot be excluded. Comparing the particle samples, the sorption of phenanthrene after 48 hours on the PA particles is slightly stronger compared to the sediment, as shown by TD-GC/MS analyses. Contrary to expectations, the presence of PA microparticles shows a reduction in mortality as well as changes in sublethal endpoints such as swimming behavior. These results can most likely be explained by similar sorption of phenanthrene to both particle types, resulting in lower bioavailability. These results are supported by Horton et al. (2018) [172]. The presence of PS microparticles alone showed no negative effect on the organism *Daphnia magna*. However, negative effects on mobility were observed in the presence of TOrcs dimethoate, which were independent of microplastic presence.

6.3 Conclusion

In the collaborative experiment with the Chair of Aquatic Systems Biology, initial conclusions can already be drawn about the influence on the toxicity of TOrcs in the presence of microplastics or sediment. The presence of both the sorption materials microplastics and sediment significantly reduced the phenanthrene content in the samples and by this lethal effects on *G. roeseli* so that *G. roeseli* died only at a higher phenanthrene concentration of 0.5 mg/L.

However, only the residual phenanthrene concentration in the aqueous phase was investigated in the current study. It has not yet been investigated how much phenanthrene is lost into the gas phase through the continuous mixing of the assays alone and whether phenanthrene also settles on the glass materials used. This could influence the available phenanthrene concentration and thus the toxicity to the target organism.

Thus, the hypothesis that **sublethal and lethal effects of particles in *in vitro* and *in vivo* assays depend on particle type (plastic or silica) and size can partially be accepted.**

7 Overall conclusions, prospects and future research challenges

Since the global pollution by micro- and nanoplastics is increasing, there is a growing interest in validated methods to enable a better classification of the extent of pollution. In this context the high sorption potential of different plastic particles and the determination of sorbed substances have to be taken into account. However, up to now, mainly time-consuming and laborious analytical techniques have been used to identify type of plastic particles and to identify and quantify sorbed TOrCs. In order to increase efficiency of analytical methods, TD-Pyr-GC/MS offers a valuable alternative.

7.1 Impacts and Conclusions of the Research Results

This work provides a validated method development of an analytical procedure for the identification or quantification of sorbed TOrCs on micro- or nanoplastic particles and also the polymer determination of the particles and addresses three main parts:

- (i) **The development of a method for the analysis of TOrCs and polymers in a single analytical setup using TD-Pyr-GC/MS.**

The analysis of sorbed TOrCs for micro- and nanoplastics is very laborious with current analytical methods due to e.g., extraction steps and time-consuming analytical procedures. TD-Pyr-GC/MS offers an alternative and potential for improvement. With reference particles (PS, PE, PMMA) and selected TOrCs (phenanthrene, triclosan, α -cypermethrin) a suitable method was developed. In the first step, the volatile substances were desorbed from the particle applying TD. Subsequently, the polymer was subjected to pyrolysis and by this disintegrated into characteristic fragments. GC/MS was used to analyze the desorbed molecules and the pyrolysis products. The method development and validation included the selection of the optimal TD temperature of 200 °C, ensuring the analysis of the highly volatile compounds (TOrCs) and simultaneously producing as few pyrolysis products as possible. The subsequent optimum pyrolysis temperature was set at 800 °C. This ensured complete fragmentation of the selected reference particles.

- (ii) **The application of the developed TD-Pyr-GC/MS method to define sorption processes and their dependencies on particle size and polymer type, the mixture of sorbed TOrCs and particle aging.**

The novel TD-Pyr-GC/MS method was subsequently applied to examine the dependence of TOrCs sorption on particle size and type, mixture of sorbed TOrCs and particle age. For this purpose, different micro- and nanoplastic particles (PS 40 μm , PS 41 μm , PS 78 nm;

PMMA 48 µm; PE 48 µm) were treated with selected TOrcs (phenanthrene, triclosan, α-cypermethrin). Samples were taken over a period of 48 h (sampling after 1 h, 24 h, 48 h) and sorption of the TOrcs was analyzed. Calculating the particle surface area, it was found that the high sorption on the PS 78 nm nanoparticles resulted mainly from the high number of particles and the therefrom resulting higher specific surface area. Taking this factor into account, the highest sorption was shown on the PE 48 µm particles. In further experiments, a mixture of TOrcs (phenanthrene, triclosan, α-cypermethrin) was simultaneously sorbed on PS 78 nm and 48 µm. In summary, sorption onto the PS nanoparticles was higher, which was evident in both the aqueous and particulate phases. In laboratory experiments, untreated PS and PA microplastic particles were treated with H₂O₂ to simulate aging of the particles. The treated particles were then analyzed by TD-Pyr-GC/MS. Based on the chromatograms and pyrograms, a change in the PS and PA particles was observed. In additional experiments, different TOrcs concentrations (1 mg/L, 5 mg/L, 10 mg/L) were used and by this it could be proven that quantification of TOrcs on nanoplastic particles (PS 78 nm) is possible.

(iii) The application of TD-GC/MS method to determine the residual TOrcs concentration in an ecotoxicological experiment.

In cooperation with the Chair of Aquatic Systems Biology, the first experiment demonstrated the relationship and effect between the presence of microplastic particles (PMMA) and a TOrc (phenanthrene) using the aquatic organism *G. roeseli*. The presence of microplastics or, in the control, sediment, significantly reduced the lethal effect. In addition to reducing mortality, the presence of the microplastic particles led to changes in sublethal endpoints such as swimming behavior. However, so far the TOrcs concentration could only be determined in the aqueous solution by TD-GC/MS and Gerstel Twister®. Phenanthrene concentration ranges of 0.05 - 0.5 mg/L were thus quantified. Quantification of the sorbed phenanthrene concentration on the PMMA particles was not performed in this experiment.

7.2 Remaining Challenges and Suggestions for Future Research

7.2.1 Screening of different micro- and nanoplastic polymers and TOrcs

In this work, seven different types of polymers (PE, PMMA, PS, PLA, PET, PA, PP) were investigated by TD-Pyr-GC/MS, sorption experiments were performed with PE, PMMA and PS. Three selected TOrcs (phenanthrene, triclosan, α-cypermethrin) were used for the sorption experiments. Based on the developed method of TD-Pyr-GC/MS, further sorption experiments, especially with nanoplastics, should be performed. Since it was shown that quantification of

sorbed TOrCs is possible, this provides further options for analysis of environmentally relevant TOrCs. Since TOrCs usually do not occur singularly in the environment, further mixing TOrCs experiments are recommended in order to enable environmentally relevant statements.

7.2.2 Application in screening procedures for ecotoxicological and laboratory tests

TD-Pyr-GC/MS could be used in the future to support qualitative and quantitative experiments, with environmental samples from ecotoxicological or laboratory wastewater treatment plant assays. However, the sample preparation of the particles has to be considered, which requires a specific design for each analytical problem. In addition, to validate TOrC concentrations on particles, the aqueous phase can be analyzed by TD-GC/MS.

7.2.3 Quantification of sorbed TOrCs by TD-Pyr-GC/MS compared with modeling

In order to better predict the sorption mechanisms and capacities, modeling will be used in the future, such as poly-parameter linear free - energy relationships (pp-LFERS) [144]. The pp-LFER models can be used to predict the partition coefficients for different environmental phases with high accuracy [144, 176]. The pp-LFERS between the sample (TOrCs), the air and the sorption material (polymers) can be calculated using the UFZ database [177]. So far, however, this is only possible for the polymers PDMS and PA. The combination of TD-GC/MS and TD-Pyr-GC/MS can be used to validate further models. This can also be applied to generate data on the concentration in the aqueous phase as well as on the particles. However, to date, these databases have been based on microplastic particles due to the lack of analytical techniques to validate sorption onto nanoplastic particles. TD-Pyr-GC/MS could provide the missing link here.

References

1. Wagner, M., et al., Microplastics in freshwater ecosystems: what we know and what we need to know. *Environmental Sciences Europe* **2014**.
2. de Souza Machado, A. A., et al., Microplastics as an emerging threat to terrestrial ecosystems. *Glob Chang Biol* **2017**.
3. Horton, A. A., et al., Microplastics in freshwater and terrestrial environments: Evaluating the current understanding to identify the knowledge gaps and future research priorities. *Sci Total Environ* **2017**.
4. Alimi, O. S., et al., Microplastics and Nanoplastics in Aquatic Environments: Aggregation, Deposition, and Enhanced Contaminant Transport. *Environ Sci Technol* **2018**, 52, (4), 1704-1724.
5. Andrady, A. L., The plastic in microplastics: A review. *Mar Pollut Bull* **2017**, 119, (1), 12-22.
6. Hidalgo-Ruz, V., et al., Microplastics in the marine environment: a review of the methods used for identification and quantification. *Environ Sci Technol* **2012**, 46, 3060–3075.
7. Thompson, R., et al., Lost at Sea: Where Is All the Plastic? *Science* **2004**.
8. Browne, M. A., et al., Microplastic—an emerging contaminant of potential concern? *Integrated Environmental Assessment and Management* **2007**, 3, (4), 559–566.
9. da Costa, J. P., et al., (Nano)plastics in the environment - Sources, fates and effects. *Sci Total Environ* **2016**, 566-567, 15-26.
10. Elert, A. M., et al., Comparison of different methods for MP detection: What can we learn from them, and why asking the right question before measurements matters? *Environ Pollut* **2017**, 231, 1256-1264.
11. Andrady, A. L., Microplastics in the marine environment. *Mar Pollut Bull* **2011**.
12. Senathirajah, K., et al., Estimation of the mass of microplastics ingested - A pivotal first step towards human health risk assessment. *J Hazard Mater* **2021**, 404, (Pt B), 124004.
13. Rossi, G., et al., Polystyrene Nanoparticles Perturb Lipid Membranes. *J Phys Chem Lett* **2014**.
14. Forte, M., et al., Polystyrene nanoparticles internalization in human gastric adenocarcinoma cells. *Toxicol In Vitro* **2016**.
15. Canesi, L., et al., Evidence for immunomodulation and apoptotic processes induced by cationic polystyrene nanoparticles in the hemocytes of the marine bivalve *Mytilus*. *Mar Environ Res* **2015**.
16. Velzeboer, I., et al., Strong sorption of PCBs to nanoplastics, microplastics, carbon nanotubes, and fullerenes. *Environ Sci Technol* **2014**, 48, 4869–4876.
17. Koelmans, A. A., et al., Microplastic as a Vector for Chemicals in the Aquatic Environment: Critical Review and Model-Supported Reinterpretation of Empirical Studies. *Environ Sci Technol* **2016**, 50, 3315–3326.
18. Ziccardi, L. M., et al., Microplastics as vectors for bioaccumulation of hydrophobic organic chemicals in the marine environment: A state-of-the-science review. *Environ Toxicol Chem* **2016**, 35, (7), 1667–1676.
19. Teuten, E. L., et al., Transport and release of chemicals from plastics to the environment and to wildlife. *Philos Trans R Soc Lond B Biol Sci* **2009**, 364, 2027–2045.
20. Hüffer, T.; Hofmann, T., Sorption of non-polar organic compounds by micro-sized plastic particles in aqueous solution. *Environ Pollut* **2016**, 214, 194e201.
21. Seidensticker, S., et al., Shift in Mass Transfer of Wastewater Contaminants from Microplastics in the Presence of Dissolved Substances. *Environ Sci Technol* **2017**, 51, 12254-12263.

22. Fries, E.; Zarfl, C., Sorption of polycyclic aromatic hydrocarbons (PAHs) to low and high density polyethylene (PE). *Environ Sci Pollut Res Int* **2012**, 19, 1296–1304.
23. Wang, J., et al., Size effect of polystyrene microplastics on sorption of phenanthrene and nitrobenzene. *Ecotoxicol Environ Saf* **2019**, 173, 331–338.
24. Löder, M. G. J., et al., Focal plane array detector-based micro-Fourier-transform infrared imaging for the analysis of microplastics in environmental samples. *Environmental Chemistry* **2015**, 12, (5).
25. Song, Y. K., et al., A comparison of microscopic and spectroscopic identification methods for analysis of microplastics in environmental samples. *Mar Pollut Bull* **2015**, 93, (1-2), 202-9.
26. Duemichen, E., et al., Fast identification of microplastics in complex environmental samples by a thermal degradation method. *Chemosphere* **2017**, 174, 572-584.
27. Shim, W. J., et al., Identification methods in microplastic analysis: a review. *Analytical Methods* **2017**, 9, (9), 1384-1391.
28. Browne, M. A., et al., Accumulation of microplastic on shorelines worldwide: sources and sinks. *Environ Sci Technol* **2011**, 45, (21), 9175-9.
29. Fischer, M.; Scholz-Bottcher, B. M., Simultaneous Trace Identification and Quantification of Common Types of Microplastics in Environmental Samples by Pyrolysis-Gas Chromatography-Mass Spectrometry. *Environ Sci Technol* **2017**, 51, 5052–5060.
30. Koelmans, A. A., et al., Microplastics in freshwaters and drinking water: Critical review and assessment of data quality. *Water Res* **2019**, 155, 410-422.
31. Mintenig, S. M., et al., Identification of microplastic in effluents of waste water treatment plants using focal plane array-based micro-Fourier-transform infrared imaging. *Water Res* **2017**.
32. Gregory, M., Plastic ‘Scrubbers’ in Hand Cleansers: a Further (and Minor) Source for Marine Pollution Identified. *Marine Pollution Bulletin* **1996**, 32, (12), 867-871.
33. Anger, P. M., et al., Raman microspectroscopy as a tool for microplastic particle analysis. *TrAC Trends in Analytical Chemistry* **2018**, 109, 214-226.
34. Cole, M., et al., Isolation of microplastics in biota-rich seawater samples and marine organisms. *Sci Rep* **2014**.
35. Imhof, H. K., et al., Contamination of beach sediments of a subalpine lake with microplastic particles. *Curr Biol* **2013**, 23, (19), R867-8.
36. Imhof, H. K., et al., A novel, highly efficient method for the separation and quantification of plastic particles in sediments of aquatic environments. *Limnology and Oceanography: Methods* **2012**, 10, (7), 524-537.
37. Anger, P. M., et al., Implementation of an open source algorithm for particle recognition and morphological characterisation for microplastic analysis by means of Raman microspectroscopy. *Analytical Methods* **2019**, 11, (27), 3483-3489.
38. Schwaferts, C., et al., Nanoplastic Analysis by Online Coupling of Raman Microscopy and Field-Flow Fractionation Enabled by Optical Tweezers. *Anal Chem* **2020**, 92, (8), 5813-5820.
39. Rial-Otero, R., et al., A Review of Synthetic Polymer Characterization by Pyrolysis–GC–MS. *Chromatographia* **2009**.
40. Duemichen, E., et al., Analysis of polyethylene microplastics in environmental samples, using a thermal decomposition method. *Water Res* **2015**, 85, 451-457.
41. Fries, E., et al., Identification of polymer types and additives in marine microplastic particles using pyrolysis-GC/MS and scanning electron microscopy. *Environ Sci Process Impacts* **2013**, 15, 1949–1956.
42. Herrera, M., et al., Fast identification of polymer additives by pyrolysis-gas chromatography/mass spectrometry. *Journal of Analytical and Applied Pyrolysis* **2003**, 70, (1), 35-42.

43. Klein, S., et al., Occurrence and Spatial Distribution of Microplastics in River Shore Sediments of the Rhine-Main Area in Germany. *Environ Sci Technol* **2015**.
44. Mei, W., et al., Interactions between microplastics and organic compounds in aquatic environments: A mini review. *Sci Total Environ* **2020**, 736, 139472.
45. Wang, F., et al., Sorption Behavior and Mechanisms of Organic Contaminants to Nano and Microplastics. *Molecules* **2020**, 25, (8).
46. Menendez-Pedriz, A.; Jaumot, J., Interaction of Environmental Pollutants with Microplastics: A Critical Review of Sorption Factors, Bioaccumulation and Ecotoxicological Effects. *Toxics* **2020**, 8, (2).
47. Karapanagioti, H. K.; Werner, D., Sorption of Hydrophobic Organic Compounds to Plastic in the Marine Environment: Sorption and Desorption Kinetics. *Hazardous Chemicals Associated with Plastics in the Marine Environment, Hdb Env Chem (2019)* **2018**.
48. Endo, S.; Koelmans, A. A., Sorption of Hydrophobic Organic Compounds to Plastics in the Marine Environment: Equilibrium. In *Hazardous Chemicals Associated with Plastics in the Marine Environment*, 2016; Vol. 78, pp 185-204.
49. Mattsson, K., et al., Nano-plastics in the aquatic environment. *Environ Sci Process Impacts* **2015**, 17, 1712–1721.
50. Wagner, M.; Lambert, S., Freshwater Microplastics Emerging Environmental Contaminants? *The Handbook of Environmental Chemistry* **2018**.
51. Hartmann, N. B., et al., Microplastics as vectors for environmental contaminants: Exploring sorption, desorption, and transfer to biota. *Integr Environ Assess Manag* **2017**.
52. Lee, H., et al., Sorption capacity of plastic debris for hydrophobic organic chemicals. *Sci Total Environ* **2014**.
53. Scherrer, R. A.; Howard, S. M., Use of distribution coefficients in quantitative structure-activity relations. *Journal of Medicinal Chemistry* **1977**.
54. Karapanagioti, H. K.; Klontza, I., Testing phenanthrene distribution properties of virgin plastic pellets and plastic eroded pellets found on Lesbos island beaches (Greece). *Mar Environ Res* **2008**.
55. Ter Halle, A., et al., To what extent are microplastics from the open ocean weathered? *Environ Pollut* **2017**, 227, 167-174.
56. Kooi, M.; Koelmans, A. A., Simplifying Microplastic via Continuous Probability Distributions for Size, Shape, and Density. *Environmental Science & Technology Letters* **2019**, 6, (9), 551-557.
57. Uber, T. H., et al., Sorption of non-ionic organic compounds by polystyrene in water. *Sci Total Environ* **2019**, 682, 348-355.
58. Bakir, A., et al., Competitive sorption of persistent organic pollutants onto microplastics in the marine environment. *Marine Pollution Bulletin* **2012**, 64, 2782–2789.
59. Liu, J., et al., Polystyrene Nanoplastics-Enhanced Contaminant Transport: Role of Irreversible Adsorption in Glassy Polymeric Domain. *Environ Sci Technol* **2018**.
60. Li, Y., et al., Effects of particle size and solution chemistry on Triclosan sorption on polystyrene microplastic. *Chemosphere* **2019**, 231, 308-314.
61. Ma, J., et al., Effect of microplastic size on the adsorption behavior and mechanism of triclosan on polyvinyl chloride. *Environ Pollut* **2019**, 254, (Pt B), 113104.
62. Zhan, Z., et al., Sorption of 3,3',4,4'-tetrachlorobiphenyl by microplastics: A case study of polypropylene. *Mar Pollut Bull* **2016**, 110, (1), 559-563.
63. Teuten, E., et al., Potential for Plastics to Transport Hydrophobic Contaminants. *Environ Sci Technol* **2007**, 41, 7759-7764.
64. Pascall, M. A., et al., Uptake of Polychlorinated Biphenyls (PCBs) from an Aqueous Medium by Polyethylene, Polyvinyl Chloride, and Polystyrene Films. *Journal of Agricultural and Food Chemistry* **2005**.

65. Reichel, J., et al., Systematic Development of a Simultaneous Determination of Plastic Particle Identity and Adsorbed Organic Compounds by Thermodesorption–Pyrolysis GC/MS (TD-Pyr-GC/MS). *Molecules* **2020**, 25, (4985).
66. Zhang, J., et al., Adsorption behavior and mechanism of 9-Nitroanthracene on typical microplastics in aqueous solutions. *Chemosphere* **2020**, 245, 125628.
67. Xu, B., et al., Microplastics play a minor role in tetracycline sorption in the presence of dissolved organic matter. *Environ Pollut* **2018**, 240, 87-94.
68. Wang, F., et al., The partition behavior of perfluorooctanesulfonate (PFOS) and perfluorooctanesulfonamide (FOSA) on microplastics. *Chemosphere* **2015**.
69. Bakir, A., et al., Transport of persistent organic pollutants by microplastics in estuarine conditions. *Estuarine, Coastal and Shelf Science* **2014**, 140, 14-21.
70. Seidensticker, S., et al., A combined experimental and modeling study to evaluate pH-dependent sorption of polar and non-polar compounds to polyethylene and polystyrene microplastics. *Environ Sci Eur* **2018**, 30, (30).
71. Guo, X.; Wang, J., Sorption of antibiotics onto aged microplastics in freshwater and seawater. *Mar Pollut Bull* **2019**, 149, 110511.
72. Zhang, H., et al., Enhanced adsorption of oxytetracycline to weathered microplastic polystyrene: Kinetics, isotherms and influencing factors. *Environ Pollut* **2018**, 243, (Pt B), 1550-1557.
73. Zuo, L. Z., et al., Sorption and desorption of phenanthrene on biodegradable poly(butylene adipate co-terephthalate) microplastics. *Chemosphere* **2019**, 215, 25-32.
74. Qiu, Y., et al., Sorption of polyhalogenated carbazoles (PHCs) to microplastics. *Mar Pollut Bull* **2019**, 146, 718-728.
75. Zhang, X., et al., Sorption of 3,6-dibromocarbazole and 1,3,6,8-tetrabromocarbazole by microplastics. *Mar Pollut Bull* **2019**, 138, 458-463.
76. Lin, W., et al., Sorption properties of hydrophobic organic chemicals to micro-sized polystyrene particles. *Sci Total Environ* **2019**, 690, 565-572.
77. Wang, W.; Wang, J., Different partition of polycyclic aromatic hydrocarbon on environmental particulates in freshwater: Microplastics in comparison to natural sediment. *Ecotoxicol Environ Saf* **2018**, 147, 648-655.
78. Bartonitz, A., et al., Modulation of PAH toxicity on the freshwater organism *G. roeseli* by microparticles. *Environmental Pollution* **2020**, 260.
79. Zhang, X., et al., Sorption of three synthetic musks by microplastics. *Mar Pollut Bull* **2018**, 126, 606-609.
80. Reichel, J., et al., Organic Contaminants and Interactions with Micro- and Nano-Plastics in the Aqueous Environment: Review of Analytical Methods. *Molecules* **2021**, 26, (4).
81. La Nasa, J., et al., Microwave-assisted solvent extraction and double-shot analytical pyrolysis for the quali-quantitation of plasticizers and microplastics in beach sand samples. *J Hazard Mater* **2020**, 401, 123287.
82. Guo, X., et al., Sorption properties of tylosin on four different microplastics. *Chemosphere* **2018**, 209, 240-245.
83. Li, S., et al., Aggregation kinetics of microplastics in aquatic environment: Complex roles of electrolytes, pH, and natural organic matter. *Environ Pollut* **2018**.
84. Zhao, L., et al., Sorption of five organic compounds by polar and nonpolar microplastics. *Chemosphere* **2020**, 257, 127206.
85. Liu, X., et al., Microplastics as Both a Sink and a Source of Bisphenol A in the Marine Environment. *Environ Sci Technol* **2019**, 53, (17), 10188-10196.
86. Liu, L., et al., Sorption of polycyclic aromatic hydrocarbons to polystyrene nanoplastic. *Environ Toxicol Chem* **2016**.
87. Hüffer, T., et al., Sorption of organic compounds by aged polystyrene microplastic particles. *Environmental Pollution* **2018**, 236, 218-225.

88. Llorca, M., et al., Adsorption and Desorption Behaviour of Polychlorinated Biphenyls onto Microplastics' Surfaces in Water/Sediment Systems. *Toxics* **2020**, 8, (3).
89. Endo, S., et al., Concentration of polychlorinated biphenyls (PCBs) in beached resin pellets: variability among individual particles and regional differences. *Mar Pollut Bull* **2005**, 50, (10), 1103-14.
90. Guo, X., et al., Sorption of sulfamethoxazole onto six types of microplastics. *Chemosphere* **2019**, 228, 300-308.
91. Chen, X., et al., Comparison of adsorption and desorption of triclosan between microplastics and soil particles. *Chemosphere* **2020**, 263, 127947.
92. Li, J., et al., Adsorption of antibiotics on microplastics. *Environ Pollut* **2018**.
93. Liu, P., et al., Effect of aging on adsorption behavior of polystyrene microplastics for pharmaceuticals: Adsorption mechanism and role of aging intermediates. *J Hazard Mater* **2020**, 384, 121193.
94. Liu, Z., et al., Adsorption of chlorophenols on polyethylene terephthalate microplastics from aqueous environments: Kinetics, mechanisms and influencing factors. *Environ Pollut* **2020**, 265, (Pt A), 114926.
95. Wu, X., et al., Adsorption of triclosan onto different aged polypropylene microplastics: Critical effect of cations. *Sci Total Environ* **2020**, 717, 137033.
96. Puckowski, A., et al., Sorption of pharmaceuticals on the surface of microplastics. *Chemosphere* **2020**, 263, 127976.
97. Ho, W. K., et al., Effects of Weathering on the Sorption Behavior and Toxicity of Polystyrene Microplastics in Multi-solute Systems. *Water Res* **2020**, 187, 116419.
98. Fan, X., et al., Investigation on the adsorption and desorption behaviors of antibiotics by degradable MPs with or without UV ageing process. *Journal of Hazardous Materials* **2021**, 401.
99. Zhang, H., et al., Sorption of fluoroquinolones to nanoplastics as affected by surface functionalization and solution chemistry. *Environ Pollut* **2020**, 262, 114347.
100. Wu, C., et al., Sorption of pharmaceuticals and personal care products to polyethylene debris. *Environ Sci Pollut Res Int* **2016**, 23, (9), 8819-26.
101. Xu, B., et al., The sorption kinetics and isotherms of sulfamethoxazole with polyethylene microplastics. *Mar Pollut Bull* **2018**, 131, (Pt A), 191-196.
102. Araujo, C. F., et al., Identification of microplastics using Raman spectroscopy: Latest developments and future prospects. *Water Res* **2018**, 142, 426-440.
103. Kappler, A., et al., Analysis of environmental microplastics by vibrational microspectroscopy: FTIR, Raman or both? *Anal Bioanal Chem* **2016**, 408, 8377-8391.
104. Duemichen, E., et al., Assessment of a new method for the analysis of decomposition gases of polymers by a combining thermogravimetric solid-phase extraction and thermal desorption gas chromatography mass spectrometry. *J Chromatogr A* **2014**, 1354, 117-128.
105. Sobhani, Z., et al., Identification and visualisation of microplastics/nanoplastics by Raman imaging (i): Down to 100 nm. *Water Res* **2020**, 174, 115658.
106. La Nasa, J., et al., A review on challenges and developments of analytical pyrolysis and other thermoanalytical techniques for the quali-quantitative determination of microplastics. *Journal of Analytical and Applied Pyrolysis* **2020**, 149.
107. Reichel, J., et al., A Novel Analytical Approach to Assessing Sorption of Trace Organic Compounds into Micro- and Nanoplastic Particles. *Biomolecules* **2022**, 12, (7).
108. Bakir, A., et al., Enhanced desorption of persistent organic pollutants from microplastics under simulated physiological conditions. *Environ Pollut* **2014**, 185, 16-23.
109. Al-Azzawi, M. S. M., et al., Validation of Sample Preparation Methods for Microplastic Analysis in Wastewater Matrices—Reproducibility and Standardization. *Water* **2020**, 12, (9).

110. Samanta, S. K., et al., Polycyclic aromatic hydrocarbons: environmental pollution and bioremediation. *TRENDS in Biotechnology* **2002**, 20, (6), 243-248.
111. Polat, H., et al., Investigation of acute toxicity of beta-cypermethrin on guppies *Poecilia reticulata*. *Chemosphere* **49** (2002) 39–44 **2002**.
112. Elbetieha, A., et al., Evaluation of the toxic potentials of cypermethrin pesticide on some reproductive and fertility parameters in the male rats. *Arch Environ Contam Toxicol* **2001**.
113. Yu, F., et al., Adsorption behavior of organic pollutants and metals on micro/nanoplastics in the aquatic environment. *Sci Total Environ* **2019**, 694, 133643.
114. Kawaguchi, M., et al., Simultaneous analysis of benzophenone sunscreen compounds in water sample by stir bar sorptive extraction with in situ derivatization and thermal desorption-gas chromatography-mass spectrometry. *J Chromatogr A* **2008**.
115. Baltussen, E., et al., Stir Bar Sorptive Extraction (SBSE), a Novel Extraction Technique for Aqueous Samples: Theory and Principles. *J. Microcolumn Separations* **1999**.
116. David, F., et al., Stir-Bar Sorptive Extraction of Trace Organic Compounds from Aqueous Matrices. *LC GC Europe* **2003**.
117. Horák, T., et al., Determination of Some Beer Flavours by Stir Bar Sorptive Extraction and Solvent Back Extraction. *Journal of the institute of Brewing* **2007**.
118. Ochiai, N., et al., Optimization of a multi-residue screening method for the determination of 85 pesticides in selected food matrices by stir bar sorptive extraction and thermal desorption GC-MS. *Journal of Separation Science* **2005**, 28, 1083–1092.
119. Ettre, L. S., Nomenclature for chromatography. *Pure & Appl. Chem.* **1993**, 65, (4), 819-872.
120. Tsuge Shin, et al., Pyrolysis - GC MS Data Book of Synthetic Polymers - Pyrograms Thermograms and MS of Pyrolyzates. **2011**.
121. Serrano, D. P., et al., An investigation into the catalytic cracking of LDPE using Py-GC/MS. *Journal of Analytical and Applied Pyrolysis* **2005**, 74, 370–378.
122. Soják, L., et al., High resolution gas chromatographic–mass spectrometric analysis of polyethylene and polypropylene thermal cracking products. *Journal of Analytical and Applied Pyrolysis* **2007**, 78, 387–399.
123. Kebelmann, K., et al., Intermediate pyrolysis and product identification by TGA and Py-GC/MS of green microalgae and their extracted protein and lipid components. *Biomass and Bioenergy* **2013**, 49, 38-48.
124. Bakir, A., et al., Transport of persistent organic pollutants by microplastics in estuarine conditions. *Estuarine, Coastal Shelf Sci.* **2014**, 140, 14-21.
125. Duemichen, E., et al., Automated Thermal Extraction - Desorption Gas Chromatography Mass Spectrometry: A Multifunctional Tool for Comprehensive Characterization of Polymers and their Degradation Products. *Journal of Chromatography A* **2019**.
126. Kleine-Benne, E.; Rose, B., Versatile Automated Pyrolysis GC Combining a Filament Type Pyrolyzer with a Thermal Desorption Unit. *Application note 4/2011* **2011**.
127. Bergmann, M., et al., Marine Anthropogenic Litter. *Springer, Berlin* **2015**.
128. Rochman, C. M., et al., Long-term field measurement of sorption of organic contaminants to five types of plastic pellets: implications for plastic marine debris. *Environ Sci Technol* **2013**.
129. Atugoda, T., et al., Adsorptive interaction of antibiotic ciprofloxacin on polyethylene microplastics: Implications for vector transport in water. *Environmental Technology & Innovation* **2020**, 19.
130. Gonzalez-Pleiter, M., et al., Microplastics as vectors of the antibiotics azithromycin and clarithromycin: Effects towards freshwater microalgae. *Chemosphere* **2021**, 268, 128824.
131. Tourinho, P. S., et al., Partitioning of chemical contaminants to microplastics: Sorption mechanisms, environmental distribution and effects on toxicity and bioaccumulation. *Environ Pollut* **2019**, 252, (Pt B), 1246-1256.

132. Barnes, D. K., et al., Accumulation and fragmentation of plastic debris in global environments. *Philos Trans R Soc Lond B Biol Sci* **2009**.
133. Roy, P. K., et al., Degradable polyethylene: fantasy or reality. *Environ Sci Technol* **2011**.
134. Lambert, S.; Wagner, M., Characterisation of nanoplastics during the degradation of polystyrene. *Chemosphere* **2016**.
135. Lowry, G. V., et al., Transformations of nanomaterials in the environment. *Environ Sci Technol* **2012**.
136. Zhang, H., et al., Enhanced Adsorption of Molecules on Surfaces of Nanocrystalline Particles. *J. Phys. Chem. B* **1999**, 103, 4656-4662.
137. Stark, J. V.; Klabunde, K. J., Nanoscale Metal Oxide Particles/Clusters as Chemical Reagents. Adsorption of Hydrogen Halides, Nitric Oxide, and Sulfur Trioxide on Magnesium Oxide Nanocrystals and Compared with Microcrystals. *Chem. Mater.* **1996**, 8, 1913-1918.
138. Hüffer, T., et al., Microplastic Exposure Assessment in Aquatic Environments: Learning from Similarities and Differences to Engineered Nanoparticles. *Environ Sci Technol* **2017**, 51, 2499–2507.
139. Koelmans, A. A., et al., Nanoplastics in the Aquatic Environment. Critical Review. In *Marine Anthropogenic Litter*, 2015; pp 325-340.
140. Parida, S. K., et al., Adsorption of organic molecules on silica surface. *Adv Colloid Interface Sci* **2006**.
141. Napper, I. E., et al., Characterisation, quantity and sorptive properties of microplastics extracted from cosmetics. *Mar Pollut Bull* **2015**, 99, 178-185.
142. Xing, B.; Pignatello, J., Dual-Mode Sorption of Low-Polarity Compounds in Glassy Poly(Vinyl Chloride) and Soil Organic Matter. *Environ. Sci. Technol.* **1997**, 31, 792-799.
143. Vieira, Y., et al., Microplastics physicochemical properties, specific adsorption modeling and their interaction with pharmaceuticals and other emerging contaminants. *Sci Total Environ* **2020**, 753, 141981.
144. Fred-Ahmadu, O. H., et al., Interaction of chemical contaminants with microplastics: Principles and perspectives. *Sci Total Environ* **2020**, 706, 135978.
145. Ward, C. P., et al., Sunlight Converts Polystyrene to Carbon Dioxide and Dissolved Organic Carbon. *Environmental Science & Technology Letters* **2019**, 6, (11), 669-674.
146. Luo, H., et al., Environmental behaviors of microplastics in aquatic systems: A systematic review on degradation, adsorption, toxicity and biofilm under aging conditions. *J Hazard Mater* **2022**, 423, (Pt A), 126915.
147. Rummel, C. D., et al., Impacts of Biofilm Formation on the Fate and Potential Effects of Microplastic in the Aquatic Environment. *Environmental Science & Technology Letters* **2017**, 4, (7), 258-267.
148. Liu, P., et al., Review of the artificially-accelerated aging technology and ecological risk of microplastics. *Sci Total Environ* **2021**, 768, 144969.
149. Brandon, J., et al., Long-term aging and degradation of microplastic particles: Comparing in situ oceanic and experimental weathering patterns. *Mar Pollut Bull* **2016**, 110, (1), 299-308.
150. Liu, G., et al., Sorption behavior and mechanism of hydrophilic organic chemicals to virgin and aged microplastics in freshwater and seawater. *Environ Pollut* **2019**, 246, 26-33.
151. Kwon, B. G., et al., Global styrene oligomers monitoring as new chemical contamination from polystyrene plastic marine pollution. *J Hazard Mater* **2015**, 300, 359-367.
152. Liu, X., et al., Hydrophobic sorption behaviors of 17beta-Estradiol on environmental microplastics. *Chemosphere* **2019**, 226, 726-735.
153. Xue, X. D., et al., Adsorption behaviors of the pristine and aged thermoplastic polyurethane microplastics in Cu(II)-OTC coexisting system. *J Hazard Mater* **2021**, 407, 124835.

154. Luo, H., et al., Aging of microplastics affects their surface properties, thermal decomposition, additives leaching and interactions in simulated fluids. *Sci Total Environ* **2020**, 714, 136862.
155. Razanajatovo, R. M., et al., Sorption and desorption of selected pharmaceuticals by polyethylene microplastics. *Mar Pollut Bull* **2018**, 136, 516-523.
156. Rochman, C. M., et al., Polystyrene plastic: a source and sink for polycyclic aromatic hydrocarbons in the marine environment. *Environ Sci Technol* **2013**.
157. Behera, S. K., et al., Sorption of triclosan onto activated carbon, kaolinite and montmorillonite: Effects of pH, ionic strength, and humic acid. *Journal of Hazardous Materials* **2010**, 179, (1-3), 684-691.
158. Xu, J., et al., Sorption of triclosan on electrospun fibrous membranes: Effects of pH and dissolved organic matter. *Emerging Contaminants* **2015**, 1, (1), 25-32.
159. Sun, T., et al., Microplastics aggravate the bioaccumulation and toxicity of coexisting contaminants in aquatic organisms: A synergistic health hazard. *J Hazard Mater* **2022**, 424, (Pt B), 127533.
160. Au, S. Y., et al., Responses of *Hyalella azteca* to acute and chronic microplastic exposures. *Environ Toxicol Chem* **2015**.
161. Nugnes, R., et al., Toxic impact of polystyrene microplastic particles in freshwater organisms. *Chemosphere* **2022**, 299, 134373.
162. Na, J., et al., Synergistic effect of microplastic fragments and benzophenone-3 additives on lethal and sublethal *Daphnia magna* toxicity. *J Hazard Mater* **2021**, 402, 123845.
163. Eerkes-Medrano, D., et al., Microplastics in freshwater systems: a review of the emerging threats, identification of knowledge gaps and prioritisation of research needs. *Water Res* **2015**.
164. Windsor, F. M., et al., Microplastic ingestion by riverine macroinvertebrates. *Sci Total Environ* **2019**.
165. Bour, A., et al., Environmentally relevant microplastic exposure affects sediment-dwelling bivalves. *Environ Pollut* **2018**, 236, 652-660.
166. Sussarellu, R., et al., Oyster reproduction is affected by exposure to polystyrene microplastics. *Proc Natl Acad Sci U S A* **2016**, 113, (9), 2430-5.
167. von Moos, N., et al., Uptake and effects of microplastics on cells and tissue of the blue mussel *Mytilus edulis* L. after an experimental exposure. *Environ Sci Technol* **2012**, 46, (20), 11327-35.
168. Scherer, C., et al., Feeding type and development drive the ingestion of microplastics by freshwater invertebrates. *Sci Rep* **2017**.
169. Hoang, T. C.; Felix-Kim, M., Microplastic consumption and excretion by fathead minnows (*Pimephales promelas*): Influence of particles size and body shape of fish. *Sci Total Environ* **2020**, 704, 135433.
170. Cormier, B., et al., Chemicals sorbed to environmental microplastics are toxic to early life stages of aquatic organisms. *Ecotoxicol Environ Saf* **2021**, 208, 111665.
171. Vethaak, A. D.; Leslie, H. A., Plastic Debris Is a Human Health Issue. *Environ Sci Technol* **2016**.
172. Horton, A. A., et al., Acute toxicity of organic pesticides to *Daphnia magna* is unchanged by co-exposure to polystyrene microplastics. *Ecotoxicol Environ Saf* **2018**.
173. Besseling, E., et al., Nanoplastic Affects Growth of *S. obliquus* and Reproduction of *D. magna*. *Environmental Science & Technology* **2014**.
174. Kokalj, A. J., et al., Screening study of four environmentally relevant microplastic pollutants: Uptake and effects on *Daphnia magna* and *Artemia franciscana*. *Chemosphere* **2018**.
175. Rehse, S., et al., Short-term exposure with high concentrations of pristine microplastic particles leads to immobilisation of *Daphnia magna*. *Chemosphere* **2016**.

176. Stenzel, A., et al., Determination of polyparameter linear free energy relationship (pp-LFER) substance descriptors for established and alternative flame retardants. *Environ Sci Technol* **2013**, 47, (3), 1399-406.
177. Lorenzo-Parodi, N., et al., Solventless microextraction techniques for water analysis. *TrAC Trends in Analytical Chemistry* **2019**, 113, 321-331.

Appendix I

Organic Contaminants and Interactions with Micro- and Nano-Plastics in the Aqueous Environment: Review of Analytical Methods

Molecules 2021, 26, 1164.

This review article examines the analysis of trace organic chemicals (TOrcs) sorbed onto micro- and nano-plastic particles. It discusses various analytical methods, including gas chromatography (GC), liquid chromatography (LC), and ultraviolet-visible spectroscopy (UV-VIS). The article also explores factors influencing sorption, such as particle size, shape, polymer type, and aging effects. Overall, it provides a comprehensive overview of methods for identifying and quantifying TOrcs on plastic particles.

Julia Reichel conducted the literature study and wrote the manuscript. Oliver Knoop contributed to the chapter 3.4. and reviewed the manuscript. Johanna Grassmann, Jörg E. Drewes and Thomas Letzel reviewed the manuscript and contributed to the discussion.

Review

Organic Contaminants and Interactions with Micro- and Nano-Plastics in the Aqueous Environment: Review of Analytical Methods

 Julia Reichel ¹, Johanna Graßmann ¹, Oliver Knoop ¹ , Jörg E. Drewes ¹  and Thomas Letzel ^{1,2,*}

¹ Urban Water Systems Engineering, Technical University of Munich, Am Coulombwall 3, 85748 Garching, Germany; julia.reichel@tum.de (J.R.); j.grassmann@tum.de (J.G.); oliver.knoop@tum.de (O.K.); jdrewes@tum.de (J.E.D.)

² Analytisches Forschungsinstitut für Non-Target Screening GmbH (AFIN-TS GmbH), Am Mittleren Moos 48, 86167 Augsburg, Germany

* Correspondence: T.Letzel@tum.de; Tel.: +49-(0)151-56330216

Abstract: Micro- and nanoplastic particles are increasingly seen not only as contaminants themselves, but also as potential vectors for trace organic chemicals (TOCs) that might sorb onto these particles. An analysis of the sorbed TOCs can either be performed directly from the particle or TOCs can be extracted from the particle with a solvent. Another possibility is to analyze the remaining concentration in the aqueous phase by a differential approach. In this review, the focus is on analytical methods that are suitable for identifying and quantifying sorbed TOCs on micro- and nano-plastics. Specific gas chromatography (GC), liquid chromatography (LC) and ultraviolet-visible spectroscopy (UV-VIS) methods are considered. The respective advantages of each method are explained in detail. In addition, influencing factors for sorption in the first place are being discussed including particle size and shape (especially micro and nanoparticles) and the type of polymer, as well as methods for determining sorption kinetics. Since the particles are not present in the environment in a virgin state, the influence of aging on sorption is also considered.

Keywords: sorption; microplastic; nanoplastic; analytic methods; GC; HPLC



Citation: Reichel, J.; Graßmann, J.; Knoop, O.; Drewes, J.E.; Letzel, T. Organic Contaminants and Interactions with Micro- and Nano-Plastics in the Aqueous Environment: Review of Analytical Methods. *Molecules* **2021**, *26*, 1164. <https://doi.org/10.3390/molecules26041164>

Academic Editors: Constantinos K. Zacharis and Joselito P. Quirino

Received: 10 January 2021
Accepted: 18 February 2021
Published: 22 February 2021

Publisher's Note: MDPI stays neutral with regard to jurisdictional claims in published maps and institutional affiliations.



Copyright: © 2021 by the authors. Licensee MDPI, Basel, Switzerland. This article is an open access article distributed under the terms and conditions of the Creative Commons Attribution (CC BY) license (<https://creativecommons.org/licenses/by/4.0/>).

1. Introduction

Micro- and nanoplastic particles can serve both as sources and sinks for pollutants in the environment. Therefore, on the one hand, sorption of pollutants on microplastics might pose a problem; on the other hand, microplastic itself must be considered as a contaminant. Monomers, additives, plasticizers, and others can desorb and may cause additional potential risks [1–7].

In recently published reviews, sorption of trace organic chemicals (TOCs) on micro- and nanoplastics has already been examined in detail [8–11]. In these studies, the focus is on the influence of the physical properties of particles (such as size, surface, crystallinity) and the resulting interaction properties of TOCs and polymers. The sorption mechanisms and ecotoxicological factors are also considered. In contrast to the previously published articles, the purpose of this article is to provide an overview of suitable analytical approaches for determining the sorption of TOCs on particles. The focus is on GC, HPLC, and UV-VIS methods. Furthermore, typical sorption strategies will be discussed.

Concerns about the possible harmful effects of microplastics relates not only to the particles themselves but also to their ability to transport pollutants. Those pollutants can be divided into two groups: (i) hydrophobic chemicals adsorbed from the aquatic environment due to their affinity for the hydrophobic surface of plastics and (ii) additives, monomers, and oligomers present as constituents of polymers [12]. Adsorbed hydrophobic pollutants with low water solubility become more mobile indirectly by binding to plastic

particles. Thus, their transport on particles can increase their distribution in environmental matrices and organisms as well as their bioavailability.

The sorption processes depend mainly on the nature of the polymer and can be divided into adsorption to the surface or absorption into the polymer [5,13,14]. The principle of both sorption types is to achieve an equilibrium of TOrcs concentrations between the solid and liquid phases. The sorption equilibrium can be reached either quickly by adsorption (onto particles) or slower by absorption (into the particle structure) [15]. In recent years, the analysis of pure micro- and nanoplastics has gained great interest but also the analysis of sorbed TOrcs on these particles [8,16]. With optical analysis methods like Raman spectroscopy or Fourier-transform infrared spectroscopy (FTIR) analysis, quantitative analyses of particles and analyses of particle size as well as shape can be conducted [17,18]. Thermal analysis methods such as pyrolysis gas chromatography-mass spectrometry (Py-GC/MS) can be used to analyze TOrcs or the additives in the polymers [19,20]. This review summarizes the current state-of-the-art in analyzing the degree of TOrcs sorption on micro- and nanoparticles.

2. Analysis of TOrcs on Micro- and Nanoplastic Particles: Typical Methods and Techniques

Analysis of sorbed TOrcs on particles in a liquid phase can be performed in either the aqueous or gas phase, or on the particles, respectively [5,13,20,21]. Different techniques like GC/MS, HPLC-DAD, UHPLC-MS/MS, UV spectrometer, or liquid scintillation counting are commonly used for this purpose [21–24].

2.1. General Experimental Design of Sorption Experiments

Principally, the experimental design studying sorption kinetics or processes in aqueous suspensions is identical in all experimental approaches. Selected particles and TOrcs are added to a liquid phase such as ultrapure water, freshwater, sea water, or synthetic water containing humic acids to mimic natural organic matter [13,20,25]. Variations in pH, salinity, or humic substances are made to simulate different environmental conditions [26–28]. Some studies use microparticles, additive-free particles, or extracted particles from cosmetics covering a certain size range [29,30]. Commonly targeted TOrcs used as sorbates in these investigations represent antibiotics, additives, pesticides, biocides, endocrine disrupting chemicals, hormones, or disinfection byproducts [24,31–36]. A schematic of the sample preparation is shown in Figure 1. In the aqueous solution, particles and TOrcs are incubated for a certain period of time and the suspension is subsequently shaken for various time periods (Tables 1 and 2). Subsequently, the particles must be separated from the aqueous phase for analysis. This is achieved for instance by filtration or centrifugation [20,37,38]. The analysis of the sorbed substances happens either directly on the particles or indirectly by solvent extraction (e.g., n-hexane, dichloromethane) decoupled from the particles [13,20,39,40]. An indirect analysis of the aqueous phase via liquid/liquid extraction or by a passive sampler is also possible [4,21,41,42]. Due to the remaining concentration in the aqueous phase, an assessment can be made on the amount of sorbed substances on the particles [43]. Furthermore, the gas phase can also be investigated [5,44].

The final analysis can be performed by various analytical techniques, such as GC/MS, GC/ECD, HPLC/MS, HPLC/UV, liquid scintillation counter, or spectrophotometer [4,6,24,30,45–49]. An overview of the workflow from a sample preparation for the analytical technique is illustrated in Figure 1. A detailed consideration of the different analytical techniques is presented in the following sections.

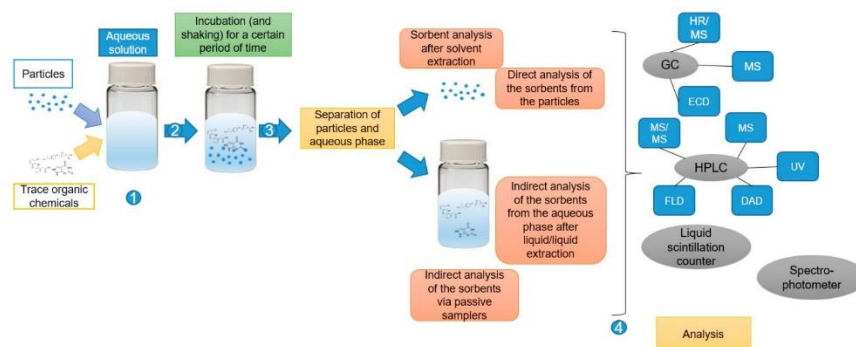


Figure 1. Workflow from a sample preparation of sorption experiments for analytical detection techniques. First, the particles and the TOrcs are incubated in aqueous solution for a certain period of time. This is followed by the separation of the particles and the aqueous phase. Depending on the choice of analytical technique, either the aqueous or the particle phase is processed. The analysis is either based on a gas chromatography method followed by high resolution/mass spectrometry (HR/MS), mass spectrometry (MS) or electron capture detection (ECD) analysis or based on a high performance liquid chromatography (HPLC) method followed by MS/MS, MS, ultraviolet (UV), diode-array detector (DAD) or fluorescence detector (FLD). Further analytical methods are liquid scintillation counter and spectrophotometer.

2.2. GC/MS

With GC/MS, volatile substances can be determined. This method is often used for the investigation of sorbed substances on polymer particles [13,26,45,46]. In a GC/MS analysis, either the aqueous phase, the particles, or the gas phase can be examined for TOrcs [5,13,39]. An overview of different sorption studies of microplastic particles performed with GC/MS is shown in Table 1. The advantages of GC analysis are that it allows direct analysis of TOrcs from the particle, requires little sample preparation, and is, thus, quick to perform (2–3 h per sample) [20,50,51]. By coupling with, e.g., a pyrolysis unit, polymers can be identified in addition to sorbed TOrcs [50]. In combination with an MS, detailed results for target and non-target analysis can be provided.

2.2.1. Direct Analysis by Pyrolysis and TED-GC/MS

Currently, GC/MS analysis is mainly used for microplastic analysis and polymer identification. For this purpose, the GC/MS is coupled with a pyrolysis unit (Pyr) or a thermal-extraction-desorption (TED)/thermogravimetric (TGA) unit [19,50–54]. A recently published review provides a good summary of these methods [55]. In general, only the polymer can be identified and quantified with the thermoanalytical systems. A determination of size is not possible. An established method for the identification of plastics in various environmental matrices is Pyrolysis-GC/MS. [52,56–60]. One advantage of this method is that both micro- and nanoplastics can be analyzed [61]. Recently, pyrolysis methods have been developed further by coupling with for instance a sequential pyrolysis, a double shot pyrolysis, or a thermal desorption (TD) unit with pyrolysis [19,20,50,53]. The aim of these methods is to identify not only the polymer itself but also additives or sorbed substances.

Double shot pyrolysis can be run in two different modes [53]: (1) in desorption mode, the volatile substances such as additives are desorbed; (2) in pyrolysis mode, the polymers are degraded. In sequential pyrolysis, several runs with different temperature maxima are performed in series [50].

TD-Pyr-GC/MS (thermodesorption-pyrolysis-GC/MS) combines these two systems into one analytical setup to investigate sorbed TOrcs before analyzing the polymer [20].

After method development, the TOrcs can be identified in the first step and the polymer type in the second step.

Another method for the determination of polymers and additives is via Thermal-Extraction-Desorption-GC/MS (TED-GC/MS) coupled with thermogravimetric analysis (TGA) [54]. In TGA, the polymers are heated and their volatile decomposition products are trapped on a solid-phase adsorber such as a Gerstel Twister or a Sorb-Star[®] [62,63]. The trapped substances are heated and then analyzed by GC/MS. An advantage of this method is that the number of particles can also be quantified.

The benefit of these thermoanalytical systems is that the samples can be analyzed in a short amount of time (2–3 h) [20]. There is no need for complex extraction procedures, but the samples can usually be analyzed directly. Often, however, there is a carry-over of the samples during the Pyr-GC/MS [64]. Therefore, it is recommended to run many blanks to identify and eliminate them. Analytical reproducibility can also be problematic [64].

2.2.2. GC/MS Analysis after Extraction of Sorbents

For indirect analysis of sorbed substances or additives, these can be extracted from the microplastic particles with solvents, see Table 1. Table 1 shows the phase that is analyzed to obtain the concentrations of TOrcs. For this purpose, the trace organic chemical can be extracted from the particle, for instance by means of soxhlet extraction [65]. The TOrcs are washed off the particle with a solvent (e.g., dichloromethane), concentrated, purified, and finally analyzed. Another possibility is the indirect determination of the concentration via the aqueous phase [21,41]. Therefore, a liquid/liquid extraction is performed. A portion of the aqueous solution is mixed with a solvent (e.g., hexane), placed in an ultrasonic bath and then stirred. The upper solution layer is then used for the GC/MS analysis [41].

Table 1. Summary of GC/MS methods to analyze sorbed substances on various microplastic particles like polyethylene (PE), polystyrene (PS), polyamide (PA), polyvinyl chloride (PVC), polypropylene (PP), polyethylene terephthalate (PET) and polymethyl methacrylate (PMMA).

Particle Type	Particle Size (μm)	Sorbate	Analytical Method	Analyzed Phase	Reference
PE	260	Phenanthrene, Tonalide, Benzophenone	GC/MS after extraction with cyclohexane	Particle (Extraction)	[13]
PE, PS	PE: 260, PS: 250	Atrazine, Benzotriazole, Caffeine, Carbamazepine, Carbendazim, DEET, Diazinon, Diclofenac, Ibuprofen, MCPA, Mecoprop, 4-Nonylphenol, Phenanthrene, Propiconazole, Tris(2-chloroisopropyl)-phosphate (TCPP), Tebuconazole, Terbutryn, Torasemide, Triclosan	GC/MS, LC-MS/MS after extraction with cyclohexane	Particle (Extraction)	[26]
PA, PE, PVC, PS	<250	n-Hexane, Cyclohexane, Benzene, Toluene, Chlorobenzene, Ethylbenzoate, Naphtalene	Headspace GC/MS or in-tube-microextraction	Gaseous phase	[5]
PS (aged)	125–250	Various aliphatics and aromatics	GC/MS headspace from three-phase system	Gaseous phase	[44]
PE, PS, Fullerene, Sediment	PE: 10–180 PS: 0.07	17 Polychlorinated biphenyls (PCBs)	GC/MS after extraction with pentane-dichloromethane	Aqueous phase via passive sampler	[45]
PE, PP, PS	320–440	8 Polycyclic aromatic hydrocarbons (PAHs), 4 Hexachlorocyclohexanes (HCHs), 2 Chlorinated benzenes (CBs)	GC-ECD after extraction with n-hexane	Aqueous phase and PDMS phase	[4]
PP	450–850	Tonalide, Musk xylene, Musk ketone	GC/MS after extraction with n-hexane and dichloromethane	Particle (extraction)	[46]
PS, PE, PET	PE: 3–16 PS: 10 PET: <300	38 PCB congeners	GC-HRMS after soxhlet extraction with dichloromethane	Particle (extraction)	[65]
PE, PP (environmental samples)	<500	PCBs (IUPAC nos. 28, 52, 101, 118, 138, 153, 180)	GC-ECD after soxhlet extraction with dichloromethane	Particle (extraction)	[66]
PS	2; 1; 0.1	Eighteen unsubstituted hydrophobic organic chemicals (HOCs)	GC/MS after liquid / liquid extraction	Aqueous phase via passive sampler	[41]
PE, PS, PVC	<150	Five polyhalogenated carbazoles (PHCs)	GC/MS after washing with n-hexane and dichloromethane	Particle (extraction)	[39]
PE, PP, PS	100–150	9-Nitroanthracene	GC/MS after liquid/liquid extraction	Aqueous phase	[21]
PP	450–850	3,6-Dibromocarbazole and 1,3,6,8-Tetrabromocarbazole	GC/MS after extraction with n-hexane and dichloromethane	Particle (extraction)	[40]
PS, PE, PMMA	PS: 40, 41, 0.078 PMMA: 48 PE: 48	Phenanthrene, Triclosan, α -Cypermethrin	TD-Pyr-GC/MS	Particle (directly)	[20]

2.3. HPLC

In addition to GC, high performance liquid chromatography (HPLC) is also an established chromatographic method for determining the sorption of TORCs on micro- and nanoparticles [67–69]. Samples are usually filtered prior to analysis and the concentration on the particles is then determined indirectly via the supernatant.

Another method is solvent extraction of the particles or solid phase extraction. The HPLC is typically coupled to a UV-detector (UV), a diode array detector (DAD), a fluorescence detector (FD), or a mass spectrometer [38,47,67,70]. A summary of selected studies performed by HPLC is shown in Table 2. In most studies, chromatography was performed with a C-18 column, which captures nonpolar to intermediate polar TORCs [22,28,34,38,48,67,70–76]. Advantages of an HPLC analysis are that an individual separation of the individual molecules takes place and detailed results can be (re)produced [47,70,71].

Table 2. Summary of HPLC methods to analyze sorbed substances on micro- and nanoplastic particles like polybutylenadipat-terephthalat (PBAT), low-density polyethylene (LD-PE) or high-density polyethylene (HD-PE).

Particle Type	Particle Size (μm)	Sorbate	Analytical Method	Analysis	Reference
PS	0.5, 0.235, 0.80, 30, 50, 102, 170	Phenanthrene, Nitrobenzene	HPLC	Supernatant	[37]
PE, PP, PS, PVC	<200	Tylosin	HPLC + DAD	Supernatant	[67]
PA, PE, PET, PS, PVC, PP	100, 150	Sulfamethoxazole	HPLC	Supernatant	[77]
PBAT, PE, PS	PBAT: 2338 \pm 486, PE: 2628 \pm 623 / Reference Particles: PE: 400PS: 250 PE: 225 + 41 PS: 313 + 48	Phenanthrene	HPLC + -UV	Supernatant	[38]
PE, PS, soil	75–180	Triclosan	HPLC + UV	Methanol extraction of the particles	[34]
PE, PS, PP, PA, PVC	75–180	Sulfadiazine, Amoxicillin, Tetracycline, Ciprofloxacin, Trimethoprim	HPLC + UV	Supernatant	[71]
PS	75.4, 106.9, 150.5, 214.6	Triclosan	HPLC + UV	Supernatant	[72]
PS	0.07	Phenanthrene, Anthracene, Fluoranthene, Pyrene, Benzo[a]anthracene, Chrysene, Benzo[b]fluoranthene, Benzo[k]fluoranthene, Benzo[a]pyrene, Benzo [g,h,i] perylene	HPLC + FD	Extraction via Polyoxymethylene sheets	[70]
PS (aged)	50.4 \pm 11.9	Atorvastatin, Amlodipine	HPLC + UV	Supernatant	[78]
PET	<150	4-Chlorophenol, 2,4,6-Trichlorophenol, Fulvic acid	HPLC + UV	Supernatant	[48]
PP (aged)	<180	Triclosan	HPLC + UV	Supernatant	[73]
PE, LD-PE, HD-PE, PVC	63–125	Enrofloxacin, Ciprofloxacin, Norfloxacin, 5-Fluorouracil, Methotrexate, Flubendazole, Fenbendazole, Propranolol, Nadolol	HPLC + DAD	Supernatant	[74]
PS (weathered)	139–207	4-Hydroxybenzophenone, Benzophenone-1, ethylhexyl methoxycinnamate, Octocrylene	UHPLC + S/MS	Supernatant	[79]
PVC, PLA	PLA: 250–550 PVC: 75–150	Tetracycline, Ciprofloxacin	HPLC	Supernatant	[31]
nano-PS, carboxyl-functionalized polystyrene nano-PS-COOH	Nano-PS: 0.05 Nano-PS-COOH: 0.055	Norfloxacin, Levofloxacin	HPLC + FD	Supernatant	[75]
PE, PS, PP	<280	Tetracycline	HPLC + FD	Supernatant	[22]
PE	250–280	Carbamazepine, 4-methylbenzylidene camphor, Triclosan, 17 α -ethinyl estradiol	HPLC + PAD (Solid phase extraction)	Supernatant	[28]
PE	150	Sulfamethoxazole	HPLC + UV	Supernatant	[76]

2.4. Further Analytical Techniques for the Determination of Sorbed TORCs

Besides the GC and LC methods for the identification of sorbed substances, other methods such as ultraviolet/visible spectroscopy (UV/VIS) or spectrophotometers can also be used [30,80,81], see Table 3. Here, a direct analysis of the sorbed substances is not possible; therefore, the supernatant is analyzed. During UV/VIS analysis, the concentrations of the pollutants were calculated from their absorbance. The advantages of UV-VIS analysis are the robustness of the system, the easy handling, the short measuring times, and that it is available in most laboratories.

Table 3. Summary of UV/VIS spectroscopic methods to analyze sorbed substances on micro- and nanoplastic particles.

Polymer Type	Particle Size (μm)	Sorbate	Analytical Method	Analysis	Reference
PVC	<1.74	Triclosan	UV/VIS (282 nm)	Supernatant	[30]
PVC, PP, PS, PE	<1000	Co-existing surfactants	UV/VIS (665, 618, 627, 546, 224 nm)	Supernatant	[80]
PE	710–850	Imidacloprid, Buprofezin, Difenconazole	UV Spectrophotometer	Supernatant	[81]

Measurement by liquid scintillation counting is another method for analyzing sorbed TORCs in laboratory experiments [6,24–84]. For this purpose, a ^{14}C labeled standard of the trace substance is used. The concentration of the trace compound is then determined by counting the decay of the ^{14}C trace compound using liquid scintillation counting.

3. Analysis of TORCs on Micro- and Nanoplastic Particles: Typical Sorption Strategies

In the initial microplastic studies, the focus was mainly on detection in environmental systems to get an overview of the distribution of the plastic [84,85]. A detailed review by Li et al. (2019) summarizes the occurrence of microplastics in freshwater systems in terms of microplastic sources, distribution, sampling, and processing methods, as well as polymer characterization [86]. The difficulties of qualitative and quantitative analyses are also addressed. In order to investigate the distribution of micro- and nanoplastics in general, numerous studies have been conducted in fresh water and salt water [87–91]. In these studies, the analysis of the particles was performed using Raman and μFTIR .

Recently, many reviews have been published dealing with interactions between plastic particles (micro and nano) and TORCs [8,9,11,92–95]. Firstly, the plastic itself is examined more closely, including polymer type, the specific surface of the particles with their functional groups and physicochemical properties, crystallinity, polarity, and additives [8,16,55,92,96]. The factors of the surrounding matrix, such as salinity, pH, dissolved organic matter (DOM), coexisting organic contaminants, and ionic strength [9,93] are also considered. The main retention mechanisms from TORCs to micro- and nanoplastics are pore filling, hydrophobic hydrogen bonding, π - π , electrostatic interactions, and van der Waals forces [9]. A further important issue is the ageing of polymers and the resulting influence on the sorption of TORCs [97]. Finally, the influences of the plastic and TORCs are examined regarding their toxicological relevance for the aquatic environment and the possible impact on human health [11,94,95].

3.1. Strategies Characterizing the Polymer Type

Several methods are available to identify the polymer type of the plastic particle, such as physical characterization (e.g., microscopy) and chemical characterization (e.g., Fourier transform infrared (FTIR) and Raman spectroscopy) and were summarized in a recent review by Shim et al., 2017 [16]. Spectroscopic analysis of polymers requires purification and isolation of environmental samples [97]. FTIR and Raman spectroscopy are non-destructive and the polymer type can be determined with the help of a database [16]. Thermoanalytical methods such as Pyr-GC/MS, TED-GC/MS can be used to identify and quantify polymers by their characteristic products, presented by La Nasa et al. (2020) and Yakovenko et al. (2020) [55,96]. Thermoanalytical methods have no size limitations

and several polymer types can be identified in parallel. However, a minimum amount of polymer is required. For example, a minimum of 10 mg is required for a TED-GC/MS analysis or 60 µg for a Pyr-GC/MS analysis [52,54].

Main characteristics affecting sorption on a plastic particle are crystallinity, density, structure, hydrophobicity, and the glass transition temperature T_g . These factors were discussed comprehensively in detail in a recently published short review [8]. In a study comparing the sorption of different polycyclic aromatic hydrocarbons (PAHs) with low-density polyethylene (LDPE) and high-density polyethylene (HDPE), the density of the polymers was observed to have a negative effect on the sorption rate. The sorption capacity decreased with increasing density of the polymers used [14]. However, the density of polymers with crystalline and amorphous components, such as HDPE, was determined by the ratio of crystallinity. In amorphous materials, the hydrophobic bonds are less stable than in crystalline materials [98]. Since only the amorphous fraction can dissolve substances, polymers with a high crystallinity content should have a limited absorption capacity [99,100]. The amorphous region within polymers can be classified as either glassy or rubbery, which is also an indication of sorption capability [12]. The surface appearance is also important for sorption processes. Napper et al. (2015) showed that rough polyethylene (PE) microplastic particles adsorbed more DDT and phenanthrene than smooth ones [29]. The crystallinity of polymers can be measured by X-ray diffraction [101].

Notably, desorption hysteresis was only observed for nonpolar/weakly polar contaminants, likely because nonpolar compounds tended to adsorb in the inner matrices of glassy polymeric structure of polystyrene (resulting in physical entrapment of adsorbates), whereas polar compounds favored surface adsorption [32]. The glass transition temperature (T_g) defines whether a polymeric rubber-like or glass-like material is present. The T_g can be determined by using a thermogravimetric differential scanning calorimetry analyzer (TG-DSC) [73]. Rubber-like polymers are normally above their T_g values if they are not plasticized. At room temperature, this results in greater flexibility, which facilitates sorption of impurities. Glassy polymers are usually below their T_g and are also referred to as condensed (glasslike) [2]. In general, rubbery polymers (such as HDPE, LDPE, or PP) are expected to allow greater diffusion of impurities into the polymer than glassy polymers (such as polyethylene terephthalate (PET) or polyvinyl chloride (PVC)) [2,3]. However, there are exceptions, such as polystyrene (PS). The average sorption capacity is higher than the T_g predicts [1,2,4,5]. A possible explanation for this is the presence of benzene. The phenyl group increases the distance between the polymer chains and can facilitate adhesion and integration of impurities into the polymer [2,5]. However, when comparing polyethylene (PE) and PS in the adsorption and desorption of triclosan, a higher sorption rate was found on PE particles. Triclosan also desorbed faster from the PE particles [34].

A summary of studies in which the sorption capacity of TORCs and their mechanisms were tested on different particle types is shown in Table 4. Here, reference particles were used in all experiments and were, therefore, not further analyzed in any of the studies.

Table 4. Sorption capacity of different polymers. The following criteria were considered for study selection: particles should be approximately the same size and sorption mechanisms and capacities should be addressed.

Polymer Type	Sorbate	Sorbate Analytics	Sorption Capacity	Mechanisms	Reference
PE, PP, PS, PVC	Tylosin	HPLC + DAD	PE < PP < PS < PVC	electrostatic interactions, surface complexation and hydrophobic interactions	[67]
PE, PS, soil	Triclosan	HPLC + UV	PE > PS = soil	PS: π - π interactions, PE: liquid-film and intra-particle diffusion	[34]
PE, PS, PP, PA, PVC	Sulfadiazine, Amoxicillin, Tetracycline, Ciprofloxacin, Trimethoprim	HPLC + UV	PA > PS, PP, PVC, PE	Polar-polar interactions	[71]
PS, PP, PE	Tetracycline	HPLC-FD	PS > PP > PE	Polar interactions, π - π interactions	[22]
PE, PP, PVC	3,6-dibromocarbazole, 3,6-dichlorocarbazole, 3,6-diodocarbazole, 2,7-dibromocarbazole, 3-bromocarbazole	GC/MS after washing with n-hexane and dichloromethane	PVC >> PP, PE	Intraparticle, film diffusion	[39]
PE, PS, soil	Triclosan	HPLC + UV	PE > PS = soil	PE: hydrophobic interactions PS: π - π interactions	[34]

3.2. Strategies Characterizing Particle Size and Shape (Micro vs. Nano)

Micro- and nanoplastic particles may be derived from fragmentation of larger plastic items by means of photolytic, mechanical, and biological degradation without significant chemical degradation [85,102,103]. Thereby, microplastic particles can further disintegrate into nanoplastics [104–106]. As the surface area increases with decreasing particle size, it is assumed that smaller particles are of greater ecotoxicological relevance since the capacity for adsorption of TOxCs increases.

Typical methods for particle sizing can be performed by microscope, FTIR, and Raman spectroscopy [16]. However, there are also limitations. A determination with an optical microscope is often only possible up to 100 μm because smaller particles can also consist of sediment particles [107]. No distinction is then possible using an optical microscope. A FTIR analysis is possible up to 10 μm , a Raman analysis is limited to 100 nm [108,109]. The relationship between particle, surface size, and sorption capacity is considered in more detail in the recently published review by Wang et al., 2020 [9].

In a study by Li et al. using different PS microparticles, it was shown that the sorption capacity of triclosan increases with decreasing particle size of PS [72]. During sorption experiments with micro- and nanoplastic particles, aggregation must also be taken into account. This can happen between two similar (homoaggregation) or two different (heteroaggregation) particles [1]. Aggregation is generally controlled by the ionic strength and valence of the electrolytes in the surrounding media; however, the polymer coating of the particles may also play a role [1,110]. Wang et al. (2019) also showed that the sorption of phenanthrene on the particles was reduced by aggregation of the particles [37]. It has also been shown that nanoparticles agglomerate more and, thus, the specific surface area is reduced again, which can lead to low sorption [37]. A new study by Sun et al. (2020) shows that the agglomeration is strongly dependent on the surrounding matrix [111]. Nanoplastic particles are stable in fresh water due to the Brownian motion and structural layer force, but aggregate in brackish or seawater. In a study with nano-PS, however, it was also shown that the aggregation of the nanoparticles does not change the sorption capacity [70]. The sorption isotherms were the same for aggregated and non-aggregated particles. This indicates that the TOxCs were reaching the sorption sites on the original nanoparticles regardless of the aggregation state. In order to enable comparison of data, the methods for detection, analysis and toxicological assessment of nanoplastics, which are currently still in their initial stages, must first be improved [112].

3.3. Strategies Characterizing Weathered/Aged Particles

Factors that can influence the aging of plastics are, e.g., UV-radiation, temperature, salt content in the environment, and biofilm formation [113]. These causes the plastic to break into smaller and smaller pieces and additives can be released. Induced aging of particles can be carried out for instance by Photo-Fenton oxidation, UV-irradiation, or microbial degradation [79,97].

Investigating aged and unaged microplastic particles, scanning electron microscopy (SEM), transmission electron microscopy (TEM), and FTIR can be used to determine the physical dimensions, morphologies, and chemical compositions [73,78,101,114]. The specific surface area and micropore volume can be studied with an accelerated surface and porosimetry system (ASAP) [83].

Differences in the sorption of aged particles compared to untreated particles are evident in the sorption mechanisms. It was shown that the adsorption of TOxCs in untreated PS particles is based on π - π interaction, whereas in aged PS particles, electrostatic interaction and hydrogen bonding prevail [78]. The results of this study indicated that aging of PS significantly changed the adsorption behavior via the changes of oxygen-containing functional groups and specific surface area. Considering aged and non-aged PP particles in combination with the trace substance triclosan, the aged ones have a higher adsorption capacity than pure microplastics [73]. The sorption affinity was increased with the increase of ionic strength. Study results suggest that particles exposed to weathering processes and

the simultaneous presence of several organic trace compounds may affect the biological ecosystem in the natural environment [79]. This is in contrast to a study by Koelmans et al. (2016) on microplastics and hydrophobic organic chemicals (HOCs). The authors conclude that more HOCs accumulate in natural prey and, thus, the risks from microplastics are not increased [10]. Aged PS particles are shown to generally exhibit higher levels of oxygenated functionality with lower surface hydrophobicity than unaged particles, which also influences the sorption capacity [79]. Due to the UV aging of the particles, the surface becomes rougher. In a study by Fan et al. (2021), it was shown that the surface area of PVC particles increased by 1.85 times and that of PLA by 2.66 times [31]. At the same time, the zeta potential decreased and the adsorption capacity of the particles increased due to the aging process. Charge neutralization is one of the important mechanisms of adsorption. Studies show that the surface charge of the adsorbent is closely related to its ability to absorb pollutants [31,115,116].

3.4. TOrC–Microplastics Sorption and Desorption Kinetics

For the determination of the ad- and absorption kinetics, the above-mentioned analytical approaches can be applied in general [33,67,77]. However, there can be some limitations for smaller particles concerning the sampling frequency, since filtration for the separation of particles from the liquid phase requires longer periods of time with decreasing size of the investigated particles. Hence, if the analytical method requires a separation by filtration, such a limitation needs to be considered in the experimental design, especially for particles in the sub-micrometer range. Studies either did not report such limitations since the particles were either too big ($>1\ \mu\text{m}$) to encounter the problem [9,30,39,48,76,77], or a filtration step was avoided, i.e., by negligible depletion solid phase extraction, the aqueous boundary layer permeation method, head space extraction techniques, or else [4,5,32,82].

For the investigation of the desorption kinetics, another issue needs to be overcome. Since the equilibrium of the sorption mechanism is mostly on the side for the polymer phase, especially for hydrophobic compounds, low aqueous concentration TOrCs must be expected and slow desorption kinetics must also be assumed [117,118]. For hydrophobic compounds, a third phase can be included since TOrCs-sink within the experimental design, such as either virgin polymer particles or another sorptive phase, such as solid-phase microextraction. Here, the sorbent acting as sink should be available in excess to ensure the desorption from the loaded polymer particles as the limiting step [32,117,119].

A desorption hysteresis is reported to be higher for hydrophobic compounds than for polar compounds, but also depends strongly on the polymer. For PE [118], and glassy polymeric domains of PS [32], a significant hysteresis for hydrophobic compounds has been reported. Therefore, desorption of hydrophobic compounds even within more complex matrices such as gut fluids is more unlikely than for polar compounds [120]. The desorption hysteresis is also a critical parameter of TOrC–polymer interaction concerning bioaccessibility and, therefore, the environmental impact [10].

4. Conclusions and Outlook

Established analytical methods for the determination of micro- and nanoplastic particles are FTIR, Raman spectroscopy, and thermal methods such as TED-GC/MS and Pyr-GC/MS. FTIR and Raman spectroscopy can be used to identify polymers, but these methods are limited in size [52,54,108,109].

Considering sample preparations for the generation of sorption kinetics, properties, or processes, the experimental set-up is in most cases the same: the selected particles are incubated with the defined TOrCs over a defined period of time. Afterwards, the aqueous phase is separated from the particle phase. The following analysis of the sorbed TOrCs can be performed either via the filtrate or the particles.

For a simple and fast target analysis of TOrCs in the supernatant, a UV-VIS method is recommended, since this is easy to use and is available in most laboratories. Specific absorbance of individual trace compounds can be determined. However, this method is

not as sensitive as separation coupled detections, such as with HPLC and GC. Using HPLC coupled with a UV, MS, FD, or DAD, this technique provides more detailed results because the molecules can be separated individually. Direct trace analysis of the particle is not possible with either UV-VIS or HPLC methods. The most established method for polymer analysis is a GC based one. By coupling specific systems such as TED-GC/MS, TD-Pyr-GC/MS, double shot pyrolysis, or sequential pyrolysis the possibility is even offered to perform a direct TOrCs analysis of the particles followed by polymer analysis.

Considering future research, the focus should be mainly on the following points:

- (1) Up to now, either the sorbed TOrCs on the particles or the supernatant have only been analyzed. For the preparation of a mass balance, a complete analysis of particles and aqueous phase would be interesting.
- (2) In most conducted studies, the TOrCs are individually adsorbed onto the polymer. However, it is not to be expected that TOrCs will occur individually in the environment, but are present in mixtures. Napper et al. (2015) and Velzeboer et al. (2014) investigated the competitive sorption of phenanthrene and DDT on PE and PVC, respectively, and both found that DDT sorbed slightly more than phenanthrene [29,45]. Future studies should focus more on how TOrCs affect each other regarding sorption strength and capacity.
- (3) The largest challenge in the analysis of TOrCs on micro- and nanoplastic particles will certainly be the removal of inorganics and larger organics such as biofilms without adversely affecting the sorbed TOrCs.

Author Contributions: Conceptualization, J.R., J.G. and T.L.; methodology, J.R., J.G. and T.L.; validation J.R., J.G. and T.L.; formal analysis, J.R., J.G. and T.L.; investigation, J.R., J.G., O.K. and T.L.; resources, J.E.D.; writing—original draft preparation, J.R., J.G., O.K. and T.L.; writing—review and editing, J.R., J.G., O.K., T.L. and J.E.D.; visualization, J.R.; supervision, J.G., T.L., J.E.D.; project administration, O.K. and J.E.D. All authors have read and agreed to the published version of the manuscript.

Funding: This research was partially funded by the German Federal Ministry of Education and Research (BMBF) in the project Sub μ Track, grant number 02WPL1443A.

Institutional Review Board Statement: Not applicable.

Informed Consent Statement: Not applicable.

Data Availability Statement: Data is contained within the article.

Conflicts of Interest: The authors declare no conflict of interest.

References

1. Alimi, O.S.; Budarz, J.F.; Hernandez, L.M.; Tufenkji, N. Microplastics and Nanoplastics in Aquatic Environments: Aggregation, Deposition, and Enhanced Contaminant Transport. *Environ. Sci. Technol.* **2018**, *52*, 1704–1724. [[CrossRef](#)] [[PubMed](#)]
2. Pascall, M.A.; Zabik, M.E.; Zabik, M.J.; Hernandez, R.J. Uptake of Polychlorinated Biphenyls (Pcbs) from an Aqueous Medium by Polyethylene, Polyvinyl Chloride, and Polystyrene Films. *J. Agric. Food Chem.* **2005**, *53*, 164–169. [[CrossRef](#)] [[PubMed](#)]
3. Rochman, C.M.; Hoh, E.; Hentschel, B.T.; Kaye, S. Long-Term Field Measurement of Sorption of Organic Contaminants to Five Types of Plastic Pellets: Implications for Plastic Marine Debris. *Environ. Sci. Technol.* **2013**, *47*, 1646–1654. [[CrossRef](#)]
4. Lee, H.; Shim, W.J.; Kwon, J.-H. Sorption capacity of plastic debris for hydrophobic organic chemicals. *Sci. Total Environ.* **2014**, *1545–1552*. [[CrossRef](#)]
5. Hüffer, T.; Hofmann, T. Sorption of non-polar organic compounds by micro-sized plastic particles in aqueous solution. *Environ. Pollut.* **2016**, *214*, 194–201. [[CrossRef](#)] [[PubMed](#)]
6. Teuten, E.L.; Rowland, S.J.; Galloway, T.S.; Thompson, R.C. Potential for Plastics to Transport Hydrophobic Contaminants. *Environ. Sci. Technol.* **2007**, *4*, 7759–7764. [[CrossRef](#)]
7. Karapanagioti, H.K.; Klontza, I. Testing phenanthrene distribution properties of virgin plastic pellets and plastic eroded pellets found on Lesbos island beaches (Greece). *Mar. Environ. Res.* **2008**, *65*, 283–290. [[CrossRef](#)]
8. Mei, W.; Chen, G.; Bao, J.; Song, M.; Li, Y.; Luo, C. Interactions between microplastics and organic compounds in aquatic environments: A mini review. *Sci. Total Environ.* **2020**, *736*, 139472. [[CrossRef](#)] [[PubMed](#)]
9. Wang, F.; Zhang, M.; Sha, W.; Wang, Y.; Hao, H.; Dou, Y.; Li, Y. Sorption Behavior and Mechanisms of Organic Contaminants to Nano and Microplastics. *Molecules* **2020**, *25*, 1827. [[CrossRef](#)] [[PubMed](#)]

10. Koelmans, A.A.; Bakir, A.; Burton, G.A.; Janssen, C.R. Microplastic as a Vector for Chemicals in the Aquatic Environment: Critical Review and Model-Supported Reinterpretation of Empirical Studies. *Environ. Sci. Technol.* **2016**, *50*, 3315–3326. [[CrossRef](#)] [[PubMed](#)]
11. Menéndez-Pedriza, A.; Jaumot, J. Interaction of Environmental Pollutants with Microplastics: A Critical Review of Sorption Factors, Bioaccumulation and Ecotoxicological Effects. *Toxics* **2020**, *8*, 40. [[CrossRef](#)]
12. Teuten, E.L.; Saquing, J.M.; Knappe, D.R.U.; Barlaz, M.A.; Jonsson, S.; Björn, A.; Rowland, S.J.; Thompson, R.C.; Galloway, T.S.; Yamashita, R.; et al. Transport and release of chemicals from plastics to the environment and to wildlife. *Philos. Trans. R. Soc. B Biol. Sci.* **2009**, *364*, 2027–2045. [[CrossRef](#)] [[PubMed](#)]
13. Seidensticker, S.; Zarfl, C.; Cirkpa, O.A.; Fellenberg, G.; Grathwohl, P. Shift in Mass Transfer of Wastewater Contaminants from Microplastics in the Presence of Dissolved Substances. *Environ. Sci. Technol.* **2017**, *51*, 12254–12263. [[CrossRef](#)]
14. Fries, E.; Zarfl, C. Sorption of polycyclic aromatic hydrocarbons (PAHs) to low and high density polyethylene (PE). *Environ. Sci. Pollut. Res.* **2012**, *19*, 1296–1304. [[CrossRef](#)]
15. Karapanagioti, H.K.; Werner, D. Sorption of Hydrophobic Organic Compounds to Plastics in the Marine Environment: Sorption and Desorption Kinetics. In *The Handbook of Environmental Chemistry*; Springer International Publishing: Basel, Switzerland, 2018; pp. 205–219.
16. Shim, W.J.; Hong, S.H.; Eo, S.E. Identification methods in microplastic analysis: A review. *Anal. Methods* **2017**, *9*, 1384–1391. [[CrossRef](#)]
17. Araujo, C.F.; Nolasco, M.M.; Ribeiro, A.M.; Ribeiro-Claro, P.J. Identification of microplastics using Raman spectroscopy: Latest developments and future prospects. *Water Res.* **2018**, *142*, 426–440. [[CrossRef](#)] [[PubMed](#)]
18. Käßler, A.; Fischer, D.; Oberbeckmann, S.; Schernewski, G.; Labrenz, M.; Eichhorn, K.-J.; Voit, B. Analysis of environmental microplastics by vibrational microspectroscopy: FTIR, Raman or both? *Anal. Bioanal. Chem.* **2016**, *408*, 8377–8391. [[CrossRef](#)] [[PubMed](#)]
19. La Nasa, J.; Biale, G.; Mattonai, M.; Modugno, F. Microwave-assisted solvent extraction and double-shot analytical pyrolysis for the quali-quantitation of plasticizers and microplastics in beach sand samples. *J. Hazard. Mater.* **2020**, *401*, 123287. [[CrossRef](#)]
20. Reichel, J.; Graßmann, J.; Letzel, T.; Drewes, J.E. Systematic Development of a Simultaneous Determination of Plastic Particle Identity and Adsorbed Organic Compounds by Thermodesorption–Pyrolysis GC/MS (TD-Pyr-GC/MS). *Molecules* **2020**, *25*, 4985. [[CrossRef](#)]
21. Zhang, J.; Chen, H.; He, H.; Cheng, X.; Ma, T.; Hu, J.; Yang, S.; Li, S.; Zhang, L. Adsorption behavior and mechanism of 9-Nitroanthracene on typical microplastics in aqueous solutions. *Chemosphere* **2020**, *245*, 125628. [[CrossRef](#)] [[PubMed](#)]
22. Xu, B.; Liu, F.; Brookes, P.C.; Xu, J. Microplastics play a minor role in tetracycline sorption in the presence of dissolved organic matter. *Environ. Pollut.* **2018**, *240*, 87–94. [[CrossRef](#)] [[PubMed](#)]
23. Wang, F.; Shih, K.M.; Li, X.Y. The partition behavior of perfluorooctanesulfonate (PFOS) and perfluorooctanesulfonamide (FOSA) on microplastics. *Chemosphere* **2015**, *119*, 841–847. [[CrossRef](#)] [[PubMed](#)]
24. Bakir, A.; Rowland, S.J.; Thompson, R.C. Transport of persistent organic pollutants by microplastics in estuarine conditions. *Estuar. Coast. Shelf Sci.* **2014**, *140*, 14–21. [[CrossRef](#)]
25. Guo, X.; Wang, J. Sorption of antibiotics onto aged microplastics in freshwater and seawater. *Mar. Pollut. Bull.* **2019**, *149*, 110511. [[CrossRef](#)] [[PubMed](#)]
26. Seidensticker, S.; Grathwohl, P.; Lamprecht, J.; Zarfl, C. A Combined Experimental and Modeling Study to Evaluate Ph-Dependent Sorption of Polar and Non-Polar Compounds to Polyethylene and Polystyrene Microplastics. *Environ. Sci. Eur.* **2018**, *30*, 30. [[CrossRef](#)]
27. Llorca, M.; Schirinzi, G.; Martínez, M.; Barceló, D.; Farré, M. Adsorption of perfluoroalkyl substances on microplastics under environmental conditions. *Environ. Pollut.* **2018**, *235*, 680–691. [[CrossRef](#)] [[PubMed](#)]
28. Wu, C.; Zhang, K.; Huang, X.; Liu, J. Sorption of pharmaceuticals and personal care products to polyethylene debris. *Environ. Sci. Pollut. Res.* **2016**, *23*, 8819–8826. [[CrossRef](#)] [[PubMed](#)]
29. Napper, I.E.; Bakir, A.; Rowland, S.J.; Thompson, R.C. Characterisation, quantity and sorptive properties of microplastics extracted from cosmetics. *Mar. Pollut. Bull.* **2015**, *99*, 178–185. [[CrossRef](#)]
30. Ma, J.; Zhao, J.; Zhu, Z.; Li, L.; Yu, F. Effect of microplastic size on the adsorption behavior and mechanism of triclosan on polyvinyl chloride. *Environ. Pollut.* **2019**, *254*, 113104. [[CrossRef](#)]
31. Fan, X.; Zou, Y.; Geng, N.; Liu, J.; Hou, J.; Li, D.; Yang, C.; Li, Y. Investigation on the adsorption and desorption behaviors of antibiotics by degradable MPs with or without UV ageing process. *J. Hazard. Mater.* **2021**, *401*, 123363. [[CrossRef](#)]
32. Liu, J.; Ma, Y.; Zhu, D.; Xia, T.; Qi, Y.; Yao, Y.; Guo, X.; Ji, R.; Chen, W. Polystyrene Nanoplastics-Enhanced Contaminant Transport: Role of Irreversible Adsorption in Glassy Polymeric Domain. *Environ. Sci. Technol.* **2018**, *52*, 2677–2685. [[CrossRef](#)]
33. Gong, W.; Jiang, M.; Han, P.; Liang, G.; Zhang, T.; Liu, G. Comparative analysis on the sorption kinetics and isotherms of fipronil on nondegradable and biodegradable microplastics. *Environ. Pollut.* **2019**, *254*, 112927. [[CrossRef](#)] [[PubMed](#)]
34. Chen, X.; Gu, X.; Bao, L.; Ma, S.; Mu, Y. Comparison of adsorption and desorption of triclosan between microplastics and soil particles. *Chemosphere* **2020**, *263*, 127947. [[CrossRef](#)]
35. Wu, P.; Cai, Z.; Jin, H.; Tang, Y. Adsorption mechanisms of five bisphenol analogues on PVC microplastics. *Sci. Total Environ.* **2019**, *650*, 671–678. [[CrossRef](#)]

36. Liu, X.; Xu, J.; Zhao, Y.; Shi, H.; Huang, C.H. Hydrophobic Sorption Behaviors of 17beta-Estradiol on Environmental Microplastics. *Chemosphere* **2019**, *226*, 726–735. [[CrossRef](#)]
37. Wang, J.; Liu, X.; Liu, G.; Zhang, Z.; Wu, H.; Cui, B.; Bai, J.; Zhang, W. Size effect of polystyrene microplastics on sorption of phenanthrene and nitrobenzene. *Ecotoxicol. Environ. Saf.* **2019**, *173*, 331–338. [[CrossRef](#)]
38. Zuo, L.-Z.; Li, H.-X.; Lin, L.; Sun, Y.-X.; Diao, Z.-H.; Liu, S.; Zhang, Z.-Y.; Xu, X.-R. Sorption and desorption of phenanthrene on biodegradable poly(butylene adipate co-terephthalate) microplastics. *Chemosphere* **2019**, *215*, 25–32. [[CrossRef](#)]
39. Qiu, Y.; Zheng, M.; Wang, L.; Zhao, Q.; Lou, Y.; Shi, L.; Qu, L. Sorption of polyhalogenated carbazoles (PHCs) to microplastics. *Mar. Pollut. Bull.* **2019**, *146*, 718–728. [[CrossRef](#)]
40. Zhang, X.; Zheng, M.; Yin, X.; Wang, L.; Lou, Y.; Qu, L.; Liu, X.; Zhu, H.; Qiu, Y. Sorption of 3,6-dibromocarbazole and 1,3,6,8-tetrabromocarbazole by microplastics. *Mar. Pollut. Bull.* **2019**, *138*, 458–463. [[CrossRef](#)]
41. Lin, W.; Jiang, R.; Wu, J.; Wei, S.; Yin, L.; Xiao, X.; Hu, S.; Shen, Y.; Ouyang, G. Sorption properties of hydrophobic organic chemicals to micro-sized polystyrene particles. *Sci. Total Environ.* **2019**, *690*, 565–572. [[CrossRef](#)]
42. Wang, W.; Wang, J. Different partition of polycyclic aromatic hydrocarbon on environmental particulates in freshwater: Microplastics in comparison to natural sediment. *Ecotoxicol. Environ. Saf.* **2018**, *147*, 648–655. [[CrossRef](#)] [[PubMed](#)]
43. Bartonitz, A.; Anyanwu, I.N.; Geist, J.; Imhof, H.K.; Reichel, J.; Graßmann, J.; Drewes, J.E.; Beggel, S. Modulation of PAH toxicity on the freshwater organism *G. roeseli* by microparticles. *Environ. Pollut.* **2020**, *260*, 113999. [[CrossRef](#)] [[PubMed](#)]
44. Hüffer, T.; Weniger, A.-K.; Hofmann, T. Sorption of organic compounds by aged polystyrene microplastic particles. *Environ. Pollut.* **2018**, *236*, 218–225. [[CrossRef](#)]
45. Velzeboer, L.; Kwadijk, C.J.A.F.; Koelmans, A.A. Strong Sorption of PCBs to Nanoplastics, Microplastics, Carbon Nanotubes, and Fullerenes. *Environ. Sci. Technol.* **2014**, *48*, 4869–4876. [[CrossRef](#)] [[PubMed](#)]
46. Zhang, X.; Zheng, M.; Wang, L.; Lou, Y.; Shi, L.; Jiang, S. Sorption of three synthetic musks by microplastics. *Mar. Pollut. Bull.* **2018**, *126*, 606–609. [[CrossRef](#)]
47. Liu, X.; Shi, H.; Xie, B.; Dionysiou, D.D.; Zhao, Y. Microplastics as Both a Sink and a Source of Bisphenol A in the Marine Environment. *Environ. Sci. Technol.* **2019**, *53*, 10188–10196. [[CrossRef](#)]
48. Liu, Z.; Qin, Q.; Hu, Z.; Yan, L.; Jeong, U.-I.; Xu, Y. Adsorption of chlorophenols on polyethylene terephthalate microplastics from aqueous environments: Kinetics, mechanisms and influencing factors. *Environ. Pollut.* **2020**, *265*, 114926. [[CrossRef](#)]
49. Yu, H.; Yang, B.; Waigi, M.G.; Peng, F.; Li, Z.; Hu, X. The effects of functional groups on the sorption of naphthalene on microplastics. *Chemosphere* **2020**, *261*, 127592. [[CrossRef](#)]
50. Fries, E.; Dekiff, J.H.; Willmeyer, J.; Nuelle, M.T.; Ebert, M.; Remy, D. Identification of polymer types and additives in marine microplastic particles using pyrolysis-GC/MS and scanning electron microscopy. *Environ. Sci. Process. Impacts* **2013**, *15*, 1949–1956. [[CrossRef](#)] [[PubMed](#)]
51. Dümichen, E.; Barthel, A.-K.; Braun, U.; Bannick, C.G.; Brand, K.; Jekel, M.; Senz, R. Analysis of polyethylene microplastics in environmental samples, using a thermal decomposition method. *Water Res.* **2015**, *85*, 451–457. [[CrossRef](#)]
52. Fischer, M.; Scholz-Böttcher, B.M. Simultaneous Trace Identification and Quantification of Common Types of Microplastics in Environmental Samples by Pyrolysis-Gas Chromatography–Mass Spectrometry. *Environ. Sci. Technol.* **2017**, *51*, 5052–5060. [[CrossRef](#)]
53. Herrera, M.; Matuschek, G.; Ketrup, A. Fast identification of polymer additives by pyrolysis-gas chromatography/mass spectrometry. *J. Anal. Appl. Pyrolysis* **2003**, *70*, 35–42. [[CrossRef](#)]
54. Duemichen, E.; Braun, U.; Senz, R.; Fabian, G.; Sturm, H. Assessment of a new method for the analysis of decomposition gases of polymers by a combining thermogravimetric solid-phase extraction and thermal desorption gas chromatography mass spectrometry. *J. Chromatogr. A* **2014**, *1354*, 117–128. [[CrossRef](#)] [[PubMed](#)]
55. La Nasa, J.; Biale, G.; Fabbri, D.; Modugno, F. A Review on Challenges and Developments of Analytical Pyrolysis and Other Thermoanalytical Techniques for the Quali-Quantitative Determination of Microplastics. *J. Anal. Appl. Pyrolysis* **2020**, *149*, 104841. [[CrossRef](#)]
56. Fischer, M.; Goßmann, I.; Scholz-Böttcher, B.M. Fleur de Sel—An interregional monitor for microplastics mass load and composition in European coastal waters? *J. Anal. Appl. Pyrolysis* **2019**, *144*, 104711. [[CrossRef](#)]
57. Nuelle, M.-T.; Dekiff, J.H.; Remy, D.; Fries, E. A new analytical approach for monitoring microplastics in marine sediments. *Environ. Pollut.* **2014**, *184*, 161–169. [[CrossRef](#)]
58. Kebelmann, K.; Hornung, A.; Karsten, U.; Griffiths, G. Intermediate pyrolysis and product identification by TGA and Py-GC/MS of green microalgae and their extracted protein and lipid components. *Biomass Bioenergy* **2013**, *49*, 38–48. [[CrossRef](#)]
59. Funck, M.; Yildirim, A.; Nickel, C.; Schram, J.; Schmidt, T.C.; Tuerk, J. Identification of microplastics in wastewater after cascade filtration using Pyrolysis-GC–MS. *MethodsX* **2020**, *7*, 100778. [[CrossRef](#)] [[PubMed](#)]
60. Peters, C.A.; Hendrickson, E.; Minor, E.C.; Schreiner, K.; Halbur, J.; Bratton, S.P. Pyr-GC/MS analysis of microplastics extracted from the stomach content of benthivore fish from the Texas Gulf Coast. *Mar. Pollut. Bull.* **2018**, *137*, 91–95. [[CrossRef](#)] [[PubMed](#)]
61. Ter Halle, A.; Jeanneau, L.; Martignac, M.; Jardé, E.; Pedrono, B.; Brach, L.; Gigault, J. Nanoplastic in the North Atlantic Subtropical Gyre. *Environ. Sci. Technol.* **2017**, *51*, 13689–13697. [[CrossRef](#)]
62. Duemichen, E.; Eisentraut, P.; Celina, M.; Braun, U. Automated thermal extraction-desorption gas chromatography mass spectrometry: A multifunctional tool for comprehensive characterization of polymers and their degradation products. *J. Chromatogr. A* **2019**, *1592*, 133–142. [[CrossRef](#)] [[PubMed](#)]

63. Dümichen, E.; Eisentraut, P.; Gerhard, C.; Barthel, A.; Senz, R.; Braun, U. Fast identification of microplastics in complex environmental samples by a thermal degradation method. *Chemosphere* **2017**, *174*, 572–584. [[CrossRef](#)] [[PubMed](#)]
64. Rial-Otero, R.; Galesio, M.; Capelo, J.L.; Simal-Gándara, J. A Review of Synthetic Polymer Characterization by Pyrolysis–Gc–Ms. *Chromatographia* **2009**, *70*, 339–348. [[CrossRef](#)]
65. Llorca, M.; Ábalos, M.; Vega-Herrera, A.; Adrados, M.A.; Abad, E.; Farré, M. Adsorption and Desorption Behaviour of Polychlorinated Biphenyls onto Microplastics' Surfaces in Water/Sediment Systems. *Toxics* **2020**, *8*, 59. [[CrossRef](#)]
66. Endo, S.; Takizawa, R.; Okuda, K.; Takada, H.; Chiba, K.; Kanehiro, H.; Ogi, H.; Yamashita, R.; Date, T. Concentration of polychlorinated biphenyls (PCBs) in beached resin pellets: Variability among individual particles and regional differences. *Mar. Pollut. Bull.* **2005**, *50*, 1103–1114. [[CrossRef](#)]
67. Guo, X.; Pang, J.; Chen, S.; Jia, H. Sorption properties of tylosin on four different microplastics. *Chemosphere* **2018**, *209*, 240–245. [[CrossRef](#)]
68. Li, S.; Liu, H.; Gao, R.; Abdurahman, A.; Dai, J.; Zeng, F. Aggregation kinetics of microplastics in aquatic environment: Complex roles of electrolytes, pH, and natural organic matter. *Environ. Pollut.* **2018**, *237*, 126–132. [[CrossRef](#)]
69. Zhao, L.; Rong, L.; Xu, J.; Lian, J.; Wang, L.; Sun, H. Sorption of five organic compounds by polar and nonpolar microplastics. *Chemosphere* **2020**, *257*, 127206. [[CrossRef](#)] [[PubMed](#)]
70. Liu, L.; Fokkink, R.; Koelmans, A.A. Sorption of polycyclic aromatic hydrocarbons to polystyrene nanoplastic. *Environ. Toxicol. Chem.* **2016**, *35*, 1650–1655. [[CrossRef](#)]
71. Li, J.; Zhang, K.; Zhang, H. Adsorption of antibiotics on microplastics. *Environ. Pollut.* **2018**, *237*, 460–467. [[CrossRef](#)] [[PubMed](#)]
72. Li, Y.; Li, M.; Li, Z.; Yang, L.; Liu, X. Effects of particle size and solution chemistry on Triclosan sorption on polystyrene microplastic. *Chemosphere* **2019**, *231*, 308–314. [[CrossRef](#)] [[PubMed](#)]
73. Wu, X.; Liu, P.; Huang, H.; Gao, S. Adsorption of triclosan onto different aged polypropylene microplastics: Critical effect of cations. *Sci. Total Environ.* **2020**, *717*, 137033. [[CrossRef](#)]
74. Puckowski, A.; Cwiąg, W.; Mioduszczyńska, K.; Stepnowski, P.; Białk-Bielińska, A. Sorption of pharmaceuticals on the surface of microplastics. *Chemosphere* **2020**, *263*, 127976. [[CrossRef](#)] [[PubMed](#)]
75. Zhang, H.; Liu, F.-F.; Wang, S.-C.; Huang, T.-Y.; Li, M.-R.; Zhu, Z.-L.; Liu, G.-Z. Sorption of fluoroquinolones to nanoplastics as affected by surface functionalization and solution chemistry. *Environ. Pollut.* **2020**, *262*, 114347. [[CrossRef](#)] [[PubMed](#)]
76. Xu, B.; Liu, F.; Brookes, P.C.; Xu, J. The sorption kinetics and isotherms of sulfamethoxazole with polyethylene microplastics. *Mar. Pollut. Bull.* **2018**, *131*, 191–196. [[CrossRef](#)]
77. Guo, X.; Chen, C.; Wang, J. Sorption of sulfamethoxazole onto six types of microplastics. *Chemosphere* **2019**, *228*, 300–308. [[CrossRef](#)] [[PubMed](#)]
78. Liu, P.; Lu, K.; Li, J.; Wu, X.; Qian, L.; Wang, M.; Gao, S. Effect of aging on adsorption behavior of polystyrene microplastics for pharmaceuticals: Adsorption mechanism and role of aging intermediates. *J. Hazard. Mater.* **2020**, *384*, 121193. [[CrossRef](#)]
79. Ho, W.-K.; Law, J.C.-F.; Zhang, T.; Leung, K.S.-Y. Effects of Weathering on the Sorption Behavior and Toxicity of Polystyrene Microplastics in Multi-solute Systems. *Water Res.* **2020**, *187*, 116419. [[CrossRef](#)]
80. Xia, Y.; Zhou, J.-J.; Gong, Y.-Y.; Li, Z.-J.; Zeng, E.Y. Strong influence of surfactants on virgin hydrophobic microplastics adsorbing ionic organic pollutants. *Environ. Pollut.* **2020**, *265*, 115061. [[CrossRef](#)] [[PubMed](#)]
81. Li, H.; Wang, F.; Li, J.; Deng, S.; Zhang, S. Adsorption of three pesticides on polyethylene microplastics in aqueous solutions: Kinetics, isotherms, thermodynamics, and molecular dynamics simulation. *Chemosphere* **2020**, *264*, 128556. [[CrossRef](#)]
82. Bakir, A.; Rowland, S.J.; Thompson, R.C. Enhanced desorption of persistent organic pollutants from microplastics under simulated physiological conditions. *Environ. Pollut.* **2014**, *185*, 16–23. [[CrossRef](#)] [[PubMed](#)]
83. Liu, J.; Zhang, T.; Tian, L.; Liu, X.; Qi, Z.; Ma, Y.; Ji, R.; Chen, W. Aging Significantly Affects Mobility and Contaminant-Mobilizing Ability of Nanoplastics in Saturated Loamy Sand. *Environ. Sci. Technol.* **2019**, *53*, 5805–5815. [[CrossRef](#)]
84. Thompson, R.C.; Olsen, Y.; Mitchell, R.P.; Davis, A.; Rowland, S.J.; John, A.W.; McGonigle, D.; Russell, A.E. Lost at Sea: Where Is All the Plastic? *Science* **2004**, *304*, 838. [[CrossRef](#)]
85. Barnes, D.K.A.; Galgani, F.; Thompson, R.C.; Barlaz, M. Accumulation and fragmentation of plastic debris in global environments. *Philos. Trans. R. Soc. B Biol. Sci.* **2009**, *364*, 1985–1998. [[CrossRef](#)]
86. Li, C.; Busquets, R.; Campos, L.C. Assessment of microplastics in freshwater systems: A review. *Sci. Total Environ.* **2020**, *707*, 135578. [[CrossRef](#)]
87. Imhof, H.K.; Wiesheu, A.C.; Anger, P.M.; Niessner, R.; Ivleva, N.P.; Laforsch, C. Variation in plastic abundance at different lake beach zones—A case study. *Sci. Total Environ.* **2018**, *613–614*, 530–537. [[CrossRef](#)]
88. Cincinelli, A.; Martellini, T.; Guerranti, C.; Scopetani, C.; Chelazzi, D.; Giarrizzo, T. A potpourri of microplastics in the sea surface and water column of the Mediterranean Sea. *TrAC Trends Anal. Chem.* **2019**, *110*, 321–326. [[CrossRef](#)]
89. Kazour, M.; Jemaa, S.; Issa, C.; Khalaf, G.; Amara, R. Microplastics pollution along the Lebanese coast (Eastern Mediterranean Basin): Occurrence in surface water, sediments and biota samples. *Sci. Total Environ.* **2019**, *696*, 133933. [[CrossRef](#)] [[PubMed](#)]
90. Llorca, M.; Vega-Herrera, A.; Schirinzi, G.; Savva, K.; Abad, E.; Farré, M. Screening of suspected micro(nano)plastics in the Ebro Delta (Mediterranean Sea). *J. Hazard. Mater.* **2021**, *404*, 124022. [[CrossRef](#)]
91. Simon-Sánchez, L.; Grelaud, M.; Garcia-Orellana, J.; Ziveri, P. River Deltas as hotspots of microplastic accumulation: The case study of the Ebro River (NW Mediterranean). *Sci. Total Environ.* **2019**, *687*, 1186–1196. [[CrossRef](#)] [[PubMed](#)]

63. Dümichen, E.; Eisentraut, P.; Gerhard, C.; Barthel, A.; Senz, R.; Braun, U. Fast identification of microplastics in complex environmental samples by a thermal degradation method. *Chemosphere* **2017**, *174*, 572–584. [CrossRef] [PubMed]
64. Rial-Otero, R.; Galesio, M.; Capelo, J.L.; Simal-Gándara, J. A Review of Synthetic Polymer Characterization by Pyrolysis–Gc–Ms. *Chromatographia* **2009**, *70*, 339–348. [CrossRef]
65. Llorca, M.; Ábalos, M.; Vega-Herrera, A.; Adrados, M.A.; Abad, E.; Farré, M. Adsorption and Desorption Behaviour of Polychlorinated Biphenyls onto Microplastics' Surfaces in Water/Sediment Systems. *Toxics* **2020**, *8*, 59. [CrossRef]
66. Endo, S.; Takizawa, R.; Okuda, K.; Takada, H.; Chiba, K.; Kanehiro, H.; Ogi, H.; Yamashita, R.; Date, T. Concentration of polychlorinated biphenyls (PCBs) in beached resin pellets: Variability among individual particles and regional differences. *Mar. Pollut. Bull.* **2005**, *50*, 1103–1114. [CrossRef]
67. Guo, X.; Pang, J.; Chen, S.; Jia, H. Sorption properties of tylosin on four different microplastics. *Chemosphere* **2018**, *209*, 240–245. [CrossRef]
68. Li, S.; Liu, H.; Gao, R.; Abdurahman, A.; Dai, J.; Zeng, F. Aggregation kinetics of microplastics in aquatic environment: Complex roles of electrolytes, pH, and natural organic matter. *Environ. Pollut.* **2018**, *237*, 126–132. [CrossRef]
69. Zhao, L.; Rong, L.; Xu, J.; Lian, J.; Wang, L.; Sun, H. Sorption of five organic compounds by polar and nonpolar microplastics. *Chemosphere* **2020**, *257*, 127206. [CrossRef] [PubMed]
70. Liu, L.; Fokink, R.; Koelmans, A.A. Sorption of polycyclic aromatic hydrocarbons to polystyrene nanoplastic. *Environ. Toxicol. Chem.* **2016**, *35*, 1650–1655. [CrossRef]
71. Li, J.; Zhang, K.; Zhang, H. Adsorption of antibiotics on microplastics. *Environ. Pollut.* **2018**, *237*, 460–467. [CrossRef] [PubMed]
72. Li, Y.; Li, M.; Li, Z.; Yang, L.; Liu, X. Effects of particle size and solution chemistry on Triclosan sorption on polystyrene microplastic. *Chemosphere* **2019**, *231*, 308–314. [CrossRef] [PubMed]
73. Wu, X.; Liu, P.; Huang, H.; Gao, S. Adsorption of triclosan onto different aged polypropylene microplastics: Critical effect of cations. *Sci. Total Environ.* **2020**, *717*, 137033. [CrossRef]
74. Puckowski, A.; Cwiąg, W.; Mioduszczyńska, K.; Stepnowski, P.; Białk-Bielińska, A. Sorption of pharmaceuticals on the surface of microplastics. *Chemosphere* **2020**, *263*, 127976. [CrossRef] [PubMed]
75. Zhang, H.; Liu, F.-F.; Wang, S.-C.; Huang, T.-Y.; Li, M.-R.; Zhu, Z.-L.; Liu, G.-Z. Sorption of fluoroquinolones to nanoplastics as affected by surface functionalization and solution chemistry. *Environ. Pollut.* **2020**, *262*, 114347. [CrossRef] [PubMed]
76. Xu, B.; Liu, F.; Brookes, P.C.; Xu, J. The sorption kinetics and isotherms of sulfamethoxazole with polyethylene microplastics. *Mar. Pollut. Bull.* **2018**, *131*, 191–196. [CrossRef]
77. Guo, X.; Chen, C.; Wang, J. Sorption of sulfamethoxazole onto six types of microplastics. *Chemosphere* **2019**, *228*, 300–308. [CrossRef] [PubMed]
78. Liu, P.; Lu, K.; Li, J.; Wu, X.; Qian, L.; Wang, M.; Gao, S. Effect of aging on adsorption behavior of polystyrene microplastics for pharmaceuticals: Adsorption mechanism and role of aging intermediates. *J. Hazard. Mater.* **2020**, *384*, 121193. [CrossRef]
79. Ho, W.-K.; Law, J.C.-F.; Zhang, T.; Leung, K.S.-Y. Effects of Weathering on the Sorption Behavior and Toxicity of Polystyrene Microplastics in Multi-solute Systems. *Water Res.* **2020**, *187*, 116419. [CrossRef]
80. Xia, Y.; Zhou, J.-J.; Gong, Y.-Y.; Li, Z.-J.; Zeng, E.Y. Strong influence of surfactants on virgin hydrophobic microplastics adsorbing ionic organic pollutants. *Environ. Pollut.* **2020**, *265*, 115061. [CrossRef] [PubMed]
81. Li, H.; Wang, F.; Li, J.; Deng, S.; Zhang, S. Adsorption of three pesticides on polyethylene microplastics in aqueous solutions: Kinetics, isotherms, thermodynamics, and molecular dynamics simulation. *Chemosphere* **2020**, *264*, 128556. [CrossRef]
82. Bakir, A.; Rowland, S.J.; Thompson, R.C. Enhanced desorption of persistent organic pollutants from microplastics under simulated physiological conditions. *Environ. Pollut.* **2014**, *185*, 16–23. [CrossRef] [PubMed]
83. Liu, J.; Zhang, T.; Tian, L.; Liu, X.; Qi, Z.; Ma, Y.; Ji, R.; Chen, W. Aging Significantly Affects Mobility and Contaminant-Mobilizing Ability of Nanoplastics in Saturated Loamy Sand. *Environ. Sci. Technol.* **2019**, *53*, 5805–5815. [CrossRef]
84. Thompson, R.C.; Olsen, Y.; Mitchell, R.P.; Davis, A.; Rowland, S.J.; John, A.W.; McGonigle, D.; Russell, A.E. Lost at Sea: Where Is All the Plastic? *Science* **2004**, *304*, 838. [CrossRef]
85. Barnes, D.K.A.; Galgani, F.; Thompson, R.C.; Barlaz, M. Accumulation and fragmentation of plastic debris in global environments. *Philos. Trans. R. Soc. B Biol. Sci.* **2009**, *364*, 1985–1998. [CrossRef]
86. Li, C.; Busquets, R.; Campos, L.C. Assessment of microplastics in freshwater systems: A review. *Sci. Total Environ.* **2020**, *707*, 135578. [CrossRef]
87. Imhof, H.K.; Wiesheu, A.C.; Anger, P.M.; Niessner, R.; Ivleva, N.P.; Laforsch, C. Variation in plastic abundance at different lake beach zones—A case study. *Sci. Total Environ.* **2018**, *613–614*, 530–537. [CrossRef]
88. Cincinelli, A.; Martellini, T.; Guerranti, C.; Scopetani, C.; Chelazzi, D.; Giarrizzo, T. A potpourri of microplastics in the sea surface and water column of the Mediterranean Sea. *TrAC Trends Anal. Chem.* **2019**, *110*, 321–326. [CrossRef]
89. Kazour, M.; Jemaa, S.; Issa, C.; Khalaf, G.; Amara, R. Microplastics pollution along the Lebanese coast (Eastern Mediterranean Basin): Occurrence in surface water, sediments and biota samples. *Sci. Total Environ.* **2019**, *696*, 133933. [CrossRef] [PubMed]
90. Llorca, M.; Vega-Herrera, A.; Schirinzi, G.; Savva, K.; Abad, E.; Farré, M. Screening of suspected micro(nano)plastics in the Ebro Delta (Mediterranean Sea). *J. Hazard. Mater.* **2021**, *404*, 124022. [CrossRef]
91. Simon-Sánchez, L.; Grelaud, M.; Garcia-Orellana, J.; Ziveri, P. River Deltas as hotspots of microplastic accumulation: The case study of the Ebro River (NW Mediterranean). *Sci. Total Environ.* **2019**, *687*, 1186–1196. [CrossRef] [PubMed]

63. Dümichen, E.; Eisentraut, P.; Gerhard, C.; Barthel, A.; Senz, R.; Braun, U. Fast identification of microplastics in complex environmental samples by a thermal degradation method. *Chemosphere* **2017**, *174*, 572–584. [CrossRef] [PubMed]
64. Rial-Otero, R.; Galesio, M.; Capelo, J.L.; Simal-Gándara, J. A Review of Synthetic Polymer Characterization by Pyrolysis–Gc–Ms. *Chromatographia* **2009**, *70*, 339–348. [CrossRef]
65. Llorca, M.; Ábalos, M.; Vega-Herrera, A.; Adrados, M.A.; Abad, E.; Farré, M. Adsorption and Desorption Behaviour of Polychlorinated Biphenyls onto Microplastics' Surfaces in Water/Sediment Systems. *Toxics* **2020**, *8*, 59. [CrossRef]
66. Endo, S.; Takizawa, R.; Okuda, K.; Takada, H.; Chiba, K.; Kanehiro, H.; Ogi, H.; Yamashita, R.; Date, T. Concentration of polychlorinated biphenyls (PCBs) in beached resin pellets: Variability among individual particles and regional differences. *Mar. Pollut. Bull.* **2005**, *50*, 1103–1114. [CrossRef]
67. Guo, X.; Pang, J.; Chen, S.; Jia, H. Sorption properties of tylosin on four different microplastics. *Chemosphere* **2018**, *209*, 240–245. [CrossRef]
68. Li, S.; Liu, H.; Gao, R.; Abdurahman, A.; Dai, J.; Zeng, F. Aggregation kinetics of microplastics in aquatic environment: Complex roles of electrolytes, pH, and natural organic matter. *Environ. Pollut.* **2018**, *237*, 126–132. [CrossRef]
69. Zhao, L.; Rong, L.; Xu, J.; Lian, J.; Wang, L.; Sun, H. Sorption of five organic compounds by polar and nonpolar microplastics. *Chemosphere* **2020**, *257*, 127206. [CrossRef] [PubMed]
70. Liu, L.; Fokink, R.; Koelmans, A.A. Sorption of polycyclic aromatic hydrocarbons to polystyrene nanoplastic. *Environ. Toxicol. Chem.* **2016**, *35*, 1650–1655. [CrossRef]
71. Li, J.; Zhang, K.; Zhang, H. Adsorption of antibiotics on microplastics. *Environ. Pollut.* **2018**, *237*, 460–467. [CrossRef] [PubMed]
72. Li, Y.; Li, M.; Li, Z.; Yang, L.; Liu, X. Effects of particle size and solution chemistry on Triclosan sorption on polystyrene microplastic. *Chemosphere* **2019**, *231*, 308–314. [CrossRef] [PubMed]
73. Wu, X.; Liu, P.; Huang, H.; Gao, S. Adsorption of triclosan onto different aged polypropylene microplastics: Critical effect of cations. *Sci. Total Environ.* **2020**, *717*, 137033. [CrossRef]
74. Puckowski, A.; Cwiąg, W.; Mioduszewska, K.; Stepnowski, P.; Białk-Bielińska, A. Sorption of pharmaceuticals on the surface of microplastics. *Chemosphere* **2020**, *263*, 127976. [CrossRef] [PubMed]
75. Zhang, H.; Liu, F.-F.; Wang, S.-C.; Huang, T.-Y.; Li, M.-R.; Zhu, Z.-L.; Liu, G.-Z. Sorption of fluoroquinolones to nanoplastics as affected by surface functionalization and solution chemistry. *Environ. Pollut.* **2020**, *262*, 114347. [CrossRef] [PubMed]
76. Xu, B.; Liu, F.; Brookes, P.C.; Xu, J. The sorption kinetics and isotherms of sulfamethoxazole with polyethylene microplastics. *Mar. Pollut. Bull.* **2018**, *131*, 191–196. [CrossRef]
77. Guo, X.; Chen, C.; Wang, J. Sorption of sulfamethoxazole onto six types of microplastics. *Chemosphere* **2019**, *228*, 300–308. [CrossRef] [PubMed]
78. Liu, P.; Lu, K.; Li, J.; Wu, X.; Qian, L.; Wang, M.; Gao, S. Effect of aging on adsorption behavior of polystyrene microplastics for pharmaceuticals: Adsorption mechanism and role of aging intermediates. *J. Hazard. Mater.* **2020**, *384*, 121193. [CrossRef]
79. Ho, W.-K.; Law, J.C.-F.; Zhang, T.; Leung, K.S.-Y. Effects of Weathering on the Sorption Behavior and Toxicity of Polystyrene Microplastics in Multi-solute Systems. *Water Res.* **2020**, *187*, 116419. [CrossRef]
80. Xia, Y.; Zhou, J.-J.; Gong, Y.-Y.; Li, Z.-J.; Zeng, E.Y. Strong influence of surfactants on virgin hydrophobic microplastics adsorbing ionic organic pollutants. *Environ. Pollut.* **2020**, *265*, 115061. [CrossRef] [PubMed]
81. Li, H.; Wang, F.; Li, J.; Deng, S.; Zhang, S. Adsorption of three pesticides on polyethylene microplastics in aqueous solutions: Kinetics, isotherms, thermodynamics, and molecular dynamics simulation. *Chemosphere* **2020**, *264*, 128556. [CrossRef]
82. Bakir, A.; Rowland, S.J.; Thompson, R.C. Enhanced desorption of persistent organic pollutants from microplastics under simulated physiological conditions. *Environ. Pollut.* **2014**, *185*, 16–23. [CrossRef] [PubMed]
83. Liu, J.; Zhang, T.; Tian, L.; Liu, X.; Qi, Z.; Ma, Y.; Ji, R.; Chen, W. Aging Significantly Affects Mobility and Contaminant-Mobilizing Ability of Nanoplastics in Saturated Loamy Sand. *Environ. Sci. Technol.* **2019**, *53*, 5805–5815. [CrossRef]
84. Thompson, R.C.; Olsen, Y.; Mitchell, R.P.; Davis, A.; Rowland, S.J.; John, A.W.; McGonigle, D.; Russell, A.E. Lost at Sea: Where Is All the Plastic? *Science* **2004**, *304*, 838. [CrossRef]
85. Barnes, D.K.A.; Galgani, F.; Thompson, R.C.; Barlaz, M. Accumulation and fragmentation of plastic debris in global environments. *Philos. Trans. R. Soc. B Biol. Sci.* **2009**, *364*, 1985–1998. [CrossRef]
86. Li, C.; Busquets, R.; Campos, L.C. Assessment of microplastics in freshwater systems: A review. *Sci. Total Environ.* **2020**, *707*, 135578. [CrossRef]
87. Imhof, H.K.; Wiesheu, A.C.; Anger, P.M.; Niessner, R.; Ivleva, N.P.; Laforsch, C. Variation in plastic abundance at different lake beach zones—A case study. *Sci. Total Environ.* **2018**, *613–614*, 530–537. [CrossRef]
88. Cincinelli, A.; Martellini, T.; Guerranti, C.; Scopetani, C.; Chelazzi, D.; Giarrizzo, T. A potpourri of microplastics in the sea surface and water column of the Mediterranean Sea. *TrAC Trends Anal. Chem.* **2019**, *110*, 321–326. [CrossRef]
89. Kazour, M.; Jemaa, S.; Issa, C.; Khalaf, G.; Amara, R. Microplastics pollution along the Lebanese coast (Eastern Mediterranean Basin): Occurrence in surface water, sediments and biota samples. *Sci. Total Environ.* **2019**, *696*, 133933. [CrossRef] [PubMed]
90. Llorca, M.; Vega-Herrera, A.; Schirinzi, G.; Savva, K.; Abad, E.; Farré, M. Screening of suspected micro(nano)plastics in the Ebro Delta (Mediterranean Sea). *J. Hazard. Mater.* **2021**, *404*, 124022. [CrossRef]
91. Simon-Sánchez, L.; Grelaud, M.; Garcia-Orellana, J.; Ziveri, P. River Deltas as hotspots of microplastic accumulation: The case study of the Ebro River (NW Mediterranean). *Sci. Total Environ.* **2019**, *687*, 1186–1196. [CrossRef] [PubMed]

119. Cornelissen, G.; van Noort, P.C.; Govers, H.A. Desorption Kinetics of Chlorobenzenes, Polycyclic Aromatic Hydrocarbons, and Polychlorinated Biphenyls: Sediment Extraction with Tenax and Effects of Contact Time and Solute Hydrophobicity. *Environ. Toxicol. Chem.* **1997**, *16*, 1351–1357. [[CrossRef](#)]
120. Liu, X.; Gharasoo, M.; Shi, Y.; Sigmund, G.; Hüffer, T.; Duan, L.; Wang, Y.; Ji, R.; Hofmann, T.; Chen, W. Key Physicochemical Properties Dictating Gastrointestinal Bioaccessibility of Microplastics-Associated Organic Xenobiotics: Insights from a Deep Learning Approach. *Environ. Sci. Technol.* **2020**, *54*, 12051–12062. [[CrossRef](#)] [[PubMed](#)]

Appendix II

Systematic Development of a Simultaneous Determination of Plastic Particle Identity and Adsorbed Organic Compounds by Thermodesorption–Pyrolysis GC/MS (TD-Pyr-GC/MS)

Molecules, 2020, 25, 4985;

This study introduces a novel thermal desorption pyrolysis gas chromatography mass spectrometry (TD-Pyr-GC/MS) method for identifying trace organic chemicals adsorbed on micro-, submicro-, and nanoparticles, along with their associated polymer types. This method streamlines the analysis process, eliminating the need for complex extraction steps. The study demonstrates the applicability of this method using reference polymers (polystyrene, polymethyl methacrylate, and polyethylene) and various particle sizes. Results indicate that the sorption of specific trace organic chemicals varies significantly depending on the polymer type and particle size. This innovative approach offers rapid and efficient analysis capabilities, particularly for nanoplastic particles, with a short 2-hour per-sample analysis time.

Julia Reichel designed, performed, evaluated the experiment and wrote the manuscript. Johanna Grassmann, Thomas Letzel and Jörg E. Drewes reviewed the manuscript and contributed to the discussion.

Article

Systematic Development of a Simultaneous Determination of Plastic Particle Identity and Adsorbed Organic Compounds by Thermodesorption–Pyrolysis GC/MS (TD-Pyr-GC/MS)

Julia Reichel ¹, Johanna Graßmann ¹, Thomas Letzel ^{1,2} and Jörg E. Drewes ^{1,*} 

¹ Chair of Urban Water Systems Engineering, Technical University of Munich, Am Coulombwall 3, 85748 Garching, Germany; julia.reichel@tum.de (J.R.); j.grassmann@tum.de (J.G.); t.letzel@tum.de (T.L.)

² AFIN-TS GmbH, Am Mittleren Moos 48, 86167 Augsburg, Germany

* Correspondence: jdrewes@tum.de; Tel.: +49-89-289-13713

Academic Editors: Teresa A. P. Rocha-Santos and João P. da Costa

Received: 9 September 2020; Accepted: 26 October 2020; Published: 28 October 2020



Abstract: Micro-, submicro- and nanoplastic particles are increasingly regarded as vectors for trace organic chemicals. In order to determine adsorbed trace organic chemicals on polymers, it has usually been necessary to carry out complex extraction steps. With the help of a newly designed thermal desorption pyrolysis gas chromatography mass spectrometry (TD-Pyr-GC/MS) method, it is possible to identify adsorbed trace organic chemicals on micro-, submicro- and nanoparticles as well as the particle short chain polymers in one analytical setup without any transfers. This ensures a high sample throughput for the qualitative analysis of trace substances and polymer type. Since the measuring time per sample is only 2 h, a high sample throughput is possible. It is one of the few analytical methods which can be used also for the investigation of nanoplastic particles. Initially adsorbed substances are desorbed from the particle by thermal desorption (TD); subsequently, the polymer is fragmented by pyrolysis (PYR). Both particle treatment techniques are directly coupled with the same GC-MS system analyzing desorbed molecules and pyrolysis products, respectively. In this study, we developed a systematic and optimized method for this application. For method development, the trace organic chemicals phenanthrene, α -cypermethrin and triclosan were tested on reference polymers polystyrene (PS), polymethyl methacrylate (PMMA) and polyethylene (PE). Well-defined particle fractions were used, including polystyrene (sub)micro- (41 and 40 μm) and nanoparticles (78 nm) as well as 48- μm sized PE and PMMA particles, respectively. The sorption of phenanthrene (PMMA \ll PS 40 μm < 41 μm < PE < PS 78 nm) and α -cypermethrin (PS 41 μm < PS 40 μm < PE < PMMA < PS 78 nm) to the particles was strongly polymer-dependent. Triclosan adsorbed only on PE and on the nanoparticles of PS (PE < PS78).

Keywords: microplastic; nanoplastic; thermodesorption; pyrolysis; desorption

1. Introduction

More than 300 million tons of plastics are annually produced worldwide and about 8 million tons migrate from land surfaces into the ocean [1,2]. It is estimated that currently more than five trillion plastic particles with a total weight of over 250,000 tons float in the oceans [3]. Most of them are microplastics with a size of less than 5 mm [4]. To date, no uniform definition has been established to distinguish between micro- and nanoplastics [5]. Plastic particles with a size between 1 mm and 1 μm are usually referred to as microplastics, while plastic particles smaller than 1 μm are defined as

meso- or nanoplastic or submicroparticles [6,7]. Micro-, submicro- and nanoplastics may potentially not only be harmful by themselves but also serve as vectors due to ad- or absorbed contaminants [5]. Detailed and robust analysis of these sorbed contaminants is challenging and requires several analytical steps [5,8–10]. Using established analytical methods, such as thermal extraction desorption gas chromatography mass spectrometry (TED-GC/MS), double-shot analytical pyrolysis and sequential pyrolysis, it has already been shown that it is possible to detect additives and identify polymers with one analytical setup [11–14]. Considering established methods to analyze sorbed substances, initially, trace organic chemicals have to be extracted with solvents such as n-hexane, cyclohexane or dichloromethane [8,15,16] prior to analysis via GC/MS [10,15,17], LC/MS [8,9], or using radioisotopic marked trace organic chemicals [18,19]. Simultaneous identification of the polymer is not possible.

So far, several methods exist to identify the polymers. Currently, spectroscopic methods, such as Raman microscopy (RM) or Fourier transform infrared spectroscopy (FTIR), and thermoanalytical methods, such as pyrolysis gas chromatography mass spectrometry (Pyr-GC-MS) or thermal extraction desorption gas chromatography mass spectrometry (TED-GC-MS), are used [14,20–24]. Especially thermoanalytical methods are becoming more important for general identification and quantification of micro- and nanoplastics [25,26].

As the surface area of plastic particles increases the smaller the particle becomes, it is assumed that smaller particles are of higher ecotoxicological relevance since the capacity for adsorption of trace organic chemicals increases [4,27,28]. However, the effective surface area of nano-sized particles can be limited due to particle aggregation by increased hydrodynamic diameter [29]. Already, with other particle types (e.g., titanium particles or magnesium oxide particles), it could be shown that the relative sorption increases, the smaller the particle becomes [30,31]. These observations can be supported by research with (sub)micro- and nanoplastics, where sorption of polychlorinated biphenyls on nano-PS is 1–2 orders of magnitude higher than on micro-PE [16].

The aim of this study is to develop an innovative analytical method of combined thermodesorption- and pyrolysis-gas chromatography/mass spectrometry (TD-GC/MS + Pyr-GC/MS) in order to enable the identification of sorbed organic chemicals and the type of polymer in one single analytical setup. For doing so, initially, the trace organic chemicals are desorbed from the particles by thermodesorption and analyzed using GC/MS. Subsequently, the polymers are decomposed by pyrolysis and the decomposition products and by this the type of polymer and contained additives are identified via GC/MS analysis. The fields of application of such a method are mainly directed to environmental screening studies, e.g., those resulting from ecotoxicological assays employing micro- or nanoplastics and sorbed organic chemicals, where a quick analytical method is desired that is able to handle high sample numbers. This method is especially suitable for water samples. After filtration of the samples, the inorganics should be removed for analysis. For an analysis of the sorbed trace substances, the samples should also be as free as possible from organic substances, such as biofilms. A quantification of the trace organic chemicals sorbed on the particles is beyond the scope of this paper and will be performed in the future.

2. Analytical Systems, Materials and Methods

2.1. Instrumental Systems

The combined thermodesorption- and pyrolysis-gas chromatography/mass spectrometry (TD-GC/MS + Pyr-GC/MS) analysis was performed using a Gerstel Thermal-Desorption-Unit (TDU) 2 equipped with a TDU pyrolysis module, a Gerstel Multi-Purpose-Sampler (MPS) robotic^{PRO}, a Cooled Injections System (CIS) 4 with Controller C506 and an Agilent 7890B gas chromatograph equipped with an DB-5MS Ultra Inert column coupled with an electron ion source to an Agilent 5977B MSD mass spectrometer. The particle samples are directly transferred into the pyrolysis module by the MPS for further analysis. A preprogrammed temperature protocol is executed to evaporate the volatile substances in a first step. Subsequently, in the CIS, the substances are trapped and then

totally transferred to the GC column entry by CIS heating. Due to the direct coupling of the pyrolysis module, it is possible to execute first a thermodesorption step (TD-GC/MS), subsequently followed by an independent pyrolysis step (Pyr-GC/MS). The total process is visualized in Figure 1; a more detailed scheme of the pyrolysis unit is shown in Figure 2a.

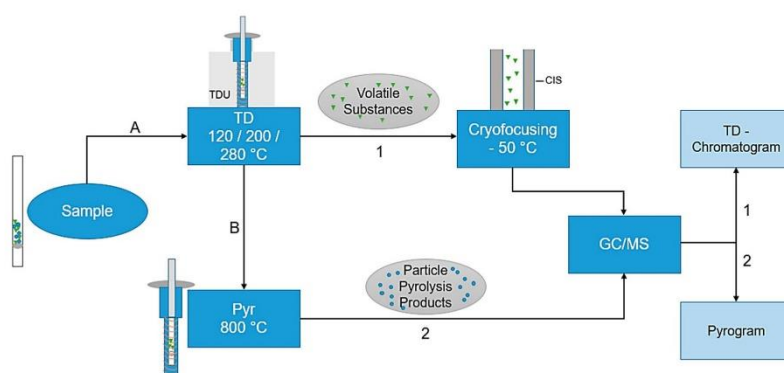


Figure 1. Flowchart of the thermodesorption- and pyrolysis-gas chromatography/mass spectrometry (TD-Pyr-GC/MS) analysis. First, (A) the sample is thermodesorbed (120–280 °C), thereby desorbing the volatile substances and cryofocusing them in the Cooled Injections System (CIS) at –50 °C. This is followed by a transfer to the GC column with an MS analysis (TD-GC/MS). The same sample (B) is subsequently pyrolyzed at 800 °C, followed by a GC/MS analysis (Pyr-GC/MS). The evaluations are carried out using the TD-Chromatogram and the Pyrogram.

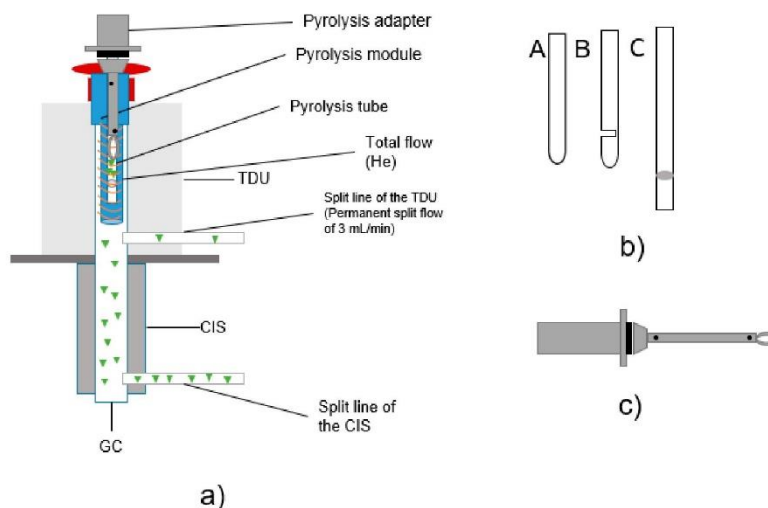


Figure 2. (a) Structure TD-GC/MS + Pyr-GC/MS; (b) design of different pyrolysis tubes (sample tubes); (c) drawing of pyrolysis transport adapter.

TD-GC/MS: The final thermal desorption temperature was set to three endpoints (120 °C, 200 °C and 280 °C). The initial temperature of the thermal desorption unit (TDU) is set to 20 °C with a delay of 0.3 min and an initial hold time of 1.0 min. The sample is heated to the respective endpoint temperature of 120 °C/200 °C/280 °C at 60 °C/min over a gradient and held for 5 min (Figure 1, step A). The desorption of the sample in the TDU occurs subsequently after the injection into the cooled injection system (CIS). In the CIS, the substances are trapped at −50 °C and heated to 120 °C/200 °C/280 °C with a 10 °C/min gradient, in order to transfer the trapped analytes onto the GC column (Figure 1, arrow 1). The transfer line temperature is 300 °C; the desorption mode is split-less, except for the permanent split flow. The GC/MS method (Figure 1; line 1 on the right) is adopted from Ochiai et al. (2005) [32]. However, the temperature for cryo-focusing is set to −50 °C instead of −150 °C. The initial temperature is set to 70 °C and is held for 2 min. The sample is then heated up to 150 °C with a gradient of 25 °C/min, followed by a heating rate of 3 °C/min to 200 °C. In the last step, the sample is heated by a gradient of 8 °C/min to 300 °C.

Pyr-GC/MS: Next, a pyrolysis step is performed (Figure 1, step B). The initial temperature of the TDU in the pyrolysis step is set to 50 °C with a hold time of 5.4 min. The sample is heated at 720 °C/min to 320 °C and this temperature is held for 1.4 min. After 0.3 min, the pyrolysis module heats the sample to a final temperature of 800 °C with a follow up time of 5 min. The transfer temperature is set to 350 °C and the desorption mode is split-less. The pyrolysis products are trapped in the CIS at 350 °C (Figure 1, arrow 2). The sample injection in the CIS is operated in split mode, i.e., the inlet ratio into the column is set to 100:1. The GC/MS method (Figure 1; line 2 on the right) is as follows: the initial temperature is set to 50 °C and is held for 2 min. The sample is then heated to 320 °C with a 10 °C/min gradient. This temperature is maintained for 3 min. Helium is used as carrier gas. In order to detect carry-over or impurities, an empty tube is measured after each sample.

The particle samples to be tested were placed in pyrolysis tubes for subsequent analysis (see Figure 2a). For the sample transfer into the CIS, three different pyrolysis tubes were tested. All were made of quartz glass and purchased from Gerstel GmbH (Mühlheim an der Ruhr, Germany). Since the design of the sample holder is an essential aspect regarding potential carry-over [33], several tube types were tested (visual setup details, see Figure 2b), including the following: pyrolysis tubes (A) with one open end and one closed end with a length of 17 mm, (B) with one open end and one closed end with an additional slot of 17 mm in length and (C) with two open ends and a length of 25 mm sealed with quartz wool. Thus, quartz wool is only used in type (C) and is contained in the tube and in contact with the sample. With the closed type (A) tube, the carrier gas flow is non-uniform; in the slotted type (B) tube, a more uniform carrier gas flow is ensured [33]. (C) is open at both ends, which should improve the carrier gas flow. The weight of the pyrolysis tubes was between 90 and 110 mg.

2.2. Materials and Methods

The reference particles were free of additives and provided by BS Partikel GmbH (Mainz, Germany). Polystyrene (PS) suspended in ethanol was supplied in the sizes of 78 nm and 41 µm, respectively. Further dry PS particles were delivered in sizes of 40 µm, and the polymethyl methacrylate (PMMA) and polyethylene (PE) particles in sizes of 48 µm, respectively. All PS particles were spherical and the shape of PMMA and PE particles was unknown. Phenanthrene (CAS: 85-01-8) and triclosan (CAS: 3380-34-5) were purchased from Sigma-Aldrich (Taufkirchen, Germany) and α -cypermethrin (CAS: 67375-30-8) from greyhoundchrom (Birkenhead, UK). All chemicals were stored at 4 °C. Methanol ($\geq 99.8\%$) in HPLC-grade was purchased from VWR (Ismaning, Germany). Ultrapure water with pH 5 was obtained from a Sartorius arium pro ultrapure water system (Göttingen, Germany). For the weighing of the samples, a Sartorius Cubis[®] Ultramicro Balance (Göttingen, Germany) was used.

2.3. Sample Preparation for Reference and Ecotoxicological Samples

Initial experiments were conducted for TD temperature optimization (with lowest expected pyrolysis products) and no trace organic chemicals. The final sets of TD temperatures were observed at 120/200/280 °C to determine that no pyrolysis products occurred during the TD step.

In all experiments, 10 mg of particles were suspended in 10 mL ultrapure water. The suspension was shaken for 1 h at room temperature at 1000 rpm. The solution was filtered by vacuum filtration to obtain dry particles. The particles were scraped off the filter with a spatula and directly transferred into a vial. The particles were freeze-dried for one hour. Subsequently, the particles were weighed into the pyrolysis tubes with a minimum and maximum weight of 30–80 to ensure reproducible results. The particles were transferred into the pyrolysis tubes using a syringe cannula. Each sample was weighed three times and the mean value was calculated to increase reproducibility. This sample tube was then subjected to TD-Pyr-GC/MS analysis. The entire sample preparation is summarized in the workflow in Figure 3. For the preparation of environmental samples from, for example, ecotoxicological assays, the sample preparation was carried out analogously.

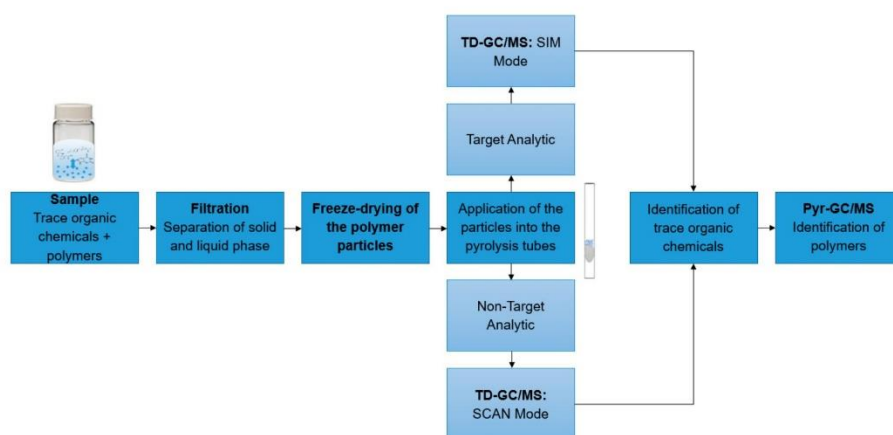


Figure 3. Workflow of sample analysis: First, the samples to be analyzed are filtered to separate the solid from the liquid phase. Then, the samples are applied into the pyrolysis tubes. Depending on the test setup, a non-target analytic (SCAN mode) or a target analytic (SIM mode) can be performed. Finally, a TD-Pyr-GC/MS analysis is conducted.

In the sorption experiments with the target substances phenanthrene, α -cypermethrin and triclosan, the principle was the same as described above without trace organic chemicals. In these studies, the trace organic chemicals were added to the 10-mg particles in concentrations of 1000 $\mu\text{g/L}$ and 100 $\mu\text{g/L}$. For the preparation of the stock solution of 1000 mg/L , the trace organic chemicals were dissolved in methanol and diluted further in methanol. The particles were suspended in 10 mL ultrapure water and treated as described above. The experiments for the measurements in SCAN and SIM mode were performed on PS 78 nm particles. The concentration was 1000 $\mu\text{g/L}$ for each trace organic chemical. All experiments were carried out in triplicate on two different days, i.e., in total, six replicates.

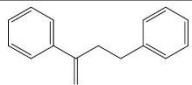
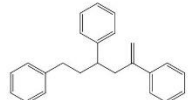

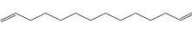

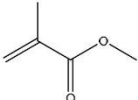
2.4. Evaluation of the TD-Pyr-GC/MS Data

The mass spectrometer operated in full-scan mode (m/z range 40 to 550) with electron impact ionization (70 eV) for non-target analysis. For a target analysis, PS 78-nm particles and the trace

organic chemicals phenanthrene (m/z 178), α -cypermethrin (m/z 163, 181, 165, 91, 77) and triclosan (m/z 290, 288, 218) were measured as references in SIM mode. Data analysis was conducted with Mass Hunter Workstation Software (Ver.B.08.000, Agilent). The identification of the substances was validated via MS spectra, and a NIST database comparison was conducted, as well as the retention index (RI) comparison [34].

Specific mass spectrometric signals were selected (Tables 1 and 2) to extract and identify the data of the different polymers or trace organic chemicals (by means of their pyrolysis products). The data were standardized to make the sorption of trace organic chemicals on the particles comparable. The peak areas obtained after the specific extraction were divided by the weighed particle amount.

Table 1. Characteristic pyrolysis products of selected polymers for identification.

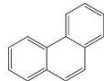
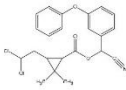
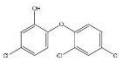
Polymer Type	Characteristic Pyrolysis Fragments	Formula	Molecular Weight (g/mol)	m/z (Intensity Ratio (%)) *	Structure
PS	3-butene-1,3-diyldibenzene (styrene dimer)	C ₁₆ H ₁₆	208	91 (100), 104 (27), 130 (23), 208 (30)	
PS	5-hexene-1,3,5-triyltribenzene (styrene trimer)	C ₂₄ H ₂₄	312	91 (100), 117 (32), 194 (19), 207 (25)	
PE	1,12-tridecadiene	C ₁₃ H ₂₄	180	55 (52), 81 (44), 67 (38), 95 (26)	
PE	1,13-tetradecadiene	C ₁₄ H ₂₆	194	81 (42), 95 (27), 109 (13)	
PE	1,15-hexadecadiene	C ₁₆ H ₃₀	222	55 (63), 81 (50), 96 (45), 69 (37)	
PMMA	Methyl methacrylate	C ₅ H ₈ O ₂	100	41 (77), 69 (100), 100 (57)	

* intensity ratio to largest peak in spectra.

Three different polymers (PE, PS and PMMA) were selected for thermodesorption temperature optimization. Characteristic fragments were chosen for the unique identification of the individual polymers. Characteristic fragments that can be used for the identification of PS are the styrene mono-, di- and trimer. However, the monomer is also present in environmental samples because it also occurs in biogenic polymers, such as chitin or wool fibers [34], thus it can also be detected in the pyrolysis step. Therefore, solely the dimer and trimer serve as final indicator fragment for PS samples. The decomposition into small aliphatic chains (saturated, mono-saturated and di-unsaturated hydrocarbons) is typical for PE [22,35,36]. In environmental matrices, mono-unsaturated and saturated hydrocarbons also occur naturally since they result, for instance, from the decomposition of fatty acids and lipids [37]. Therefore, exclusively the di-unsaturated hydrocarbons (C13, C14 and C16) were used for the identification of PE [38]. The only pyrolysis product that could be detected reproducibly for PMMA was methyl methacrylate, which was used for identification.

The sorption data were evaluated with respect to sample 'peak area' to 'particle weight' ratio and the ratio of 'peak area' to 'particle surface'. The evaluation of the ratio of 'particle area' to particle weight' compares the peak area of the selected trace organic chemicals with the weighed-in particle mass. This allows conclusions to be drawn about the sorption capacity of the individual polymer types and sizes. The ratio peak area to particle surface reflects the peak areas of the trace organic chemicals on the calculated particle surface.

Table 2. Characteristic signals, properties and structure of chosen substances.

Substance	Characteristic Signals (m/z)	Molecular Weight (g/mol)	Log D Value (pH 5.5) *	Environmental Relevance	Boiling Point (°C) at 760 mmHg	Structure
Phenanthrene	178	178	5.27	High toxicity, mutagenic [39], typical waste water pollutant [9]	337.4 ± 9.0	
α-Cypermethrin	163, 184, 209	416	6.05	The most widespread product of Type II pyrethroid pesticide [9,40]	511.3 ± 50	
Triclosan	290, 288, 218, 63	290	5.27	Antimicrobial agent which is used in personal care products [41,42]	344.6 ± 42.0	

* values from chemspider.com database.

3. Results and Discussion

The aim of this study was to develop a method for the simultaneous analysis of trace organic chemicals on micro- and nanoplastic particles and polymer identification using a new analytical technique combining TD-GC/MS and Pyr-GC/MS. First, it had to be ensured that the method was reproducible and free of carry-over for the analysis of reference polymers. In a next step, this method was validated using selected trace organic chemicals that were sorbed onto reference particles. As indicator chemicals, in this study, we used phenanthrene, α-cypermethrin, and triclosan. The three trace organic chemicals were selected considering their different structural formulas, hydrophobicities (represented by different log K_{OW} values) and environmental relevance (Table 2). In this study, PS (41, 40, 0.078 μm), PE (48 μm) and PMMA (48 μm) particles were used.

3.1. Scope of Application for TD-Pyr-GC/MS

The application area of TD-Pyr-GC/MS is mainly in the rapid qualitative analysis of environmental samples targeting interactions of trace organic chemicals and different polymer types, e.g., ecotoxicological assays or spiked samples of lab- or pilot-scale wastewater treatment processes. Since no additional extraction steps are required for the analysis of trace organic chemicals, the sample preparation time is short. The pure measuring time for one sample is 2 h, which allows a high sample throughput. Figure 3 illustrates a possible workflow of sample analysis. The particles to be analyzed are separated from the liquid phase by filtration and freeze-drying. For analysis, the samples are applied to the pyrolysis tubes. Depending on the assay, a target analysis (SIM mode) or a non-target analysis (SCAN mode) can be performed. Then, the coupled TD-Pyr-GC/MS analysis is carried out as described in 2.1. The final data analysis results in a quick qualitative overview of possible trace organic chemicals present and the types of polymers.

3.2. Sources of Contamination in the TD-Pyr-GC/MS System

One aim of this study was to establish an analytical approach by minimizing carry-over. Preliminary experiments were carried out with PS containing styrene dimers and trimers as characteristic substances for identification in the MS fragment spectrum. An accumulation of the characteristic substances in the system was observed with increasing numbers of measurements. This carry-over was

verified by measuring an empty tube with TD-GC/MS followed by Pyr-GC/MS after each measurement. The results imply that the analytes are transferred from incomplete pyrolysis of the sample to the subsequent TD measurement of the empty tube. It is assumed that during pyrolysis, not the whole content of substances reaches the GC column but accumulates in the system [43].

(a) Sample Inlet Tubes

Carryover was observed using tube types A and B (Figure 2b). Measurements with tube type C showed good results and significantly reduced the problem of substance transfer. Therefore, type C tubes were used for all temperature optimization tests and sorption experiments. Pyrolysis tubes type A and B are closed at the bottom. Therefore, a constant flow of helium cannot be guaranteed.

(b) Transport Adapters

Pyrolysis tubes type C were mounted on transport adapters (Figure 2c) which can also be a source of contamination. To avoid contamination inside of the adapter, the lower part of the adapter was cleaned after each measurement for 15 min in dichloromethane and an ultrasonic bath. In addition, the filament of the pyrolysis unit is another wearing part carrying a risk of contamination.

(c) Filament for pyrolysis

After approximately 300–350 measurements with the same filament, more impurities appeared during the empty tube measurements. The filament was examined more closely and black dots and soot discolorations were visible. However, this source of contamination could easily be eliminated by changing the filament regularly.

3.3. Influence of Different TD Temperature Programs on Pyrolysis of Particles of Different Materials and Size

Reference particles without indicator substances were used to study and optimize the thermal desorption temperature. Thereby, characteristic pyrolysis products of each polymer were used for the Pyr-GC/MS data evaluation. Particle samples with adsorbed substances were thermodesorbed (TD-GC/MS) and subsequently pyrolyzed (Pyr-GC/MS). In this way, already, pyrolysis fragments eluting in the TD-GC/MS could be identified. The resulting chromatograms and pyrograms of the individual polymers were extracted according to their characteristic fragments (as shown in Table 1). As examples, PS chromatograms and pyrograms are shown in Figure 4. These were extracted for the di- and trimer in TD (Figure 4a) and Pyr (Figure 4b), respectively. The pyrogram shown in Figure 4a reveals that polystyrene particles (78 nm) are, in large part, already fragmented into the di- and trimer in the TD. In Figure 4b, the pyrogram is contrasted with the di- and trimer of the polystyrene particle (78 nm).

For TD temperature optimization, measurements with the selected particles (PMMA, PE and PS) were performed at the final temperatures of 120, 200 and 280 °C and results are shown in Figure 5. A significant increase in PMMA pyrolysis products in the thermodesorption step occurred with an increase in TD temperature. Differences can be seen for the PS microplastic particles (PS 40 µm and PS 41 µm). Since the PS 40 µm particles were stored dry but the PS 41 µm were suspended in ethanol, it seems that the storage conditions of the particles might have an influence. The TD temperature variation has no influence on the PE particles, independent of the temperature the characteristic products are only visible in the pyrogram. The final thermal desorption temperature was chosen at 200 °C, considering that 120 °C is too low to achieve quantitative desorption of most trace organic chemicals. A TD temperature of 200 °C is also more suitable than 280 °C for the analysis of thermolabile substances.

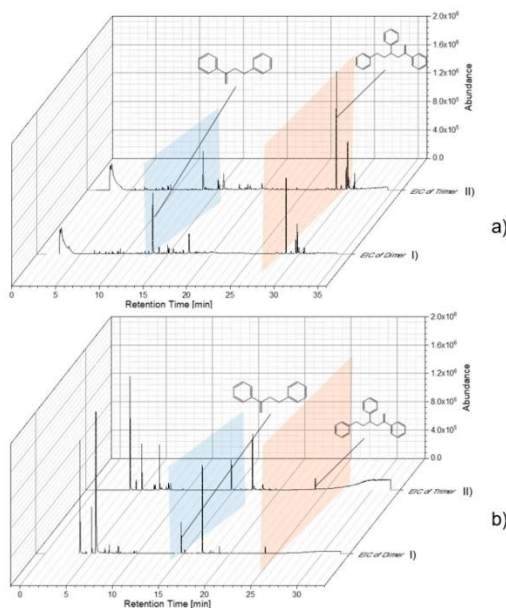


Figure 4. Evaluation of chromatogram/pyrogram of PS 78-nm particles by extracted-ion chromatogram (EIC) of dimer (I) and Trimer (II) (a) TD-Chromatogram (TD-GC/MS), (b) Pyrogram (Pyr-GC/MS).

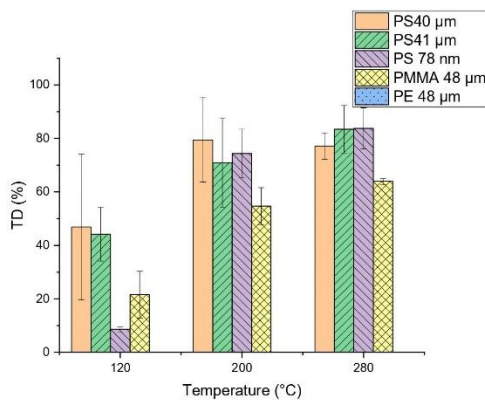


Figure 5. Percentage of the characteristic pyrolysis products of the polymers (Table 1) of the single polymers (polymethyl methacrylate (PMMA), polyethylene (PE) and polystyrene (PS)) already visible in the TD Chromatogram calculated from the peak areas. The remaining percentage of the characteristic pyrolysis products is visible in the Pyrogram.

3.4. Desorption Behavior of Phenanthrene, α -Cypermethrin and Triclosan

For the validation of the newly developed TD-Pyr-GC/MS method, the sorption behavior of the target trace organic chemicals (Table 2) at two final concentrations (1000 $\mu\text{g/L}$ and 100 $\mu\text{g/L}$) on the different particles was investigated. The boiling points of the trace organic chemicals used in this study are reported in Table 2. If more polymer products are present in the TD, there is a risk of interference with trace organic chemicals and that both the trace organic chemicals and the characteristic substances of the polymers can no longer be clearly identified. Figure 6a–c illustrate the measured peak area of the trace organic chemicals divided by the weighed mass for the three target trace organic chemicals. The results are discussed in the following sections.

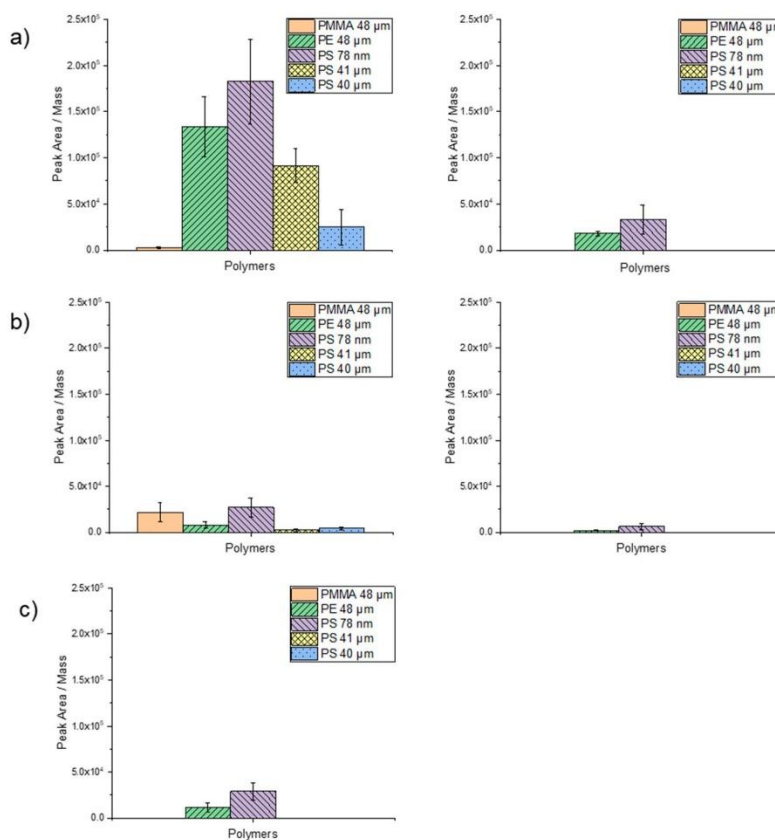


Figure 6. Sorption of the selected trace substances on PMMA (48 μm), PE (48 μm), PS (78 μm), PS (41 μm) and PS (40 μm) particles: (a) 1 $\mu\text{g/mL}$ (left) and 0.1 $\mu\text{g/mL}$ (right) phenanthrene, (b) 1 $\mu\text{g/mL}$ (left) and 0.1 $\mu\text{g/mL}$ (right) α -cypermethrin and (c) 1 $\mu\text{g/mL}$ triclosan. For evaluation, the peak area of the trace substance was divided by the weighed mass.

Phenanthrene at a concentration of 1000 $\mu\text{g/L}$ exhibited the highest degree of peak area per mass on PS nanoparticles (78 nm), followed by PE (48 μm), PS (41 μm) and PS (40 μm). Almost no sorption

occurred on PMMA (48 μm) (Figure 6a). These findings suggest a significant influence of particle size on sorption ability. For phenanthrene at a concentration of 100 $\mu\text{g/L}$, only sorption on PS 78 nm and PE particles was observed. The lowest degree of sorption of phenanthrene was noticed on the PMMA particles. A difference was also observed for the PS particles, although they almost have the same size (i.e., 40 and 41 μm). The particles suspended in ethanol (PS 41 μm) exhibited a higher degree of sorption than the dry particles (PS 40 μm). Here, ethanol might have served as an adsorption mediator.

The normalized degree of sorption of 1000 $\mu\text{g/L}$ α -cypermethrin on the particles was in general lower compared to phenanthrene (Figure 6b). Applying α -cypermethrin at a concentration of 100 $\mu\text{g/L}$ sorption was only observed on PS 78 nm and PE particles. Due to a more complex structure and the higher molecular weight of α -cypermethrin compared to phenanthrene, a contact time of 1 h may have been too short to achieve a higher degree of adsorption. Interestingly, however, sorption is higher on PMMA and lower on PE. Here, too, the highest degree of sorption was observed on PS 78-nm particles.

Triclosan at a concentration of 1000 $\mu\text{g/L}$ adsorbed only on PS 78-nm and PE 48- μm particles within a contact time of 1 h (Figure 6c). Applying triclosan at a concentration of 100 $\mu\text{g/L}$, no sorption was observed on any particle type. This contact time was likely too short, since Li et al. (2019) reported that the sorption equilibrium of triclosan was only reached after 72 h [44]. Nevertheless, also for triclosan, the highest degree of sorption was observed for the nanoparticles.

Due to the relatively short contact time of 1 h, the sorption equilibrium may not yet have been reached and further experiments with longer contact times are pending. However, the sorption kinetics and the individual detection limits of trace substances are beyond the scope of this paper and are currently under investigation.

3.5. Comparison of the Desorption Behavior of the Selected Trace Organic Chemicals in TD and PYR

In order to assess the tendency of trace organic chemicals to desorb from particles, the percentage of phenanthrene desorption during TD was considered and is illustrated in Figure 7. Although values fluctuate, almost 100% of phenanthrene was already desorbing from PE particles during the TD step, while PS particles (41 and 40 μm) exhibited desorption varying between 25 and 60%. These significant differences may be due to the different pretreatments of the particles. The PS 41- μm particles were suspended in ethanol whereas the PS 40- μm particles were stored dry. By comparing different concentration levels of applied trace organic chemicals, the concentration does not seem to influence the desorption for PE, PS 40- μm , and PS 78-nm particles significantly (Figure 7). These findings suggest that the desorption behavior depends on both the particle size and the particle type. α -cypermethrin and triclosan were both completely desorbed within the TD (data not shown).

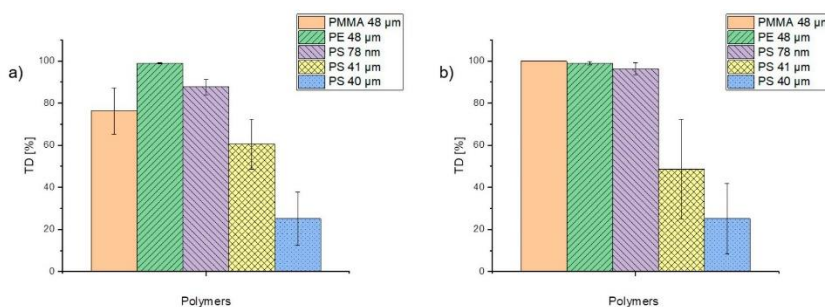


Figure 7. Percentage of phenanthrene in the concentrations of 1 $\mu\text{g/mL}$ (a) and 0.1 $\mu\text{g/mL}$ (b) desorbed during TD from the particles.

On the basis of these experiments, it is not yet possible to draw any conclusions regarding the quantity of trace organic chemicals adsorbed on microparticles. However, those conclusions will potentially be possible in the near future when both the trace organic chemicals on the particles and the remaining trace organic chemicals in the aqueous phase will be examined. The aqueous phase is analyzed via stir bar sorptive extraction (SBSE) and TD-GC/MS, the particles via TD-Pyr-GC/MS. It was demonstrated that desorption behavior depends on both the particle type and the particle size. In addition to size and shape, the main characteristics that are considered to influence sorption on a plastic particle are crystallinity, density, structure and hydrophobicity [5,10,45].

3.6. Comparison of SCAN and SIM Mode for Selected Trace Organic Chemicals on PS Nanoparticles

The three target trace organic chemicals were incubated at the concentration of 1000 µg/L on PS 78 nm particles and measured in TD-GC/MS using SIM mode. The SIM mode was optimized for the respective trace substance; see Section 2.4. The peak areas, and thus the sensitivity, increased in SIM mode for all trace substances: phenanthrene (+33% ± 2%), α-cypermethrin (+54% ± 12%), and triclosan (+58% ± 12%). For target analysis, it is, therefore, recommended to measure in SIM mode.

3.7. Trace Organic Chemical Sorption in Relation to the Particle Surface

Since the polystyrene particles are assumed to be spherical in shape, their surface area could be calculated. Subsequently, the calculated surface was divided by the measured peak area in the chromatogram. The number of particles was calculated on the basis of the weighed mass (Table 3). As expected, the number of nanoparticles (78 nm) is significantly higher compared to microparticles (40 and 41 µm). In addition, the calculated surface area of the nanoparticles confirms that the surface area is significantly larger for almost the same mass, thus providing more opportunities for the trace organic chemicals to adsorb.

Table 3. Mass and number of polystyrene particles.

Particle Size (µm)	Particle Type	Mass (µg)	Number of Particles	Surface Particles (m ²)
41	PS	22–63	586–1679	3.10×10^{-6} – 8.86×10^{-6}
40	PS	23–64	660–1837	3.32×10^{-6} – 9.23×10^{-6}
0.078	PS	29–69	1.12×10^{11} – 2.67×10^{11}	2.14×10^{-3} – 5.10×10^{-3}
48	PE		Not spherical	
48	PMMA		Not spherical	

The degree of sorption of trace organic chemicals as a function of the peak area per particle surface is illustrated in Figure 8. Comparing these findings with the results in which the polymers were plotted as a function of particle per mass reveals that the higher degree of sorption of nanoparticles is mainly due to the high number of particles and the higher specific surface area. The results also suggest that the sorption on PS 41-µm particles suspended in ethanol works better than on dry 40-µm particles.

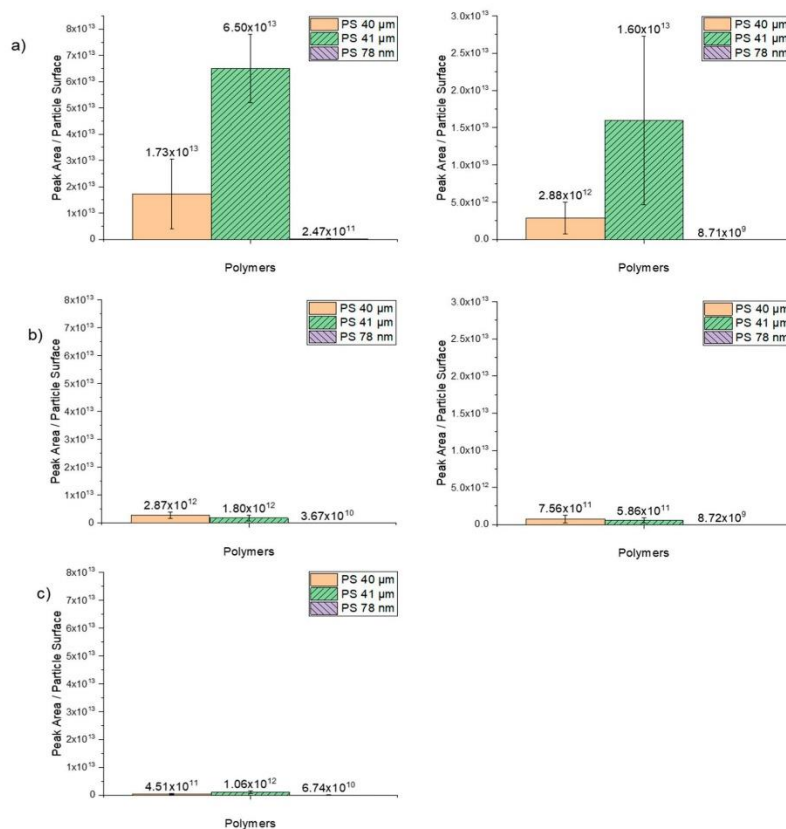


Figure 8. Sorption of the selected trace substances as a function of peak area/particle surface on the spherical PS particles in sizes 40 μm , 41 μm and 78 nm. (a) 1 $\mu\text{g/mL}$ (right) and 0.1 $\mu\text{g/mL}$ (left) phenanthrene, (b) 1 $\mu\text{g/mL}$ (right) and 0.1 $\mu\text{g/mL}$ (left) α -cypermethrin, (c) 1 $\mu\text{g/mL}$ (right) triclosan.

4. Conclusions and Outlook

The results of this study confirm that a new method can simultaneously identify trace organic chemicals and polymer type in one analytical setup. This method offers fast sample analysis within a short time period of 2 h. In comparison to Herrera et al., 2003 and Fries et al., 2013, who use a double shot pyrolysis or a sequential pyrolysis GC/MS for the characterization of additives in polymers, the sorption behavior of trace organic substances on different polymers and sizes without extraction steps could be shown for the first time in this work [12,14]. The method development for the determination of the optimal TD-temperature for the TD-Pyr-GC/MS also showed that this temperature significantly influences the desorption behavior. In addition, it could be shown that TD-Pyr-GC/MS is particularly suitable for the analysis of nanoplastic particles. The following objectives were achieved through the TD-Pyr-GC/MS method development:

1. Temperature optimization of the proposed TD-GC/MS method requires that the thermal desorption temperature should be as high as possible in order to desorb all sorbed substances, and at the same time, the temperature must be so low that as few pyrolysis products as possible are generated during the thermal desorption step. In this regard, the optimal TD-temperature was identified to be 200 °C.
2. A suitable Pyr-GC/MS method was developed which completely depolymerizes all targeted polymers (i.e., PS, PE and PMMA) without leaving residues in the system and therefore avoiding carry-over issues. For this purpose, an optimum pyrolysis temperature of 800 °C was determined.

In the experiments carried out, it was confirmed that sorption of trace organic chemicals depends on both particle size and polymer type. In all sorption tests, it could be shown that the sorption on nanoplastic particles was highest. Phenanthrene and α -cypermethrin exhibited a higher degree of sorption on PS nanoparticles and on PS microparticles. For triclosan, no sorption on PMMA and PS microplastic particles was observed. The sorption of phenanthrene on the particles was strongly polymer-dependent (PMMA \ll PS 40 μm < 41 μm < PE < PS 78 nm). This adsorption trend was also observed for α -cypermethrin (PS 41 μm < PS 40 μm < PE < PMMA < PS 78 nm). Triclosan adsorbed only on PE and PS 78-nm nanoplastic particles (PE < PS78). In this study, however, the contact time was limited to one hour and the sorption equilibrium might not have been reached after this time period. The focus of this study, however, was not on sorption kinetics but on the establishment and practical application of a new method for the analysis of trace organic chemicals on micro- and nanoplastic particles. In further experiments, the contact time should be extended in order to assure that the sorption equilibrium between the trace organic chemicals on the particles and the aqueous phase is reached and to elucidate sorption kinetics.

Author Contributions: Conceptualization, J.R., J.G. and T.L.; methodology, J.R. and J.G.; software, J.R.; validation, J.R., J.G. and T.L.; formal analysis, J.R. and J.G.; investigation, J.R. and J.G.; resources, J.E.D.; data curation, J.R.; writing—original draft preparation, J.R.; writing—review and editing, J.R., J.G., T.L. and J.E.D.; visualization, J.R.; supervision, J.C., T.L. and J.E.D.; project administration, J.C. and J.E.D. All authors have read and agreed to the published version of the manuscript.

Funding: This research was funded by the German Federal Ministry of Education and Research (BMBF) in the project SubµTrack, grant number 02WPL1443A.

Acknowledgments: We are grateful for the support by BS Partikel, who produced the micro- and nanoplastic particles, Thomas Wagner from Gerstel for technical support, Caroline Feyerabend for practical assistance in the lab and Oliver Knoop for valuable discussions.

Conflicts of Interest: The authors declare no conflict of interest.

References

1. Jambeck, J.R.; Geyer, R.; Wilcox, C.; Siegler, T.R.; Perryman, M.; Andrady, A.L.; Narayan, R.; Law, K.L. Plastic waste inputs from land into the ocean. *Science* **2015**, *347*, 768–771. [[CrossRef](#)] [[PubMed](#)]
2. GESAMP. *Sources, Fate and Effects of Microplastics in the Marine Environment: A Global Assessment*; International Maritime Organization: London, UK, 2015.
3. Eriksen, M.; Lebreton, L.C.; Carson, H.S.; Thiel, M.; Moore, C.J.; Borerro, J.C.; Galgani, F.; Ryan, P.G.; Reisser, J. Plastic Pollution in the World's Oceans: More than 5 Trillion Plastic Pieces Weighing over 250,000 Tons Afloat at Sea. *PLoS ONE* **2014**, *9*, e111913. [[CrossRef](#)] [[PubMed](#)]
4. Mattsson, K.; Hansson, L.A.; Cedervall, T. Nano-plastics in the aquatic environment. *Environ. Sci. Process. Impacts* **2015**, *17*, 1712–1721. [[CrossRef](#)]
5. Alimi, O.S.; Farner Budarz, J.; Hernandez, L.M. Tufenkji, Microplastics and Nanoplastics in Aquatic Environments: Aggregation, Deposition, and Enhanced Contaminant Transport. *Environ. Sci. Technol.* **2018**, *52*, 1704–1724. [[CrossRef](#)] [[PubMed](#)]
6. da Costa, J.P.; Santos, P.S.M.; Duarte, A.C.; Rocha-Santos, T. (Nano) plastics in the environment—Sources, fates and effects. *Sci. Total Environ.* **2016**, *566–567*, 15–26. [[CrossRef](#)] [[PubMed](#)]
7. Browne, M.A.; Galloway, T.; Thompson, R. Microplastic—An emerging contaminant of potential concern? *Integr. Environ. Assess. Manag.* **2007**, *3*, 559–566. [[CrossRef](#)]

8. Seidensticker, S.; Gratwohl, P.; Lamprecht, J.; Zarfl, C. A combined experimental and modeling study to evaluate pH-dependent sorption of polar and non-polar compounds to polyethylene and polystyrene microplastics. *Environ. Sci. Eur.* **2018**, *30*, 30. [[CrossRef](#)] [[PubMed](#)]
9. Seidensticker, S.; Zarfl, C.; Cirpka, O.A.; Fellenberg, G.; Gratwohl, P. Shift in Mass Transfer of Wastewater Contaminants from Microplastics in the Presence of Dissolved Substances. *Environ. Sci. Technol.* **2017**, *51*, 12254–12263. [[CrossRef](#)]
10. Hüffer, T.; Hofmann, T. Sorption of non-polar organic compounds by micro-sized plastic particles in aqueous solution. *Environ. Pollut.* **2016**, *214*, 194–201. [[CrossRef](#)]
11. Duemichen, E.; Eisentraut, P.; Celina, M.; Braun, U. Automated Thermal Extraction-Desorption Gas Chromatography Mass Spectrometry: A Multifunctional Tool for Comprehensive Characterization of Polymers and their Degradation Products. *J. Chromatogr. A* **2019**, *1592*, 133–142. [[CrossRef](#)]
12. Herrera, M.; Matuschek, G.; Kettrup, A. Fast identification of polymer additives by pyrolysis-gas chromatography/mass spectrometry. *J. Anal. Appl. Pyrolysis* **2003**, *70*, 35–42. [[CrossRef](#)]
13. La Nasa, J.; Biale, G.; Fabbri, D.; Modugno, F. Microwave-assisted solvent extraction and double-shot analytical pyrolysis for the quali-quantitation of plasticizers and microplastics in beach sand samples. *J. Hazard Mater.* **2020**, *401*, 123287. [[CrossRef](#)] [[PubMed](#)]
14. Fries, E.; Dekiff, J.H.; Willmeyer, J.; Nuelle, M.-T.; Ebert, M.; Remy, D. Identification of polymer types and additives in marine microplastic particles using pyrolysis-GC/MS and scanning electron microscopy. *Environ. Sci. Process. Impacts* **2013**, *15*, 1949–1956. [[CrossRef](#)] [[PubMed](#)]
15. Zhang, X.; Zheng, M.; Wang, L.; Lou, Y.; Shi, L.; Jiang, S. Sorption of three synthetic musks by microplastics. *Mar. Pollut. Bull.* **2018**, *126*, 606–609. [[CrossRef](#)] [[PubMed](#)]
16. Velzeboer, L.; Kwadijk, C.J.A.F.; Koelmans, A.A. Strong sorption of PCBs to nanoplastics, microplastics, carbon nanotubes, and fullerenes. *Environ. Sci. Technol.* **2014**, *48*, 4869–4876. [[CrossRef](#)] [[PubMed](#)]
17. Hüffer, T.; Weniger, A.-K.; Hofmann, T. Sorption of organic compounds by aged polystyrene microplastic particles. *Environ. Pollut.* **2018**, *236*, 218–225. [[CrossRef](#)] [[PubMed](#)]
18. Bakir, A.; Rowland, S.J.; Thompson, R.C. Enhanced desorption of persistent organic pollutants from microplastics under simulated physiological conditions. *Environ. Pollut.* **2014**, *185*, 16–23. [[CrossRef](#)]
19. Bakir, A.; Rowland, S.J.; Thompson, R.C. Transport of persistent organic pollutants by microplastics in estuarine conditions. *Estuar. Coast. Shelf Sci.* **2014**, *140*, 14–21. [[CrossRef](#)]
20. Hidalgo-Ruz, V.; Gutow, L.; Thompson, R.C.; Thiel, M. Microplastics in the marine environment: A review of the methods used for identification and quantification. *Environ. Sci. Technol.* **2012**, *46*, 3060–3075. [[CrossRef](#)]
21. Käppler, A.; Fischer, D.; Oberbeckmann, S.; Schernewski, G.; Labrenz, M.; Eichhorn, K.-J.; Voit, B. Analysis of environmental microplastics by vibrational microspectroscopy: FTIR, Raman or both? *Anal. Bioanal. Chem.* **2016**, *408*, 8377–8391. [[CrossRef](#)]
22. Duemichen, E.; Barthel, A.-K.; Braun, U.; Bannick, C.G.; Brand, K.; Jekel, M.; Senz, R. Analysis of polyethylene microplastics in environmental samples, using a thermal decomposition method. *Water Res.* **2015**, *85*, 451–457. [[CrossRef](#)]
23. Elert, A.M.; Becker, R.; Duemichen, E.; Eisentraut, P.; Falkenhagen, J.; Sturm, H.; Braun, U. Comparison of different methods for MP detection: What can we learn from them, and why asking the right question before measurements matters? *Environ. Pollut.* **2017**, *231*, 1256–1264. [[CrossRef](#)]
24. Klein, S.; Dimzon, I.K.; Eubeler, J.; Knepper, T.P. Analysis, Occurrence, and Degradation of Microplastics in the Aqueous Environment. In *Freshwater Microplastics*; Springer: Frankfurt am Main, Germany, 2018; Volume 58, pp. 51–67.
25. La Nasa, J.; Biale, G.; Fabbri, D.; Modugno, F. A review on challenges and developments of analytical pyrolysis and other thermoanalytical techniques for the quali-quantitative determination of microplastics. *J. Anal. Appl. Pyrolysis* **2020**, *149*, 104841. [[CrossRef](#)]
26. Yakovenko, N.; Carvalho, A.; ter Halle, A. Emerging use thermo-analytical method coupled with mass spectrometry for the quantification of micro(nano)plastics in environmental samples. *TrAC Trends Anal. Chem.* **2020**, *131*, 115979. [[CrossRef](#)]
27. Ziccardi, L.M.; Edgington, A.; Hentz, K.; Kulacki, K.J.; Kane Discroll, S. Microplastics as vectors for bioaccumulation of hydrophobic organic chemicals in the marine environment: A state-of-the-science review. *Environ. Toxicol. Chem.* **2016**, *35*, 1667–1676. [[CrossRef](#)] [[PubMed](#)]

28. Teuten, E.; Rowland, S.; Galloway, T.S.; Thompson, R.C. Potential for Plastics to Transport Hydrophobic Contaminants. *Environ. Sci. Technol.* **2007**, *41*, 7759–7764. [[CrossRef](#)] [[PubMed](#)]
29. Wang, J.; Liu, X.; Liu, G.; Zhang, Z.; Wu, H.; Cui, B.; Bai, J.; Zhang, W. Size effect of polystyrene microplastics on sorption of phenanthrene and nitrobenzene. *Ecotoxicol. Environ. Saf.* **2019**, *173*, 331–338. [[CrossRef](#)]
30. Zhang, H.; Penn, R.; Hamers, R.; Banfield, J. Enhanced Adsorption of Molecules on Surfaces of Nanocrystalline Particles. *J. Phys. Chem. B* **1999**, *103*, 4656–4662. [[CrossRef](#)]
31. Stark, J.V.; Klabunde, K.J. Nanoscale Metal Oxide Particles/Clusters as Chemical Reagents. Adsorption of Hydrogen Halides, Nitric Oxide, and Sulfur Trioxide on Magnesium Oxide Nanocrystals and Compared with Microcrystals. *Chem. Mater.* **1996**, *8*, 1913–1918. [[CrossRef](#)]
32. Ochiai, N.; Sasamoto, K.; Kanda, H.; Yamagami, T.; David, F.; Tienpont, B.; Sandra, P. Optimization of a multi-residue screening method for the determination of 85 pesticides in selected food matrices by stir bar sorptive extraction and thermal desorption GC-MS. *J. Sep. Sci.* **2005**, *28*, 1083–1092. [[CrossRef](#)]
33. Kleine-Benne, E.; Rose, B. *Versatile Automated Pyrolysis GC Combining a Filament Type Pyrolyzer with a Thermal Desorption Unit*; Gerstel GmbH&Co. KG: Mülheim an der Ruhr, Germany, 2011.
34. Fischer, M.; Scholz-Bottcher, B.M. Simultaneous Trace Identification and Quantification of Common Types of Microplastics in Environmental Samples by Pyrolysis-Gas Chromatography-Mass Spectrometry. *Environ. Sci. Technol.* **2017**, *51*, 5052–5060. [[CrossRef](#)]
35. Serrano, D.P.; Aguado, J.; Escola, J.M.; Rodríguez, J.M.; San Miguel, G. An investigation into the catalytic cracking of LDPE using Py-GC/MS. *J. Anal. Appl. Pyrolysis* **2005**, *74*, 370–378. [[CrossRef](#)]
36. Soják, L.; Kubinec, R.; Jurdáková, H.; Hájeková, E.; Bajus, M. High resolution gas chromatographic-mass spectrometric analysis of polyethylene and polypropylene thermal cracking products. *J. Anal. Appl. Pyrolysis* **2007**, *78*, 387–399. [[CrossRef](#)]
37. Kebelmann, K.; Hornung, A.; Karsten, U.; Griffiths, G. Intermediate pyrolysis and product identification by TGA and Py-GC/MS of green microalgae and their extracted protein and lipid components. *Biomass Bioenergy* **2013**, *49*, 38–48.
38. Duemichen, E.; Eisentraut, P.; Bannick, C.G.; Barthel, A.-K.; Senz, R.; Braun, U. Fast identification of microplastics in complex environmental samples by a thermal degradation method. *Chemosphere* **2017**, *174*, 572–584. [[CrossRef](#)] [[PubMed](#)]
39. Samanta, S.K.; Singh, S.K.; Jain, R.K. Polycyclic aromatic hydrocarbons: Environmental pollution and bioremediation. *Trends Biotechnol.* **2002**, *20*, 243–248.
40. Yu-Tao, T.; Zhao-Wei, L.; Yang, Y.; Zhuo, Y.; Tao, Z. Effect of alpha-cypermethrin and theta-cypermethrin on delayed rectifier potassium currents in rat hippocampal neurons. *Neurotoxicology* **2009**, *30*, 269–273. [[CrossRef](#)]
41. Adolffsson-Erici, M.; Pettersson, M.; Parkkonen, J.; Sturve, J. Triclosan, a commonly used bactericide found in human milk and in the aquatic environment in Sweden. *Chemosphere* **2002**, *46*, 1485–1489. [[CrossRef](#)]
42. Bester, K. Fate of triclosan and triclosan-methyl in sewage treatment plants and surface waters. *Arch. Environ. Contam. Toxicol.* **2005**, *49*, 9–17. [[CrossRef](#)]
43. Rial-Otero, R.; Galesio, M.; Capelo, J.-L.; Simal-Gándara, J. A Review of Synthetic Polymer Characterization by Pyrolysis-GC-MS. *Chromatographia* **2009**, *70*, 339–348. [[CrossRef](#)]
44. Li, Y.; Li, M.; Li, Z.; Yang, L.; Liu, X. Effects of particle size and solution chemistry on Triclosan sorption on polystyrene microplastic. *Chemosphere* **2019**, *231*, 308–314. [[CrossRef](#)] [[PubMed](#)]
45. Endo, S.; Koelmans, A.A. Sorption of Hydrophobic Organic Compounds to Plastics in the Marine Environment: Equilibrium. In *Hazardous Chemicals Associated with Plastics in the Marine Environment*; Springer: Cham, Switzerland, 2016; Volume 78, pp. 185–204.

Sample Availability: Samples of the compounds are available from the authors.

Publisher's Note: MDPI stays neutral with regard to jurisdictional claims in published maps and institutional affiliations.



© 2020 by the authors. Licensee MDPI, Basel, Switzerland. This article is an open access article distributed under the terms and conditions of the Creative Commons Attribution (CC BY) license (<http://creativecommons.org/licenses/by/4.0/>).

Appendix III

A Novel Analytical Approach to Assessing Sorption of Trace Organic Compounds into Micro- and Nanoplastic Particles




Biomolecules 2022, 12, 953.

This study introduced a new method, combining thermal extraction/desorption–gas chromatography/mass spectrometry (TD-Pyr-GC/MS), to analyze the sorption of trace organic compounds (TOrcs) into micro- and nanoplastic particles. It allowed direct TOrc analysis from the particles without extensive preparation. The study examined different polymer types and sizes, finding PS nanoparticles (78 nm) showed the highest and fastest sorption. Additionally, it demonstrated the feasibility of directly quantifying TOrcs from PS nanoparticles and showed that multiple TOrcs could sorb onto the particles simultaneously in mixed solutions.

Julia Reichel designed, performed, evaluated the experiments and wrote the manuscript. Johanna Grassmann, Oliver Knoop, Thomas Letzel and Jörg E. Drewes reviewed the manuscript and contributed to the discussion.

Article

A Novel Analytical Approach to Assessing Sorption of Trace Organic Compounds into Micro- and Nanoplastic Particles

 Julia Reichel ¹, Johanna Graßmann ¹, Oliver Knoop ¹ , Thomas Letzel ^{1,2}  and Jörg E. Drewes ^{1,*} 
¹ Chair of Urban Water Systems Engineering, Technical University of Munich, 85748 Garching, Germany; julia.reichel@tum.de (J.R.); j.grassmann@tum.de (J.G.); oliver.knoop@tum.de (O.K.); t.letzel@tum.de (T.L.)

² Analytisches Forschungsinstitut für Non-Target Screening GmbH (AFIN-TS GmbH), Am Mittleren Moos 48, 86167 Augsburg, Germany

* Correspondence: jdrewes@tum.de

Abstract: Assessing the sorption of trace organic compounds (TOCs) into micro- and nanoplastic particles has traditionally been performed using an aqueous phase analysis or solvent extractions from the particle. Using thermal extraction/desorption–gas chromatography/mass spectrometry (TD-Pyr-GC/MS) offers a possibility to analyze the TOCs directly from the particle without a long sample preparation. In this study, a combination of two analytical methods is demonstrated. First, the aqueous phase is quantified for TOC concentrations using Gerstel Twister[®] and TD-GC/MS. Subsequently, the TOCs on the particles are analyzed. Different polymer types and sizes (polymethyl methacrylate (PMMA), 48 µm; polyethylene (PE), 48 µm; polystyrene (PS), 41 µm; and PS, 78 nm) were analyzed for three selected TOCs (phenanthrene, triclosan, and α -cypermethrin). The results revealed that, over a period of 48 h, the highest and fastest sorption occurred for PS 78 nm particles. This was confirmed with a theoretical calculation of the particle surface area. It was also shown for the first time that direct quantification of TOCs from PS 78 nm nanoparticles is possible. Furthermore, in a mixed solute solution, the three selected TOCs were sorbed onto the particles simultaneously.

Keywords: microplastic; nanoplastic; desorption; sorption processes; TD-Pyr-GC/MS


Citation: Reichel, J.; Graßmann, J.; Knoop, O.; Letzel, T.; Drewes, J.E. A Novel Analytical Approach to Assessing Sorption of Trace Organic Compounds into Micro- and Nanoplastic Particles. *Biomolecules* **2022**, *12*, 953. <https://doi.org/10.3390/biom12070953>

Academic Editors: Marisa P. Sárria, Dmitri Petrovykh and Andreia Gomes

Received: 24 May 2022

Accepted: 29 June 2022

Published: 6 July 2022

Publisher's Note: MDPI stays neutral with regard to jurisdictional claims in published maps and institutional affiliations.



Copyright: © 2022 by the authors. Licensee MDPI, Basel, Switzerland. This article is an open access article distributed under the terms and conditions of the Creative Commons Attribution (CC BY) license (<https://creativecommons.org/licenses/by/4.0/>).

1. Introduction

Due to the wide range of beneficial properties of polymers (such as low cost, durability, and light weight), it is hard to imagine our everyday life without plastics [1,2]. However, improper disposal of plastic products worldwide is causing more and more plastic waste to enter the environment [3]. Larger plastic litter is subsequently being converted into microplastics by the fragmentation of larger plastic pieces through photolytic, mechanical, and biological degradation processes, while the chemical structure remains intact [4–6]. Microplastic particles can further disintegrate into nanoplastic [7–9]. Recently, micro- and nanoplastics have been defined by an ISO standard (ISO/TR 21960:2020). According to this standard, microplastics are water-insoluble particles with a size of 1 µm to 1 mm and nanoplastics are particles smaller than 1 µm.

The porous polymer structure and high surface area of micro- and nanoplastics enables both the adsorption of chemicals onto the particle surface and the absorption into the particles [10]. Due to the hydrophobicity of plastics and their high surface-to-volume ratio, trace organic compounds (TOCs) might sorb readily to micro- and nanoplastics. This can lead to the accumulation of TOCs on plastic particles from the aqueous phase [2,9,11,12]. Thus, micro- and nanoplastics might act as vectors distributing persistent TOCs into the environment and causing bioaccumulation in organisms [9,11,13,14]. A number of persistent organic pollutants have been found to readily sorb into polymer particles, such as polychlorinated biphenyls (PCBs), dichlorodiphenyldichloroethylene (DDE), dichlorodiphenyl-trichloroethane (DDT), and polycyclic aromatic hydrocarbons (PAHs) [11,15,16]. However, the environmental risk associated with exposure of microplastics carrying TOCs also

depends on their relative source contribution. One review reports that the amount of bioaccumulated hydrophobic organic chemicals from natural prey in rivers is higher than the amount of ingested microplastics [17].

The identification or quantification of polymers can be achieved either spectroscopically by Fourier transform infrared spectroscopy (FTIR) or Raman spectroscopy in terms of particle numbers and sizes, or by thermal analysis in terms of polymer masses [18–21]. Thermal analysis-based methods include, for instance, thermal desorption–gas chromatography mass spectrometry (TD-GC/MS) or pyrolysis–gas chromatography mass spectrometry (Pyr-GC/MS) [20,22–24]. However, here, only the polymer is being analyzed and not the sorbed TORCs. To quantify sorbed TORCs, two different approaches are commonly applied: either the sorbed TORCs are analyzed indirectly by examining the aqueous phase under controlled conditions or the sorbed substances are extracted from the particles in specific extraction steps with solvents and subsequently analyzed [25–32]. A limitation of the extraction of TORCs from particles with a subsequent analysis is that not all solvents are suitable for all polymers. For instance, methanol seems not to be suitable for the extraction of DDE from polypropylene (PP) particles and others [15]. A comprehensive summary of current analytical approaches was summarized in a recent review [33].

TD-Pyr-GC/MS offers the possibility to identify the sorbed TORCs and polymers using one analytical setup [34]. For this purpose, the TORCs are initially thermo-desorbed from the particles and analyzed by GC/MS. In the subsequent pyrolysis step, the polymer is pyrolyzed and can then be identified by its characteristic monomers. Due to a simple modification of the TD-Pyr-GC/MS not only the particles but also the aqueous phase concentration of TORCs can be investigated by stir bar analysis (Gerstel Twister®) and TD-GC/MS.

The concept of a combined TD-GC/MS and TD-Pyr-GC/MS analysis is applied in this study for the first time. The degree of sorption of selected TORCs, phenanthrene, triclosan, and α -cypermethrin on polyethylene (PE), polystyrene (PS), and polymethyl methacrylate (PMMA) is investigated with TD-Pyr-GC/MS. In all experiments, both the aqueous phase (TD-GC/MS) and the particles (TD-Pyr-GC/MS) are analyzed directly. The aim of this study is to investigate the degree of sorption of each TORCs after 1 h, 24 h, and 48 h on representative micro- and nanoparticles.

2. Analytical Systems, Materials, and Methods

2.1. Instrumental Systems

For the analysis of aqueous solutions, stir bars (Gerstel Twister®) were employed and purchased from Gerstel GmbH & Co. KG (Mühlheim an der Ruhr, Germany). The TD-Pyr-GC/MS analysis was equipped with a Gerstel Thermal Desorption Unit (TDU) 2, a Gerstel Multi-PurposeSampler (MPS) robotic^{PRO}, a Cooled Injection System (CIS) 4 with C506, and an Agilent 7890B gas chromatograph equipped with an DB-5MS Ultra Inert column coupled to an Agilent 5977B MSD mass spectrometer.

The particles were analyzed using a TD-Pyr-GC/MS system. The setup was basically the same, except that a pyrolysis module was integrated into the TDU 2 [34]. In the thermodesorption phase (TD-GC/MS), the sample was first heated up to a temperature of 200 °C to desorb the TORC. At –50 °C, the volatiles were trapped in the CIS and transferred to the GC column while heating to 200 °C. The GC method was adopted from Ochiai et al. (2005) [35]. The MS analysis was conducted in SIM mode. The same sample was now pyrolyzed at 800 °C (Pyr-GC/MS). Since not all volatile TORCs completely desorb from the particle at a TD temperature, subsequent pyrolysis is essential. The pyrolysis products were trapped and released at 350 °C. The sample injection of the CIS was operated in split mode (100:1) to avoid contamination by polymer products. The sample was subsequently analyzed by GC/MS. The initial temperature was set to 50 °C and maintained for 2 min. The GC oven was subsequently heated to 320 °C with a gradient of 10 °C/min. This temperature was held for 3 min. The final evaluations were carried out using the TD-

Chromatogram for TOxC analysis and the Pyrogram for polymer analysis. A more detailed method description can be found in Reichel et al., 2020 [34].

2.2. Materials

The reference micro- and nanoplastic particles were provided by BS-Partikel GmbH (Mainz, Germany). The spherical polystyrene particles in sizes of 78 nm and 41 μm , respectively, were supplied suspended in EtOH. The PE and PMMA particles with a size of 48 μm were available in a dry state. α -cypermethrin (CAS: 67375-30-8) was purchased from greyhoundchrom (Birkenhead, UK), phenanthrene (CAS: 85-01-8), and triclosan (CAS: 3380-34-5) from Sigma Aldrich (Taufkirchen, Germany). The deuterated standards phenanthrene-d10 (CAS: 1217-22-2) and cypermethrin-(phenoxy-d5) were purchased from Sigma Aldrich (Taufkirchen, Germany). Triclosan-d3 (CAS: 1020719-98-5) was purchased from Toronto Research Chemicals (Toronto, Canada). All chemicals were dissolved in methanol and stored at 4 $^{\circ}\text{C}$. Methanol ($\geq 99.8\%$) in HPLC-grade was purchased from VWR (Ismaning, Germany). For the simulation of real environmental conditions, tap water from Garching (Germany) was used for all sorption experiments. For the weighing of the samples, a Sartorius Cubis[®] Ultramicro Balance (Göttingen, Germany) was used. For filtration, nucleopore hydrophilic membrane filters (0.03 μm pore size) were purchased from Whatman/GE Healthcare (Marlborough, MA, USA).

2.3. Sample Preparation for Sorption Processes Experiments

In an aqueous solution, the selected TOxCs (phenanthrene, triclosan, and α -cypermethrin) were incubated with the defined micro- or nanoplastic particles. Depending on the experiment, either the incubation time or the TOxC concentration were varied. In addition, an experiment was performed with a mixture of the three selected TOxCs (phenanthrene, triclosan, and α -cypermethrin). The three model substances were selected based on their ecotoxicological relevance [36–39]. The particle concentration was always 1 g/L for all polymers and sizes. After incubation, the suspensions were filtered to separate the aqueous phase from the particulate phase. Both the aqueous and particulate phases were analyzed to establish a mass balance between sorbed and unsorbed TOxCs.

The entire sample preparation workflow is shown in Figure 1.

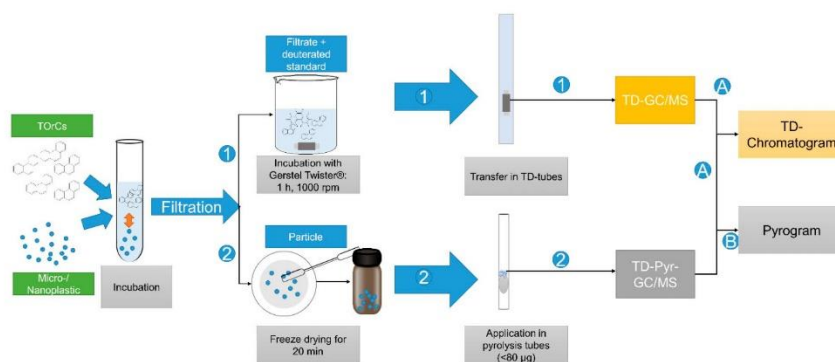


Figure 1. First, the TOxCs and microplastic particles are incubated in aqueous solution. Then, the sample is filtered. The filtrate (1) is mixed with the deuterated standard and stirred for 1 h with the Twister. The Twister is added to the TD tube and analyzed via TD-GC/MS. The TOxCs are analyzed via the TD chromatogram (A). The particles (2) are scraped off the filter with a spatula, placed in a vial, and freeze dried. The dried particles are weighed directly into the pyrolysis tube and analyzed by TD-Pyr-GC/MS. The TD chromatogram is used to evaluate the volatiles (A), and the pyrogram is used for the polymers (B).

The respective methods are explained in the following sections.

2.3.1. Analysis of the Aqueous Phase

After incubation and filtration, the filtrate was diluted 1:10 for quantitative analysis. The deuterated standards phenanthrene-d10 (50 ng/L), cypermethrin-(phenoxy-d5) (0.1 mg/L), and triclosan-d3 (0.01 mg/L) were added corresponding to the TOrc filtrate to obtain a final volume of 10 mL. A stir bar sorptive extraction (SBSE; Gerstel Twister[®], Mühlheim an der Ruhr, Germany) was used for the TD-GC/MS quantification of the TOrcs. The Gerstel Twisters[®] were coated with a polydimethylsiloxane (PDMS, film thickness 0.5 mm, length 10 mm) layer. In all experiments, the Gerstel Twisters[®] were stirred on a Thermo Fisher (Waltham, MA, USA) magnetic stirrer (15 positions) for 1 h at room temperature and 1000 rpm. The Gerstel Twister[®] was removed, washed with ultra-pure water, and dried with a lint-free tissue. The Gerstel Twister[®] was then transferred to the thermal desorption tube and analyzed by TD-GC/MS.

Calibration curves were prepared in each case using the appropriate deuterated standards to quantitatively determine the TOrcs in the filtrate. In order to eliminate the influence of filtration, the calibration standards were also filtered.

2.3.2. Particle Analysis

After filtration, the particles were scraped off the filter with a spatula, freeze-dried for 20 min, and stored at 4 °C for a maximum of 24 h. These were then weighed directly into the pyrolysis tubes, with a maximum of 80 µg to avoid a system overload. This sample was then analyzed by TD-Pyr-GC/MS.

2.3.3. Sorption Processes as a Function of Time

For the determination of the sorption of the selected TOrcs as a function of time (1 h, 24 h, and 48 h), 10 mg of particles were suspended in 10 mL of tap water in each case. The TOrcs phenanthrene, triclosan, and α -cypermethrin were added with a final concentration of 1 mg/L. The stock solution of the TOrcs was previously prepared in methanol. The suspension was shaken for 1 h, 24 h, and 48 h at room temperature at 1000 rpm. All experiments were performed in quadruplicates.

2.3.4. Sorption Processes with Different TOrc Concentrations on Nanoparticles

In order to determine whether TD-Pyr-GC/MS can also be used to reliably determine concentration differences on the particles, three concentrations (1 mg/L, 5 mg/L, and 10 mg/L) of each of the selected TOrcs (phenanthrene/triclosan/ α -cypermethrin) were sorbed onto the PS 78 nm particles in aqueous solution (10 g/L), respectively. Since rapid sorption into the PS 78 nm particles was observed within 1 h in previous experiments, the incubation time was set to 1 h. Both the aqueous phase (TD-GC/MS) and the particles (TD-Pyr-GC/MS) were analyzed.

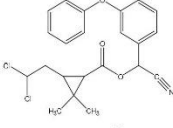
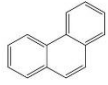
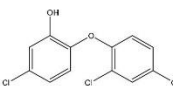
2.3.5. Sorption Processes with Mixtures of TOrcs

To investigate how the three TOrcs phenanthrene, triclosan, and α -cypermethrin affect each other, the three TOrcs were added simultaneously to the PS 78 nm and PE 48 µm particles (10 g/L) at concentrations of 1 mg/L and 10 mg/L, respectively. After an incubation period of 1 h, the samples were filtered and analyzed by TD-GC/MS and TD-Pyr-GC/MS.

2.4. Evaluation of the TD-GC/MS and TD-Pyr-GC/MS Data

TD-GC/MS: The mass spectrometer operated in SIM mode and the TOrcs phenanthrene (m/z 178), triclosan (m/z 290), and α -cypermethrin (m/z 163), and their corresponding deuterated standards were analyzed (Table 1).

Table 1. Characteristic signals for MS analysis, properties, and structure of selected TORCs.

Substance	Characteristic Signals (<i>m/z</i>)	Molecular Weight (g/mol)	Van der Waals Surface * (\AA^2)	log D (pH 7) *	Structure
α -Cypermethrin	163, 184, 209	416	571	5.35	
Phenanthrene	178	178	261	3.95	
Triclosan	290, 288, 218, 63	290	319	5.80	

* calculated via MarvinSketch 21.3. All data were statistically analyzed for significant outliers using Dixon's Q-test and Grubbs test at a level of 0.05. The significant outliers were no longer included in data evaluation.

TD-Pyr-GC/MS: In the thermodesorption step, analysis was performed in a combined SIM/full scan mode to identify the selected TORCs in the SIM mode and, at the same time, also to identify any characteristic substances of the polymers in the full scan mode. Pyrolysis was performed in full scan mode to identify potential carryover or contamination of polymer products. Moreover, pyrolysis can also identify the TORCs (e.g., phenanthrene) that do not completely desorb in the TD.

Data analysis was performed using Mass Hunter Workstation software (Ver.B.08.000, Agilent) for TD-GC/MS and TD-Pyr-GC/MS analysis. Compound identification was validated via MS spectra, and a NIST database comparison was performed.

Specific mass spectrometric signals were selected for the identification of the selected TORCs in the aqueous and in the particulate phases via TD-GC/MS (Table 1). A more detailed description of the data analysis can be found in Reichel et al., 2020 [34]. The data were standardized (peak area over weighed particle mass in the pyrolysis tube) to provide a basis of comparison for the sorption of TORCs on polymers.

3. Results and Discussion

The aim of the study was to establish the analysis of TORCs directly from particles and to validate it with an aqueous phase analysis. For the sorption tests with phenanthrene, triclosan, and α -cypermethrin, a TORC concentration of 1 mg/L was applied in each case. PE 48 μm , PMMA 48 μm , PS 41 μm , and PS 78 nm were used as reference particles. The concentration of the particle suspension was 1 g/L.

3.1. Sorption Behavior of Phenanthrene, Triclosan, and α -Cypermethrin onto Reference Particles

Up until now, most sorption studies have investigated either only the aqueous or the particulate phase [25–27,29,31,40]. So far, no mass balances of the sorbed substances, consisting of aqueous and particulate phases, have been performed. In the following, sorption of the TORCs phenanthrene, α -cypermethrin, and triclosan in the aqueous phase and onto the particles after incubation times of 1 h, 24 h, and 48 h are considered.

3.1.1. Phenanthrene

Phenanthrene is a non-polar chemical and easily sorbs into non-polar polymers. Consequently, the results shown in Figure 2a confirm that phenanthrene is no longer present in the aqueous filtrate of the PE 48 μm , PS 78 nm, and PMMA 48 μm particles already after an exposure time of 1 h. For PS 41 μm particles, the phenanthrene concentration

in the aqueous filtrate decreases over time. Considering the sorption onto the different polymers illustrated in Figure 2, it can be seen that, despite large deviations, the sorption onto PE 48 μm (Figure 2b) and PS 78 nm (Figure 2a) particles is already completed after 1 h. Deviations can occur due to the weighing of the particles or due to incomplete pyrolysis of the particles. The sorption results of the particle phase analysis (TD-Pyr-GC/MS) are supported by the aqueous phase results (TD-GC/MS). A slight increase in phenanthrene concentration on the PS 41 μm particles from 1 h to 48 h is indicated.

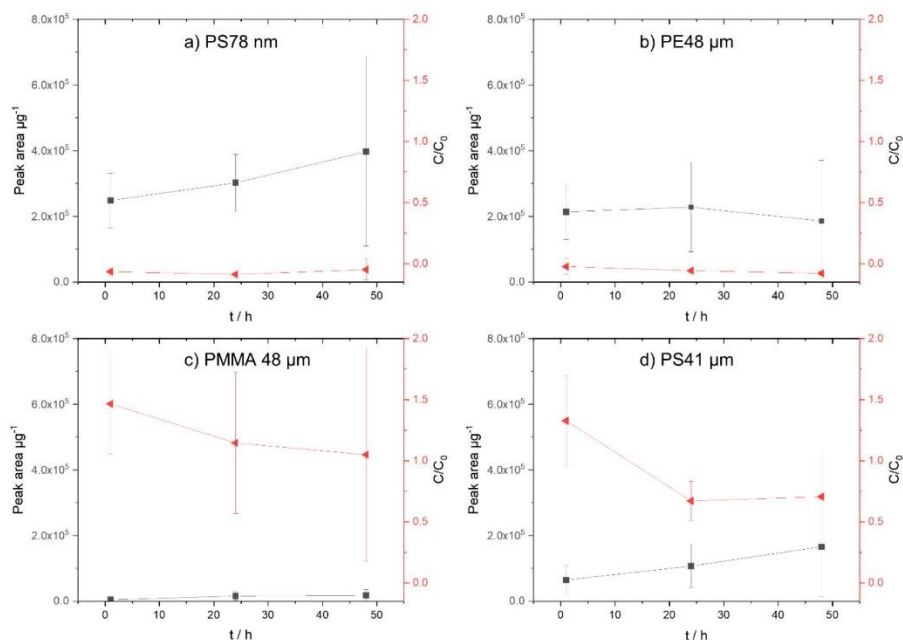


Figure 2. Concentration of phenanthrene on micro- and nanoplastic particles. On the left y -axis (black, square), the sorption on the particles (peak area μg^{-1}) is shown; on the right y -axis (red, triangle), the normalized concentration in the aqueous phase (C/C_0) is presented. (a) PS 78 nm, (b) PE 48 μm , (c) PMMA 48 μm , and (d) PS41 μm .

Compared with PS and PE, PMMA is relatively polar. Therefore, even after 48 h, hardly any sorption of phenanthrene onto the particles was noticed (Figure 2c). This is confirmed by the remaining high concentrations of TOxCs in the aqueous phase.

Compared with the other polymers studied, PE is the least polar. Therefore, its high affinity for phenanthrene is to be expected. In the case of the polymer PS and phenanthrene, which are both aromatic compounds, a non-covalent interaction occurs by “stacking” benzene rings and π - π interactions. Phenanthrene, with a rigid planar surface, may approach the PS particle surface [41,42]. In addition, there is an additional effect of benzene rings on sorption capability, with absorption being enhanced by a greater distance between polymer chains due to the benzene rings [43]. Comparing the similar sized particles of PE 48 μm and PS 41 μm , the sorption onto the PE particles is clearly increased. According to Pascall et al. (2005), this might be due to the different distances between the polymer chains in PS and PE [43]. The polymer backbone of PS consists of a benzene molecule, while that of PE consists of hydrogen atoms. As a result, the segmental mobility within

the polystyrene chains is temperature dependent, whereas that of PE is not. If the segment mobility is high and the distance between the polymer chains is large, the TORCs can easily diffuse into the polymer matrix. In addition, the segmental mobility of PS is reduced by the presence of benzene.

Considering the sorption of phenanthrene based on the aqueous and particulate phase data over a period of 48 h (sampling: 1 h, 24 h, and 48 h), the sorption follows the following order: PMMA 48 μm < PS 41 μm < PE 48 μm < PS 78 nm.

3.1.2. Triclosan

Due to its fairly high symmetry, triclosan shows little polarity (Table 1). After only 1 h, almost all of the triclosan is sorbed onto the PS 78 nm nanoparticles (Figure 3a). The aqueous phase and the particle data have been examined. In contrast to the PS nanoparticles, sorption onto the PS microparticles (PS 41 μm) is not yet complete even after 48 h (Figure 3d). The data of triclosan and the comparably polar PMMA (Figure 3c) clearly indicate that sorption onto the particles has not yet occurred after 48 h.

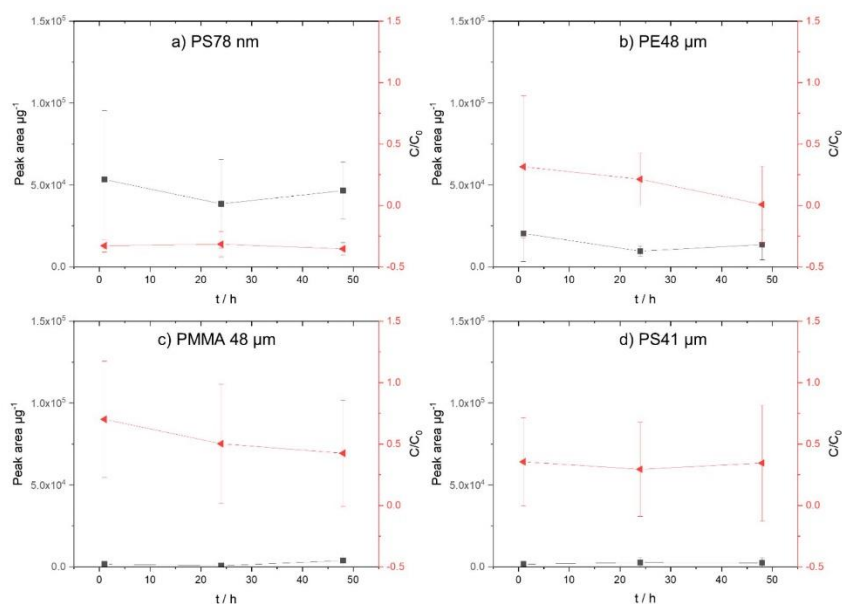


Figure 3. Concentration of triclosan on micro- and nanoplastic particles. On the left y -axis (black, square), the sorption on the particles (peak area μg^{-1}) is shown; on the right y -axis (red, triangle) the concentration in the aqueous phase (C/C_0) is presented. (a) PS 78 nm, (b) PE 48 μm , (c) PMMA 48 μm , and (d) PS41 μm .

Due to the benzene rings in the structure of triclosan, it can form π - π interactions with those of PS [26]. Additionally, the higher sorption of triclosan onto the nanoparticles (PS 78 nm) compared with the microparticles (PS 41 μm) is clearly evident. This confirms the results of Li et al. (2019), who reported an increased sorption capacity of triclosan with decreasing PS particle size [44]. According to the literature, the sorption of triclosan onto the polymers occurs mainly due to hydrophobic, hydrogen-bonding, and π - π -bonding interactions [45,46].

The analysis of the aqueous phase concentration of triclosan revealed the following order: PMMA 48 μm < PS 41 μm < PE 48 μm < PS78 nm. If only the particle phase is considered, the following order appears: PMMA 48 μm = PS 41 μm < PE 48 μm < PS78 nm. Comparing the same polymers PS, a significantly higher sorption onto the nanoparticles is evident. These results are supported by Ma et al. (2019), reporting that particle size affects the sorption behavior of triclosan [47], confirming that smaller particles provide a larger surface area for sorption.

3.1.3. α -Cypermethrin

α -cypermethrin is a mixture of the two enantiomers 1*R*-*cis*- α S and 1*S*-*cis*- α R. As reported by Qin and Gan/2007), the substances can undergo isomerization in some organic solvents such as methanol [48]. Since the standard solutions of α -cypermethrin were prepared in methanol, it is likely that they also contain the diastereomers. The observed signals in the chromatogram are therefore caused by the isomers, where the two sets of enantiomers each produced one signal in the chromatogram. The same isomerization has also been reported due to the high temperatures in the GC inlet, which could also cause the presence of two signals in the chromatogram [49]. This could also affect the final evaluation of α -cypermethrin, especially in the aqueous phase with the deuterated standard.

The concentration of α -cypermethrin in the aqueous phase is consistently very low for all polymers (Figure 4a–d). Since the deuterated standard cypermethrin-(phenoxy-d5) was used as a reference in the aqueous phase, this could have influenced the measurements due to the presence of four isomers. Based on the polymer data, the highest sorption occurs on the PS 78 nm particles (Figure 4a). However, deviations over 1 h, 24 h, and 48 h are very large. For the PE 48 μm (Figure 4b), PMMA 48 μm (Figure 4c), and PS 41 μm (Figure 4d) particles, the sorption onto the particles is lower.

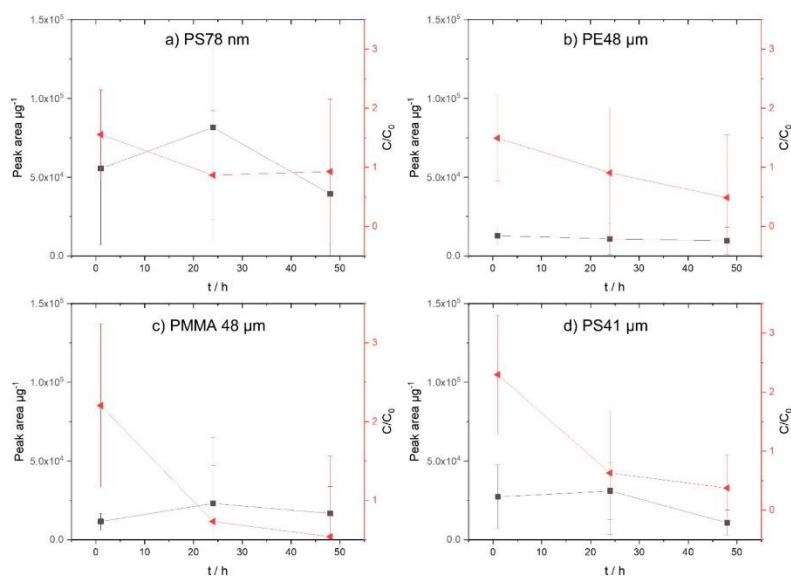


Figure 4. Concentration of α -cypermethrin on micro- and nanoplastic particles. On the left y -axis (black, square), the sorption on the particles (peak area μg^{-1}) is shown; on the right y -axis (red, triangle), the concentration in the aqueous phase (C/C_0) is presented. (a) PS 78 nm, (b) PE 48 μm , (c) PMMA 48 μm , and (d) PS41 μm .

The analysis of the aqueous phase concentration of triclosan revealed the following order: PMMA 48 μm < PS 41 μm < PE 48 μm < PS78 nm. If only the particle phase is considered, the following order appears: PMMA 48 μm = PS 41 μm < PE 48 μm < PS78 nm. Comparing the same polymers PS, a significantly higher sorption onto the nanoparticles is evident. These results are supported by Ma et al. (2019), reporting that particle size affects the sorption behavior of triclosan [47], confirming that smaller particles provide a larger surface area for sorption.

3.1.3. α -Cypermethrin

α -cypermethrin is a mixture of the two enantiomers 1*R*-*cis*- α S and 1*S*-*cis*- α R. As reported by Qin and Gan/2007), the substances can undergo isomerization in some organic solvents such as methanol [48]. Since the standard solutions of α -cypermethrin were prepared in methanol, it is likely that they also contain the diastereomers. The observed signals in the chromatogram are therefore caused by the isomers, where the two sets of enantiomers each produced one signal in the chromatogram. The same isomerization has also been reported due to the high temperatures in the GC inlet, which could also cause the presence of two signals in the chromatogram [49]. This could also affect the final evaluation of α -cypermethrin, especially in the aqueous phase with the deuterated standard.

The concentration of α -cypermethrin in the aqueous phase is consistently very low for all polymers (Figure 4a–d). Since the deuterated standard cypermethrin-(phenoxy-d5) was used as a reference in the aqueous phase, this could have influenced the measurements due to the presence of four isomers. Based on the polymer data, the highest sorption occurs on the PS 78 nm particles (Figure 4a). However, deviations over 1 h, 24 h, and 48 h are very large. For the PE 48 μm (Figure 4b), PMMA 48 μm (Figure 4c), and PS 41 μm (Figure 4 d) particles, the sorption onto the particles is lower.

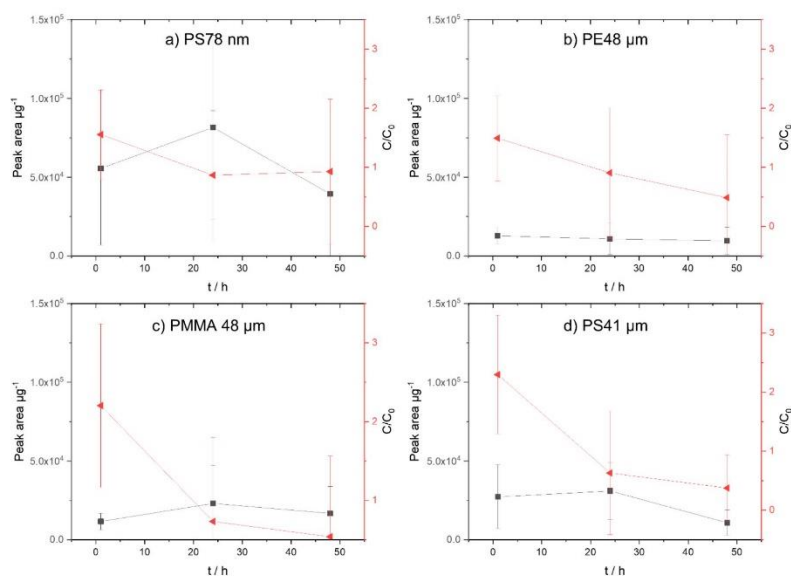


Figure 4. Concentration of α -cypermethrin on micro- and nanoplastic particles. On the left y -axis (black, square), the sorption on the particles (peak area μg^{-1}) is shown; on the right y -axis (red, triangle), the concentration in the aqueous phase (C/C_0) is presented. (a) PS 78 nm, (b) PE 48 μm , (c) PMMA 48 μm , and (d) PS41 μm .

3.2.3. α -Cypermethrin

Based on the particle data (Figure 4a), it can be clearly seen that, here, too, the highest degree of sorption occurs on the PS 78 nm particles. This is explained by the low surface coverage with α -cypermethrin (ratio α -cypermethrin/PS 78 nm: 0.05). The ratio of triclosan to PE 48 μ m, PS 41 μ m, and PMMA 48 μ m is approximately the same. This is confirmed by the sorption results of the particle data.

These results are confirmed by other studies reporting that the sorption of TOrcs on nanoplastics is much stronger than on microplastics [26,50]. Sorption of polychlorinated biphenyls (PCBs) to nano-PS (70 nm) was 1–2 orders of magnitude stronger than to micro-PE (10–180 μ m) due to the higher aromaticity and larger surface-to-volume ratio of nano-PS [26]. In the further study, three different synthetic musks and their sorption onto polypropylene (PP) particles of different sizes (2–5, 0.85–2, 0.425–0.85, or 0.125–0.45 mm) were investigated. Again, the adsorption capacity was found to increase with smaller particle size [50].

3.3. Sorption of Selected TOrcs as a Function of TOrc Concentrations on Nanoparticles

Based on the previous experiments, the PS 78 nm particles were selected to conduct further experiments with different concentrations (1 mg/L, 5 mg/L, and 10 mg/L) of TOrcs to be sorbed onto the PS 78 nm particles. The aim of the experiment was to evaluate whether a quantitative analysis of the sorbed TOrcs on the nanoparticles is in principle feasible by TD-Pyr-GC/MS.

3.3.1. Phenanthrene + PS 78 nm Particles

The phenanthrene concentration in the aqueous phase and on the particles was investigated (Figure 5a). For the initial concentration of 1 mg/L, there is no more phenanthrene in the aqueous phase after an incubation time of 1 h. Concentrations of less than 0.2 mg/L were observed for the 5 mg/L and 10 mg/L concentrations after 1 h of exposure in the aqueous phase. In the TD-Pyr-GC/MS particle analysis, a distinct increase in sorbed phenanthrene was noted. A quantification of this TOrc should therefore be possible.

3.3.2. Triclosan + PS 78 nm Particles

The triclosan concentration in the aqueous solution and the corresponding amount on the particles of the initial concentrations of 1 mg/L, 5 mg/L, and 10 mg/L were studied (Figure 5b). For all initial concentrations, the final concentration after 1 h incubation is below 1 mg/L. Considering the particle analysis (TD-Pyr-GC/MS), also here, a clear increase in the triclosan concentration on the particles can be seen, so that quantification of triclosan on the particles is possible.

3.3.3. α -Cypermethrin + PS 78 nm Particles

The concentration in the aqueous phase and in the particulate phase with the TOrc α -cypermethrin after 1 h incubation with PS 78 nm particles and initial concentrations of 1 mg/L, 5 mg/L, and 10 mg/L were investigated (Figure 5c). Compared with phenanthrene and triclosan, the remaining concentrations and the deviations in the aqueous phase are significantly higher. Based on these results (Figure 5c), a quantification of the sorbed amount on the particles is possible.

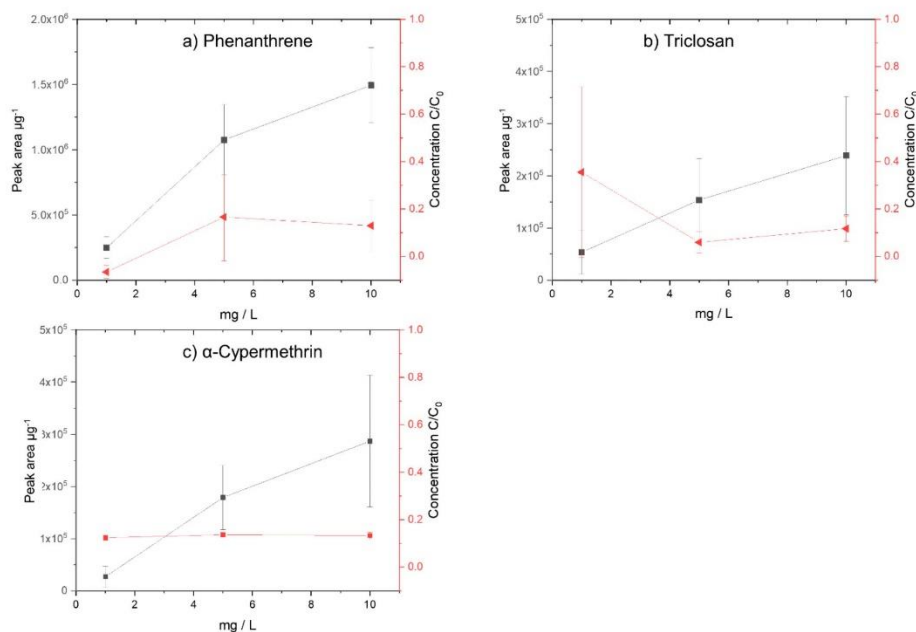


Figure 5. Analysis of initial concentration of 1 mg/L, 5 mg/L, and 10 mg/L in the aqueous phases via TD-GC/MS (C/C_0) and the particle phases via TD-Pyr-GC/MS (peak area μg^{-1}) for the TORCs (a) phenanthrene, (b) triclosan, and (c) α -cypermethrin. On the left y-axis (black, square), the sorption on the particles (peak area μg^{-1}) is shown; on the right y-axis (red, triangle) the concentration in the aqueous phase (C/C_0) is presented.

3.4. Sorption of the TORC Mixture onto Reference Particles

Most studies on sorbed TORCs on micro- or nanoplastic particles examine single substances [10,30,44,51–53]. However, it is not to be expected that TORCs will occur individually in the aquatic environment, but that they are always present in mixtures [16,26]. If a mixture of substances is used, the sorption capacity of the single substance may be affected. Therefore, in an additional experiment, the three selected TORCs phenanthrene, triclosan, and α -cypermethrin were sorbed simultaneously at concentrations of 1 mg/L and 10 mg/L onto the polymers PS 78 nm and PE 48 μm (1 g/L each). These particles were selected because the sorption equilibrium had been rapidly established after 1 h in the sorption experiments. In each of the experiments, the aqueous phase (TD-GC/MS) and the particles (TD-Pyr-GC/MS) were analyzed.

The three TORCs were sorbed onto PS 78 nm particles with an initial concentration of 10 mg/L (Figure 6a). The concentrations of the individual TORCs (α -cypermethrin phenanthrene and triclosan) are compared with the mixed sorbed substances. Considering the results from the aqueous phase and from the particle measurements, only minor differences of the mixed measured TORCs compared with the single substances were observed which are in the range of the measurement fluctuations. In the case of these three substances, the sorption capacity of the selected TORCs neither increased nor decreased. The calculated particle surface areas (Section 3.2) indicate that the surface of the nanoparticles is only slightly occupied, and therefore, no agonistic or antagonistic effects occur.

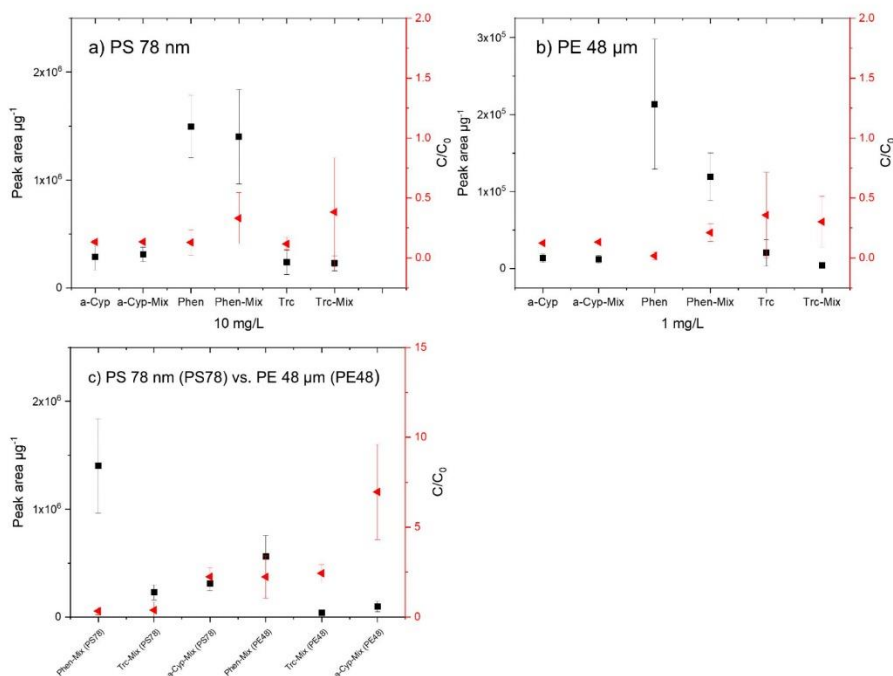


Figure 6. Comparison of the results of the measured single substances (α -cypermethrin (a-Cyp), Phenanthrene (Phen), and Triclosan (Trc) and the measurement of the mixed TOrcs (a-Cyp-Mix, Phen-Mix, Trc-Mix) with an initial concentration of 10 mg/L and sorption on PS 78 nm (a), with an initial concentration of 1 mg/L and sorption on PE 48 μ m particles (b), and with an initial concentration of 10 mg/L on PS78 nm and PE 48 μ m (c); measurements of the aqueous phase were conducted via Gerstel Twister[®] and TD-GC/MS measurements of the particles were carried out with TD-Pyr-GC/MS. On the left y-axis (black, square), the sorption on the particles (peak area μ g⁻¹) is shown; on the right y-axis (red, triangle), the concentration in the aqueous phase (C/C_0) is presented.

Analogous to the sorption on PS 78 nm particles, the single and mixed substances were sorbed onto PE 48 μ m particles (Figure 6b). Based on the surface occupancy, a final concentration of 1 mg/L was selected for all TOrcs. The sorption of α -cypermethrin is not affected by the presence of the other TOrcs. Both in the aqueous phase and on the particles, the sorption differs only marginally. Phenanthrene sorbs more strongly as a single substance on PE 48 μ m. This could indicate an antagonistic effect, which was already observed by Bakir et al. (2012) for phenanthrene and DDT [54]. Triclosan, similar to α -cypermethrin, is hardly affected by the presence of the other TOrcs. Both the aqueous phase and the particle analysis indicate similar sorption.

Comparison of the sorption of the mixing experiments of PS 78 nm and PS 48 μ m particles with an initial TOrc concentration of 10 mg/L shows that the degree of sorption of all TOrcs is higher on the PS nanoparticles (Figure 6c). This is reflected in the aqueous phase as well as in the particle phase.

3.5. Stability and Reproducibility of Data in TD-GC/MS and TD-Pyr-GC/MS Analysis

The quantitative analysis of an aqueous sample with stir bar sorptive extraction (via Gerstel Twister[®]) and a GC/MS analysis is an established routine procedure [38,55,56]. Nevertheless, high standard deviations occurred in some cases. One reason for this could be the filtration step. Although nanofilters were used, it cannot be ruled out that smaller particle fractions enter the aqueous phase and interact with the Gerstel Twisters[®]. Additionally, the duration of filtration varies and depends on how quickly the filter clogs.

Regarding the TD-Pyr-GC/MS data of the sorbed TORCs, they show high standard deviations with partly low reproducibility, especially in the incubation experiment over 48 h. However, only a concentration of 1 mg/L was investigated in these experiments. If the quantification experiments with concentrations of 1 mg/L, 5 mg/L, and 10 mg/L are considered, the data still have large deviations in some cases, but the different sorbed concentrations are clearly visible. In these experiments, it was demonstrated for the first time that quantification of TORCs directly from the micro- and nanoparticle is possible. Previous analyses directly from the microplastic particle have so far only been able to identify substances such as polymer additives [22,23] and to quantify phthalates [57]. Quantification of TORCs on nanoparticles has not been possible up until now.

4. Conclusions and Outlook

Based on the results of this study, the combination of TD-GC/MS and TD-Pyr-GC/MS can be applied as a novel and quick method for the analysis and quantification of sorbed TORCs on micro- and nanoparticles and for polymer identification [34]. With the analysis of both phases, the concentration in the aqueous phase and the peak area/weight on polymers could be shown for the first time.

Sorption of the three selected TORCs (phenanthrene, triclosan, and α -cypermethrin) onto three different polymer types and sizes (PS 78 nm, PS 41 μ m, PE 48 μ m, and PMMA 48 μ m) within 48 h was demonstrated. The results showing that the highest sorption occurs on the PS 78 nm nanoparticles is supported by the calculation of the high surface-to-volume ratio of the particles.

It was demonstrated for the first time that quantification directly from the particles is possible using TD-Pyr-GC/MS. By showing clear peak area/weight differences for all three selected TORCs at concentrations of 1 mg/L, 5 mg/L, and 10 mg/L, a calibration based on TORC-loaded nanoparticles can be constructed. All data were statistically analyzed for significant outliers using the Dixon Q test and the Grubbs test at a level of 0.05. The quantification of TORCs on particles could be particularly interesting for use in ecotoxicological assays or in experiments using controlled laboratory-scale wastewater treatment plants.

By means of TD-Pyr-GC/MS, quantitative experiments especially regarding environmental samples, could be performed in the future. Nevertheless, sample preparation must be taken into account here and will need a specific design for each analytical question. The samples should be free of organic material, such as biofilms. At the same time, the presence of potentially interfering inorganics should be avoided. Additionally, the investigation of the amount truly sorbed into the particles under the influence of various factors such as pH, temperature, or salinity should be feasible using this analytical method. For future experiments, it would be useful to consider different polymer types in the nanometer range. As long as no chemical interactions during desorption occur, the sorbed TORCs can be quantified directly from the particle regardless of the polymer type and extraction methods.

In the future, the experimentally obtained sorption data obtained by TD-Pyr-GC/MS analysis could still be validated by modeling (e.g., pp-LSER). However, so far, these modeling approaches for sorption experiments have been performed mainly with microplastic particles and not with nanoplastic particles, so the number of databases is likely to be limited [58,59].

Author Contributions: Conceptualization, J.R., J.G. and T.L.; methodology, J.R. and J.G.; software, J.R.; validation, J.R., J.G. and T.L.; formal analysis, J.R. and J.G.; investigation, J.R. and J.G.; resources, J.E.D.; data curation, J.R.; writing—original draft preparation, J.R.; writing—review and editing, J.R., J.G., T.L., O.K. and J.E.D.; visualization, J.R.; supervision, J.G., T.L., O.K. and J.E.D.; project administration, O.K. and J.E.D. All authors have read and agreed to the published version of the manuscript.

Funding: This research was funded by the German Federal Ministry of Education and Research (BMBF) in the project SubµTrack, grant number 02WPL1443A.

Institutional Review Board Statement: Not applicable.

Informed Consent Statement: Not applicable.

Data Availability Statement: Data is contained within the article.

Acknowledgments: We are grateful for the support by BS Partikel GmbH, who produced the micro- and nanoplastic particles and Thomas Wagner from Gerstel GmbH & Co. KG for technical support.

Conflicts of Interest: The authors declare that there are no conflict of interest or competing interests.

References

- Teuten, E.L.; Saquing, J.M.; Knappe, D.R.; Barlaz, M.A.; Jonsson, S.; Björn, A.; Rowland, S.J.; Thompson, R.C.; Galloway, T.S.; Yamashita, R.; et al. Transport and release of chemicals from plastics to the environment and to wildlife. *Philos. Trans. R. Soc. B Biol. Sci.* **2009**, *364*, 2027–2045. [\[CrossRef\]](#)
- Bergmann, M.; Gutow, L.; Klages, M. (Eds.) *Marine Anthropogenic Litter*; Springer: Berlin, Germany, 2015.
- Geyer, R.; Jambeck, J.R.; Law, K.L. Production, use, and fate of all plastics ever made. *Sci. Adv.* **2017**, *3*, e1700782. [\[CrossRef\]](#)
- Barnes, D.K.A.; Galgani, F.; Thompson, R.C.; Barlaz, M. Accumulation and fragmentation of plastic debris in global environments. *Philos. Trans. R. Soc. Lond. B Biol. Sci.* **2009**, *364*, 1985–1998. [\[CrossRef\]](#)
- Roy, P.K.; Hakkarainen, M.; Varma, I.K.; Albertsson, A.-C. Degradable Polyethylene: Fantasy or Reality. *Environ. Sci. Technol.* **2011**, *45*, 4217–4227. [\[CrossRef\]](#)
- Browne, M.A.; Galloway, T.; Thompson, R. Microplastic—an emerging contaminant of potential concern? *Integr. Environ. Assess. Manag.* **2007**, *3*, 559–566. [\[CrossRef\]](#) [\[PubMed\]](#)
- Lambert, S.; Wagner, M. Characterisation of nanoplastics during the degradation of polystyrene. *Chemosphere* **2016**, *145*, 265–268. [\[CrossRef\]](#)
- Mattsson, K.; Hansson, L.-A.; Cedervall, T. Nano-plastics in the aquatic environment. *Environ. Sci. Process. Impacts* **2015**, *17*, 1712–1721. [\[CrossRef\]](#)
- Da Costa, J.P.; Santos, P.S.M.; Duarte, A.C.; Rocha-Santos, T. (Nano) plastics in the environment—Sources, fates and effects. *Sci. Total Environ.* **2016**, *566–567*, 15–26. [\[CrossRef\]](#)
- Hüffer, T.; Hofmann, T. Sorption of non-polar organic compounds by micro-sized plastic particles in aqueous solution. *Environ. Pollut.* **2016**, *214*, 194–201. [\[CrossRef\]](#) [\[PubMed\]](#)
- Rochman, C.M.; Hoh, E.; Hentschel, B.T.; Kaye, S. Long-Term Field Measurement of Sorption of Organic Contaminants to Five Types of Plastic Pellets: Implications for Plastic Marine Debris. *Environ. Sci. Technol.* **2013**, *47*, 1646–1654. [\[CrossRef\]](#) [\[PubMed\]](#)
- Andrady, A.L. Microplastics in the marine environment. *Mar. Pollut. Bull.* **2011**, *62*, 1596–1605. [\[CrossRef\]](#)
- Alimi, O.S.; Farmer Budarz, J.; Hernandez, L.M.; Tufenkji, N. Microplastics and Nanoplastics in Aquatic Environments: Aggregation, Deposition, and Enhanced Contaminant Transport. *Environ. Sci. Technol.* **2018**, *52*, 1704–1724. [\[CrossRef\]](#) [\[PubMed\]](#)
- González-Pleiter, M.; Pedrouzo-Rodríguez, A.; Verdú, I.; Leganés, F.; Marco, E.; Rosal, R.; Fernández-Piñas, F. Microplastics as vectors of the antibiotics azithromycin and clarithromycin: Effects towards freshwater microalgae. *Chemosphere* **2021**, *268*, 128824. [\[CrossRef\]](#)
- Mato, Y.; Isobe, T.; Takada, H.; Kanehiro, H.; Ohtake, C.; Kaminuma, T. Plastic Resin Pellets as a Transport Medium for Toxic Chemicals in the Marine Environment. *Environ. Sci. Technol.* **2001**, *35*, 318–324. [\[CrossRef\]](#) [\[PubMed\]](#)
- Napper, I.E.; Bakir, A.; Rowland, S.J.; Thompson, R.C. Characterisation, quantity and sorptive properties of microplastics extracted from cosmetics. *Mar. Pollut. Bull.* **2015**, *99*, 178–185. [\[CrossRef\]](#) [\[PubMed\]](#)
- Koelmans, A.A.; Bakir, A.; Allen Burton, G.; Janssen, C. Microplastic as a Vector for Chemicals in the Aquatic Environment: Critical Review and Model-Supported Reinterpretation of Empirical Studies. *Environ. Sci. Technol.* **2016**, *50*, 3315–3326. [\[CrossRef\]](#)
- Thompson, R.C.; Olsen, Y.; Mitchell, R.P.; Davis, A.; Rowland, S.J.; John, A.W.; Russell, A.E. Lost at Sea: Where Is All the Plastic? *Science* **2004**, *304*, 838. [\[CrossRef\]](#) [\[PubMed\]](#)
- Klein, S.; Worch, E.; Knepper, T.P. Occurrence and Spatial Distribution of Microplastics in River Shore Sediments of the Rhine-Main Area in Germany. *Environ. Sci. Technol.* **2015**, *49*, 6070–6076. [\[CrossRef\]](#) [\[PubMed\]](#)
- Duemichen, E.; Braun, U.; Senz, R.; Fabian, G.; Sturm, H. Assessment of a new method for the analysis of decomposition gases of polymers by a combining thermogravimetric solid-phase extraction and thermal desorption gas chromatography mass spectrometry. *J. Chromatogr. A* **2014**, *1354*, 117–128. [\[CrossRef\]](#) [\[PubMed\]](#)

21. Fischer, M.; Scholz-Böttcher, B.M. Simultaneous Trace Identification and Quantification of Common Types of Microplastics in Environmental Samples by Pyrolysis-Gas Chromatography–Mass Spectrometry. *Environ. Sci. Technol.* **2017**, *51*, 5052–5060. [[CrossRef](#)]
22. Fries, E.; Dekiff, J.H.; Willmeyer, J.; Nuelle, M.T.; Ebert, M.; Remy, D. Identification of polymer types and additives in marine microplastic particles using pyrolysis-GC/MS and scanning electron microscopy. *Environ. Sci. Process. Impacts* **2013**, *15*, 1949–1956. [[CrossRef](#)] [[PubMed](#)]
23. Herrera, M.; Matuschek, G.; Kettrup, A. Fast identification of polymer additives by pyrolysis-gas chromatography/mass spectrometry. *J. Anal. Appl. Pyrolysis* **2003**, *70*, 35–42. [[CrossRef](#)]
24. Dümichen, E.; Barthel, A.K.; Braun, U.; Bannick, C.G.; Brand, K.; Jekel, M.; Senz, R. Analysis of polyethylene microplastics in environmental samples, using a thermal decomposition method. *Water Res.* **2015**, *85*, 451–457. [[CrossRef](#)] [[PubMed](#)]
25. Seidensticker, S.; Zarfl, C.; Cirkpa, O.A.; Fellenberg, G.; Grathwohl, P. Shift in Mass Transfer of Wastewater Contaminants from Microplastics in the Presence of Dissolved Substances. *Environ. Sci. Technol.* **2017**, *51*, 12254–12263. [[CrossRef](#)]
26. Velzeboer, L.; Kwadijk, C.J.A.F.; Koelmans, A.A. Strong Sorption of PCBs to Nanoplastics, Microplastics, Carbon Nanotubes, and Fullerenes. *Environ. Sci. Technol.* **2014**, *48*, 4869–4876. [[CrossRef](#)] [[PubMed](#)]
27. Zhang, J.; Chen, H.; He, H.; Cheng, X.; Ma, T.; Hu, J.; Yang, S.; Li, S.; Zhang, L. Adsorption behavior and mechanism of 9-Nitroanthracene on typical microplastics in aqueous solutions. *Chemosphere* **2020**, *245*, 125628. [[CrossRef](#)] [[PubMed](#)]
28. Zhang, X.; Zheng, M.; Yin, X.; Wang, L.; Lou, Y.; Qu, L.; Liu, X.; Zhu, H.; Qiu, Y. Sorption of 3,6-dibromocarbazole and 1,3,6,8-tetrabromocarbazole by microplastics. *Mar. Pollut. Bull.* **2019**, *138*, 458–463. [[CrossRef](#)]
29. Wang, J.; Liu, X.; Liu, G.; Zhang, Z.; Wu, H.; Cui, B.; Bai, J.; Zhang, W. Size effect of polystyrene microplastics on sorption of phenanthrene and nitrobenzene. *Ecotoxicol. Environ. Saf.* **2019**, *173*, 331–338. [[CrossRef](#)]
30. Guo, X.; Pang, J.; Chen, S.; Jia, H. Sorption properties of tylosin on four different microplastics. *Chemosphere* **2018**, *209*, 240–245. [[CrossRef](#)]
31. Fan, X.; Zou, Y.; Geng, N.; Liu, J.; Hou, J.; Li, D.; Yang, C.; Li, Y. Investigation on the adsorption and desorption behaviors of antibiotics by degradable MPs with or without UV ageing process. *J. Hazard. Mater.* **2021**, *401*, 123363. [[CrossRef](#)]
32. Wu, P.; Cai, Z.; Jin, H.; Tang, Y. Adsorption mechanisms of five bisphenol analogues on PVC microplastics. *Sci. Total Environ.* **2019**, *650*, 671–678. [[CrossRef](#)] [[PubMed](#)]
33. Reichel, J.; Graßmann, J.; Knoop, O.; Drewes, J.; Letzel, T. Organic Contaminants and Interactions with Micro- and Nano-Plastics in the Aqueous Environment: Review of Analytical Methods. *Molecules* **2021**, *26*, 1164. [[CrossRef](#)] [[PubMed](#)]
34. Reichel, J.; Graßmann, J.; Letzel, T.; Drewes, J. Systematic Development of a Simultaneous Determination of Plastic Particle Identity and Adsorbed Organic Compounds by Thermodesorption–Pyrolysis GC/MS (TD-Pyr-GC/MS). *Molecules* **2020**, *25*, 4985. [[CrossRef](#)] [[PubMed](#)]
35. Ochiai, N.; Sasamoto, K.; Kanda, H.; Yamagami, T.; David, F.; Tienpont, B.; Sandra, P. Optimization of a multi-residue screening method for the determination of 85 pesticides in selected food matrices by stir bar sorptive extraction and thermal desorption GC-MS. *J. Sep. Sci.* **2005**, *28*, 1083–1092. [[CrossRef](#)] [[PubMed](#)]
36. Browne, M.A.; Niven, S.J.; Galloway, T.S.; Rowland, S.J.; Thompson, R. Microplastic Moves Pollutants and Additives to Worms, Reducing Functions Linked to Health and Biodiversity. *Curr. Biol.* **2013**, *23*, 2388–2392. [[CrossRef](#)] [[PubMed](#)]
37. Karlsson, M.V.; Carter, L.J.; Agatz, A.; Boxall, A.B.A. Novel Approach for Characterizing pH-Dependent Uptake of Ionizable Chemicals in Aquatic Organisms. *Environ. Sci. Technol.* **2017**, *51*, 6965–6971. [[CrossRef](#)] [[PubMed](#)]
38. Bartonitz, A.; Anyanwu, I.N.; Geist, J.; Imhof, H.K.; Reichel, J.; Graßmann, J.; Drewes, J.E.; Beggel, S. Modulation of PAH toxicity on the freshwater organism *G. roeseli* by microparticles. *Environ. Pollut.* **2020**, *260*, 113999. [[CrossRef](#)]
39. Yordanova, V.; Stoyanova, T.; Traykov, L.; Boyanovsky, B. Toxicological Effects of Fastac Insecticide (Alpha—Cypermethrin) to *Daphnia Magna* and *Gammarus Pulex*. *Biotechnol. Biotechnol. Equip.* **2009**, *23* (Suppl. S1), 393–395. [[CrossRef](#)]
40. Seidensticker, S.; Grathwohl, P.; Lamprecht, J.; Zarfl, C. A combined experimental and modeling study to evaluate pH-dependent sorption of polar and non-polar compounds to polyethylene and polystyrene microplastics. *Environ. Sci. Eur.* **2018**, *30*, 30. [[CrossRef](#)]
41. Penner, N.A.; Nesterenko, P.N.; Ilyin, M.M.; Tsyurupa, M.P.; Davankov, V.A. Investigation of the properties of hypercrosslinked polystyrene as a stationary phase for high-performance liquid chromatography. *Chromatographia* **1999**, *50*, 611–620. [[CrossRef](#)]
42. Liu, L.; Fokkink, R.; Koelmans, A.A. Sorption of polycyclic aromatic hydrocarbons to polystyrene nanoplastic. *Environ. Toxicol. Chem.* **2016**, *35*, 1650–1655. [[CrossRef](#)] [[PubMed](#)]
43. Pascall, M.A.; Zabik, M.E.; Zabik, M.J.; Hernandez, R.J. Uptake of Polychlorinated Biphenyls (PCBs) from an Aqueous Medium by Polyethylene, Polyvinyl Chloride, and Polystyrene Films. *J. Agric. Food Chem.* **2005**, *53*, 164–169. [[CrossRef](#)] [[PubMed](#)]
44. Li, Y.; Li, M.; Li, Z.; Yang, L.; Liu, X. Effects of particle size and solution chemistry on Triclosan sorption on polystyrene microplastic. *Chemosphere* **2019**, *231*, 308–314. [[CrossRef](#)] [[PubMed](#)]
45. Behera, S.K.; Oh, S.-Y.; Park, H.-S. Sorption of triclosan onto activated carbon, kaolin and montmorillonite: Effects of pH, ionic strength, and humic acid. *J. Hazard. Mater.* **2010**, *179*, 684–691. [[CrossRef](#)]
46. Xu, J.; Niu, J.; Zhang, X.; Liu, J.; Cao, G.; Kong, X. Sorption of triclosan on electrospun fibrous membranes: Effects of pH and dissolved organic matter. *Emerg. Contam.* **2015**, *1*, 25–32. [[CrossRef](#)]
47. Ma, J.; Zhao, J.; Zhu, Z.; Li, L.; Yu, F. Effect of microplastic size on the adsorption behavior and mechanism of triclosan on polyvinyl chloride. *Environ. Pollut.* **2019**, *254*, 113104. [[CrossRef](#)]

48. Qin, S.; Gan, J. Abiotic Enantiomerization of Permethrin and Cypermethrin: Effects of Organic Solvents. *J. Agric. Food Chem.* **2007**, *55*, 5734–5739. [[CrossRef](#)]
49. Liu, W.; Qin, A.S.; Gan, J. Chiral Stability of Synthetic Pyrethroid Insecticides. *J. Agric. Food Chem.* **2005**, *53*, 3814–3820. [[CrossRef](#)]
50. Zhang, X.; Zheng, M.; Wang, L.; Lou, Y.; Shi, L.; Jiang, S. Sorption of three synthetic musks by microplastics. *Mar. Pollut. Bull.* **2018**, *126*, 606–609. [[CrossRef](#)]
51. Wang, W.; Wang, J. Comparative evaluation of sorption kinetics and isotherms of pyrene onto microplastics. *Chemosphere* **2018**, *193*, 567–573. [[CrossRef](#)]
52. Gong, W.; Jiang, M.; Han, P.; Liang, G.; Zhang, T.; Liu, G. Comparative analysis on the sorption kinetics and isotherms of fipronil on nondegradable and biodegradable microplastics. *Environ. Pollut.* **2019**, *254*, 112927. [[CrossRef](#)] [[PubMed](#)]
53. Xu, B.; Liu, F.; Brookes, P.C.; Xu, J. Microplastics play a minor role in tetracycline sorption in the presence of dissolved organic matter. *Environ. Pollut.* **2018**, *240*, 87–94. [[CrossRef](#)] [[PubMed](#)]
54. Bakir, A.; Rowland, S.J.; Thompson, R.C. Competitive sorption of persistent organic pollutants onto microplastics in the marine environment. *Mar. Pollut. Bull.* **2012**, *64*, 2782–2789. [[CrossRef](#)] [[PubMed](#)]
55. Camino-Sanchez, F.J.; Zafra-Gomez, A.; Perez-Trujillo, J.P.; Conde-Gonzalez, J.E.; Marques, J.C.; Vilchez, J.L. Validation of a GC-MS/MS method for simultaneous determination of 86 persistent organic pollutants in marine sediments by pressurized liquid extraction followed by stir bar sorptive extraction. *Chemosphere* **2011**, *84*, 869–881. [[CrossRef](#)] [[PubMed](#)]
56. Kolahgar, B.; Hoffmann, A.; Heiden, A.C. Application of stir bar sorptive extraction to the determination of polycyclic aromatic hydrocarbons in aqueous samples. *J. Chromatogr. A* **2002**, *963*, 225–230. [[CrossRef](#)]
57. La Nasa, J.; Biale, G.; Mattonai, M.; Modugno, F. Microwave-assisted solvent extraction and double-shot analytical pyrolysis for the quali-quantitation of plasticizers and microplastics in beach sand samples. *J. Hazard. Mater.* **2020**, *401*, 123287. [[CrossRef](#)]
58. Mosca Angelucci, D.; Tomei, M.C. Uptake/release of organic contaminants by microplastics: A critical review of influencing factors, mechanistic modeling, and thermodynamic prediction methods. *Crit. Rev. Environ. Sci. Technol.* **2020**, *52*, 1356–1400. [[CrossRef](#)]
59. Xu, J.; Wang, L.; Sun, H. Adsorption of neutral organic compounds on polar and nonpolar microplastics: Prediction and insight into mechanisms based on pp-LFERs. *J. Hazard. Mater.* **2021**, *408*, 124857. [[CrossRef](#)] [[PubMed](#)]

Appendix IV

Validation of Sample Preparation Methods for Microplastic Analysis in Wastewater Matrices—Reproducibility and Standardization

Water 2020, 12, 2445

This study aimed to develop a sample preparation method for wastewater samples to analyze microplastics. Three protocols (KOH, H₂O₂, and Fenton reactions) were evaluated for their effectiveness in removing organic matter from microplastic samples without altering polymer properties. Results showed that H₂O₂ and Fenton reactions were effective, while KOH dissolved certain polymer particles.

Mohammed S. M. Al-Azzawi designed and wrote the manuscript. Mohammed S. M. Al-Azzawi and Simone Kefer performed the size analysis and evaluated the experiments. Mohammed S. M. Al-Azzawi and Jana Weißer performed the FTIR analysis and evaluated the experiments. Mohammed S. M. Al-Azzawi and Julia Reichel performed the Pyr-GC/MS analysis and evaluated the experiments. Christoph Schwaller, Karl Glas, Oliver Knoop and Jörg E. Drewes reviewed the manuscript and contributed to the discussion.



Article

Validation of Sample Preparation Methods for Microplastic Analysis in Wastewater Matrices—Reproducibility and Standardization

Mohammed S. M. Al-Azzawi ¹, Simone Kefer ², Jana Weißer ³, Julia Reichel ¹, Christoph Schwaller ¹, Karl Glas ³, Oliver Knoop ^{1,*} and Jörg E. Drewes ¹

¹ Chair of Urban Water Systems Engineering, Technical University of Munich, 85748 Garching, Germany; mohammed.al-azzawi@tum.de (M.S.M.A.-A.); julia.reichel@tum.de (J.R.); c.schwaller@tum.de (C.S.); jdrewes@tum.de (J.E.D.)

² Chair of Brewing and Beverage Technology, Technical University Munich, 85354 Freising, Germany; simone.kefer@tum.de

³ Chair of Food Chemistry and Molecular Sensory Science, Technical University of Munich, 85354 Freising, Germany; jana.weisser@tum.de (J.W.); karl.glas@tum.de (K.G.)

* Correspondence: oliver.knoop@tum.de

Received: 24 July 2020; Accepted: 27 August 2020; Published: 31 August 2020



Abstract: There is a growing interest in monitoring microplastics in the environment, corresponding to increased public concerns regarding their potential adverse effects on ecosystems. Monitoring microplastics in the environment is difficult due to the complex matrices that can prevent reliable analysis if samples are not properly prepared first. Unfortunately, sample preparation methods are not yet standardized, and the various efforts to validate them overlook key aspects. The goal of this study was to develop a sample preparation method for wastewater samples, which removes natural organic matter without altering the properties of microplastics. Three protocols, based on KOH, H₂O₂, and Fenton reactions, were chosen out of ten protocols after a literature review and pre-experiments. In order to investigate the effects of these reagents on seven polymers (PS, PE, PET, PP, PA, PVC, and PLA), this study employed μ FTIR, laser diffraction-based particle size analysis, as well as TD-Pyr-GC/MS. Furthermore, the study discussed issues and inconsistencies with the Fenton reactions reported in the literature in previous validation efforts. The findings of this study suggest that both H₂O₂ and Fenton reactions are most effective in terms of organic matter removal from microplastic samples while not affecting the tested polymers, whereas KOH dissolved most PLA and PET particles.

Keywords: microplastics; wastewater; Fenton reaction; hydrogen peroxide; digestion methods; sample preparation

1. Introduction

The first studies regarding microplastic contamination in oceans appeared in the 1970s and since then, interest in the topic has been rapidly growing, especially in recent years [1,2]. Microplastics are defined differently in the literature, either as plastic particles smaller than 5 mm, or smaller than 1 mm [1,3–5]. Due to the difficulty of monitoring microplastics in the environment, even decades later there are still not enough data to obtain a full picture of microplastic contamination [2]. The difficulty in assessing microplastics in the environment lies in distinguishing microplastics from the complex mixture of natural organic and inorganic particles in any given environmental matrix. These can be, for example, inorganic particles like sand and silt, but also organic particles originating from biofilms, plant, and animal debris [6]. Even with the advent of modern analytical methods such as

Fourier-transform infrared spectroscopy (FTIR) and Raman spectroscopy, a natural matrix can still hinder the detection of microplastics or at least increase the error factor considerably. Therefore, appropriate sample preparation steps are necessary.

Inorganic matter is usually separated from microplastics by using density differences. Common microplastics have a density close to that of water ($0.83\text{--}1.1\text{ g/cm}^3$), whereas most inorganic constituents have higher densities. Using a concentrated salt solution, such as sodium chloride (NaCl) or sodium iodine (NaI) solutions (with density of 1.2 and 1.8 g/cm^3 , respectively), microplastics and inorganics can be separated based on the difference of their respective densities [7,8].

On the other hand, organic matter has a similar density to microplastics and cannot be separated based on density differences [8,9]. Thus, a matrix rich in organic matter, such as biosolids, wastewater effluents, or streambed sediments, needs to be treated via chemical digestion protocols such as oxidative, acidic, alkaline, as well as enzymatic digestions [8]. However, the use of strong chemical reagents can inadvertently affect the characteristics of the microplastics being analyzed [7,10]. Although enzymatic digestion protocols are usually safe for microplastics, they require long digestion times, which limits their applicability [7]. To date, there are no standardized sample preparation methods. This is one of the main factors limiting the comparability between various efforts to monitor microplastics in the environment [7].

1.1. Sample Preparation Methods for Removing Organic Matter

Oxidative digestion methods are common in the literature, most of which are protocols utilizing hydrogen peroxide (H_2O_2). It was utilized under various conditions with different concentrations ($15\text{--}35\%$), temperatures (room temperature up to $70\text{ }^\circ\text{C}$), and reaction times (a few hours to a week) [7,11–14]. Table A1 summarizes the hydrogen peroxide protocols used in microplastic studies and the effects on both organics as well as polymers [7,11–14]. In general, it can be observed that hydrogen peroxide provided effective digestion and little degradation in polymers when using lower temperatures (up to $60\text{ }^\circ\text{C}$) and/or shorter reaction times (up to 24 h). Therefore, hydrogen peroxide was identified as a viable candidate to be investigated in this study.

Fenton reaction is a viable alternative to hydrogen peroxide, as it usually requires lower reaction times [15–17]. Similar to the situation with hydrogen peroxide, Fenton reactions were applied differently in the literature. The utilized reaction times varied from 20 min to 24 h, depending on the applied protocols [17–19]. Table A2 summarizes some of the Fenton protocols used in microplastic studies [7,15–17]. There, it can be observed that Fenton can provide effective digestion, while causing minimal effects on the investigated microplastics. Therefore, Fenton was considered as a candidate to be investigated in this study.

Acid-based digestion methods, such as hydrochloric acid (HCl) and nitric acid (HNO_3), have been traditionally used to digest biological samples such as fish tissues [11,20,21]. Studies reported that some polymers are sensitive to acids and might be affected or dissolved during treatment [12,13,21–25]. Table A3 summarizes some of the acid-based protocols used in the literature [11–13,20–22,25]. Some acid digestions were tested in pre-experiments in this study (SI Section S1.1), where they were found to result in microplastics deterioration. Based on this and reports from the literature about the degradation of several polymers, acid-based digestions were excluded from this study.

Alkaline treatments, such as potassium hydroxide (KOH) and sodium hydroxide (NaOH), were also often used for biological samples [11,13,22,25–28]. Some studies reported that alkaline digestion might cause discoloration or damage to the investigated microplastics, especially NaOH [27,29]. On the other hand, Hurley et al. [7] tested a digestion method with 10% of KOH at $60\text{ }^\circ\text{C}$, and achieved around 57% removal of organic matter from sludge, while observing minimal changes of the microplastics tested. Table A4 summarizes some of the alkaline-based protocols used in the literature [7,11,13,22,25–29]. Alkaline digestions were tested in the pre-experiments performed in this study (SI Section S1.1), and a protocol based on KOH (10%) was selected as a possible candidate to be investigated further.

Finally, enzymatic digestions can be an alternative to chemical digestions, especially for biological tissues such as those from fish or plankton [25,27]. They have also been used in conjunction with other treatment methods to treat wastewater samples [30]. The problem with such protocols is usually the long period of time (days) required for complete digestions. In addition, applying this digestion can be expensive or might be incomplete, especially for wastewater samples, which can require a follow-up application of other chemical reagents for a complete digestion [7]. For this reason, enzymatic digestions were excluded from this study, as a rapid reaction and efficiency were key attributes desired in the protocol selection.

1.2. Parameters Used in Microplastic Monitoring

An important goal when analyzing microplastic particles found in environmental samples is the determination of size and abundance [31–33]. Chemical digestion methods might dissolve microplastic particles and cause a general decrease in their size or a loss of particles under a certain size range. This would cause an underestimation of the microplastics and represent serious consequences for the conclusions of some studies. Furthermore, identifying polymer types is also desirable during microplastic monitoring and often involves specific pyrograms from gas chromatography coupled with mass spectrometry (GC-MS), or spectra from Fourier-transform infrared spectroscopy (FTIR). An improper digestion method might interfere with these specific pyrograms/spectra and hinder unambiguous microplastic identification. Therefore, it is important that the selected chemical digestion method neither alters the size of the investigated particles, nor interfere with their identification.

1.3. Research Objectives and State-of-the-Art

The objective of this study was to investigate the most common sample preparation methods for isolating microplastic particles from organic matrices, as well as to discuss the inconsistencies that have been identified in different studies. Then, this knowledge was used to develop and validate sample preparation methods to extract microplastics from wastewater samples, without effecting the important identifying parameters for microplastics that were discussed in the previous section.

Several recent studies have already attempted to validate sample preparation methods for microplastics [7,8,11,15,17,22,26]. However, these studies contained one or more of the following shortcomings: (A) working with larger microplastic particles (>500 μm) due to easier handling and analysis [7,15,22,26]; smaller particles have a larger surface area to volume ratio and might be far more susceptible to unintended effects from the chemical reagents used in sample preparation. (B) Using a small number of microplastic particles, which can limit the statistical significance of the findings [7,11,17,22,26]. (C) When using FTIR to compare the IR spectra of microplastic particles before and after exposure to the chemical treatment. It is common to compare the spectra of treated particles against their reference spectra to observe any changes. However, due to easy handling, reference spectra are often obtained in attenuated total reflection (ATR) mode, while for environmental samples, usually FTIR microscopy (μFTIR) spectra are used [7,8,15,17]. These modes of analysis do not always yield the exact same results, thus, they cannot be used interchangeably. Some FTIR researchers mentioned that ATR and μFTIR spectra differ from one another due to different beam penetration depths [34]. However, this has never been addressed in studies concerning microplastics, where the practice of obtaining reference spectra using ATR and comparing it to μFTIR spectra of the treated environmental sample is very common. This can lead to confusion in spectra interpretation if not addressed. (D) For studies implementing a digestion protocol based on the Fenton reaction, handling of the large amounts of precipitated iron (III) particles usually is not mentioned. This phenomenon can negatively affect microplastic detection by covering the entire sample with a layer of iron (III) particles. (E) Finally, studies reported completely different behaviors and contact times for the Fenton reaction [7,15–19]. Some studies even reported reaction times up to 24 h [19], which seems unlikely in terms of reaction kinetics, as the Fenton reaction forms hydroxyl radicals, which result in diffusion limited reaction rates. Thus, the process should be rapid. Lastly, studies like Masura et al. [16] heated

the reactants to 75 °C, which is surprising as the Fenton reaction is exothermic and sometimes, cooling is recommended to protect polymers from excessive temperatures [7].

To allow a comprehensive validation and to consider the shortcomings of the mentioned previous validation efforts, the experimental design in this study was adapted accordingly: (A) Microplastic particles with sizes between 80–330 µm were selected. (B) For size distribution analysis, depending on the microplastic type, approximately 4×10^3 – 2×10^5 particles were investigated. (C) µFTIR analysis was applied to both the reference and treated microplastic particles in order to minimize bias in interpretation. (D) The Fenton reaction as a possible digestion method for microplastics was further investigated by adapting the protocol from Tagg et al. [17] and refining it to address the issues associated with the precipitation of iron (III). (E) Finally, an experimental setup was dedicated to investigating Fenton reaction kinetics. This was intended to elucidate the reasons behind the discrepancies and long reaction times required for the Fenton reaction, as reported in some studies [15,19].

2. Materials and Methods

2.1. Selection of Sample Preparation Protocols

Ten feasible sample preparation protocols were selected based on a comprehensive review of the peer-reviewed literature [7,14,17,21,27,35–37]. They were then investigated in pre-experiments using 250 µm PS-particles (BS-Partikel, Mainz, Germany) and an optical microscope (Axioplan 2, Carl Zeiss AG, Oberkochen, Germany) to assess visual changes to the particles' surface. For further details, refer to Supplementary Materials Section S1.1.

Furthermore, questionnaires were sent to the project partners within the research consortium 'Plastic in the Environment' sponsored by the German Federal Ministry of Education and Research, to gather more information about the most common methods utilized to digest environmental samples. The findings from these reviews along with observations from the pre-experiments resulted in a final selection of three methods for further testing. An overview of the selected protocols is provided in Table 1. Furthermore, a workflow for applying the protocols to real sludge/wastewater samples is provided in Figure 1.

Table 1. Protocols investigated in this study.

Protocols	Temperature	Time
Fenton (30% H ₂ O ₂ + 20 g/L FeSO ₄) [17]	Unregulated	10 min + 10 min cooling
KOH (10%) [22]	60 °C	24 h
H ₂ O ₂ (30%) [7]	60 °C	24 h

In case other sample volumes are used than what is specified in Figure 1, the ratios of reactants should be kept the same. For KOH and hydrogen peroxide protocols, the ratio of reagent to sample is 10:1. As for Fenton, the ratios can be back calculated from the procedure described in Figure 1. Alternatively, a scaling factor (K) is utilized to achieve this goal; a complete explanation is given in the Supplementary Materials Section S1.2.

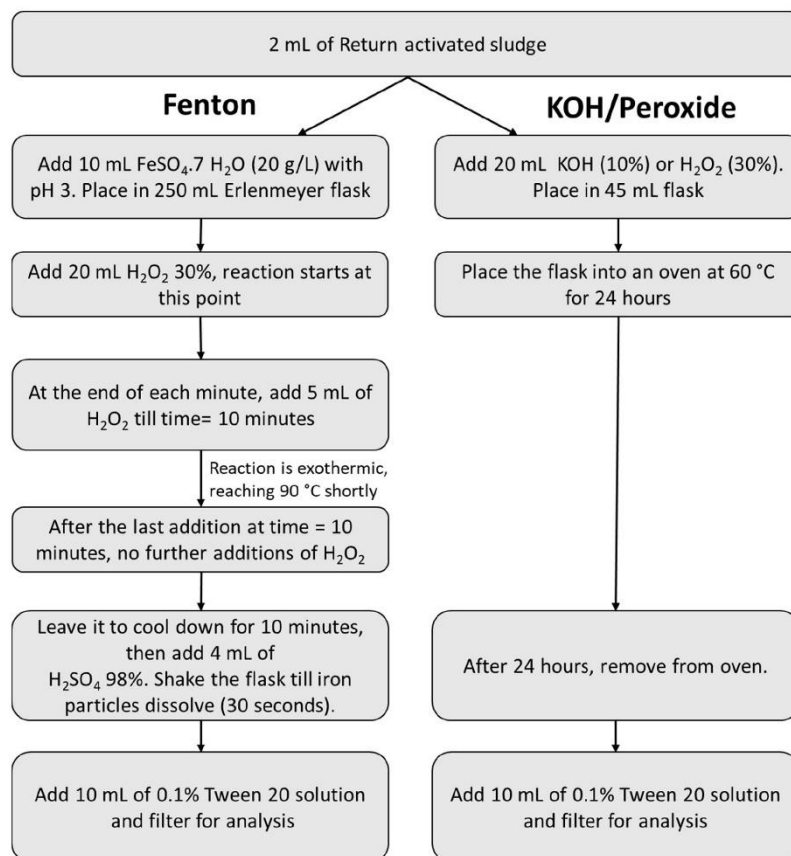


Figure 1. Workflows of the three selected protocols for processing microplastics from wastewater sludge samples.

2.2. Materials

Seven different polymers were used in this study: Polystyrene (PS), low density polyethylene (LDPE), polyvinyl chloride (PVC) (Ineos, London, UK), polypropylene (PP) (Borealis, Vienna, Austria), polyethylene terephthalate (PET) (TPL, Zurich, Switzerland), polyamide (PA) (Lanxess, Cologne, Germany), and polylactic acid (PLA) (Nature Works, Minnetonka, MN, USA). The particle sizes for all polymers were between 80 and 330 μm (detailed information in Supplementary Materials Table S2).

Ultra-pure water (UPW) was produced using an arium[®] pro VF (Sartorius, Göttingen, Germany) with an ultra-filter and used for all steps. Hydrogen peroxide (H_2O_2) (30%) was purchased from Merck, Germany and Carl Roth, Karlsruhe, Germany. Different batches were tested (ISO/Ph.Eur. stabilized; for synthesis, stabilized, Carl Roth, Germany and VWR, Germany) to observe the impact of the different manufacturing standards of hydrogen peroxide quality on Fenton reaction kinetics. The ferric sulfate (FeSO_4) catalyst was prepared using $\text{FeSO}_4 \cdot 7\text{H}_2\text{O}$ (Merck, Germany), which was weighed and dissolved in UPW and the pH was subsequently adjusted to 3 using sulfuric acid (H_2SO_4 ,

0.5 M; VWR, Germany). Potassium hydroxide (KOH, 10 wt%) was prepared from dissolving pure KOH pellets (Merck, Germany) in UPW. To minimize contamination by foreign particles, all reagents were filtered prior to application, using 0.2 μm syringe filters.

Sample filtration was performed using a vacuum filtration unit made of glass (DURAN, Mainz, Germany). The filters used were track etched polycarbonate filters, 25 mm in diameter with a pore size of 0.2 μm (PCTE, unsterile, Carl Roth, Germany). For rinsing glass apparatuses and producing stable microplastic suspensions, 0.1% (*v/v*) of the surfactant Tween 20 (Merck, Germany) in UPW was utilized (Supplementary Materials Section S1.5).

2.3. Contamination Mitigation and Quality Assurance

To ensure minimal airborne microparticle cross-contamination, all experiments were conducted in a laminar flow box (Laminar Flow Module FMS series SuSi, Spetec, Erding, Germany). The samples were handled outside of this setup only when weighing the microplastics. During this process, the samples were always covered with aluminum foil to prevent cross-contamination. Lab coats made only out of cotton were worn at all times to avoid plastic fibers contaminating the samples.

2.4. Investigating the Discrepancies in Fenton Reactions

The authors of the current study were perplexed by the widely different Fenton reaction kinetics and behaviors reported in the literature, and the lack of discussion thereof [7,15–19]. The Fenton reaction is exothermic and should not require any external heating to exceed temperatures of 40 °C [38]. This was in accordance with the pre-experiments performed in this study, as well as reactions described by Hurley et al. [7] and Tagg et al. [17], where the digestion reactions with organic matrices were quick, needing merely 20 min to complete, and required cooling to prevent them from exceeding 40 °C. On the other hand, some studies mentioned reaction times up to 24 h, or described heating the reactants externally to 75 °C [16,19].

To investigate if the source of those discrepancies is somehow related to the various manufacturing processes used to produce hydrogen peroxide, identical H_2O_2 concentrations (30%) were used, albeit from five different commercially available batches: (i) Hydrogen peroxide 30%, stabilized, (Perhydro[®]) EMSURE[®] ISO analytical reagent, Supelco[®] (Merck, Germany), (ii) Hydrogen peroxide 30% ROTIPURAN[®] p.a., ISO, stabilized (Carl Roth, Germany), (iii) Hydrogen peroxide 30%, Ph. Eur, stabilized (Carl Roth, Germany), (iv) Hydrogen peroxide 30% for synthesis, stabilized (Carl Roth, Germany), as well as (v) Hydrogen peroxide 30% stabilized, EMPROVE[®] ESSENTIAL Ph. Eur., BP, USP, SAFC[®] (Merck, Germany).

The Fenton protocol was performed identically with each one of these batches of hydrogen peroxide. No microplastics were used in these experiments, as the investigation was concerned merely with the kinetics and general behavior of the Fenton reaction itself. Thus, samples comprised only the filtered reagents (hydrogen peroxide and iron sulfate); no additional particles or organic matter were added to prevent any unforeseen implications. The reaction was performed as explained in Figure 1 and the Supplementary Materials Section S1.2, with a scaling factor (*K*) of 2 mL (Supplementary Materials Section S1.2), or simply 2 mL of $\text{FeSO}_4 \cdot 7\text{H}_2\text{O}$ and 4 mL of H_2O_2 as starting volumes (Figure 1), resulting in a final total reagents volume of 16 mL. The experiments were performed in duplicates in 100 mL Erlenmeyer flasks. The temperature and pH of the reactions were recorded over time. To understand the effects of thermal dissipation/insulation on reaction kinetics, additional experiments for the selected hydrogen peroxide batches were performed by placing the 100 mL Erlenmeyer flasks on an aluminum bench to simulate a larger heat dissipation condition, whereas plastic centrifugal tubes (50 mL) were used to simulate heat insulation.

Subsequently, the experiments with the 100 mL Erlenmeyer flasks were repeated but a 1.5 × 1.5 cm piece of tissue paper was placed inside each flask and allowed to react as before in order to observe the effects of different reaction kinetics on the removal of organic matter.

2.5. Investigating the Effects of Sample Preparation on Microplastics

To ensure that sample preparation protocols do not interfere with the characterization of microplastic parameters as mentioned in Section 1.2, they were investigated for changes in their size distributions as well as their characterization by μ FTIR and Thermal Desorption–Gas Chromatography coupled with mass spectrometry (TD-Pyr-GC/MS), before and after applying the digestion protocols. Table 2 shows the samples that were prepared for these investigations. The samples were prepared in 50 mL glass flasks for Fenton samples, and 10 mL glass tubes for the rest. Polymers were each made as individual samples for all the tests listed below in order to assess the changes to each of them individually.

Table 2. Protocols that were investigated for their effects on the polymers.

Protocols	Description
Control	5 mL UPW @ Room Temperature
Fenton	As described in Figure 1 (2 mL FeSO ₄ as a starting volume)
H ₂ O ₂	As described in Figure 1 (5 mL H ₂ O ₂)
KOH	As described in Figure 1 (5 mL KOH)
** Temperature control 60 °C	5 mL UPW @ 60 °C and 24 h
** Temperature control 90 °C	5 mL UPW @ 90 °C and 20 Minutes

** Only performed for size distribution analysis in order to isolate the melting or agglomerating effects of the elevated temperature from the effect of the chemical reagents.

The temperature controls simulated the maximum temperatures and durations encountered in each of the protocols (60 and 90 °C for H₂O₂/KOH and Fenton protocols, respectively), and were made for the same exposure times (24 h and 20 min, respectively).

2.5.1. Size Distribution Analysis by Laser Diffraction

Laser diffraction measurements for particle size distribution analysis were conducted using a Malvern “Mastersizer S long bed”, a small volume sample dispersion unit (SVSDU), and a sample disperser, all manufactured by Malvern Panalytical (UK). In the optical unit, a 2 mW He-Ne laser with 633 nm wavelength, 18 mm beam width, and 2.4 mm beam length, was sent through a 300 RF lens, whose measurement range is 0.05–900 μ m. The wet standard scattering model was applied. The refractive index of water was used as the refractive index of the medium. The refractive indices applied were 1.5295 (real) and 0.1 (imaginary) in 1.33 (medium). All measurements were carried out according to ISO 13320:2009-10 [39].

Duplicate samples and controls, each consisting of 200 ± 50 mg for PS, PE, PET, PA, PLA, and PVC as well as 60 ± 15 mg for PP, were used as per Table 2. Each sample was further subdivided into two repetitions to improve the reliability of the analysis. All samples were suspended in 10 mL UPW containing a concentration of 0.1% (v/v) of the surfactant Tween 20, vortexed for 40 s at 2500 RPM prior to analysis and then, poured into the wet dispersion unit. Measurements were only made after waiting for 2 min to ensure full dispersion. The laser was aligned at the beginning of each measuring session. The background scattering was determined before adding the sample aliquots into the SVSDU, which was pre-filled with deionized water and then, stirred for 2 min to ensure proper dispersion in the system. After each measurement, the SVSDU was cleaned with a 0.1% (v/v) Tween 20 solution. The weighted average of each size distribution was calculated to compare the treated samples against their corresponding control samples. Further, the smallest 10th percentile of the size distribution was also compared in order to observe if the smallest particles in the size distribution exhibited more size changes than the average size particles. Finally, to test the statistical significance, the frequency tables from the Mastersizer measurements were transformed to raw data by using the Real Statistics Resource Pack add-in for Microsoft Excel™, after which the data were exported to IBM's SPSS® Statistics package, where a Kruskal–Wallis 1-way analysis of variance (ANOVA) was performed for each polymer type across all treatment methods. These results were subsequently compared against

their respective controls with a post hoc analysis. The differences were only considered significant if the probability (p) of the null hypothesis being true was smaller than 0.05.

2.5.2. FTIR Analysis

Samples and controls were prepared according to the protocols listed in Table 2, by weighing 2.5 mg of each of the microplastic types (PS, PE, PET, PP, PVC, PA, and PLA). Samples were then filtered through a gold-coated polycarbonate membrane (diameter 25 mm, pore size 0.8 μm , Analytische Produktions-, Steuerungs- und Kontrollgeräte GmbH, Germany) and measured by μFTIR spectroscopy on an Agilent Cary 620 spectrometer coupled to an Agilent Cary 670 FTIR microscope, equipped with a 128×128 pixel Focal Plane Array detector. IR images were measured in reflectance mode at a spectral resolution of 8 cm^{-1} within a spectral range from 3750 to 800 cm^{-1} and a number of 30 scans. Before IR imaging, a mosaic photograph of the samples was taken in order to visualize any changes of the particle's surface morphology (Supplementary Materials Figures S2–S8). For each polymer type and treatment, spectra from ten particles were extracted from the IR image and their average spectra were calculated and normalized to values from 0 to 1. Additionally, further control particles were measured in ATR mode (Germanium crystal) in order to illustrate the differences between the ATR and reflectance μFTIR analysis modes.

2.5.3. Thermal Analysis by TD-Pyr-GC/MS

The TD-Pyr-GC/MS analysis was conducted with a thermal desorption unit (TDU) equipped with a TDU Pyrolysis module, a Multipurpose sampler (MPS) robotic^{PRO}, a Cooled Injections System CIS 4 with C506 (all by Gerstel, Mülheim an der Ruhr, Germany), and a 7890B gas chromatograph equipped with a DB-5MS Ultra Inert column in combination with a 5977B MSD mass spectrometer (all by Agilent, Santa Clara, CA, USA). In the first step, the samples were thermodesorbed to analyze volatile compounds at a final thermodesorption (TD) temperature of $200 \text{ }^\circ\text{C}$. The sample was then cryofocused in the cooled injection system (CIS) at $-50 \text{ }^\circ\text{C}$. The desorption mode was split-less. The GC/MS method for the TD step was adopted from Ochiai et al., 2005. [40]. However, the cryofocusing was conducted at $-50 \text{ }^\circ\text{C}$ instead of $-150 \text{ }^\circ\text{C}$. In the second step, the sample was pyrolyzed with a final temperature of $800 \text{ }^\circ\text{C}$, followed by a GC/MS analysis. The mass spectrometer was operated in full-scan mode (m/z range 40 to 550) with electron impact ionization (70 eV). For further details, refer to Reichel et al. (submitted).

Duplicate samples were prepared as per Table 2, by weighing 2.5 mg of each of the microplastic types. The reference particles of the polymers PS, PE, PLA, PET, PA, and PP were analyzed using TD-Pyr-GC/MS: once without treatment (control) and once after applying the sample preparation method. The chromatograms of the TD and pyrograms were compared in order to detect possible changes for the untreated and treated polymers regarding the characteristic pyrolysis products. PVC analysis could not be conducted due to the limitation of the TD-Pyr-GC/MS.

2.6. Determination of the Organic Matter Removal Efficiency from Sludge Samples

Thickened sludge samples were collected from the return-activated sludge (RAS) at a local wastewater treatment plant in the city of Freising, Germany. The organic content of the sludge was first determined via loss on ignition (LOI) by placing it in a furnace at $550 \text{ }^\circ\text{C}$ according to DIN 38409-1:1987-01 [41].

To gravimetrically determine the effectiveness of the three selected protocols, papers such as by Hurley et al. [7] used a procedure where sludge was first dried at $105 \text{ }^\circ\text{C}$ for 24 h to establish the starting dry weight of the sludge before treatment. Digestion protocols were applied to the dried sludge, and what remained was then filtered, dried, and weighed. The difference in weight between the starting dry weight and the final weight was assumed to correspond directly to the removal of organic matter.

This seemingly logical approach proved to be insufficient and error prone. The pre-experiments in this study revealed that following the aforementioned approach resulted in dried and hardened clay-like material that clumped and did not readily digest via the applied protocols (Supplementary Materials Section S7). Therefore, a new approach was created where the sludge was not dried before treatment; instead, its starting dry weight would be based on a control sample (surrogate). The process was performed in parallel, as shown below in Figure 2.

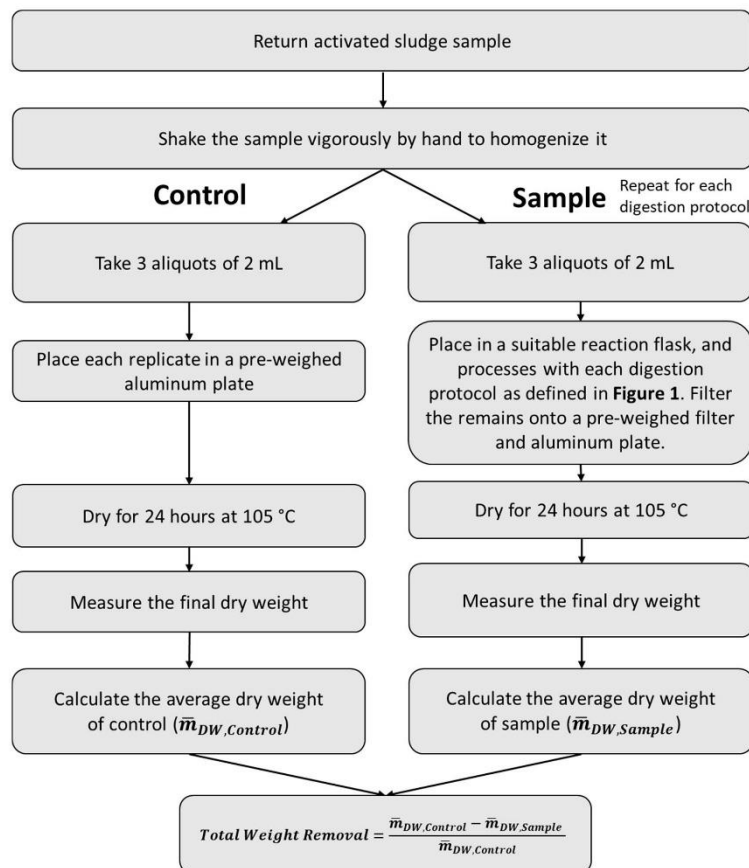


Figure 2. The workflow used in this study for investigating the organic matter removal efficiency.

Finally, the studies assumed that all weight loss from digestion protocols corresponded directly to organic matter removal [7], even though there is a certain number of inorganic and organic constituents that will dissolve during digestion, thus, presenting additional weight loss that could be misconstrued as organic matter removal. This might explain the findings of some studies, like Hurley et al. [7], who reported organic matter removal efficiencies over 100%. To showcase that the total weight loss after digestion may not entirely be due to organic matter removal, ultrapure water was added to 2 mL sludge aliquots. They were then left for 2 h to dissolve readily solvable inorganic and organic fractions,

filtered, and subsequently, dried for weight determination. This was done in duplicates, following the workflow described in Figure 2.

3. Results and Discussion

3.1. Discrepancies in Fenton Reactions

The reasons behind the aforementioned surprising descriptions of Fenton reactions in the literature can finally be understood based on the experiments of this study, as two general behaviors for the Fenton reaction were observed, when testing the five aforementioned batches of hydrogen peroxide. These differences occurred despite employing identical protocols and concentrations. To the best of the authors' knowledge, these different reaction behaviors have not been discussed in the literature before. Thus, it is important to understand the mechanism behind these behaviors. This is important to assure reproducible Fenton-based sample preparation methods. These two general behaviors of the Fenton reaction are subsequently referred to as type I and type II Fenton reactions:

Type I Fenton reaction: This reaction type has been used and validated in this study and can be reproduced when using batches i, ii, iv, and v. Its typical behavior was to start fizzing immediately after mixing the reactants, accompanied by a rapid temperature increase, which peaked at the range of 82–90 °C within 2–4 min, depending on the flask's thermal insulation, as the reaction reached its maximum intensity. This can be described as a boiling-like behavior and a change in color from an initial dark color to orange due to the formation of iron precipitates. The reaction kinetic showed some variation but it was largely consistent between runs as well as between different hydrogen peroxide batches, as can be seen by the similar maximum temperatures and low standard deviation for the four batches presented in Table 3.

Table 3. The reaction differences for the five batches of hydrogen peroxide when using 100 mL Erlenmeyer flasks on the rubberized bench. T_{max} —Maximum temperature.

H ₂ O ₂ Batches	T_{max} [°C]	pH @ T_{max} [-]	Time Till T_{max} [sec]
(i)	86.9 ± 0.9	1.62 ± 0.03	157 ± 4
(ii)	87.2 ± 0.2	1.67 ± 0.06	167 ± 19
(iii)	70.4 ± 23	1.72 ± 0.23	510 ± 127
(iv)	85 ± 0.4	1.67 ± 0.05	173 ± 11
(v)	84.9 ± 1.7	1.69 ± 0.04	192 ± 5

Type II Fenton reaction: This type was observed only when using batch iii of hydrogen peroxide. It typically exhibited a slower reaction kinetic than type I reactions. The initial fizzing was either very weak or missing. Temperatures increased at a lower rate than type I reactions and a critical temperature of 55 °C was needed in order to initialize boiling, which when occurring, would reach 82–90 °C within 7–10 min. However, the reaction was erratic, as can be seen in the elevated standard deviation values of batch iii compared to the remaining batches in Table 3. Identical parallel tests were performing differently, some reaching the boiling phase and others staying below 55 °C and failing to initialize boiling. This was especially true when the Erlenmeyer flasks were placed on the aluminum bench to simulate larger heat dissipation (Table 4). The experiments were repeated with two different bottles of batch iii to ensure that this was not a coincidence.

Table 4. The reaction difference for type I and II Fenton reaction when using 100 mL Erlenmeyer flasks on the aluminum bench for heat dissipation.

Reaction Type	T_{max} [°C]	pH @ T_{max} [-]	Time to T_{max} [sec]
Type (I) (batch (ii))	84.1 ± 3.4	1.65 ± 0.09	228 ± 3
Type (II) (batch (iii))	60.8 ± 29.3	1.7 ± 0.25	554 ± 190

Surprisingly, type II reactions exhibited much more consistent results when using the more thermally insulating 50 mL centrifugal tubes, consistently reaching 90 ± 0.5 °C within 3–4 min, very similar to the kinetics of type I when performing the same test. This indicates that heat insulation plays a much larger role for type II reactions than it does for type I, which had a very consistent behavior, regardless of the heat insulation of the used reaction flask. The color change still occurred, as was the case with type I, albeit the end color was a light yellow instead of orange, indicating that different iron species could be involved. The reactions that failed to initialize boiling had even less precipitation of iron (III), as shown in Figure 3.



Figure 3. Visual difference between type I and II Fenton reactions (end of reaction). (A): Type II that failed to initialize boiling. (B): Type II which initialized boiling. (C): Type I.

Finally, when using 100 mL Erlenmeyer flasks with tissue papers, type I consistently visually digested the paper at the end of the reaction; a similar result was observed in the tests where type II would initialize boiling. However, when type II failed to reach the critical temperature needed for the boiling phase, the tissue paper was still visibly floating at the end of the reaction (Figure 4). Since the reaction of type II is very unpredictable, it was excluded from this study and was not further validated.

Based on the observations revealed in this study, it is assumed that type II reactions were used in works like Masura et al. [16], where they needed to heat the reactants to 75 °C to exceed the critical temperature discussed above, thereby initializing the boiling phase of the reaction. This can also be seen in the study of Prata et al. [15], who heated the reaction at 50 °C for 1 h. The slower kinetics of type II could also explain the long reaction times in studies like Prata et al. and Flotron et al. [15,19], whereas type I might be the one used in investigations such as Hurley et al. and Tagg et al. [7,17] where no additional heat was needed to start the reaction and reaction times were short.

The formation of iron precipitates during Fenton reactions was not mentioned in microplastic-related studies. This might cause problems during filtration when not addressed (especially for type I), as iron precipitates tended to remain on the filters and covered the microplastics, which would have prevented particle identification. This was solved in this study by adding 5% (v/v) of 98% sulfuric acid at the end of the reaction, which quickly reacted with the precipitating iron species and dissolved them within 30s (Figure 1).

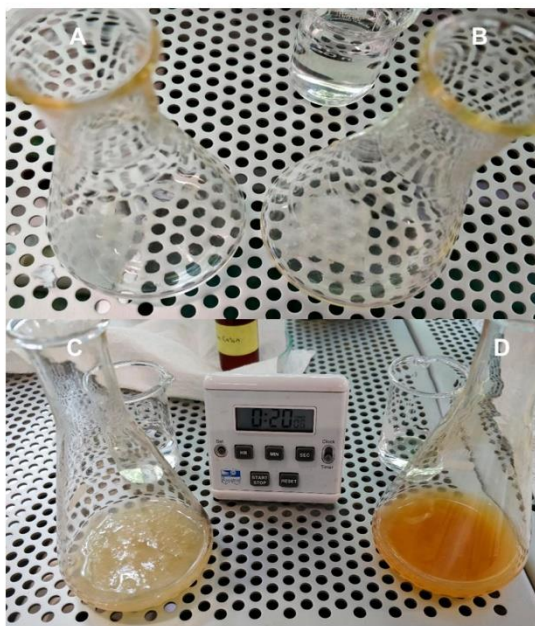


Figure 4. Differences between a type I Fenton reaction and a type II Fenton reaction that failed to initialize boiling when digesting a piece of tissue paper. (A,C): type II before and after reaction. (B,D): type I before and after reaction.

It became obvious that the reaction behavior of Fenton is influenced by the employed batch of hydrogen peroxide. It can be assumed that the stabilization agents added to the hydrogen peroxide are the critical factor for differentiation of the type I and type II reaction behaviors. However, the stabilization agents are not stated by the manufacturers directly and were not further investigated within this study.

The validations performed in this study followed the type I Fenton reaction by using batch (ii) of the hydrogen peroxide for all subsequent validation experiments.

3.2. Investigating the Effects of Sample Preparation on Microplastics

3.2.1. Variation in Size Distribution (Laser Diffraction)

Some polymers, such as PLA and PET, did not tolerate the KOH protocol. Hence, the majority of PET and PLA particles were dissolved after KOH digestion. The remaining few particles in the suspension after digestion did not produce enough signal to be reliably detected. Nevertheless, the resulting signal for PLA still showed a significant reduction in the size of the surviving particles, as can be seen in Figure 5 for PLA. On the other hand, PS exhibited a slight size increase which indicated the formation of a few small agglomerates or swelling. The rest of the polymers showed little to no change after being exposed to KOH. The effect of KOH on PLA, PET, and PS can clearly be seen in Figure 6. The changes were statistically significant after using Kruskal–Wallis post hoc pair tests, with ($p = 0.00$) for both PLA and PET and ($p = 0.006$) for PS, both of which are well below the significance value ($p > 0.05$).

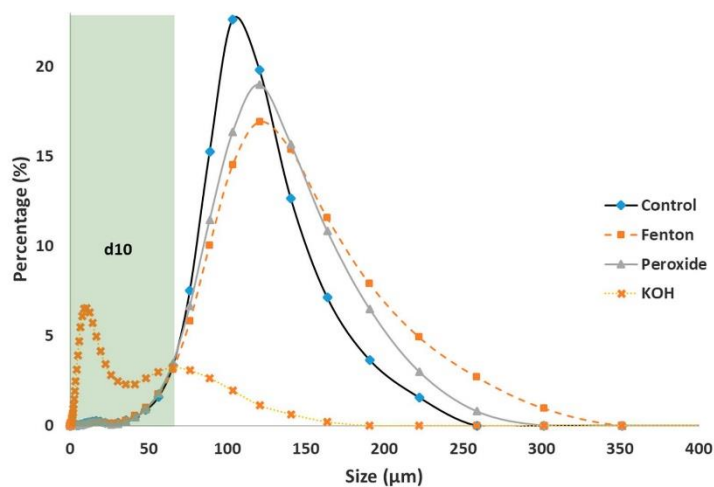


Figure 5. Size distribution analysis for PLA, the green area represents the smallest 10th percent (d10).

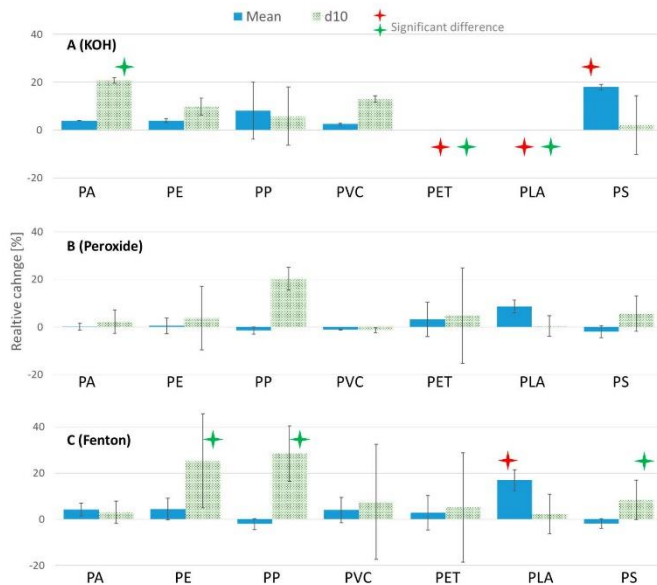


Figure 6. Relative particle size changes after treatment (A) KOH, (B) Peroxide, and (C) Fenton, compared to the controls (for weighted average sizes and 10th percentiles (d10)). The error bars represent the standard deviations. PLA and PET in (A) were completely destroyed, thus no results are given. The red and green stars indicate statistical significance for the entire distribution, as well as d10, respectively.

Using a 1 and 10 M NaOH and 60 °C for 24 h, Hurley et al. [7] observed a degradation of PET. They attributed it to the saponification of ester bonds on the polymer's surface. However, they observed no such effect when using KOH (10%) with the same conditions. Other studies also observed no adverse effect on PET particles when using different KOH protocols [22,29,42]. This might be because the aforementioned studies utilized larger microplastics (>500 µm) which possessed lower surface area to volume ratios, making them potentially less susceptible to the digestion reagents than the microplastics used in this current study. This issue, when coupled with the very small number of particles used in the aforementioned studies, can severely reduce the reliability of their results. As for PLA, no study was found that tested it specifically with the protocols chosen in the current study. However, Kühn et al. [42] tested six biodegradable microplastic particles with 1 M KOH at room temperature for 2 days. The authors observed that PLA particles, derived from biodegradable bags, were completely dissolved after applying the treatment. This agrees with the results found in the current study.

Fenton and hydrogen peroxide protocols both showed no significant changes regarding the size distribution of the tested polymers (Figure 6), with the exception of PLA, which exhibited slight agglomeration tendencies with increased temperatures, especially during Fenton reactions, which can briefly reach 90 °C. This manifested itself as an average size increase for PLA of 8.6% and 16.9% for hydrogen peroxide and Fenton, respectively (Figures 5 and 6). These changes were statistically significant only for Fenton though ($p = 0.04$). The temperature controls showed a more extreme case with 9.4% and 28.9% size increases for 60 and 90 °C, respectively (Figure 7). The temperature controls for 90 °C even showed a larger statistical significance when compared to the Fenton samples ($p = 0$). This indicated that indeed, the forming of agglomerates was caused by increased temperatures, possibly by making the particle's surface sticky, which caused some of the particles to randomly adhere to each other. This is supported by the fact that PLA has a glass transition temperature of around 60 °C, which would cause it to become sticky past this temperature [43]. Still, the changes were not disastrous, and the information about the particles was not lost as a result of melting. Although, when accurate size assessments for PLA are needed, when using these Fenton or hydrogen peroxide protocols, it is recommended to apply a correction to the average sizes to account for these results. This was also the main reason for suspending the particles after treatment in 0.1% Tween 20 solution and vortexing for 40 s before an analysis was made, as it helped to break some of the agglomerates.

In order to understand the effect on smaller particles, the changes to the smallest 10th percentile of the size distribution ($D(v,0.1)$), abbreviated here as (d10), were investigated. Figure 5 provides a visual representation of d10 (green highlight). The smaller particles can be more susceptible to degradation during treatment because of their larger surface area to volume ratios. Based on the d10 fractions, the tendency for severer size changes on smaller particles could be observed, although the accuracy of the measurement degraded when measuring the smallest 10th percentile. This can be seen in Figures 6 and 7 by the larger standard deviations for d10, compared to the mean size measurements. This might be attributed to the reduction in accuracy in light scattering techniques when larger and smaller particles are present in the same sample, as larger particles scatter the light at larger angles than smaller particles and might cover them.

It can be further inferred from the results presented in Figures 6 and 7 that there are more statistically significant size changes for d10 than when testing the larger particles. However, due to the reduced measuring accuracy of the Mastersizer under these conditions, concrete conclusions cannot be drawn, other than there is probably an increased tendency for smaller particles to be affected by the applied treatments.

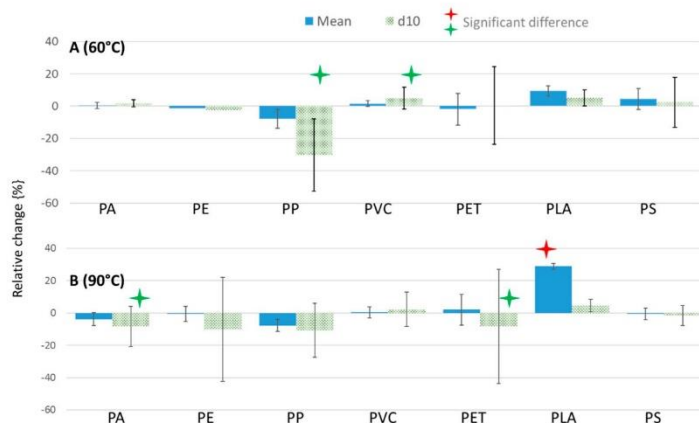


Figure 7. Relative particle size changes after temperature treatments compared to controls (for weighted average sizes and 10th percentiles (d10)). The error bars represent the standard deviations. (A): 60 °C for 24 h, (B): 90 °C for 20 min. The red and green stars indicate statistical significance for the entire distribution, as well as d10, respectively.

3.2.2. Variation in Infrared Spectra (FTIR)

μ FTIR spectra of the treated microplastic particles in general revealed only few alterations compared to untreated (reference) particle spectra (Supplementary Materials Figures S9–S15). Most of the modifications were small and are not suspected to hamper polymer identification.

As discussed for the size distribution experiments, the majority of PLA and PET microparticles were dissolved after the KOH treatment and consequently, their spectra were expected to be altered severely. However, only small changes were observed in the spectra of the few remaining particles after KOH treatment (Appendix A Figures A1 and A2). All treated PLA particles exhibited a relatively narrow band of intermediate strength at 3500 cm^{-1} (Figure A2). This band was a lot broader in untreated PLA particles. Spectra of KOH treatment induced a weak band at 3650 cm^{-1} to the PLA spectrum. Both bands indicate that OH groups were formed during sample treatment. Such OH groups were described by Zhang et al. [44] when investigating the infrared spectra of PET.

The spectra of the KOH-treated PET particles (Figure A1) lacked the shoulder present in untreated particles at the C=O band at 1720 cm^{-1} . Additionally, the band at 1945 cm^{-1} , an aromatic C-H bending overtone, was weaker compared to the other samples. This is in accordance with the fact that alkaline hydrolysis can be used in the recycling process of PET [45]. Nevertheless, these changes were quite small and are not suspected to hamper polymer identification.

In PVC, all digestion protocols induced a band at 3300 cm^{-1} , representing the formation of OH groups by the oxidative reagents, indicating a hydroxylation at the surface (Figure A3). In general, the spectral changes observed were small, however, they may lead to confusion for unexperienced users during spectra interpretation. If a spectral range above 3000 cm^{-1} is considered for polymer identification in a database search, it is recommended to include an altered PVC spectrum into the database. The rest of the microplastics exhibited no changes after the digestion protocols.

It can be concluded that if PLA and PET are among the target polymers for microplastic analysis, samples should not be treated with KOH. It is very likely that the few PLA and PET particles detected in the KOH samples investigated in this study were outliers that used to be much larger prior to the KOH digestion, whereas the vast majority of the particles were too small and dissolved during KOH digestion.

As was mentioned earlier, due to the easy handling, usually attenuated total reflection (ATR) mode is used for validation by researchers. However, ATR is suitable only for clean isolated particles that are big enough to be placed on the ATR crystal individually and therefore, this mode is not applicable for small microplastic particles (<500 μm) from environmental samples. This is where FTIR microscopy (μFTIR) is used instead. The usage of focal plane array (FPA) detectors enables the generation of FTIR images across a big sample area and therefore, reduces measurement time for real samples. Often, studies would use ATR spectra of reference particles to identify the spectra of a sample, regardless whether the latter were obtained using ATR or μFTIR . However, the spectra obtained with the two methods are not perfectly comparable without mathematical correction to account for the wavelength-dependent differences in penetration depth. Because penetration depth decreases with increasing wavenumbers for ATR measurements, the C-H stretch region around 2900 cm^{-1} exhibits very weak absorption bands. These bands are significantly larger for μFTIR spectra. That is why in this study, particle alterations due to chemical treatment were examined by comparing treated and untreated μFTIR spectra with each other to reduce bias caused by different spectral acquisition modes.

In Figure 8, a μFTIR reflectance mode spectrum of an untreated PET particle is shown in comparison to an ATR spectrum of the same material. Both spectra were normalized. The ATR spectrum is not ATR-corrected, thus, the differences between the spectra are fairly substantial, especially at higher wavenumbers. As was already discussed by von der Esch et al. [46], ATR spectra represent mostly the particle surface because of the low penetration depth compared to μFTIR spectra which, in the lower wavenumbers, penetrate more deeply into the material and therefore, represent the bulk properties of the particle. In manual data evaluation as well as in automated approaches, this can lead to confusion and misinterpretation. It is, therefore, recommended to establish a reference database comprising of μFTIR spectra in transmission and/or reflection mode, depending on the sample measurement method.

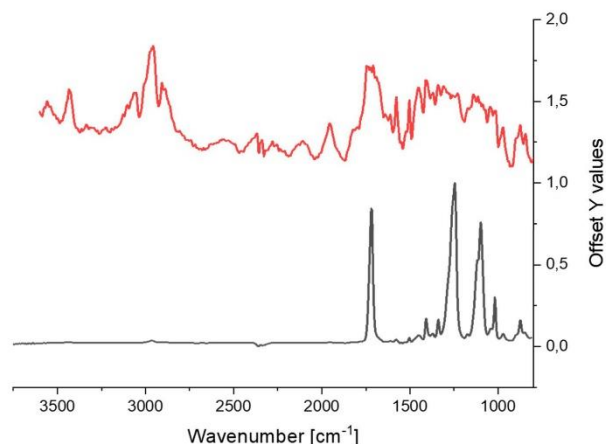


Figure 8. Normalized FTIR spectra of reference PET particles. **Top** (red line): measured in reflectance mode on FTIR microscope; **Bottom** (black line): measured in ATR mode.

3.2.3. Variations in Pyr-GC/MS Chromatograms

As KOH resulted in significant degradation of PLA and PET particles, it was excluded from this analysis. The characteristic substances of the polymers PE, PLA, PET, and PP were completely decomposed during pyrolysis. However, in the case of the polymers PA and PS, treatment with Fenton and H_2O_2 had an influence on their thermal stability. The ratio of the volatile pyrolysis products observed during the thermal desorption step at $200\text{ }^\circ\text{C}$ to the stable pyrolysis products at $800\text{ }^\circ\text{C}$ was

decreased after treatment, especially PA (Table 5). This means that the amount of pyrolysis products that were volatile at 200 °C was reduced after applying the treatments, and more of the pyrolysis products remained stable until the second pyrolysis step at 800 °C. Nevertheless, all of the polymers were still clearly identifiable in all cases. The pyrolysis products of the individual polymers are shown in the Supplementary Materials Table S3.

Table 5. Influence on the partial pyrolysis of thermal desorption (TD) products at 200 °C for both PA and PS.

Polymer Type	Particle Treatment	Pyrolysis Products in TD [%]/Standard Deviation [%]
PA	untreated	74.5/19.0
	Fenton	17.1/12.65
	H ₂ O ₂	3.0/3.67
PS	untreated	79.3/12.5
	Fenton	78.8/16.9
	H ₂ O ₂	71.9/10.9

3.3. Organic Matter Removal Efficiency

Since the KOH protocol degraded PLA and PET, only H₂O₂ and Fenton protocols were considered for further investigations. First, the dry weights of the sludge control aliquots (surrogates) were established, as was described in Figure 2. The triplicates exhibited highly consistent results with a standard deviation of <5% (average dry weight was 75.17 ± 3.55 mg). Therefore, implementing the dry weight of the controls as reference for the removal efficiency, as was described in Figure 2, can be seen as a better alternative to the reported method of drying the sludge of each sample before digestion to establish its dry-weight. As explained in the methods section, this would have had a far greater impact on the results, due to the hardening and clumping of dried sludge, thus, reducing the efficacy of the digestion. This could in fact explain the higher removal efficiency compared to Hurley et al. [7], as they used similar protocols but dried each sludge sample before applying digestion.

As indicated before, usually the lost weight is taken to correspond directly to the loss of organic matter. However, the organic content of the dry sludge was determined to be 70.5% via loss on ignition (LOI). Based on this, organic removal efficiencies >100% were obtained (Table 6). This clearly cannot be the case. This can be explained by the dissolution of some inorganic salts and inorganic carbon, which would pass through during the filtration process and be observed as extra lost weight. Hence, extra samples were investigated, where sludge aliquots were mixed with UPW, as described in the previous section. The results revealed that dissolution of the readily solvable organic and inorganic compartments in ultrapure water had a weight reduction of around 5.9% ± 2.3%. This is far from negligible and indicates that some organic and inorganic content was dissolved and registered as extra weight loss. This phenomenon is expected to intensify for lower pH values and higher temperatures, such as the ones encountered during the Fenton and hydrogen peroxide protocols. However, this was not necessary for the scope of this paper, as the comparison between protocols did not require exact knowledge of the removed inorganic components. This side experiment was only intended as a proof of concept to clarify the reported removal percentages, which are sometimes larger than 100% in the literature. In fact, a study by Karami et al. [11] did not dry the biological samples beforehand, which compromised the absolute removal values they reported; but, as a comparative tool between the investigated protocols, it was still a valid result, as all samples were treated equally. Thus, no further investigations regarding this were perused.

Table 6. Average total and corresponding organic removal efficiencies for the investigated protocols. Results represent the average \pm standard deviation for the three sample repetitions.

Protocol	Total Weight Removal	Corresponding Organic Matter Removal *
Fenton	83.5% \pm 1.8%	118.4% \pm 2.6%
H ₂ O ₂	71.3% \pm 1.2%	101.1% \pm 1.6%

* The results were not adjusted to account for the loss of inorganic matter, hence removal efficiencies over 100% are present.

Finally, Figure 9 shows a visual comparison of the filtered results from the hydrogen peroxide and Fenton protocol for the gravimetric analysis. Even though the weight difference between the sludge treated with Fenton and hydrogen peroxide protocols was not large, the characteristic of the remaining material differed between the two. Whereas the hydrogen peroxide-treated sample showed visible particulate matter after digestion, Fenton showed only coloration of the filter with no visible organic particles.

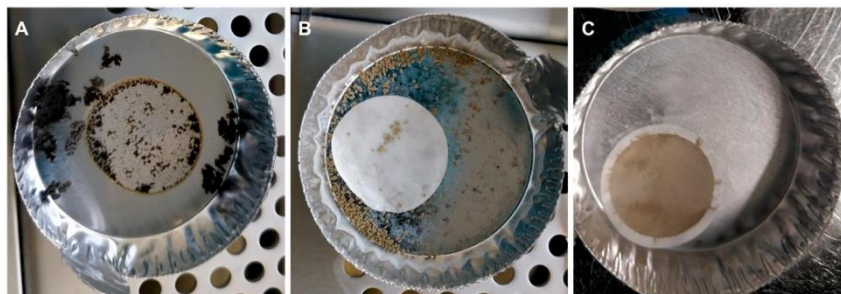


Figure 9. The end result of the gravimetric analysis done on 2 mL of sludge. (A): dried sludge (surrogate) (B): dried retentate and filter after hydrogen peroxide treatment, (C): dried retentate and filter after Fenton treatment.

4. Conclusions

If one sentence could summarize the findings of this paper, it would be: “the devil is in the details”. The initial intention of the authors was to screen through sample preparation methods in the literature and adapt and validate the most suitable methods for microplastic monitoring in wastewater samples. It was soon clear however, that large variations existed between the reported results in the peer-reviewed literature. Further, it was not always possible to simply replicate the results due to seemingly insignificant missing details, which turned out to be basic but essential to take into account when replicating someone’s work. Therefore, this study tried to consider even the smaller details in order to clarify the reasons behind the different results in the literature. Along the journey, surprising but important discoveries were made regarding the different types of Fenton reactions that exist, even when one is seemingly using identical chemical reagents and protocols. This study recommends using the Fenton reaction as described in Figure 1 as well as the Supplementary Materials Section S1.2. It provided excellent organic matter removal efficiency from wastewater samples in a very short amount of time and had very little adverse effects on the seven investigated microplastic types. However, it is of utmost importance that the used sort of hydrogen peroxide is tested beforehand to ensure that it provides a type I Fenton reaction as was defined in this study. Type II Fenton reactions were explored and defined in this study, but they were not validated and are not recommended for this application, due to their much slower reaction kinetics. The use of hydrogen peroxide also provided similar results to Fenton, but the much longer reaction times (24 h as opposed to 20 min) limit the rapid throughput

potential of the latter when compared to Fenton. Additionally, the remaining organic particles after hydrogen peroxide digestion (Figure 9) could constrain particle counting and identification.

Supplementary Materials: The following are available online at <http://www.mdpi.com/2073-4441/12/9/2445/s1>.

Author Contributions: Conceptualization, M.S.M.A.-A., C.S., J.E.D., O.K.; methodology and data analysis: Size Analysis: M.S.M.A.-A., S.K.; FTIR: M.S.M.A.-A., J.W.; Pyr-GC/MS: M.S.M.A.-A., J.R.; writing—review and editing, M.S.M.A.-A., O.K., J.W., S.K., J.R., C.S. and J.E.D.; supervision, J.E.D., O.K., and K.G. All authors have read and agreed to the published version of the manuscript.

Funding: This research was funded by the Bayerische Forschungsstiftung, grant number 1258-16 and by the German Federal Ministry of Education and Research (BMBF), grant number 02WPL1443A.

Conflicts of Interest: The authors declare no conflict of interest. The funders had no role in the design of the study; in the collection, analyses, or interpretation of data; in the writing of the manuscript, or in the decision to publish the results.

Appendix A

Abbreviations for microplastics used in the tables below:

Acrylonitrile-butadiene-styrene	ABS
Cellulose acetate	CA
Crosslinked polystyrene	PSXL
Expanded PS	EPS
High-density PE	HDPE
Low-density PE	LDPE
Linear LDPE	LLDPE
Nylon-6 or polyamide-6	NY6
Nylon12 or polyamide-12	NY12
Nylon-66 or polyamide-66	NY66
Poly 1,4-butylene terephthalate	PBT
Polyamide	PA
Polycarbonate	PC
Polyethylene	PE
Polyethylene terephthalate	PET
Poly(hexamethylene nonanediamide)	Nylon 6/9
Poly(methyl methacrylate)	PMMA
Polypropylene	PP
Polytetrafluoroethylene	PTFE
Polyurethane	PUR
Polyvinyl chloride	PVC
Styrene acrylate	SA
Un-plasticized polyvinyl chloride	uPVC

Table A1. Summary of various hydrogen peroxide protocols used in microplastic studies. RT—Room Temperature.

Protocols	Conditions	Matrix	MPs	Effects on Organics	Effects on MP
H2O2 (30%) [7]	60 °C for * 24/12 h or 70 °C for * 24 h	Sludge and soil	PP, LDPE, HDPE, PS, PET, NY66, PC, PMMA	Digestion > 80% for sludge and >96% for soil	Degradation of NY66 (at 70 °C), PP (at 70 °C). As for PS; less degradation at 60 °C and more at 70 °C
H2O2 (33%) [11]	50 °C for 96 h	Fish	LDPE, HDPE, PP, PS, PET, PVC, NY6, NY66	Digestion of 98%	Discoloration of PET, loss of NY6 and NY6
H2O2 (30%) [12]	55 °C for 7 days	Fish	PE, PS	** Extraction efficiency of 70%	No report
Density separation then H2O2 (1.5%) [12]	50 °C overnight	Fish	PE, PS	** Extraction efficiency of 95%	No effects
H2O2 (30%) [13]	RT. For 7 days	Marine sediment	PVC, PET, PA, ABS, PC, PUR, PP, LDPE, LLDPE, HDPE	50% digestion and the rest were discolored	Discoloration or degradation in PA, PC, PP, PET, LLDPE, PVC, PUR, LDPE
H2O2 (35%) [13]	RT. For 7 days	Marine sediment	PVC, PP, LDPE, PE, HDPE, PET, PUR, PS, PC, PA, ABS, EPS	92% digestion and discoloration	Size reduction PP and PE
H2O2 (30%) then density separation [14]	70 °C overnight	Sludge	PE	** Extraction efficiency of 78%	No adverse effects reported

* Contact times in the study of Hurley et al. [7] were not clearly reported. The experiments for the effects on microplastics was 24 h for all six protocols. However, the experiments for organic matter digestion were done separately and the contact time was not specified. Their protocol for H₂O₂ was based on a protocol by Suijtham et al. [11], where the contact time was defined as 12 h (overnight). ** Extraction efficiency represents only the recovery of microplastics from an environmental matrix; it does not report on the reduction of the matrix.

Table A2. Summary of various Fenton protocols used in microplastic studies. RT—Room Temperature.

Protocols	Conditions	Matrix	MPs	Effects on Organics	Effects on MP	
H2O2 (30%) + 20 g/L FeSO4 7H2O2 1:1 (v/v) [7]	<40 °C (ice bath)	*24 h/20 min	PP, LDPE, HDPE, PS, PET, NY66, PC, PMMA	Digestion 87% for sludge and 106% for soil	No adverse effects	
H2O2 (30%) + 15 g/L FeSO4 7H2O2 1:1 (v/v) [15]	50 °C for 1 h.	Plant and animal tissues	PE, PP, PS, PET, PVC, CA, PA	Digestion of 72.6% of fish tissue, 100% of algae, 26.3% driftwood, 17.5% paraffin	Degradation of CA	
H2O2 (30%) + 15 g/L FeSO4 7H2O2 1:1 (v/v) [16]	75 °C for >35 min	Water, beach and sediment	None tested	No reports	No reports	
H2O2 (30%) + 20 g/L FeSO4 7H2O2 (2:1 v/v) [17]	RT (no ice bath)	10 min reaction + 10 min cooling	Sludge	PE, PP, PVC, PA	Effective removal (No exact details provided)	No observed effects

* Contact times in the study of Hurley et al. [7] were not clearly reported. The experiments for the effects on microplastics used 24 h for all protocols. However, the experiments for organic matter digestion were done separately and the contact time was not specified. Their protocol for Fenton was based on a protocol by Tegg et al. [17], where the contact time was defined as 20 min in total.

Table A3. Summary of various acid-based digestions used in microplastic studies. RT—Room Temperature.

Protocols	Conditions	Matrix	MPs	Effects on Organics	Effects on MP
HNO3 (69%) [11]	25 °C for 96 h	Fish	LDPE, HDPE, PP, PS, PET, PVC, NY6, NY66	Removal >95%	Loss of NY6, NY66. Melting of LDPE, HDPE, PP. Recovery of PVC 69%. Discoloration of others
HNO3 (55%) [20]	Based on fish size: RT. For 3–10 h or 80 °C for 10–20 min	Fish	HDPE, PA, Nylon 6/9, PBT, PVC	Complete digestion of the fish	Tested at room temperature for 1 month. Loss of Nylon within 24 h, the rest showed no significant changes after 1 month.

Table A3. Cont.

Protocols	Conditions	Matrix	MPs	Effects on Organics	Effects on MP
HNO ₃ (22.5 M) [21]	RT. Overnight then boiling for 2 h	Mussels	PS, PA	Good digestion of the tissues	PA fibers (30 × 200 µm) were lost. PA particles 100 × 400 µm were 98% recovered. PS particles 30 µm and 10 µm were recovered.
HNO ₃ (22.5 M) [21]	60 °C for 1 h then 100 °C for 1 h	Mussels	PS, PA	Satisfactory digestion of the tissues	PS particles melting together when exposed to the reagent directly. This did not occur when PS was embedded in the tissues. PA was completely lost
HNO ₃ (22.5 M) [12]	RT. overnight then boiling for 30 min	Fish	PS, PE	** Extraction efficiency of only 4%	Almost complete loss of PS and PE
HNO ₃ (65%) [22]	RT. overnight then 60 °C for 2 h	None	LDPE, HDPE, PP, NY12, PS	Not tested due to damaged polymers	Melting of NY12, yellowing of the rest
HNO ₃ (35%) [25]	60 °C overnight	Mussels	PET, HDPE, PVC, PA	Complete digestion	Melting together of PET, HDPE, loss of PA
HCL (37%) [11]	25 °C for 96 h	Fish	LDPE, HDPE, PP, PS, PEI, PVC, NY6, NY66	Digestion efficiency >95%	Loss of NY6, NY66. Melting and clumping of PEI
HCL (20%) [13]	RT. for 7 days	Marine sediment	PVC, PET, PA, ABS, PC, PUR, PP, LDPE, LLDPE, HPDE	No complete dissolution of any biogenic organic matter	Not reported

** Extraction efficiency represents only the recovery of microplastics from an environmental matrix; it does not report on the reduction of the matrix.

Table A4. Summary of various alkaline-based digestions used in microplastic studies. RT—Room Temperature.

Protocols	Conditions	Matrix	MPs	Effects on Organics	Effects on MP
KOH (10%) [7]	60 °C for 24 h	Sludge and soil	PP, LDPE, HDPE, PS, PET, NY66, PC, PMMA	Digestion of sludge: 57% And for soil: 35%	A slight weight decrease for PC

Table A4. Cont.

Protocols	Conditions	Matrix	MPs	Effects on Organics	Effects on MP
KOH (10%) [11]	25 °C for 96 h or 40 °C for 48 h or 50 °C for 36 h or 60 °C for 24 h	Fish	LDPE, HDPE, PP, PS, PET, PVC, NY6, NY66	Removal >95% (all temperatures)	Yellowing of NY66. Reduction in PVC and PET recovery that worsens with increased temperature
KOH (10%) [22]	0 °C for 24 h	Mussels, crabs, fish	CA, HDPE, LDPE, NY6, NY12, PC, PET, PMMA, PP, PS, PSXL, PTFE, PUR, uPVC, EPS	Digestion efficiency > 99.5%	Degradation of CA
KOH (56, 224 g/L) [26]	RT. For 14 days	None	Cera Microcrystalline, PE	** Extraction efficiency > 95%	Discoloration of cera microcrystalline and PE (for 224 g/L)
KOH (10%) [28]	RT. For 2–3 weeks	Fish	No spiking: PE, PP, PET, SA	Digestion satisfactory	None tested
KOH (10%) [29]	60 °C for 24 h	Vegetal	PP, PE, PVC, PUR, PET, PS	No digestion observed	No effects observed
NaOH (1, 10 M) [7]	60 °C for 24 h	Sludge and soil	PP, LDPE, HDPE, PS, PET, NY66, PC, PMMA	Digestion of sludge: 61% (1M) 67% (10M) and soil: 68% (1 M) 65% (10 M)	Degradation of PET, PC (even more with 10 M)
NaOH (20, 30, 40, 50%) [13]	RT. For 7 days	Marine sediment	PVC, PET, PA, ABS, PC, PUR, PP, LDPE, LLDPE, HPDE	No complete dissolution of any biogenic organic matter. Strongest reaction with NaOH (20%)	Not reported
NaOH (10 M) [22]	60 °C for 24 h	None	CA, HDPE, LDPE, NY6, NY12, PC, PET, PMMA, PP, PS, PSXL, PTFE, PUR, uPVC, EPS	Not tested due to damage to polymers	Degradation of CA, PC, PET
NaOH (1 M) [25]	60 °C overnight	Mussels	PET, HDPE, PVC, PA	Complete digestion and extraction efficiency of 93%	No significant effects
NaOH (10 M) [27]	60 °C for 24 h	Zooplankton	PS, PA, PET, PE, uPVC	Digestion efficiency of 91%	Partial degradation of PA, clumping of PE, yellowing of uPVC, partial loss of PS
NaOH (10 M) [29]	60 °C for 24 h	Vegetal	PP, PE, PVC, PUR, PET, PS	Almost no digestion	Degradation of PET

** Extraction efficiency represents only the recovery of microplastics from an environmental matrix; it does not report on the reduction of the matrix.

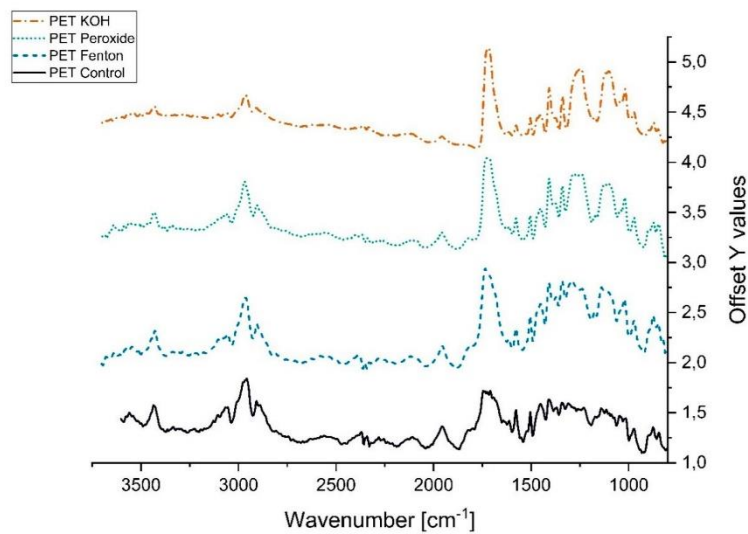
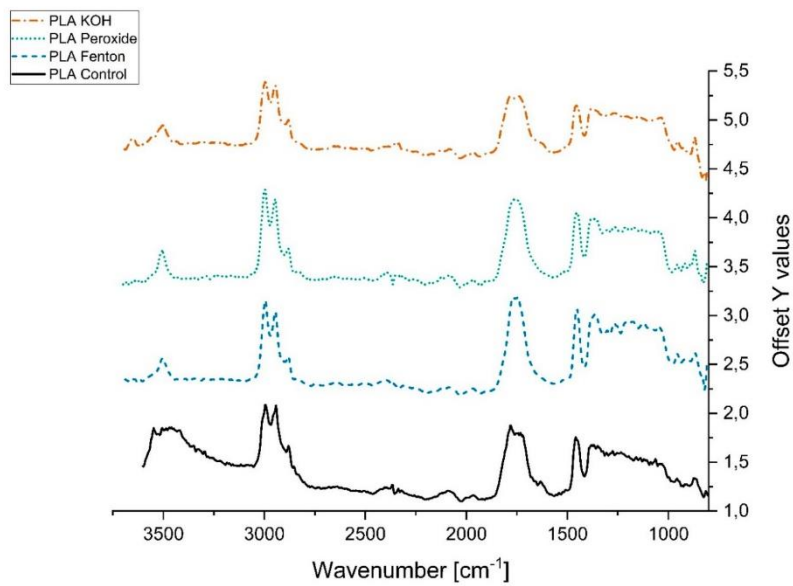
Figure A1. μ FTIR Spectra of PET.

Figure A2. FTIR Spectra of PLA.

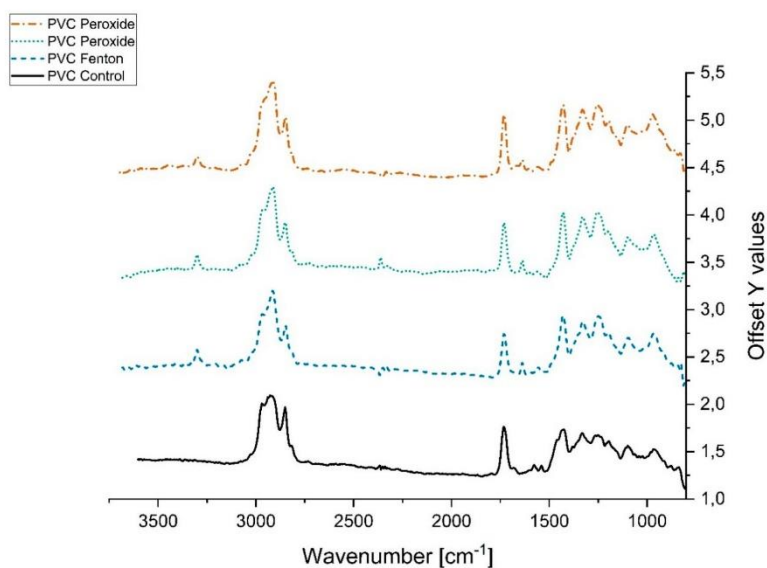


Figure A3. μ FTIR Spectra of PVC.

References

- Underwood, A.J.; Chapman, M.G.; Browne, M.A. Some problems and practicalities in design and interpretation of samples of microplastic waste. *Anal. Methods* **2017**, *9*, 1332–1345. [\[CrossRef\]](#)
- Jambeck, J.R.; Geyer, R.; Wilcox, C.; Siegler, T.R.; Perryman, M.; Andrady, A.; Narayan, R.; Law, K.L. Marine pollution. Plastic waste inputs from land into the ocean. *Science* **2015**, *347*, 768–771. [\[CrossRef\]](#) [\[PubMed\]](#)
- Hartmann, N.B.; Hüffer, T.; Thompson, R.C.; Hassellöv, M.; Verschoor, A.; Dagaard, A.E.; Rist, S.; Karlsson, T.; Brennholt, N.; Cole, M.; et al. Are we speaking the same language? Recommendations for a definition and categorization framework for plastic debris. *Environ. Sci. Technol.* **2019**, *53*, 1039–1047. [\[CrossRef\]](#) [\[PubMed\]](#)
- GESAMP. *Sources, Fate and Effects of Microplastics in the Marine Environment: A Global Assessment*; Kershaw, P., Ed.; IMO/FAO/UNESCO-IOC/UNIDO/WMO/IAEA/UN/UNEP/UNDP Joint Group of Experts on the Scientific Aspects of Marine Environmental Protection: London, UK, 2015.
- Braun, U.; Jekel, M.; Gerdtz, G.; Ivleva, N.P.; Jens, R. *Microplastics Analytics Sampling, Preparation and Detection Methods*; German Federal Ministry of Education And Research: Berlin, Germany, 2018.
- Ivleva, N.P.; Wiesheu, A.C.; Niessner, R. Microplastic in aquatic ecosystems. *Angew. Chem. Int. Ed.* **2017**, *56*, 1720–1739. [\[CrossRef\]](#) [\[PubMed\]](#)
- Hurley, R.R.; Lusher, A.L.; Olsen, M.; Nizzetto, L. Validation of a method for extracting microplastics from complex, organic-rich, environmental matrices. *Environ. Sci. Technol.* **2018**, *52*, 7409–7417. [\[CrossRef\]](#)
- Tagg, A.S.; Sapp, M.; Harrison, J.P.; Ojeda, J.J. Identification and quantification of microplastics in wastewater using focal plane array-based reflectance Micro-FT-IR imaging. *Anal. Chem.* **2015**, *87*, 6032–6040. [\[CrossRef\]](#)
- Dyachenko, A.; Mitchell, J.; Arsem, N. Extraction and identification of microplastic particles from secondary wastewater treatment plant (WWTP) effluent. *Anal. Methods* **2017**, *9*, 1412–1418. [\[CrossRef\]](#)
- Schwaferts, C.; Niessner, R.; Elsner, M.; Ivleva, N.P. Methods for the analysis of submicrometer- and nanoplastic particles in the environment. *TrAC Trends Anal. Chem.* **2019**, *112*, 52–65. [\[CrossRef\]](#)
- Karami, A.; Golieskardi, A.; Choo, C.K.; Romano, N.; Ho, Y.B.; Salamatina, B. A high-performance protocol for extraction of microplastics in fish. *Sci. Total Environ.* **2017**, *578*, 485–494. [\[CrossRef\]](#)

12. Avio, C.G.; Gorbi, S.; Regoli, F. Experimental development of a new protocol for extraction and characterization of microplastics in fish tissues: First observations in commercial species from adriatic sea. *Mar. Environ. Res.* **2015**, *111*, 18–26. [[CrossRef](#)]
13. Nuelle, M.T.; Dekiff, J.H.; Remy, D.; Fries, E. A new analytical approach for monitoring microplastics in marine sediments. *Environ. Pollut.* **2014**, *184*, 161–169. [[CrossRef](#)] [[PubMed](#)]
14. Sujathan, S.; Kniggendorf, A.-K.; Kumar, A.; Roth, B.; Rosenwinkel, K.-H.; Nogueira, R. Heat and bleach: A cost-efficient method for extracting microplastics from return activated sludge. *Arch. Environ. Contam. Toxicol.* **2017**, *73*, 641–648. [[CrossRef](#)] [[PubMed](#)]
15. Prata, J.C.; da Costa, J.P.; Girão, A.V.; Lopes, I.; Duarte, A.C.; Rocha-Santos, T. Identifying a quick and efficient method of removing organic matter without damaging microplastic samples. *Sci. Total Environ.* **2019**, *686*, 131–139. [[CrossRef](#)] [[PubMed](#)]
16. Masura, J.; Baker, J.E.; Foster, G.D.; Arthur, C.; Herring, C. *Laboratory Methods for the Analysis of Microplastics in the Marine Environment: Recommendations for Quantifying Synthetic Particles in Waters and Sediments*; National Oceanic and Atmospheric Administration: Silver Spring, MD, USA, 2015.
17. Tagg, A.S.; Harrison, J.P.; Ju-Nam, Y.; Sapp, M.; Bradley, E.L.; Sinclair, C.J.; Ojeda, J.J. Fenton's reagent for the rapid and efficient isolation of microplastics from wastewater. *Chem. Commun.* **2017**, *53*, 372–375. [[CrossRef](#)]
18. Zhang, H.; Heung, J.C.; Huang, C.P. Optimization of fenton process for the treatment of landfill leachate. *J. Hazard. Mater.* **2005**, *125*, 166–174. [[CrossRef](#)]
19. Flotron, V.; Delteil, C.; Padellec, Y.; Camel, V. Removal of sorbed polycyclic aromatic hydrocarbons from soil, sludge and sediment samples using the Fenton's reagent process. *Chemosphere* **2005**, *59*, 1427–1437. [[CrossRef](#)]
20. Naidoo, T.; Goordiyal, K.; Glassom, D. Are nitric acid (HNO₃) digestions efficient in isolating microplastics from juvenile fish? *Water, Air, Soil Pollut.* **2017**, *228*, 1–11. [[CrossRef](#)]
21. Claessens, M.; Van Cauwenberghe, L.; Vandegehuchte, M.B.; Janssen, C.R. New techniques for the detection of microplastics in sediments and field collected organisms. *Mar. Pollut. Bull.* **2013**, *70*, 227–233. [[CrossRef](#)]
22. Dehaut, A.; Cassone, A.-L.; Frère, L.; Hermabessiere, L.; Himber, C.; Rinnert, E.; Rivièrè, G.; Lambert, C.; Soudant, P.; Huvet, A.; et al. Microplastics in seafood: Benchmark protocol for their extraction and characterization. *Environ. Pollut.* **2016**, *215*, 223–233. [[CrossRef](#)]
23. Rocha-Santos, T.; Duarte, A.C. A critical overview of the analytical approaches to the occurrence, the fate and the behavior of microplastics in the environment. *TrAC Trends Anal. Chem.* **2015**, *65*, 47–53. [[CrossRef](#)]
24. Qiu, Q.; Tan, Z.; Wang, J.; Peng, J.; Li, M.; Zhan, Z. Extraction, enumeration and identification methods for monitoring microplastics in the environment. *Estuar. Coast. Shelf Sci.* **2016**, *176*, 102–109. [[CrossRef](#)]
25. Catarino, A.I.; Thompson, R.; Sanderson, W.; Henry, T.B. Development and optimization of a standard method for extraction of microplastics in mussels by enzyme digestion of soft tissues. *Environ. Toxicol. Chem.* **2017**, *36*, 947–951. [[CrossRef](#)] [[PubMed](#)]
26. Munno, K.; Helm, P.A.; Jackson, D.A.; Rochman, C.; Sims, A. Impacts of temperature and selected chemical digestion methods on microplastic particles. *Environ. Toxicol. Chem.* **2018**, *37*, 91–98. [[CrossRef](#)] [[PubMed](#)]
27. Cole, M.; Webb, H.; Lindeque, P.K.; Fileman, E.S.; Halsband, C.; Galloway, T.S. Isolation of microplastics in biota-rich seawater samples and marine organisms. *Sci. Rep.* **2014**, *4*, 1–8. [[CrossRef](#)] [[PubMed](#)]
28. Foekema, E.M.; De Gruijter, C.; Mergia, M.T.; Van Franeker, J.A.; Murk, A.J.; Koelmans, A.A. Plastic in north sea fish. *Environ. Sci. Technol.* **2013**, *47*, 8818–8824. [[CrossRef](#)]
29. Herrera, A.; Garrido-Amador, P.; Martínez, I.; Samper, M.D.; López-Martínez, J.; Gómez, M.; Packard, T.T. Novel methodology to isolate microplastics from vegetal-rich samples. *Mar. Pollut. Bull.* **2018**, *129*, 61–69. [[CrossRef](#)]
30. Mintenig, S.M.; Int-Veen, I.; Löder, M.G.J.; Primpke, S.; Gerdt, G. Identification of microplastic in effluents of waste water treatment plants using focal plane array-based micro-fourier-transform infrared imaging. *Water Res.* **2017**, *108*, 365–372. [[CrossRef](#)]
31. Zhao, S.; Zhu, L.; Li, D. Microplastic in three urban estuaries, China. *Environ. Pollut.* **2015**, *206* (Suppl. C), 597–604. [[CrossRef](#)]
32. Gewert, B.; Ogonowski, M.; Barth, A.; MacLeod, M. Abundance and composition of near surface microplastics and plastic debris in the stockholm archipelago, Baltic Sea. *Mar. Pollut. Bull.* **2017**, *120*, 292–302. [[CrossRef](#)]
33. Van Cauwenberghe, L.; Vanreusel, A.; Mees, J.; Janssen, C.R. Microplastic pollution in deep-sea sediments. *Environ. Pollut.* **2013**, *182* (Suppl. C), 495–499. [[CrossRef](#)]

34. Renner, G.; Schmidt, T.C.; Schram, J. Characterization and quantification of microplastics by infrared spectroscopy. *Compr. Anal. Chem.* **2017**, *75*, 67–118. [[CrossRef](#)]
35. Imhof, H.K.; Ivleva, N.P.; Schmid, J.; Niessner, R.; Laforsch, C. Contamination of beach sediments of a subalpine lake with microplastic particles. *Curr. Biol.* **2013**, *23*, R867–R868. [[CrossRef](#)] [[PubMed](#)]
36. Carr, S.A.; Liu, J.; Tesoro, A.G. Transport and fate of microplastic particles in wastewater treatment plants. *Water Res.* **2016**, *91*, 174–182. [[CrossRef](#)] [[PubMed](#)]
37. Cabernard, L.; Durisch-Kaiser, E.; Vogel, J.C.; Rensch, D.; Niederhauser, P.; Gewässerschutz, A.W.E.L. *Mikroplastik in Abwasser Und Gewässern*; Aqua & Gas N°7/8: Zurich, Switzerland, 2016.
38. Aramyan, S.M. Advances in fenton and fenton based oxidation processes for industrial effluent contaminants Control-A review. *Int. J. Environ. Sci. Nat. Resour.* **2017**, *2*, 1–18. [[CrossRef](#)]
39. ISO—ISO 13320:2009—Particle Size Analysis—Laser Diffraction Methods; International Organization for Standardization: Geneva, Switzerland, 2009.
40. Ochiai, N.; Sasamoto, K.; Kanda, H.; Yamagami, T.; David, F.; Tienpont, B.; Sandra, P. Optimization of a multi-residue screening method for the determination of 85 pesticides in selected food matrices by stir bar sorptive extraction and thermal desorption GC-MS. *J. Sep. Sci.* **2005**, *28*, 1083–1092. [[CrossRef](#)]
41. DIN 38409-1—1987-01, German Standard Methods for the Examination of Water, Waste Water and Sludge; Parameters Characterizing Effects and Substances (Group H); Determination of Total Dry Residue, Filtrate Dry Residue and Residue on Ignition (H 1); German Institute for Standardisation: Berlin, Germany, 1987.
42. Kühn, S.; van Werven, B.; van Oyen, A.; Meijboom, A.; Bravo Rebolledo, E.L.; van Franeker, J.A. The use of potassium hydroxide (KOH) solution as a suitable approach to isolate plastics ingested by marine organisms. *Mar. Pollut. Bull.* **2017**, *115*, 86–90. [[CrossRef](#)]
43. Lunt, J. Large-Scale production, properties and commercial applications of poly lactic acid polymers. *Polym. Degrad. Stab.* **1998**, *59*, 145–152. [[CrossRef](#)]
44. Zhang, H.; Rankin, A.; Ward, I.M. Determination of the end-group concentration and molecular weight of poly (Ethylene Naphthalene-2,6-Dicarboxylate) using infra-red spectroscopy. *Polymer (Guildf)* **1996**, *37*, 1079–1085. [[CrossRef](#)]
45. Myungwan, H. Chemical Depolymerization Of Pet Bottles Via Methanolysis And Hydrolysis Myungwan Han. In *Recycling of Polyethylene Terephthalate Bottles*; Sabu, T., Ajay, V.R., Krishnan, K., Abitha, V., Martin, G.T., Eds.; William Andrew Publishing: New York, NY, USA, 2018.
46. von der Esch, E.; Lanzinger, M.; Kohles, A.J.; Schwaferts, C.; Weisser, J.; Hofmann, T.; Glas, K.; Elsner, M.; Ivleva, N.P. Simple generation of suspensible secondary microplastic reference particles via ultrasound treatment. *Front. Chem.* **2020**, *8*, 169. [[CrossRef](#)]



© 2020 by the authors. Licensee MDPI, Basel, Switzerland. This article is an open access article distributed under the terms and conditions of the Creative Commons Attribution (CC BY) license (<http://creativecommons.org/licenses/by/4.0/>).

Appendix V

Modulation of PAH toxicity on the freshwater organism *G. roeseli* by microparticles

Environmental Pollution 2020, 260, 113999

This study explored the impact of plastic particles on the behavior of polycyclic aromatic hydrocarbons (PAHs) in the environment. It found that the presence of both plastic and natural particles reduced the acute toxicity of phenanthrene in *Gammarus roeseli*. The study showed no significant difference between plastic and natural particles in terms of their effects, suggesting that both types of particles similarly reduced the bioavailability of phenanthrene. This challenges the idea that microplastics enhance PAH toxicity.

Astrid Bartonitz designed, performed, evaluated the experiments and wrote the manuscript. Ihuoma N. Anyanwu, Juergen Geist, Hannes K. Imhof, Julia Reichel, Johanna Grassmann, Jörg E. Drewes and Sebastian Beggel reviewed the manuscript and contributed to the discussion.



Contents lists available at ScienceDirect

Environmental Pollution

journal homepage: www.elsevier.com/locate/envpol

Modulation of PAH toxicity on the freshwater organism *G. roeseli* by microparticles[☆]



Astrid Bartonitz^{a, *}, Ihuoma N. Anyanwu^b, Juergen Geist^a, Hannes K. Imhof^a,
Julia Reichel^c, Johanna Graßmann^c, Joerg E. Drewes^c, Sebastian Beggel^a

^a Aquatic Systems Biology Unit, School of Life Sciences Weihenstephan, Technical University of Munich, Mühlenweg 22, 85354, Freising Weihenstephan, Germany

^b Department of Biology/ Microbiology/ Biotechnology, Faculty of Science, Alex-Ekwueme Federal University Ndufu-Alike Ikwo, P.M.B 1010, Ebonyi State, Nigeria

^c Chair of Urban Water Systems Engineering, Department of Civil, Geo and Environmental Engineering, Technical University of Munich, Am Coulombwall 3, 85748, Garching, Germany

ARTICLE INFO

Article history:

Received 31 July 2019
Received in revised form
13 January 2020
Accepted 14 January 2020
Available online 21 January 2020

Keywords:

Phenanthrene
Gammarus
Toxicology
Microplastic
Bioavailability

ABSTRACT

Polycyclic aromatic hydrocarbons are widespread and environmentally persistent chemicals that readily bind to particles in air, soil and sediment. Plastic particles, which are also an ubiquitous global contamination problem, may thus modulate their environmental fate and ecotoxicity. First, the acute aqueous toxicity of phenanthrene in adult *Gammarus roeseli* was determined with a LC₅₀ of 471 µg/L after 24 h and 441 µg/L after 48 h. Second, considering lethal and sublethal endpoints, effects of phenanthrene concentration on *G. roeseli* were assessed in relation to the presence of anthropogenic and natural particles. The exposure of gammarids in presence of either particle type with phenanthrene resulted after 24 and 48 h in reduced effect size. Particle exposure alone did not result in any effects. The observed reduction of phenanthrene toxicity by polyamide contradicts the discussion of microplastics acting as a vector or synergistically. Especially, no difference in modulation by plastic particles and naturally occurring sediment particles was measured. These findings can most likely be explained by the similar adsorption of phenanthrene to both particle types resulting in reduced bioavailability.

© 2020 Elsevier Ltd. All rights reserved.

1. Introduction

Polycyclic aromatic hydrocarbons (PAH) are widespread and environmentally persistent chemicals of concern. Their sources and distribution are well understood and documented (Abdel-Shafy and Mansour, 2016; Baek et al., 1991; Lima et al., 2005; Rabodonirina et al., 2015). Small quantities of the PAHs can be of biological origin, but most enter the environment from anthropogenic sources (Menzie et al., 1992). The highest quantity of PAHs is emitted into the atmospheric environment, where further distribution to soil and water occurs. Because of their lipophilic characteristics, PAHs readily bind to particles in air, soils and sediments, and tend to be rarely found dissolved in water (Abdel-Shafy and Mansour, 2016; Baek et al., 1991; Srogi, 2007). PAHs are known to

cause potential adverse health effects for humans and animals (Abdel-Shafy and Mansour, 2016) and a wide range of toxicity-tests for various PAHs have been conducted (Barata Martí et al., 2005; Besse et al., 2013; McConkey et al., 1997). With respect to the lipophilic characteristics and known distribution of PAHs (Srogi, 2007), many of these studies focused on PAHs adsorbed to natural particles like sediment (Landrum et al., 1994; Lankadurai et al., 2011; Lotufo and Fleeger, 1997; Verrhiest et al., 2001). Thus, the effects of PAHs sorbed to sediment particles are well-known for many species. Due to the increasing occurrence in the environment, research has recently focused on the effects of chemicals associated with anthropogenic plastic particles (Kleinteich et al., 2018; Karami et al., 2016; Browne et al., 2013). Likewise to PAHs, plastic particles are ubiquitous in lake and stream ecosystems worldwide (Rezania et al., 2018; Sharma and Chatterjee, 2017; Strungaru et al., 2019). As reviewed by Dris et al., (2018), a median of 0.0026 particles/L surface water with a size of >50 µm was found in 63 rivers. In beach sediments, even 333 particles/kg dry weight in a size range between 0.5 and 5 mm were detectable. Water samples from

[☆] This paper has been recommended for acceptance by Maria Cristina Fossi.

* Corresponding author.

E-mail address: astrid.bartonitz@tum.de (A. Bartonitz).

anthropogenically influenced sites proved to be more burdened with microplastic in concentrations around 2.5 and 2.9 particles/L in China and 7.9 ± 7.3 microparticles/L in Germany compared to natural sites (Dris et al., 2018; Schmidt et al., 2018).

PAHs adsorb to and desorb from plastic (Alimi et al., 2017; Bakir et al., 2014a; Browne et al., 2013; Rios et al., 2010). Comparing the chemical properties, sorption capacity of microplastic seems to be slightly higher than for sediment, while adsorption kinetics of PAHs on microplastic or sediment can vary depending on many properties such as the chemicals hydrophobicity or sediment organic carbon content. Like for sediment, partitioning coefficient of the specific chemicals is one of the main drivers for sorption on microplastic and vice versa. However, the release of the chemicals from plastic particles seems to be faster (Wang and Wang, 2018). As a result, a discussion about possible synergistic effects of PAH and plastic particles evolved, specifically concerning the role of plastic particles to act as a vector (Alimi et al., 2017). Nowadays, nearly 80% of examined PE-microparticles from the north pacific central gyre were associated with PAHs (Rios et al., 2010). In samples from the Beijing river in the Feilaixia reservoir, all the microplastic particles found were associated with PAHs ranging from 282.4 ng/g for PP and 364.2 ng/g for PE (Tan et al., 2019). As many organisms ingest plastic particles (Cole et al., 2013; Cole and Galloway, 2015; Foley et al., 2018; van Cauwenberghe et al., 2015), a high potential for adverse effects exists evoked by transported chemicals due to the large surface of microparticles (Bakir et al., 2014a; Batel et al., 2016; Browne et al., 2013). However, modelling studies assume a negligible impact from plastic particles as vector, because of their insignificant small amount in the environment (Bakir et al., 2016; Koelmans et al., 2013). Yet, a tipping point may be reached at which the role of plastic in sorption, cleaning and transport of chemicals can become important (Koelmans et al., 2016) depending on the plastics' characteristics (Lee et al., 2018; Sun et al., 2019; Wang and Wang, 2018).

Studies simultaneous investigating the chemicals toxicity in the presence of anthropogenic particles, like microplastic, and natural particles are rare (Alimi et al., 2017). The studies investigating the effect of chemical-pollution-combined particles mainly addressed one aspect, e.g. toxicity of one chemical-associated-particle (sediment: Landrum et al., 1994; Lotufo and Fleeger, 1997, microplastic: Browne et al., 2013; Kleinteich et al., 2018). The comparison of the PAH-toxicity when dissolved or sorbed to different particle types remains largely unattended (Alimi et al., 2017). Due to the sorption characteristics of microplastic (described by Wang and Wang, 2018) and the previous studies with contaminant-associated particles, the combined effect of PAH and microplastic particles in the same compartment has to be tested and compared with natural microparticles. Therefore, the main goal of the present study was to compare the modulation of sublethal PAH-effects on gammarids by the presence of anthropogenic and natural microparticles. A preceding acute toxicity test for exposure of phenanthrene through water was performed to determine the LC_{50} via this exposure route and to determine the concentration range for sublethal toxicity measurements. On the assumption that sublethal endpoints are more sensitive and an earlier response than lethality (Maltby et al., 2002), *G. roeseli* were exposed to a range of sublethal phenanthrene concentrations with and without combination of polyamide (PA) or sediment microparticles (SP). These tests were intended to show the change in effect strength of phenanthrene to the gammarids by the presence of natural and anthropogenic microparticles. The measured endpoints were mortality, swimming behavior and feeding.

2. Materials and methods

2.1. Sampling and acclimatization of test organisms

Because of its environmental relevance, *G. roeseli* was chosen as test species. They have a widespread distribution, form a majority of biomass in stream ecosystems and play an important role in the food web (Gerhardt et al., 2011; Kelly et al., 2002). Furthermore, a high sensitivity towards a wide range of pollutants has been reported (Brock and van Wijngaarden, 2012; Hunting et al., 2016; Zhai et al., 2018). *G. roeseli* were collected from the river Moosach in Freising, Germany ($48^{\circ}23'38.8''N$ $11^{\circ}43'26.1''E$) between May and June 2018 and size selected (9.6 ± 1 mm, $n = 50$) by sieve passage. Acclimatization occurred in a climate chamber with constant temperature of $13^{\circ}C \pm 0.5^{\circ}C$ and a 16:8 h light:dark cycle. First, individuals were kept in aerated aquaria filled with a mix of 50% bank filtrate from the river Moosach and 50% artificial water (ISO 6341 2012) for at least three days. During this part of the acclimatization period, gammarids were fed *ad libitum* with modified DECOTABs (Kampfraath et al., 2012). 10% of cellulose was replaced with ground Tetraphyll (Tetra GmbH, Germany), which was added as a supplementary food source (DECOTAB size 1 cm \emptyset , 0.5 cm high, dry weight 30.8 ± 3.0 mg ($n = 150$)). The subsequent acclimatization phase in 100% artificial water (ISO 6341 2012) started three days before the test. Gammarids were not fed during this step (US EPA, 2016). Mortality during acclimatization did not exceed 5%.

2.2. Test substances

Phenanthrene was chosen as a standard model PAH. It is one of the smallest PAHs with three benzene rings and a known low toxicity to humans compared to other PAHs (GESTIS Substance Database, 2019; Samanta et al., 2002). Due to its well-described chemical and toxicological characteristics (Verbruggen and van Herwijnen, 2012) it is often used as standard PAH (Barata Martí et al., 2005; Verrhiest et al., 2001; Zhang et al., 1997). Water solubility is 1.15 mg/L at $25^{\circ}C$, so stock solution was made with methanol (99.8%). The $Log K_{ow}$ is 4.52 (safety data sheet, IFA substance data base) and K_{oc} is around $2.97 \cdot 10^4$ ml/g (Zhang et al., 2009). Phenanthrene for toxicity testing (Phe, CAS: 85-01-8) and phenanthrene-d10 (CAS: 1517-22-2) for chemical analysis was purchased from Sigma-Aldrich (Germany), and stored at $8^{\circ}C$. Methanol for chemical analysis of phenanthrene concentration in the artificial medium was purchased from VWR chemicals (Germany). Polyamide (PA), which has a high market share (Scheibitz and Spies, 2016), was used as an exemplary anthropogenic particle, while sediment particles from the river Moosach were used as natural reference particles. Granulates of PA were purchased from Lanxess (Cologne, Germany) as "Durethan C38F" (ISO 16396-PA 6/66, E, S14-020). The microparticles were generated by centrifugal milling the PA granulates and sieving (Ultra Centrifugal Mill Type ZM 200, Retsch, Germany). Particles were 40–63 μm in size, had a fragmental shape and were stored at room temperature (Fig. S1 B). With respect to Hartmann et al. (2015), stock solutions were prepared in 10 ml methanol, resulting in a concentration of 2.5 mg/ml for each stock solution. PA is stable in 100% methanol according to Bürkle GmbH (2011). Sediment microparticles (SP) were obtained from wet-sieved and dried fine sediment samples from the river Moosach in Freising, Germany. Particles were 45–63 μm in size, had a fragmental shape and were stored at room temperature (Fig. S1 A). A gravimetric measurement with Element Analyser EA 4000 (Analytik Jena) revealed total organic carbon of 1.64% (balancing method), limit of determination was 0.1%.

2.3. Bioassay

Toxicity determination was conducted in a two-step approach. As the main goal was to determine microparticle-induced changes in sublethal effects, an acute toxicity assay for phenanthrene was performed first to determine lethal thresholds for adult *G. roeseli*. Then, the main toxicity assay with sublethal concentrations was performed, based on the results from acute toxicity assay. Sublethal toxicity of Phe alone was compared with presence of polyamide (PA) or sediment microparticles (SP) and microparticles alone as described below.

The validity criteria and test conditions of all bioassays followed the Gammarid Amphipod Acute Toxicity Test (US EPA, 2016) with minor modifications in feeding protocol and test medium. Assays were conducted in 1 L appropriate aerated artificial water (ISO 6341 2012) in glass beakers under same conditions as acclimatization. Each beaker contained three glass stones as hiding places to reduce stress for the gammarids.

While gently mixing the stock suspension/solution to ensure a homogenous dispersion, Phe, PA and SP concentrations were pipetted directly into the medium. Following, five individuals were transferred into each prepared beaker and fed *ad libitum* with one modified DECOTAB. The parameters of the static assays were measured at the end of each treatment after 24 and 48 h with portable pH meter MultiLine® Multi 3630 IDS SET G (WTW, Ger-

many). The exposure concentration was intentionally not maintained stable during the exposure period to show the reduction due to the adsorption behavior of the chemical, which is also a more environmentally realistic scenario.

$$\text{Feeding rate} = \frac{\text{DECOTAB standard dry weight [g]} - \text{DECOTAB leftover dry weight [g]}}{\text{living gammarids} * \text{test duration [d]}} \quad (1)$$

many). The exposure concentration was intentionally not maintained stable during the exposure period to show the reduction due to the adsorption behavior of the chemical, which is also a more environmentally realistic scenario.

2.3.1. Acute toxicity

Acute toxicity of phenanthrene was determined with a control, solvent control (methanol, 1 ml/L) and five concentrations of phenanthrene (nominal concentrations: 5, 50, 500, 1,000, 1500 µg/L, n = 3). Mortality was recorded after 24, 48, 72 and 90 h in the corresponding three replicates, which were then removed from the test. Therefore, the other treatments were not disturbed or stressed. Individual gammarids were classified as dead when they were not moving (including movement of legs), unben or/and body color changed from white/grey to orange.

2.3.2. Sublethal toxicity

In order to determine the modulation of the sublethal phenanthrene toxicity in presence or absence of different microparticles, *G. roeseli* were exposed to eight sublethal exposure concentrations of phenanthrene in three exposure scenarios over 24 and 48 h: (1) phenanthrene alone (Phe), (2) phenanthrene and PA microparticles (Phe + PA), and (3) phenanthrene and natural microparticles (Phe + SP) in the water column. Nominal concentrations from 50 to 500 µg/L were chosen for the sublethal toxicity experiment in order to cover a range with expected sublethal effect concentrations. The nominal phenanthrene concentrations were: 50, 75, 100, 250, 315, 375, 435, and 500 µg/L. In consequence of the chemical analysis (2.4), the nominal concentrations were replaced by measured concentrations (Table 1) throughout the analyses and illustrations. Both, the sediment and PA microparticles were added at a

2.3.2.1. Feeding rate

For feeding rate determination, DECOTAB leftovers were removed with a spoon at the end of the experiment (24 and 48 h) and transferred to small pre-dried aluminum dishes. The leftovers were dried for one day in a drying cabinet at 45 °C and then weighed with a Sartorius R200D Analytical Balance (Sartorius GmbH, Germany, 0.01 ± 0.02 mg). For the standard DECOTAB-weight, 150 freshly made DECOTABS were also dried for one day and weighed (30.8 ± 3.0 mg). To calculate feeding rate, leftover dry weight was subtracted from the standard DECOTAB dry weight. Estimated loss of weight was divided by the amount of living gammarids at the end of the exposure and calculated per day.

2.3.2.2. Swimming behavior

A camera-based automated tracking system with the software Ethovision XT 9 (Noldus, Germany) was used for the measurement of velocity. Recording time was 10 min with a sample rate of 25 frames per second. The measurement setup was made of three cameras positioned 30 cm above 15 arenas. The five organisms of each beaker were transferred to five glass petri dishes (Ø 5.5 cm) filled with 10 ml of treatment water and placed under the camera in programmed arena position to ascertain individual swimming behavior. To avoid interfering influences of moving light or shadows a cardboard box was pulled over and a lightboard (M.Way, China) was placed under the setup. A ruler of 10 cm served as scale calibration standard in the videos. After automated tracking of *G. roeseli*, videos were manually checked for false detections and corrected if reasonable.

2.4. Chemical analysis

2.4.1. Instrumentation

Stir bars (Gerstel Twister®) coated with polydimethylsiloxane (PDMS, film thickness 0.5 mm, length 10 mm) were purchased from Gerstel GmbH & Co. KG (Germany). For incubation, 20 mL Head-space vials (Agilent, USA) with Sil/PTFE coated septa (Thermo Fisher, USA) were used. The Twisters were stirred on a multiple position magnetic stirrer (15 positions) from Thermo Fisher (USA). The thermal extraction/desorption-gas chromatography/mass spectrometry (TD-GC/MS) analysis was performed using a Gerstel

4

A. Bartonitz et al. / Environmental Pollution 260 (2020) 113999

Table 1

Nominal and measured concentration of phenanthrene only and with microparticles after 0 and 48 h. * Label for samples not centrifuged, the other samples were centrifuged to remove microparticles. LOD for Phe was 2.5×10^{-3} µg/L.

Treatment	Nominal concentration	Measured concentration	
	[µg/L]	0 h	48 h
		[µg/L] ± SD	[µg/L] ± SD
Control	< LOD	< LOD	< LOD
Solvent control	< LOD	< LOD	< LOD
SP control	< LOD	< LOD	< LOD
PA control	< LOD	< LOD	< LOD
Phe A	50	92.1 ± 0.1 *	19.9 ± 1.4 *
Phe B	75	78.9 ± 8.1 *	16.3 ± 0.5 *
Phe C	100	115.3 ± 2.2 *	21.1 ± 0.3 *
Phe D	250	329.3 ± 22.1 *	52.8 ± 10.6 *
Phe E	500	601.3 ± 42.8 *	141.8 ± 6.5 *
PA + Phe A	50	0.3 ± 0.4	0.0 ± 0.0
PA + Phe B	75	7.9 ± 5.9	2.2 ± 0.0
PA + Phe C	100	25.1 ± 3.3	4.6 ± 0.2
PA + Phe D	250	131.1 ± 3.4	28.3 ± 2.4
PA + Phe E	500	209.4 ± 5.3	34.1 ± 1
SP + Phe A	50	10.8 ± 0.3	0.9 ± 0.1
SP + Phe B	75	33.0 ± 0.6	1.5 ± 0.1
SP + Phe C	100	24.5 ± 0.6	4.3 ± 0.6
SP + Phe D	250	138.7 ± 3.4	27.0 ± 0.6
SP + Phe E	500	325.2 ± 10.1	24.4 ± 0.2

ThermalDesorptionUnit (TDU) 2 equipped with a Gerstel Multi-PurposeSampler (MPS) robotic ^{PIV}, a Cooled Injections System (CIS 4) with C506 and an Agilent 7890B gas chromatograph equipped with an DB-5MS (Agilent) column combined with an Agilent 5977B MSD mass spectrometer.

2.4.2. Sample preparation and incubation

Standard solutions of phenanthrene and phenanthrene-d10 were dissolved in methanol. To obtain a calibration curve, the standard solutions were diluted in artificial water (ISO 6341 2012), adding 0.01 mg/L phenanthrene-d10 as an internal standard to a final volume of 10 ml. Samples containing sediment and microplastic particles were centrifuged before analysis. Water samples and 0.01 mg/L phenanthrene-d10 were diluted to a final volume of 10 ml in 20 ml headspace vials together with one stir bar and stirred at 24 °C, 1000 rpm for 60 min. The stir bar was removed, washed with LC/MS water, and dried with a lint-free tissue. Subsequently the stir bar was transferred into the thermodesorption tube. The limit of detection (LOD) for phenanthrene was 2.5×10^{-3} µg/L.

2.4.3. Chemical analysis

The concentration of phenanthrene was determined with stir bar sorptive extraction via TD-GC/MS. All measurements were conducted in triplicate. The TDU method was adopted from [Ochiai et al. \(2005\)](#). The TDU was set at an initial temperature of 20 °C (delay time 0.30 min; initial time 1 min) and a following ramp at 50 °C/min to an end temperature of 280 °C, hold time 1 min. The desorbed compounds were cryo-focused at -100 °C. Transfer from the stir bar to the cold trap was done in split-less mode. The CIS was programmed from -100 °C to 280 °C (held for 5 min) at 10 °C/s. Injection was done in a 1:100 split mode and the GC oven temperature gradient was as follows: 70 °C (2 min)/25 °C/min → 150 °C/3 °C/min → 200 °C/8 °C/min → 300 °C. Helium was used as carrier gas. The mass spectrometer was operated in the full scan mode (m/z range 40–550) with electron impact ionization (70V). Calibration concentrations were 50 µg/L to 0.05 µg/L.

2.5. Statistical analyses

Statistical analyses were conducted with RStudio ([RStudio, 2015](#)). Data were tested for normality using the Shapiro-Wilk test

and homogeneity of variance with the Levene's Test. Due to low replicate number, non-normality and heterogeneity of variance, mortality was tested with exact Fisher-test (EF) for significance of deviation between the treatments to estimate whether the observed mortality is independent of the treatment and/or the microparticles. When EF showed a significant p-value (<0.05) pairwise Wilcoxon test with Benjamini-Hochberg correction (pW-BH, [Benjamini et al., 1998](#)) was used as post hoc test to identify those treatments significantly different to the control. After this, log-logistic regression (LL2.5, LL3, LL4 and LL5) was conducted to identify the best model fit. The models were compared with Likelihood Ratio-Test (LRT) and Akaike-Information-criterion (AIC). For swimming behavior, influence of beaker was tested first with ANOVA. For this, the model 'y = β₀₀ + β₁ * Treatment * beaker' was chosen because of assumed interaction of beaker and phenanthrene concentration. Since the model resulted in normal distribution and homogeneity of variance, ANOVA could be used. ANOVA showed just in one case out of five significant influence from beaker on the effect, which lead to the further exclusion of beaker effects. Due to resulting non-normality and heterogeneity, Kruskal-Wallis-test (KW) was conducted to test differences between the three exposure scenarios, followed by pairwise Wilcoxon test (pW). One-way ANOVA by Welch (AW) was used to test significant difference between the treatments. As post-hoc test pW-BH was used. Furthermore, linear regression was used to fit a model between concentration and velocity. Feeding rate was analysed with KW to test for differences between the three exposure scenarios. Additionally, AW was used to test for significant differences in the exposure scenarios, followed by the post-hoc test pW-BH. Furthermore, linear regression was used to fit a model between concentration and feeding rate. Data from GC/MS were acquired with MassHunter Workstation Software (Ver.B.08.000 from Agilent Technologies). Ion chromatograms were extracted for m/z 178.2 for phenanthrene and 188.2 for phenanthrene-d10. Integration was conducted automatically, and software supported. Data analysis was conducted with Microsoft Excel 2016.

3. Results

3.1. Water chemistry

Physicochemical parameters in medium measured at start and

termination of the exposure period were within the acceptable range for the test organism for all experiments and treatments (US EPA, 2016). The measured mean values (\pm standard deviation) were: Temperature 12.7 ± 0.6 °C; oxygen $101\% \pm 1.5\%$; pH 7.6 ± 0.2 , and conductivity 677 ± 13 μ S/cm.

3.2. Acute toxicity

The preceding test for acute toxicity was based on nominal test concentrations and revealed an increasing mortality with increasing phenanthrene concentration at all four timepoints (24, 48, 72 and 90 h). Phenanthrene revealed very similar effect responses, with low mortality at 5 (<10%) and 50 μ g/L (7% and 13%), followed by a strong increase to more than 60% up to nearly 100% in the concentrations 500, 1000 and 1500 μ g/L. LC₅₀ was reached at a nominal phenanthrene concentration of 471.9 μ g/L for 24 h, 441.1 μ g/L for 48 h, 125.9 μ g/L for 72 h and 83.6 μ g/L for 90 h (Fig. S2 and Table S1).

3.3. Chemical analysis

The chemical analysis of the water samples from the sublethal toxicity assay indicated a discrepancy between predicted nominal and measured concentrations at the beginning of the experiment, with around 20% more phenanthrene in the treatment with Phe (Table 1). Phenanthrene concentration in all control treatments was below limit of detection ($2.5 \cdot 10^{-3}$ μ g/L). Exposure scenarios of Phe with microparticles showed a reduction of phenanthrene in the water column by 60% in the highest concentrations and 99% in the lowest concentrations compared to the Phe in samples from the start of the test. Compared to exposure scenario with Phe, concentration was constantly (0 and 48 h) more than 50% lower (mean $24\% \pm 18\%$) with microparticles in the water column. Phenanthrene concentration reduction was similar in plastic and sediment particle treatments. After 48 h, the measured concentration of phenanthrene revealed a decrease down to around $20\% \pm 3\%$ of the measured initial concentrations in the Phe exposures and $17\% \pm 10\%$ (Phe + PA) and $11\% \pm 7\%$ (Phe + SP) of initial concentrations with microparticles.

3.4. Sublethal toxicity

Based on the LC₅₀ of the preceding acute toxicity test, nominal concentrations with maximum 500 μ g/L were chosen for the subsequent sublethal toxicity assay. Whole analysis was conducted with the measured concentrations of Phe after 0 h (Table 1).

3.4.1. Mortality

Phe exposure to expected sublethal concentrations resulted in a low mortality of *G. roeseli* not exceeding 20%, except for a phenanthrene concentration of 601 μ g/L after 48 h (84%, pW, $p = 0.01$). Exposure scenarios with microparticles alone did not result in any significant differences in mortality of *G. roeseli* (pW, $p > 0.7$) irrespective of microparticle species (PA or SP) and exposure time (24 h and 48 h, Fig. 1). The mortality of *G. roeseli* exposed to Phe with additional microparticles (Phe + PA and Phe + SP) did not significantly differ neither to the Phe exposure nor among each other (EF, $p > 0.2$). The combined exposure resulted in lowered mortalities < 20% after 24 h (EF, $p > 0.1$). Only after 48 h at the highest concentration a significantly increased mortality occurred (Phe + SP, 36%, pW, $p < 0.05$). Though, models show clearly lower courses in mortality with microparticles added, especially for 48 h.

3.4.2. Feeding rate

Feeding rate was independent from microparticle exposure

scenario, i.e. neither Phe nor the combination with SP or PA after 24 and 48 h influenced the gammarids' feeding (KW, $\chi^2 = 0.72$ for 24 h/0.68 for 48 h, $df = 2$, $p > 0.5$). Control feeding rates varied from 0.88 to 1.40 mg/gammarid*day within 24 h and 0.65–1.15 mg/gammarid*day within 48 h. Also, feeding rates within the treatments varied randomly (Fig. S3). In Phe exposures, there was no change in feeding rate with increasing phenanthrene concentration compared to the controls (AW, F(6,11.12) 24 h, F(6,12.13) 48 h, $p > 0.5$). Variation of feeding rates occurred only for Gammarids exposed to Phe + SP after 24 h (AW, F(7, 13.15), $p < 0.001$) at concentrations 80, 92 with higher feeding rate and 329 μ g/L with lower feeding rate (pW, $p < 0.05$) and after 48 h at the highest concentration resulting in lower feeding rate (pW, $p = 0.28$).

3.4.3. Swimming behavior

Swimming behavior did not change after exposure to microparticles compared to controls and was on average 1.5 ± 0.7 cm/s and 1.8 ± 0.7 cm/s after 24 and 48 h (pW, $p > 0.5$ (PA) and $p > 0.4$ (SP)). Effect of phenanthrene on velocity after 24 and 48 h was significantly different in the presence of microparticles (KW, $\chi^2 = 59.8$ (24 h)/35.0 (48 h), $df = 2$, $p < 0.001$). Swimming velocity during exposure with Phe was lower than in exposures with Phe and microparticles (pW, $p < 0.001$) after 24 and 48 h. Phe with microparticle exposures (Phe + PA and Phe + SP) resulted in similar decreasing velocity (pW, $p = 0.77$ for 24 h, 0.93 for 48 h). Swimming velocity of *G. roeseli* decreased significantly with increasing phenanthrene concentration for the Phe exposure (Fig. 2, AW, F(6, 40.7/16.1), $p < 0.001$). At lowest concentration (80 μ g/L), Phe resulted in decreased velocity of 0.3 cm/s slower than the control after 24 h (pW, $p = 0.018$) and 0.6 cm/s slower after 48 h (pW, $p < 0.001$). Velocity reduction coincided with increasing concentration. At highest phenanthrene concentration, gammarids swam with a speed of 0.27 (24 h) and 0.35 cm/s (48 h), which equals a reduction by 0.84 and 1.16 cm/s from control to 601 μ g/L. The same negative trend occurred in exposures with Phe + PA (AW, F(7, 40.7/33.0), $p < 0.001$) and Phe + SP (AW, F(7, 78.3/14.3), $p < 0.001$). Although velocity was reduced even at lowest concentrations for both exposure scenarios and timepoints, significant difference was detected from 115 μ g/L for Phe + PA (pW, $p < 0.01$ for 24 and 48 h) and from 92 μ g/L for Phe + SP (pW, $p < 0.01$ for 24 and 48 h). Gammarids exposed for 24 h to phenanthrene and microparticle swam 0.21 (Phe + PA) and 0.17 (Phe + SP) cm/s at 601 μ g/L, which is slightly slower than in the Phe exposure, while exposure over 48 h resulted in a comparable or faster speed in highest concentration (0.33 (PA) and 0.48 (SP)). Velocity reduction followed a linear relationship (Fig. 2).

4. Discussion

Against the common hypothesis, the measured influence of microparticles on the ecotoxicity of phenanthrene was reducing, ruling out their role as vectors. Furthermore, the potential of plastic particles acting as a more effective sorbent and carrier than natural microparticles has been relativized for polyamide and phenanthrene, because they did not modulate effects different to naturally occurring inorganic sediment particles based on effects on gammarids. Instead, the presence of microparticles revealed a reduction of mortality as well as changes in sublethal endpoints such as swimming behavior. This impact can be explained by adsorption of phenanthrene to the microparticles, resulting in a reduced bioavailability of phenanthrene.

Acute toxicity determination revealed delayed rapid mortality due the baseline toxicity of the hydrophobic chemical (Mayer and Reichenberg, 2006). Phe exposure resulted in mortality of adult *G. roeseli* following a sigmoidal dose-response curve over the

6

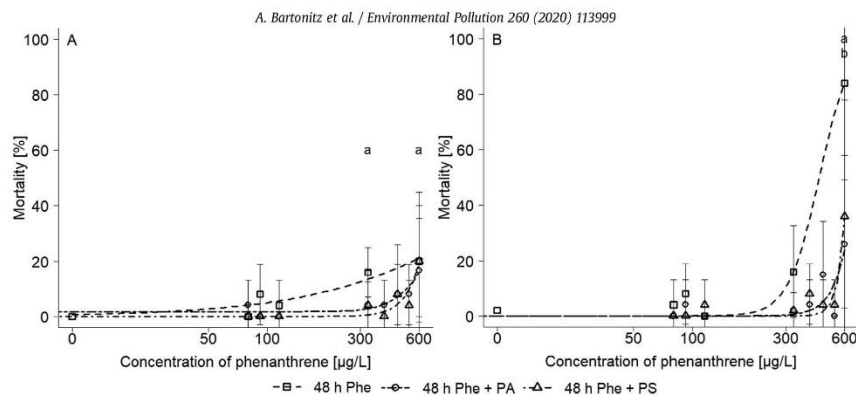


Fig. 1. Mean mortality of *G. roeseli* after 24 (A) and 48 h (B) exposure to phenanthrene alone (Phe) or in combination with PA or SP of 40–63 μm . Mortality was counted for dead (including eaten) gammarids and calculated per beaker ($n = 5$). Concentration range of phenanthrene (measured concentration 80–600 $\mu\text{g/L}$) was pre-selected from the acute toxicity test for sublethal effect concentrations. Dose-response-curves for exposure scenarios are shown by lines. Labels a (Phe), b (Phe + PA) and c (Phe + SP) mark significant differences to solvent control. Statistical information for regression are given in SI (Table S2). Error bars represent standard deviation.

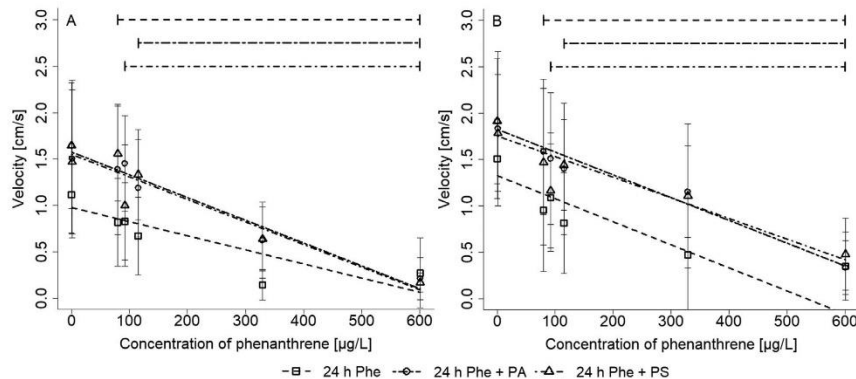


Fig. 2. Mean Velocity of *G. roeseli* after 24 (A) and 48 h (B) exposure to Phe and in combination with PA or SP. Error bars represent standard deviation. Linear regression for exposure scenarios are shown by lines. Horizontal Lines for Phe (dashed), Phe + PA (twodash) and Phe + SP (dotdash) mark significant differences to control. Velocity of individual *G. roeseli* was measured with Ethovision XT 9. Dead gammarids were excluded. Statistical information for regression are given in SI (Table S3).

course for 24, 48, 72 and 90 h. Acute toxicity thresholds (LC_{50}) of phenanthrene were 471.9 $\mu\text{g/L}$ after 24 h and 441.1 $\mu\text{g/L}$ after 48 h and further decreased over time. Thereby, *G. roeseli* was more sensitive to phenanthrene compared to other crustaceans like *Daphnia magna* (24 h LC_{50} : 678.4 $\mu\text{g/L}$ - 853.7 $\mu\text{g/L}$ (Verriest et al., 2001)) or copepods (*Oithona davisae*, 24 h LC_{50} at 440.2 $\mu\text{g/L}$ - 604.2 $\mu\text{g/L}$ (Barata Martí et al., 2005)). The sudden and strong increase in mortality after a steady low mortality can be explained by a critical concentration of the hydrophobic chemical that is reached in the lipid membranes (Mayer and Reichenberg, 2006; Mayer and Holmstrup, 2008). Phenanthrene might be tolerated by adult *G. roeseli* until a certain threshold is exceeded. Additionally, phenanthrene is hydrophobic with a $\log K_{OW}$ of 4.16–4.67 and most likely adsorbed to surrounding compartments such as food, particles or the organism (Teuten et al., 2007). As a consequence, there was after some time less phenanthrene available to the test organisms than at the beginning of the experiment, but at higher concentrations effective doses of phenanthrene remained. Also Lee et al. (2014) concluded a reduction of dissolved chemicals

concentration and bioavailability due to sorption kinetics for hydrophobic chemicals and microplastics, but with the condition of a sufficient microplastic concentration. According to Bakir et al. (2014a) the plastic particle - water equilibrium of phenanthrene and polyethylene or polyvinylchloride can be reached within 24 h at a temperature of 18 $^{\circ}\text{C}$. Therefore, this sorption is likely to happen in a relevant timescale. This is further supported by the measured phenanthrene concentrations in the sublethal toxicity experiment which were reduced remarkably after 48 h. It is thus likely that organisms not affected in the first hours of the exposure might not suffer from the bound phenanthrene in low concentrations but from remaining phenanthrene in higher concentrations.

The measurement of sublethal endpoints such as swimming behavior during the exposure of *G. roeseli* with sublethal phenanthrene concentrations proved to be highly sensitive, even at the lowest concentrations. The most important observation was the reducing toxic effect of both used microparticle types to phenanthrene, which follows a strong interaction of the contaminant with the present natural and anthropogenic microparticles. This effect is

most likely due to a reduced bioavailability of adsorbed phenanthrene. Concerning mortality and swimming behavior, another observation was that the degree of reduction was independent of added particle type. As supported by chemical analysis of the artificial water with and without particles, these outcomes can be explained by a fast and, most important, similar adsorption to both particle types. Also, with regard to the sublethal toxicity assay and as initially intended, mortality was very low in all exposure scenarios with phenanthrene (including cannibalism). Due to the low mortality, no change in mortality due to microparticles was observed. This is comparable to results of exposure with phenanthrene in combination with sediment on *Diporeia* spp., in which a low mortality around $12\% \pm 3\%$ at a phenanthrene concentration of $110.5 \mu\text{g/g}$ sediment was found (Landrum et al., 1994). Moreover, when exposed to sediment-associated phenanthrene (max. conc. 333 mg/kg) for ten days (Gust, 2006), *Hyalella azteca* also showed low mortality ($5\% \pm 8\%$). Therefore, focus in this assay was on the sublethal endpoints swimming behavior and feeding. The responses by sublethal endpoints are more sensitive compared to mortality and made an earlier detection of adverse effects possible. The exposure to polyamide and sediment particles in the used particle concentration without phenanthrene did not induce any adverse responses on the tested endpoints, as expected. Both, polyamide and sediment particles are very likely non-toxic, but it is possible that the potential toxicity of the plastic particles is not severe enough to be detected using these endpoints on the organism level. The molecular level could be a more sensitive level than organism level (Blarer and Burkhardt-Holm, 2016; Karami et al., 2016). Pplastic particle toxicity has been reported in other species exposed to a comparable size-class and concentration as used in this study. Karami et al. (2016) for instance reported damage on inner organs in *Clarias gariepinus* after exposure to $< 60 \mu\text{m}$ sized low-density polyethylene particles in concentrations of 50 and $500 \mu\text{g/L}$. Also Blarer and Burkhardt-Holm (2016) did not observe any impact on feeding rate and wet weight change, but in assimilation efficiency for *Gammarus fossarum* after application of polyamide fibres (2680 fibres/beaker) and polystyrene beads (12,500 beads/ml). This is in line with other studies not finding effects of plastic microparticles even at very high concentrations and relevant particle sizes according to endpoints from molecular to organism level (reviewed by Burns and Boxall, 2018). Consequently, it can be anticipated that there was no measurable effect from 40 to $63 \mu\text{m}$ sized polyamid microparticles as from sediments for *G. roeseli* at the tested concentration. Effect size of phenanthrene is lowered in the presence of particles due to adsorption to the particles. In this context, a strong influence of microparticles on phenanthrene-exposed gammarids' swimming velocity has been shown for 24 and 48 h. When exposed to phenanthrene and microparticles, gammarids swam in mean 0.5 cm/s faster than when exposed to Phe. Apart from this, feeding was not influenced by microparticles. Reduction of swimming velocity does not correspond with results reported by Ma et al. (2016) with *Daphnia magna* tested for 10 days with $0.05\text{--}1.2 \text{ mg/L}$ phenanthrene. They found no impact at a concentration of 500 mg/L particles ($10 \mu\text{m}$) on the phenanthrene-induced effect. Though, phenanthrene-loaded low-density polyethylene particles $< 60 \mu\text{m}$ resulted in higher molecular stress response than only phenanthrene exposure on catfish (Karami et al., 2016). The highly sensitive changes on the molecular level can thereby be seen as early warning signals, but cannot be interpreted regarding their adverse effects without a linkage to phenotypic consequences (Beggel et al., 2011; Beggel et al., 2012). Hence, rather than an undetected counteracting positive effect induced by the particles, because none was found in the particle control, this result indicates a decreasing bioavailability of phenanthrene due to adsorption to the

microparticles. Consequentially, as the chemical potential of phenanthrene is decreased when adsorbed to microparticles, the measured lowered effect is most likely caused by the remaining dissolved chemical or from the chemical in the food (Koelmans et al., 2016; Kwon et al., 2017).

Several studies dealt with the distribution of PAHs and found concentrations ranging from mg adsorbed to sediment and μg to ng dissolved in water (Kafilzadeh, 2015; Luo et al., 2008; Rabodonirina et al., 2015). Thus, the tendency of PAHs to adsorb to plastic has already been proven (Alimi et al., 2017; Bakir et al., 2014a; Wang and Wang, 2018) and sorption equilibrium of phenanthrene to polyethylene was within 24 h (Bakir et al., 2014a). This is also confirmed by the analytically determined concentrations of the phenanthrene test solutions in this study. The artificial medium clearly exhibited a fast decline of phenanthrene concentration within 48 h to 20% of initial concentration with phenanthrene only and a mere fraction with microparticles rapidly after test start. More studies with varying particle species and sizes need to be conducted to verify if the particle type is an important factor for sorption and resulting effect modulation. Nevertheless, as stated by Bakir et al. (2014a) and shown by Rochman et al. (2017) or Lee et al. (2014), it depends on both polymer and pollutant properties. Therefore, the chemical potential and toxic effect of a contaminant is modulated by the presence of microparticles in the aquatic environment and this possibly depends on the respective particles surface quality, internal diffusion and chemical properties.

An open question is whether a toxic phenanthrene concentration is also reached in the organism if the substance is transported by ingested phenanthrene-loaded particles to the organism. The study by Bakir et al. (2016) indicates to some degree that the ingestion of loaded plastic is a negligible additional pathway compared to chemical uptake from the surrounding compartment or food. Ingestion and egestion of particles via food in μm size by *G. roeseli* is very fast and nearly in equilibrium with 6 and 8 ± 5 particles per minute, while uptake from surrounding medium was lower (unpublished data). Tracking of fluorescent particles showed egestion rates within 24 h comparable to Straub et al. (2017). Whilst sorption equilibrium of phenanthrene to polyvinyl chloride and polyethylene is reached within 24 h, desorption is slower with 5 days to reach equilibrium in seawater again (Bakir et al., 2014b). Although desorption of phenanthrene is faster under simulated gut conditions (Bakir et al., 2014a), it is likely that egestion of phenanthrene-associated particles is too fast for phenanthrene to desorb in an appreciable amount or even reach equilibrium to cause significant effects (Mohamed Nor and Koelmans, 2019). Even the assumed faster desorption from microplastic (Wang and Wang, 2018) does not intervene. Additionally, uptake of particles via the water is very low compared to ingestion via food, which lowers the possibility of phenanthrene uptake with particles again. Even if the particles are ingested, the release of the hydrophobic contaminant is very unlikely, intensified by the plastics characteristics like size and intraparticle diffusion (Seidensticker et al., 2019). Due to minimal ingestion and slow desorption kinetics, it can be concluded that suspended particles are negligible carriers for sorbed chemicals compared to the surrounding compartment. The used amount of solved phenanthrene and suspended polyamide particles in medium was higher and that of sediment particles lower than the known concentrations in freshwater. Consequently, especially environmental concentrations of phenanthrene, around $3\text{--}45 \text{ ng/L}$ (Kafilzadeh, 2015; Luo et al., 2008), are most likely not leading to acute mortality or change in behavior of *Gammarus* spp. Partly, particle concentrations could represent a scenario where sediment and sand become a rare source and plastic particle concentration in environment rises as discussed by Koelmans et al. (2013) or Enders et al. (2015).

In view of environmental relevance, this study focused more on effect and modulation detection than environmental concentrations. Due to the aim of the study to see modulated effects, the higher concentrations were needed. Thus, with respect to their environmental occurrence, it seems that the impact of microplastic compared to natural microparticles is approximately equivalent. In cases like the observed, where the chemical adsorbs to microplastic and sediments to a similar extend, the higher bioavailability due to higher abundance of sediments makes sediment much more hazardous. There is an uneven higher probability for sediment to be ingested and release the chemical than for microplastic. Further, the adsorption and desorption of chemicals highly depends on the environmental parameters like abundance of organic matter (Seidensticker et al. 2017), pH or salinity (Wang et al., 2018). Also, after ingestion, the potential of the plastic particle to act as a vector and release the chemical highly depends on particle and chemical characteristics (Seidensticker et al., 2019). This indicates possible different behavior of the chemical in the environment than in static laboratory experiments and it has to be mentioned that the effects and modulation by microparticles could differ with the varying combinations. However, many recent model-based studies evaluated that the role of microplastic as a vector for anthropogenic pollutants not added to plastics is a common misconception (Mohamed Nor and Koelmans 2019; Koelmans et al., 2019). Nevertheless, it is necessary to examine a broad empirical area for chemical and (plastic) particle toxicity, as it is rising in the last years, to generate a stronger basis for risk assessment and regulation.

CRediT authorship contribution statement

Astrid Bartonitz: Conceptualization, Data curation, Formal analysis, Investigation, Methodology, Visualization, Writing - original draft, Writing - review & editing. **Ihuoma N. Anyanwu:** Conceptualization, Investigation, Methodology, Writing - review & editing. **Juergen Geist:** Conceptualization, Supervision, Resources, Writing - review & editing. **Hannes K. Imhof:** Conceptualization, Formal analysis, Supervision, Writing - review & editing. **Julia Reichel:** Methodology, Investigation, Writing - review & editing. **Johanna Graßmann:** Methodology, Supervision, Writing - review & editing. **Joerg E. Drewes:** Resources, Supervision, Writing - review & editing. **Sebastian Beggel:** Conceptualization, Formal analysis, Methodology, Supervision, Writing - review & editing.

Acknowledgement

This work was funded by the German Federal Ministry of Education and Research (BMBF) in the project Sub₄Track (grant number 02WPL1443A). Dr. Ihuoma Ngozi Anyanwu was funded by the joint program of the German Research Foundation and The World Academy of Sciences (grant number GE 2169/8-1 to JGe). We also want to thank Simone Kefer from the chair of food packaging technology, TUM, who produced PA microparticles and Gerrit Thomas, Karoline Kirschfink, and Kristina Bichler for practical assistance in the lab. AB, JGe, INA, HI, and SB conceived the study and its experimental design, INA, AB and SB conducted the laboratory assays, JR, JGr did the chemical analyses, AB, JGe, SB, HI and INA analyzed and interpreted the data; AB led the writing of the paper with JGe, HI and SB; JGe, INA and JD secured funding; all authors edited and approved the final version.

Appendix A. Supplementary data

Supplementary data to this article can be found online at <https://doi.org/10.1016/j.envpol.2020.113999>.

References

- Abdel-Shafy, H.I., Mansour, M.S.M., 2016. A review on polycyclic aromatic hydrocarbons: source, environmental impact, effect on human health and remediation. *Egypt J Pet* 25, 107–123. <https://doi.org/10.1016/j.ejpe.2015.03.011>.
- Ailimi, O., Farmer Budarz, J., Hernandez, L.M., Tufenkji, N., 2017. Microplastics and nanoplastics in aquatic environments: aggregation, deposition, and enhanced contaminant transport. *Environ. Technol.* <https://doi.org/10.1021/acs.est.7b05559>.
- Baek, S.O., Field, R.A., Goldstone, M.E., Kirk, P.W., Lester, J.N., Perry, R., 1991. A review of atmospheric polycyclic aromatic hydrocarbons: sources, fate and behavior. *Water, Air, Soil Pollut.* 60, 279–300. <https://doi.org/10.1007/BF00282628>.
- Bakir, A., Rowland, S.J., Thompson, R.C., 2014a. Enhanced desorption of persistent organic pollutants from microplastics under simulated physiological conditions. *EnvironPoll* 185, 16–23. <https://doi.org/10.1016/j.envpol.2013.10.007>. Barking, Essex : 1987.
- Bakir, A., Rowland, S.J., Thompson, R.C., 2014b. Transport of persistent organic pollutants by microplastics in estuarine conditions. *Estuar. Coast Shelf Sci.* 140, 14–21. <https://doi.org/10.1016/j.ecss.2014.01.004>.
- Bakir, A., O'Connor, I.A., Rowland, S.J., Hendriks, A.J., Thompson, R.C., 2016. Relative importance of microplastics as a pathway for the transfer of hydrophobic organic chemicals to marine life. *Environ poll* 219, 56–65. <https://doi.org/10.1016/j.envpol.2016.09.046>. Barking, Essex : 1987.
- Barata Marti, C., Calbet, A., Saiz, E., Ortiz, V.L., Bayona Termens, J.M., 2005. Predicting single and mixture toxicity of petrogenic polycyclic aromatic hydrocarbons (PAH) to the copepod *Oithona davisae*. Implications for environmental risk assessment of oil spills in the marine plankton food web. *Environ. Toxicol. Chem.* 24, 2992–2999. <https://doi.org/10.1897/05-189R.1>.
- Batel, A., Linti, F., Scherer, M., Erdinger, L., Braunbeck, T., 2016. Transfer of benzo(a)pyrene from microplastics to *Artemia nauplii* and further to zebrafish via a trophic food web experiment: CYP1A induction and visual tracking of persistent organic pollutants. *Environ. Toxicol. Chem.* 35, 1656–1666. <https://doi.org/10.1002/etc.3361>.
- Beggel, S., Connon, R., Werner, I., Geist, J., 2011. Changes in gene transcription and whole organism responses in larval fathead minnow (*Pimephales promelas*) following short-term exposure to the synthetic pyrethroid bifenthrin, 105. *Aquat Toxicol.* Amsterdam, Netherlands, pp. 180–188. <https://doi.org/10.1016/j.aquatox.2011.06.004>.
- Beggel, S., Werner, I., Connon, R.E., Geist, J.P., 2012. Impacts of the phenylpyrazole insecticide fipronil on larval fish: time-series gene transcription responses in fathead minnow (*Pimephales promelas*) following short-term exposure. *Sci. Total Environ.* 426, 160–165. <https://doi.org/10.1016/j.scitotenv.2012.04.005>.
- Benjamini, Y., Hochberg, Y., Stark, P.B., 1998. Confidence intervals with more power to determine the sign: two ends constrain the means. *J. Am. Stat. Assoc.* 93, 309–317. <https://doi.org/10.1080/01621459.1998.10474112>.
- Besse, J.-P., Coquery, M., Lopes, C., Chaumont, A., Budzinski, H., Labadie, P., Giffard, O., 2013. Caged *Gammarus fossarum* (Crustacea) as a robust tool for the characterization of bioavailable contamination levels in continental waters: towards the determination of threshold values. *Water Res.* 47, 650–660. <https://doi.org/10.1016/j.watres.2012.10.024>.
- Blarer, P., Burkhardt-Holm, P., 2016. Microplastics affect assimilation efficiency in the freshwater amphipod *Gammarus fossarum*. *EnvironSci Poll R Intl* 23, 23522–23532. <https://doi.org/10.1007/s11356-016-7584-2>.
- Brock, T.C.M., van Wijngaarden, R.P.A., 2012. Acute toxicity tests with *Daphnia magna*, *Americamysis bahia*, *Chironomus riparius* and *Gammarus pulex* and implications of new EU requirements for the aquatic effect assessment of insecticides. *EnvironSci Poll R Intl* 19, 3610–3618. <https://doi.org/10.1007/s11356-012-0930-0>.
- Browne, M.A., Niven, S.J., Galloway, T.S., Rowland, S.J., Thompson, R.C., 2013. Microplastic moves pollutants and additives to worms, reducing functions linked to health and biodiversity. *Curr. Biol. : CB (Curr. Biol.)* 23, 2388–2392. <https://doi.org/10.1016/j.cub.2013.10.012>.
- Bürkle GmbH, 2011. Chemische Beständigkeit von Kunststoffen. https://www.buerkle.de/files_pdf/wissenswertes/liste_chemische_bestaendigkeiten_de.pdf. (Accessed 18 February 2019).
- Burns, E.E., Boxall, A.B.A., 2018. Microplastics in the aquatic environment: evidence for or against adverse impacts and major knowledge gaps. *Environ. Toxicol. Chem.* 37, 2776–2796. <https://doi.org/10.1002/etc.4268>.
- Cole, M., Galloway, T.S., 2015. Ingestion of nanoplastics and microplastics by pacific oyster larvae. *EnvironSciTechnol* 49, 14625–14632. <https://doi.org/10.1021/acs.est.5b04099>.
- Cole, M., Lindeque, P., Fileman, E., Halsband, C., Goodhead, R., Moger, J., Galloway, T.S., 2013. Microplastic ingestion by zooplankton. *Environ SciTechnol* 47, 6646–6655. <https://doi.org/10.1021/es400663f>.
- Dris, R., Imhof, H.K., Löder, M.G.J., Gasperi, J., Laforsch, C., Tassin, B., 2018. Microplastic contamination in freshwater systems: methodological challenges, occurrence and sources: microplastics in rivers. In: Zeng, E.Y. (Ed.), *Microplastic Contamination in Aquatic Environments: an Emerging Matter of Environmental Urgency*. Elsevier, Amsterdam, Netherlands, pp. 51–93.
- Enders, K., Lenz, R., Stedmon, C.A., Nielsen, T.G., 2015. Abundance, size and polymer composition of marine microplastics $\geq 10\mu\text{m}$ in the Atlantic Ocean and their modelled vertical distribution. *Mar. Pollut. Bull.* 100, 70–81. <https://doi.org/10.1016/j.marpolbul.2015.09.027>.
- Foley, C.J., Feiner, Z.S., Malinich, T.D., Höök, T.O., 2018. A meta-analysis of the effects

- of exposure to microplastics on fish and aquatic invertebrates. *Sci. Total Environ.* 631–632, 550–559. <https://doi.org/10.1016/j.scitotenv.2018.03.046>.
- Gerhardt, A., Bloor, M., Mills, C.L., 2011. Gammarus: important taxon in freshwater and marine changing environments. *Int J Zool* 2011, 1–2. <https://doi.org/10.1155/2011/524276>.
- GESTIS Substance Database, 2019. Substance Datasheet Phenanthrene. [http://gestis-en.itrust.de/nxt/gateway.dll/gestis_en/022900.xml?f=templates&fn=default-doc.htm\\$3.0](http://gestis-en.itrust.de/nxt/gateway.dll/gestis_en/022900.xml?f=templates&fn=default-doc.htm$3.0). (Accessed 31 January 2019).
- Gust, K.A., 2006. Joint toxicity of cadmium and phenanthrene in the freshwater amphipod *Hyalella azteca*. *Arch. Environ. Contam. Toxicol.* 50, 7–13. <https://doi.org/10.1007/s00244-004-4163-1>.
- Hartmann, N.B., Jensen, K.A., Baun, A., Rasmussen, K., Rauscher, H., Tantra, R., Cupi, D., Gilliland, D., Pianella, F., Riego Sintes, J.M., 2015. Techniques and protocols for dispersing nanoparticle powders in aqueous media—Is there a rationale for harmonization? *J ToxEnvironHealth. Part B, Critical reviews* 18, 299–326. <https://doi.org/10.1080/10937404.2015.1074969>.
- Hunting, E.R., Vonk, J.A., Musters, C.J.M., Kraak, M.H.S., Vijver, M.G., 2016. Effects of agricultural practices on organic matter degradation in ditches. *Sci Rep-UK* 6, 21474. <https://doi.org/10.1038/srep21474>.
- ISO 6341, 2012. Water Quality – Determination of the Inhibition of the Mobility of *Daphnia magna* Straus (Cladocera, Crustacea) – Acute Toxicity Test. *Internat Organ Standard*.
- Kafilzadeh, F., 2015. Distribution and sources of polycyclic aromatic hydrocarbons in water and sediments of the Soltan Abad River, Iran. *Egypt J Aquat Res* 41, 227–231. <https://doi.org/10.1016/j.ejar.2015.06.004>.
- Kampfraath, A.A., Hunting, E.R., Mulder, C., Breure, A.M., Gessner, M.O., Kraak, M.H.S., Admiraal, W., 2012. DECOTAB: a multipurpose standard substrate to assess effects of litter quality on microbial decomposition and invertebrate consumption. *Freshw. Sci.* 31, 1156–1162. <https://doi.org/10.1899/12-075.1>.
- Karami, A., Romano, N., Galloway, T., Hamzah, H., 2016. Virgin microplastics cause toxicity and modulate the impacts of phenanthrene on biomarker responses in African catfish (*Clarias gariepinus*). *Environ. Res.* 151, 58–70. <https://doi.org/10.1016/j.envres.2016.07.024>.
- Kelly, D.W., Dick, J.T.A., Montgomery, W.L., 2002. The functional role of Gammarus (Crustacea, Amphipoda): shredders, predators, or both? *Hydrobiologia* 485, 199–203. <https://doi.org/10.1023/A:1021370405349>.
- Kleintjeck, J., Seidensticker, S., Marggrander, N., Zarfl, C., 2018. Microplastics reduce short-term effects of environmental contaminants. Part II: polyethylene particles decrease the effect of polycyclic aromatic hydrocarbons on microorganisms. *Int. J. Environ. Res. Public Health* 15. <https://doi.org/10.3390/ijerph15020287>.
- Koelmans, A.A., Besseling, E., Wegner, A., Foekema, E.M., 2013. Plastic as a carrier of POPs to aquatic organisms: a model analysis. *Environ Sci Technol* 47, 7812–7820. <https://doi.org/10.1021/es401169n>.
- Koelmans, A.A., Bakir, A., Burton, G.A., Janssen, C.R., 2016. Microplastic as a vector for chemicals in the aquatic environment: critical review and model-supported reinterpretation of empirical studies. *Environ. Sci. Technol.* 50, 3315–3326. <https://doi.org/10.1021/acs.est.5b06069>.
- Koelmans, A.A., Mohamed Nor, N.H., Hermens, E., Kooi, M., Mintenig, S.M., France, J. de, 2019. Microplastics in freshwaters and drinking water: critical review and assessment of data quality. *Water Res.* 155, 410–422. <https://doi.org/10.1016/j.watres.2019.02.054>.
- Kwon, J.-H., Chang, S., Hong, S.H., Shim, W.J., 2017. Microplastics as a vector of hydrophobic contaminants: importance of hydrophobic additives. *Integr. Environ. Assess. Manag.* 13, 494–499. <https://doi.org/10.1002/ieam.1906>.
- Landrum, P.F., Dupuis, W.S., Kukkonen, J., 1994. Toxicokinetics and toxicity of sediment-associated pyrene and phenanthrene in *Diporeia* spp.: examination of equilibrium-partitioning theory and residue-based effects for assessing hazard. *Environ. Toxicol. Chem.* 13, 1769–1780.
- Lankadurai, B.P., Wolfe, D.M., Simpson, A.J., Simpson, M.J., 2011. ¹H NMR-based metabolomic observation of a two-phased toxic mode of action in *Eisenia fetida* after sub-lethal phenanthrene exposure. *Environ. Chem.* <https://doi.org/10.1071/EN10094>.
- Lee, H., Shim, W.J., Kwon, J.-H., 2014. Sorption capacity of plastic debris for hydrophobic organic chemicals. *Sci. Total Environ.* 470–471, 1545–1552. <https://doi.org/10.1016/j.scitotenv.2013.08.023>.
- Lee, H., Byun, D.E., Kim, J.M., Kwon, J.H., 2018. Desorption modeling of hydrophobic organic chemicals from plastic sheets using experimentally determined diffusion coefficients in plastics. *Mar. Pollut. Bull.* 126, 312–317. <https://doi.org/10.1016/j.marpolbul.2017.11.032>.
- Lima, A.L.C., Farrington, J.W., Reddy, C.M., 2005. Combustion-derived polycyclic aromatic hydrocarbons in the environment—a review. *Environ. Forensics* 6, 109–131. <https://doi.org/10.1080/15275920590952739>.
- Lotufo, G.R., Fleeger, J.W., 1997. Effects of sediment-associated phenanthrene on survival, development and reproduction of two species of meiobenthic copepods. *Mar Ecol Prog Ser* 151, 91–102. <https://doi.org/10.3354/meps151091>.
- Luo, X.-J., Mai, B.-X., Yang, Q.-S., Chen, S.-J., Zeng, E.Y., 2008. Distribution and partition of polycyclic aromatic hydrocarbon in surface water of the Pearl River Estuary, South China. *Environ. Assess.* 427–436. <https://doi.org/10.1007/s10661-007-0051-2>.
- Ma, Y., Huang, A., Cao, S., Sun, F., Wang, L., Guo, H., Ji, R., 2016. Effects of nanoplastics and microplastics on toxicity, bioaccumulation, and environmental fate of phenanthrene in fresh water. *Environ Poll* 219, 166–173. <https://doi.org/10.1016/j.envpol.2016.10.061>. Barking, Essex : 1987.
- Maltby, L., Clayton, S.A., Wood, R.M., McLoughlin, N., 2002. Evaluation of the *Gammarus pulex* in situ feeding assay as a biomonitor of water quality: robustness, responsiveness, and relevance. *Environ. Toxicol.* 361–368. <https://doi.org/10.1002/etc.5620210219>.
- Mayer, P., Reichenberg, F., 2006. Can highly hydrophobic organic substances cause aquatic baseline toxicity and can they contribute to mixture toxicity? *Environ. Toxicol. Chem.* 25, 2639–2644. <https://doi.org/10.1897/06-142R1>.
- Mayer, P., Holmstrup, M., 2008. Passive dosing of soil invertebrates with polycyclic aromatic hydrocarbons: limited chemical activity explains toxicity cutoff. *Environ. Sci. Technol.* 42, 7516–7521. <https://doi.org/10.1021/es801689y>.
- McConkey, B.J., Duxbury, C.L., Dixon, D.G., Greenberg, B.M., 1997. Toxicity of a PAH photooxidation product to the bacteria *Photobacterium phosphoreum* and the duckweed *Lemna gibba*: effects of phenanthrene and its primary photoproduct, phenanthrenequinone. *Environ. Toxicol. Chem.* 16, 892–899. <https://doi.org/10.1002/etc.5620160508>.
- Menzie, C.A., Potocki, B.B., Santodonato, J., 1992. Exposure to carcinogenic PAHs in the environment. *Environ. Sci. Technol.* 26, 1278–1284. <https://doi.org/10.1021/es00031a002>.
- Mohamed Nor, N.H., Koelmans, A.A., 2019. Transfer of PCBs from microplastics under simulated gut fluid conditions is biphasic and reversible. *Environ. Sci. Technol.* 53, 1874–1883. <https://doi.org/10.1021/acs.est.8b05143>.
- Ochiai, N., Sasamoto, K., Kanda, H., Yamagami, T., David, F., Tienpont, B., Sandra, P., 2005. Optimization of a multi-residue screening method for the determination of 85 pesticides in selected food matrices by stir bar sorptive extraction and thermal desorption GC-MS. *J. Sep. Sci.* 28, 1083–1092. <https://doi.org/10.1002/jssc.200500017>.
- Rabodonirina, S., Net, S., Ouddane, B., Merhaby, D., Dumoulin, D., Popescu, T., Ravelonandro, P., 2015. Distribution of persistent organic pollutants (PAHs, Me-PAHs, PCBs) in dissolved, particulate and sedimentary phases in freshwater systems. *Environ Poll* 206, 38–48. <https://doi.org/10.1016/j.envpol.2015.06.023>. Barking, Essex : 1987.
- Rezania, S., Park, J., Md Din, M.F., Mat Taib, S., Talaiekhozani, A., Kumar Yadav, K., Kanyab, H., 2018. Microplastics pollution in different aquatic environments and biota: a review of recent studies. *Mar. Pollut. Bull.* 133, 191–208. <https://doi.org/10.1016/j.marpolbul.2018.05.022>.
- Rios, L.M., Jones, P.R., Moore, C., Narayan, U.V., 2010. Quantitation of persistent organic pollutants adsorbed on plastic debris from the Northern Pacific Gyre's "eastern garbage patch". *J. Environ. Monit. : JEM (J. Emerg. Med.)* 12, 2226–2236. <https://doi.org/10.1039/c0em00239a>.
- Rochman, C.M., Parnis, J.M., Browne, M.A., Serrato, S., Reiner, E.J., Robson, M., Young, T., Diamond, M.L., Teh, S.J., 2017. Direct and indirect effects of different types of microplastics on freshwater prey (*Corbicula fluminea*) and their predator (*Acipenser transmontanus*). *PLoS One* 12, e0187664. <https://doi.org/10.1371/journal.pone.0187664>.
- RStudio, T., 2015. RStudio: Integrated Development for R, vol. 42. RStudio, Inc., Boston, MA, p. 14.
- Samanta, S.K., Singh, O.V., Jain, R.K., 2002. Polycyclic aromatic hydrocarbons: environmental pollution and bioremediation. *Trends Biotechnol.* 20, 243–248. [https://doi.org/10.1016/S0167-7799\(02\)01943-1](https://doi.org/10.1016/S0167-7799(02)01943-1).
- Scheibitz, M., Spies, P., 2016. Polyamid 6 und 66 (PA6 und PA66): Asien und die Automobilindustrie prägen die Nachfrage an Polyamiden. *Werkstoff der Kunststoffe* 62–67.
- Schmidt, L.K., Bochow, M., Imhof, H.K., Oswald, S.E., 2018. Multi-temporal surveys for microplastic particles enabled by a novel and fast application of SWIR imaging spectroscopy - study of an urban watercourse traversing the city of Berlin, Germany. *Environ Poll* 239, 579–589. <https://doi.org/10.1016/j.envpol.2018.03.097>. Barking, Essex : 1987.
- Seidensticker, S., Zarfl, C., Cirpka, O.A., Fellenberg, G., Grathwohl, P., 2017. Shift in mass transfer of wastewater contaminants from microplastics in the presence of dissolved substances. *Environ. Sci. Technol.* 51, 12254–12263. <https://doi.org/10.1021/acs.est.7b02664>.
- Seidensticker, S., Zarfl, C., Cirpka, O.A., Grathwohl, P., 2019. Microplastic-contaminant interactions: influence of nonlinearity and coupled mass transfer. *Environ. Toxicol. Chem.* 38, 1635–1644. <https://doi.org/10.1002/etc.4447>.
- Sharma, S., Chatterjee, S., 2017. Microplastic pollution, a threat to marine ecosystem and human health: a short review. *Environ Sci Poll Res International* 24, 21530–21547. <https://doi.org/10.1007/s11356-017-9910-8>.
- Srogi, K., 2007. Monitoring of environmental exposure to polycyclic aromatic hydrocarbons: a review. *Environ. Chem. Lett.* 5, 169–195. <https://doi.org/10.1007/s10311-007-0095-0>.
- Straub, S., Hirsch, P.E., Burkhardt-Holm, P., 2017. Biodegradable and petroleum-based microplastics do not differ in their ingestion and excretion but in their biological effects in a freshwater invertebrate *Gammarus fossarum*. *Int. J. Environ. Res. Public Health* 14. <https://doi.org/10.3390/ijerph14070774>.
- Strungaru, S.-A., Jijie, R., Nicoara, M., Plavan, G., Faggio, C., 2019. Micro- (nano) plastics in freshwater ecosystems: abundance, toxicological impact and quantification methodology. *Trends Anal. Chem.* 110, 116–128. <https://doi.org/10.1016/j.trac.2018.12.025>.
- Sun, B., Hu, Y., Cheng, H., Tao, S., 2019. Releases of brominated flame retardants (BFRs) from microplastics in aqueous medium: kinetics and molecular-size dependence of diffusion. *Water Res.* 151, 215–225. <https://doi.org/10.1016/j.watres.2018.12.017>.
- Tan, X., Yu, X., Cai, L., Wang, J., Peng, J., 2019. Microplastics and associated PAHs in surface water from the Feilaixia reservoir in the beijing river, China. *Chemosphere* 221, 834–840. <https://doi.org/10.1016/j.chemosphere.2019.01.022>.
- Teuten, E.L., Rowland, S.J., Galloway, T.S., Thompson, R.C., 2007. Potential for plastics

- to transport hydrophobic contaminants. *Environ. Sci. Technol.* 41, 7759–7764. <https://doi.org/10.1021/es071737s>.
- US EPA, 2016. OCSPP 850.1020. In: Gammarid Amphipod Acute Toxicity Test: Ecological Effects Test Guidelines. OCS PP.
- van Cauwenberghe, L., Claessens, M., Vandegehuchte, M.B., Janssen, C.R., 2015. Microplastics are taken up by mussels (*Mytilus edulis*) and lugworms (*Arenicola marina*) living in natural habitats. *Environ Poll* 199, 10–17. <https://doi.org/10.1016/j.envpol.2015.01.008>. Barking, Essex : 1987.
- Verbruggen, E.M.J., van Herwijnen, R., 2012. Environmental Risk Limits for Phenanthrene. National Institute for Public Health and the Environment.
- Verrhiest, G., Clement, B., Blake, G., 2001. Single and combined effects of sediment-associated PAHs on three species of freshwater macroinvertebrates. *Ecotoxicology* 10, 363–372.
- Wang, W., Wang, J., 2018. Different partition of polycyclic aromatic hydrocarbon on environmental particulates in freshwater: microplastics in comparison to natural sediment. *Ecotoxicol. Environ. Saf.* 147, 648–655. <https://doi.org/10.1016/j.ecoenv.2017.09.029>.
- Wang, F., Wang, F., Zeng, E.Y., 2018. Sorption of toxic chemicals on microplastics. In: Zeng, E.Y. (Ed.), *Microplastic Contamination in Aquatic Environments: an Emerging Matter of Environmental Urgency*. Elsevier, Amsterdam, Netherlands, pp. 225–247.
- Zhai, Y., Brun, N.R., Bundschuh, M., Schrama, M., Hin, E., Vijver, M.G., Hunting, E.R., 2018. Microbially-mediated indirect effects of silver nanoparticles on aquatic invertebrates. *Aquat. Sci.* 80, 12968. <https://doi.org/10.1007/s00027-018-0594-z>.
- Zhang, Y., Maier, W.J., Miller, R.M., 1997. Effect of rhamnolipids on the dissolution, bioavailability, and biodegradation of phenanthrene. *Environ. Sci. Technol.* 31, 2211–2217. <https://doi.org/10.1021/es960687g>.
- Zhang, J., Zeng, J., He, M., 2009. Effects of temperature and surfactants on naphthalene and phenanthrene sorption by soil. *J Environ Sci* 21, 667–674. [https://doi.org/10.1016/S1001-0742\(08\)62297-4](https://doi.org/10.1016/S1001-0742(08)62297-4).